

**TECTONIC EVOLUTION AND CRUSTAL STRUCTURE OF THE
CENTRAL INDONESIAN REGION FROM GEOLOGY, GRAVITY
AND OTHER GEOPHYSICAL DATA**

Ir. AGUS GUNTORO

Thesis submitted for the degree of Doctor of Philosophy
Department of Geological Sciences
University College London

**UNIVERSITY OF LONDON
JULY 1995**

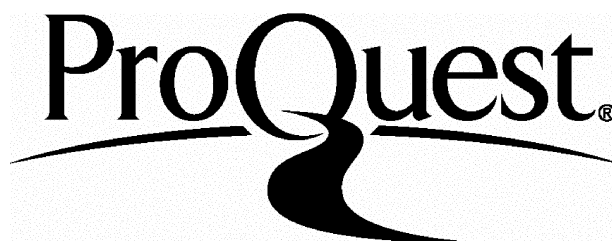
ProQuest Number: 10044387

All rights reserved

INFORMATION TO ALL USERS

The quality of this reproduction is dependent upon the quality of the copy submitted.

In the unlikely event that the author did not send a complete manuscript and there are missing pages, these will be noted. Also, if material had to be removed, a note will indicate the deletion.



ProQuest 10044387

Published by ProQuest LLC(2016). Copyright of the Dissertation is held by the Author.

All rights reserved.

This work is protected against unauthorized copying under Title 17, United States Code.
Microform Edition © ProQuest LLC.

ProQuest LLC
789 East Eisenhower Parkway
P.O. Box 1346
Ann Arbor, MI 48106-1346

ABSTRACT

Geographically, the Indonesian archipelago is often divided into eastern and western parts, the boundary between them being placed at the 200 m bathymetric contours passing through the Makassar Strait in the north to Lombok Strait in the south. In this study, a new subdivision is proposed, introducing a Central Indonesian Region (CIR) which represents a transition between the largely Eurasian elements of Western Indonesia and the Pacific and Australian related elements of Eastern Indonesia. The CIR is bounded by two major subduction zones; in the west by pre-Tertiary subduction zone at the southeastern margin of the Sundaland, and to the east by the Early Tertiary subduction zone. The latter is marked by the Selayar-Bonerate ridge. One of the most interesting features of the CIR is the existence of outcrops of deformed pre-Tertiary basement complexes in the West and Central Java, SE Kalimantan and SW Sulawesi, which are similar in age, lithology and structure (Katili 1978; Hamilton 1979; Parkinson 1991). They suggest that these terranes are fragments of a microcontinent, which accreted eastwards and was dismembered in the Late Cretaceous. The eastward migration of a subduction system during the Late Cretaceous and Early Tertiary is suggested by the eastward growth of melange terranes, by the position of the Neogene magmatic arc to the east of the Cretaceous one and by the separation of the Western Arc of Sulawesi from Kalimantan. These events are thought to have been responsible for the formation of the basins in the CIR.

As part of this study, a geological and gravity survey has been carried out on the Flores Sea Islands. The results of this survey were integrated with the published geological and geophysical data and with commercial seismic sections to allow examination of the crustal structure and tectonic development in the CIR. On the basis of gravity, magnetic and structural maps the CIR and vicinity can be divided into five major provinces, these being the Bone Bay, the Makassar Strait, the Central Java Sea, the East Java Sea and the Flores Sea provinces. Each province is examined and their stratigraphy, structural and tectonic styles correlated in order to have a complete understanding of their evolution.

Variations in gravity values and models demonstrate that the continental crust in the CIR was attenuated by subduction roll-back and then subjected to rifting by extensional forces.

The extension in the Makassar Strait, Central Java Sea and East Java Sea took place in the Eocene, forming marginal basins. Bone Bay opened due to collision between the Banggai-Sula microcontinent and Sulawesi in the Middle Miocene and was followed by clockwise rotation of Java, Sumbawa and Flores which cause the opening of the Flores Sea. The present configuration of the CIR is influenced by the collision between the Indo-Australian Plate and the Banda-Sunda arcs.

LIST OF CONTENTS

Title Page	1
Abstract	2
List of Contents	4
List of Figures	11
List of Tables	20
List of Photos	20
List of Appendixes	21
Acknowledgements	22
CHAPTER ONE	
INTRODUCTION	24
1.1 PREAMBLE	24
1.2 AIMS OF THE STUDY	26
1.3 AREA OF STUDY	26
1.4 METHOD OF STUDY	26
1.4.1 Seismic stratigraphic analysis	28
1.4.2 Gravity modelling	28
1.5 THESIS OUTLINE	29
CHAPTER TWO	
REVIEW OF TECTONIC EVOLUTION OF THE INDONESIAN REGION	30
2.1 RECONSTRUCTION OF PLATE MOTIONS IN THE INDONESIAN REGION	30
2.1.1 Late Cretaceous (70 Ma)	30
2.1.2 Late Paleocene (55 Ma)	30
2.1.3 Late Eocene (40 Ma)	32
2.1.4 Oligocene (30 Ma)	32
2.1.5 Early Miocene (20 Ma)	33
2.1.6 Middle Miocene (10 Ma)	33
2.1.7 Early Pliocene (5 Ma)	33
2.2 HYPOTHESES CONCERNING THE PLATE BOUNDARY IN THE EASTERN SUNDA SHELF	35
CHAPTER THREE	
GEOLOGY AND GEOPHYSICS OF THE CENTRAL INDONESIAN REGION	43
3.1 GEOLOGICAL REVIEW	43
3.1.1 Geological subdivisions	43
3.1.2 Pre-Tertiary Subduction zone in the Central Indonesian Region	46
3.1.2.1 Definition of melange	46
3.1.2.2 Pre-Tertiary rocks in Java	47
3.1.2.3 East Java Sea basement complex	49
3.1.2.4 Pre-Tertiary rocks in Southwest and Central Sulawesi	50
3.1.2.5 Pre-Tertiary rocks in Southeast Kalimantan	50

3.1.2.6	Summary	51
3.1.3	Volcanism in the Central Indonesian Region	51
3.1.3.1	Volcanism in Java Sea and SE Kalimantan	52
3.1.3.2	Volcanism in SW Sulawesi	54
3.1.3.2.1	Palaeogene volcanism in Southwest Sulawesi	54
3.1.3.2.2	Neogene volcanism in Southwest Sulawesi	55
3.1.3.3	Summary	55
3.2	GEOPHYSICAL REVIEW OF THE CENTRAL INDONESIAN REGION	56
3.2.1	Bathymetry	57
3.2.2	Earthquake data in the Central Indonesian Region	59
3.2.2.1	Introduction	59
3.2.2.2	Interpretation	59
3.2.3	Magnetic data	62
3.2.3.1	Introduction	62
3.2.3.2	Qualitative interpretation	65
3.2.4	Gravity data	72
3.2.4.1	Introduction	72
3.2.4.2	Qualitative interpretation	72
3.2.5	Seismic refraction in the East Java - Flores seas	72

CHAPTER FOUR

MORPHOSTRUCTURAL UNITS IN THE CENTRAL INDONESIAN REGION

		80
4.1	INTRODUCTION	80
4.2	GEOLOGICAL PROVINCES	80
4.3	SUBDUCTION ROLL-BACK	82

CHAPTER FIVE

BONE BAY PROVINCE

		85
5.1	INTRODUCTION	85
5.2	PREVIOUS STUDIES	85
5.3	GEOLOGY OF SULAWESI	85
5.3.1	Western Sulawesi Plutono- Volcano arc (WSPVA)	87
5.3.2	Central Sulawesi Metamorphic Belt (CSMB)	88
5.3.3	Eastern Sulawesi Ophiolite Belts (ESOB)	89
5.3.4	Banggai-Sula Microcontinent (BSM)	89
5.4	Bathymetry	90
5.5	SEISMIC INTERPRETATION	90
5.5.1	Seismic interpretation line IND 07	90
5.5.2	Seismic interpretation line IND 48	94
5.5.3	Seismic interpretation line IND 97	96
5.5.4	Seismic interpretation line IND 116	99
5.5	SUMMARY	101
5.6	GRAVITY DATA	102
5.6.1	Introduction	102
5.6.2	Qualitative gravity interpretation	102
5.6.3	Gravity models	104

5.6.3.1	Introduction	104
5.6.3.2	Interpretation	104
5.6.3.2.1	Gravity model IND 07	104
5.6.3.2.2	Gravity model IND 116	107
5.7	CRUSTAL STRUCTURE	110
5.8	TECTONIC IMPLICATIONS	111

CHAPTER SIX

	MAKASSAR STRAIT PROVINCE	117
6.1	INTRODUCTION	117
6.2	PREVIOUS STUDIES	117
6.3	BATHYMETRY	119
6.4	TECTONIC SETTING AND STRATIGRAPHY OF SE KALIMANTAN	119
6.4.1	Basement complexes	121
6.4.2	Sedimentary and volcanic rocks	124
6.4.3	Plutonic rocks	124
6.4.4	Implications	125
6.5	SEISMIC INTERPRETATION	125
6.5.1	Introduction	125
6.5.2	Seismic interpretation line PAC 201	125
6.5.2.1	Acoustic basement unit (Seismic sequence 1)	128
6.5.2.2	Syn-rift unit (Seismic sequence 2)	128
6.5.2.3	Post-rift unit	129
6.5.3	Seismic interpretation line PAC 202	130
6.5.3.1	Acoustic basement unit (Seismic sequence 1)	132
6.5.3.2	Syn-rift unit (Seismic sequence 2)	132
6.5.3.3	Post-rift unit	132
6.5.4	Seismic interpretation line MCP 05	133
6.5.5	Seismic interpretation line MK1 and MK3	135
6.6	WELL DATA	137
6.6.1	Well TT 2	137
6.6.2	Well TT 1	137
6.7	CORRELATION OF WELL DATA WITH SEISMIC SEQUENCES	138
6.8	SUMMARY	140
6.9	GRAVITY DATA	141
6.9.1	Introduction	141
6.9.2	Qualitative gravity interpretation	141
6.9.3	Gravity models	143
6.9.3.1	Introduction	143
6.9.3.2	Gravity model PAC 201	144
6.9.3.3	Gravity model PAC 202	144
6.9.3.4	Gravity model MCP 05	147
6.10	CRUSTAL STRUCTURE	147
6.11	TECTONIC IMPLICATIONS	149

CHAPTER SEVEN	
CENTRAL JAVA SEA PROVINCE	151
7.1 INTRODUCTION	151
7.2 PREVIOUS STUDIES	151
7.3 BATHYMETRY	153
7.4 TECTONIC SETTING AND STRATIGRAPHY	153
7.4.1 Subduction related zone	153
7.4.2 Basement rocks	153
7.4.3 Stratigraphy	156
7.5 SEISMIC REFRACTION AND REFLECTION	157
7.5.1 Refraction data	157
7.5.1.1 Introduction	157
7.5.1.2 Result and interpretation	157
7.5.2 Seismic reflection	160
7.5.2.1 Introduction	160
7.5.2.2 Interpretation	160
7.5.3 Summary	162
7.6 GRAVITY DATA	165
7.6.1 Introduction	165
7.6.2 Qualitative gravity interpretation	165
7.6.3 Gravity models	167
7.6.3.1 Introduction	167
7.6.3.2 Interpretation	167
7.6.3.2.1 Gravity model Java Sea 1	167
7.6.3.2.2 Gravity model Java Sea 2	171
7.6.3.2.3 Gravity model Java Sea 3	173
7.7 CRUSTAL STRUCTURE	175
7.8 TECTONIC IMPLICATIONS	176
CHAPTER EIGHT	
EAST JAVA SEA PROVINCE	179
8.1 INTRODUCTION	179
8.2 PREVIOUS STUDIES	179
8.3 BATHYMETRY	179
8.4 TECTONIC SETTING AND STRATIGRAPHY	179
8.4.1 Madura Zone	182
8.4.2 Kangean Island	182
8.4.3 The Bali-Lombok Sea	183
8.5 WELL DATA OF L46-1	183
8.6 SEISMIC INTERPRETATION	188
8.6.1 Introduction	188
8.6.2 Seismic interpretation line BP91-037	188
8.6.2.1 Stratigraphic framework	188
8.6.2.1.1 Basement unit	188
8.6.2.1.2 Pre-rift sediments	191
8.6.2.1.3 Syn-rift sediments	191
8.6.2.1.4 Post-rift sediments	192
8.6.2.2 Structural framework	192

8.6.3	Seismic interpretation line BP91-010	193
8.6.3.1	Stratigraphic framework	193
8.6.3.2.1	Basement unit	193
8.6.3.2.2	Pre-rift sediments	193
8.6.3.2.3	Syn-rift sediments	195
8.6.3.2.4	Post-rift sediments	195
8.6.3.2	Structural framework	195
8.6.4	Seismic interpretation line BP091-110	196
8.6.4.1	Stratigraphic framework	196
8.6.4.2.1	Basement unit	196
8.6.4.2.2	Pre-rift sediments	196
8.6.4.2.3	Syn-rift sediments	196
8.6.4.2.4	Post-rift sediments	198
8.6.4.2	Structural framework	198
8.6.5	Summary	198
8.7	GRAVITY DATA	199
8.7.1	Introduction	199
8.7.2	Qualitative gravity interpretation	199
8.7.3	Gravity models	199
8.7.3.1	Introduction	199
8.7.3.2	The effect of subducted lithosphere on the gravity models	202
8.7.3.3	Gravity model BEN 20	202
8.7.3.4	Gravity model RAMA 67	202
8.7.3.5	Gravity model BP 037	206
8.7.3.6	Gravity model MSN 14B	208
8.7.3.7	Gravity model MSN 14A	208
8.8	CRUSTAL STRUCTURE	210
8.9	TECTONIC IMPLICATIONS	213

CHAPTER NINE

GEOLOGICAL AND GRAVITY OBSERVATION ON THE FLORES

	SEA ISLANDS	216
9.1	THE FLORES SEA ISLANDS SURVEY	216
9.1.1	Introduction	216
9.1.2	Survey area	216
9.1.3	Type and period of survey	218
9.1.3.1	Gravity survey	218
9.1.3.2	Reconnaissance geological mapping	218
9.1.4	Communication and access	218
9.1.5	Currents, climate and weather	219
9.2	GEOLOGICAL SURVEY	220
9.2.1	Introduction	220
9.2.1.1	Type of geological information	220
9.2.1.2	Vegetation and outcrop conditions	220
9.2.1.3	Previous survey	220
9.2.2	Topography of the Flores Sea islands	221
9.2.2.1	Tanahjampea	221
9.2.2.2	Kajuadi	221

9.2.2.3	Kalao and Bonerate	221
9.2.2.4	Madu and Kalaotoa	222
9.2.2.5	Taka Lambaena and Karompa	222
9.2.2.6	Kepulauan Macan	222
9.2.3	Regional geological study of South Sulawesi	222
9.2.3.1	Introduction	222
9.2.3.2	Stratigraphy	223
9.2.4	Review geology on the Flores Sea Islands	228
9.2.4.1	Selayar	228
9.2.4.2	Kajuadi	228
9.2.4.3	Tanahjampea and Tanahmalala	228
9.2.4.4	Kalao	229
9.2.4.5	Kepulauan Macan (Tiger Islands)	230
9.2.5	Geological observation on the Flores Sea Islands	230
9.2.5.1	Selayar	230
9.2.5.2	Kajuadi	230
9.2.5.3	Tanahjampea and Tanahmalala	230
9.2.5.3.1	Old volcanic breccia	233
9.2.5.3.2	Bioclastic limestone	233
9.2.5.3.3	Igneous rocks	236
9.2.5.3.4	Young volcanic breccia	242
9.2.5.3.5	Coral limestone	242
9.2.5.4	Kalao	244
9.2.5.4.1	Ophiolitic rocks	244
9.2.5.4.2	Sedimentary rocks	247
9.2.5.5	Bonerate	252
9.2.5.6	Kalaotoa	254
9.2.5.7	Summary of stratigraphy of the Flores Sea islands	256
9.3	GRAVITY SURVEY ON THE FLORES SEA ISLANDS	261
9.3.1	Introduction	261
9.3.1.1	Purpose of study	261
9.3.1.2	Location of gravity stations	261
9.3.1.3	Instrumentation	261
9.3.1.4	Method of investigation	261
9.3.1.5	Observed gravity	262
9.3.1.6	Survey loops	265
9.3.2	Gravity data processing	267
9.3.2.1	Gravity data reduction	267
9.3.2.1.1	Latitude correction	268
9.3.2.1.2	Free-air correction	268
9.3.2.1.3	Bouguer correction	269
9.3.2.1.4	Terrain correction	270
9.3.2.2	Errors estimation in reduction of the gravity data	271
9.3.2.3	Bouguer anomaly and contouring	271
9.3.2.4	Description of Bouguer anomaly maps	272
9.3.2.5	Summary	276

CHAPTER TEN	
GEOPHYSICAL STUDY OF THE FLORES SEA ISLANDS AND VICINITY	277
10.1 INTRODUCTION	277
10.2 FLORES BASIN	277
10.2.1 Tectonic setting of the Flores Basin	277
10.2.2 Stratigraphy of the Flores Basin	280
10.3 SEISMIC INTERPRETATION	282
10.4 GRAVITY DATA	286
10.4.1 Introduction	286
10.4.2 Qualitative gravity interpretation	286
10.4.3 Gravity models	289
10.4.3.1 Introduction	289
10.4.3.2 Gravity model Atlantis 07	289
10.4.3.3 Gravity model MSN 13	289
10.4.3.4 Gravity model Silver 06	292
10.5 CRUSTAL STRUCTURE	294
10.6 TECTONIC IMPLICATIONS	294
CHAPTER ELEVEN	
SUMMARY AND TECTONIC EVOLUTION	290
11.1 SUMMARY OF GEOLOGICAL PROVINCES	296
11.1.1 Bone Bay Province	296
11.1.2 Makassar Strait Province	297
11.1.3 Central Java Sea Province	298
11.1.4 East Java Sea Province	298
11.1.5 Flores Sea Province	299
11.2 EVOLUTION OF THE CENTRAL INDONESIAN REGION	301
11.3 RECOMMENDATIONS FOR FUTURE WORK	311
REFERENCES	312

LIST OF FIGURES

CHAPTER ONE

- Figure 1.1 Present-day tectonic setting and the distribution of basement complexes 25
around the boundary between the Eastern and Western Indonesian
regions (Modified from Bransden and Matthews 1992; Parkinson 1991).
- 1.2 The study area 27

CHAPTER TWO

- Figure 2.1a-d Plate reconstruction in the Indonesian region in 70, 55, 40 and 30 Ma. 31
(Daly *et al.* 1991).
- 2.1e-g Plate reconstruction in the Indonesian region in 20, 10 and 5 Ma. 34
(Daly *et al.* 1991).
- 2.2 Late Cretaceous reconstruction showing the Cretaceous magmatic arc 37
and subduction zone passing from the southeast end of Sumatra across the
Java Sea and through the Meratus Mountains of SE Kalimantan (Katili 1971,
1972 and Hamilton 1972, 1979).
- 2.3 Late Cretaceous reconstruction of Asian Indonesia showing the 37
paleogeography of the Northern Tethys margin and the position of Timor
south of East Java (Audley-Charles 1976).
- 2.4 Cartoons showing evolution of the Australian continental margin, 38
Sundaland, the Banda Sea and the island of Timor from the early
Mesozoic to the present day (Barber 1981).
- 2.5 Late Cretaceous reconstruction showing the position of the West 38
Sulawesi (WS) microcontinent to the south of Borneo. The WS
microcontinent was interpreted to derive from the westernmost Banda Arc
(Parker and Gealey 1983).
- 2.6&2.7 Cartoons of the tectonic evolution of SE Kalimantan and SW Sulawesi 40
showing the main theories of the origin of present SW Sulawesi block. In
Fig.2.6 (Sikumbang 1990), the SW Sulawesi block is derived from oceanic
crust subducted at the Alino Island Arc. In Fig.2.7 (Parkinson 1991) the
block is derived from a microcontinental fragment rifted from Gondwanaland.

CHAPTER THREE

Figure 3.1	The Indonesian region in relation to the Sundaland and Australian Platform (Hamilton 1979).	44
3.2	Proposed division Western, Central and Eastern Indonesia.	45
3.3	The distribution of the pre-Tertiary basement complexes in the Indonesian region (Compiled from Hamilton 1979, Tyrrel <i>et al.</i> 1986 and Parkinson 1991).	48
3.4	The distribution of pre-Tertiary and Tertiary magmatic arcs in the Indonesian region (Modified from Hamilton 1979; Katili 1991).	53
3.5	Bathymetric map in the East Java and Flores seas (Edcon 1991).	58
3.6	Earthquake map in the Indonesian Region (Kertapati <i>et al.</i> 1992).	60
3.7	Map showing depth contours (in kilometers) to the top of the inclined seismic zone in the Central Indonesian Region (Cardwell and Isacks 1978).	61
3.8	Composite vertical cross sections of earthquake hypocentres shown in Fig.3.7 in the East Java and Banda seas (Cardwell and Isacks 1978).	63
3.9	Magnetic data coverage in the Central Indonesian Region (Edcon 1991).	64
3.10	Magnetic anomaly map in the Central Indonesian Region (redraw from Edcon 1991).	66
3.11	Magnetic profiles in the Java Sea Province.	67
3.12	Magnetic profile in the Kangean Province.	68
3.13	Magnetic profiles in the Flores Sea Province.	70
3.14	Magnetic profiles in the Selayar-Tanahjampea Province.	71
3.15	Gravity data coverage in the Central Indonesian Region (Edcon 1991).	73
3.16	Marine Bouguer anomaly map of the Central Indonesian Region (Modified from Edcon 1991).	74
3.17	Location of seismic refraction and radiosonobuoy stations in the East Java-Flores seas (Ben-Avraham and emery 1973; Curray <i>et al.</i> 1977).	76
3.18	Correlation of layers obtained from seismic refraction between stations MSN 12, MSN 13 and MSN14A&B showing the increase of crustal thickness from east to west (Curray <i>et al.</i> 1977).	78
3.19	Seismic structure section across the Java Sea, Java Trough, Java and Java Trench showing the increase in crustal thickness from south to north which	78

possibly continues into the Java Sea (Ben-Avraham and Emery 1973).

CHAPTER FOUR

Figure 4.1	Morpho-structural units in the Central Indonesian Region based on gravity, magnetic and structural maps.	81
4.2	The two models showing the different styles of extensional deformation expected with fast and slow rates of lithosphere extension (Park 1988).	83
4.3	Sketch showing the relationship between the relative velocity of subduction zone rollback (V_t) and the velocity of the upper plate (V_u) in relation to extensional and compressional stress behind the arc (After Daly <i>et al.</i> 1991).	83

CHAPTER FIVE

Figure 5.1	The four major belts and tectonic setting of Sulawesi (Sources; Hamilton 1979; Silver <i>et al.</i> 1983; Simandjuntak 1986; Daly <i>et al.</i> 1991; Parkinson 1991).	86
5.2	Bathymetric map and seismic location on Bone Bay.	91
5.3	Seismic line drawing and interpretation of line IND 07 showing two major sedimentary units; folded and flat-lying sediments in which the boundary between them marks the major tectonic event in Bone Bay.	92
5.4	Seismic line drawing and interpretation of line IND 48 showing the presence of extensional basin in Bone Bay.	95
5.5	Seismic line drawing and interpretation of line IND 97 showing the presence of extensional basin in Bone Bay.	97
5.6	Seismic line drawing and interpretation of line IND116E showing the presence of extensional basin in Bone Bay.	100
5.7	The free-air anomaly map of Bone Bay (Bouguer onland of SW Sulawesi; modified from Bowin <i>et al.</i> 1980; Silver <i>et al.</i> 1981; Simamora and Marzuki 1990; Edcon 1991; 1993 Flores Sea Islands gravity Survey).	103
5.8a	Simplified gravity model of line IND 07 showing crustal structure in northern part of Bone Bay.	105
5.8b	Alternative gravity model IND 07 showing crustal structure in northern	106

	part of Bone Bay.	
5.9a	Simplified gravity model IND 116 showing crustal structure in southern part of Bone Bay.	108
5.9b	Alternative gravity model IND 116 showing subducted oceanic crust beneath Selayar Island.	109
5.10	Possible correlation of seismic structures in Bone Bay constrained from gravity data.	114
5.11	The comparison between strike-slip faults in Sulawesi and the indentation model from Tapponnier (1982), showing the strike-slip faults in Sulawesi are in agreement with the indentation model.	115
5.12	A cartoon showing the effect of the Banggai-Sula collision to Sulawesi having caused displacement and rotation between two prominent strike-slip faults (the Walanae and Palu-Koro faults) causing the opening of Bone Bay.	116

CHAPTER SIX

Figure 6.1	Location map of the Makassar Strait	118
6.2	Bathymetric, structural and seismic location maps on the Makassar Strait.	120
6.3	Distribution of stratigraphic and tectonostratigraphic units in the Meratus Mountains and adjacent areas (Sikumbang 1992).	122
6.4	Summary of stratigraphic framework and geological evolution of the Meratus Mountains (Sikumbang 1992).	123
6.5A	Line drawing and its interpretation of western segment of line PAC 201 showing basement faults indicating extensional basin. Arrows mark cycle terminations on onlap, downlap and toplap which provide criteria for recognition of sequence boundaries. Letter H1-H6 designate seismic horizons.	126
6.5B	Seismic line drawing and its interpretation of eastern segment of line PAC 201 showing extensive thrust faults after the formation of horizon H5 forming Neogene foreland basin. Arrows mark cycle terminations onlap, downlap, toplap which provide criteria for recognition of sequence boundaries. Letters H1-H6 designate seismic horizons.	127
6.6	Seismic line drawing and interpretation showing basement faults, suggesting extensional basin. Arrows mark cycle terminations on onlap,	131

downlap and toplap which provide criteria for recognition of sequence boundaries. Letters H1-H6 designate seismic horizons.

6.7	Seismic line drawing interpretation of line MCP 05 across the Makassar Strait showing the intracratonic rifting of the Makassar Strait causing separation between SE Kalimantan and SW Sulawesi (Katili 1973).	134
6.8	Seismic line drawing of line MK 1 and MK 3 showing deep basin of the North Makassar Basin (After Buroillet and Salle 1981).	136
6.9	Lithologies of Well TT 1 and TT 2 and correlation to the seismic horizons	139
6.10	The Free-air anomaly map of the Makassar Strait (Bouguer onland of SW Sulawesi) (Sources; SIPM, obtained from Situmorang 1982; Simamora and Marzuki 1990).	142
6.11	Gravity model PAC 201 showing crustal thinning over the Makassar Basin	145
6.12	Gravity model PAC 202 showing crustal thinning over the Makassar Basin.	146
6.13	Gravity model MCP 05 showing crustal thinning over the Makassar Basin.	148

CHAPTER SEVEN

Figure 7.1	Structural setting of the Central Java Sea showing the NE-SW structural highs and lows (P.T Trias 1989).	152
7.2	Bathymetric map of the Central Java Sea (Ben-Avraham and Emery 1973).	154
7.3	Tectonic elements in the Central Java Sea and vicinity showing four major structural highs in NE-SW direction (Simplified from Ben-Avraham and Emery 1973).	155
7.4	Stratigraphic correlation between Western and Eastern Java, which is comparable to western and eastern basinal areas (P.T Trias 1989).	158
7.5	Location of oblique reflection-refraction data coverage in the Java Sea (Ben-Avraham and Emery 1973).	159
7.6	Seismic line drawing interpretation with Bouguer, Free-air and magnetic anomaly profiles (Ben-Avraham and Emery 1973).	161

7.7	Shallow seismic reflection profiles in the Central Java Sea (Silitonga and Hakim, 1990)	163
7.8	Geological cross section passing the Central Java Sea in E-W direction (Koesoemadinata and Pulunggono 1971; 1975).	164
7.9	Bouguer anomaly map of the Central Java Sea and vicinity (Modified from Edcon 1991).	166
7.10	Location of gravity models and radiosonobuoy stations in the Central Java Sea	168
7.11	Gravity model Java Sea 1	169
7.12	Gravity model Java Sea 2	172
7.13	Gravity model Java Sea 3	174

CHAPTER EIGHT

Figure 8.1	The new division of the East Java Sea into Central and East Java seas on the basis of structural and Bouguer anomaly contour patterns.	180
8.2	Bathymetric map of the East Java Sea showing E-W contour orientations and towards the Makassar Strait the contours suddenly change into N-S directions.	181
8.3	Location map of wells and the Central Lombok Block in the East Java Sea.	184
8.4a	Stratigraphy of the upper portion of the Amoco L40-1 well (Tyrrel <i>et al.</i> 1986).	185
8.4b	Stratigraphy of the Amoseas Bone-1 well (Tyrrel 1986).	185
8.4c	Stratigraphy of JS 25-1 well close to Kangean Island (Kohar 1985).	186
8.5	Location of seismic interpretation on the East Java Sea.	189
8.6	Line drawing and interpretation of seismic line BP 091-037 showing horst and graben structures and inversion structure.	190
8.7	Line drawing and interpretation of line BP 091-010 showing horst and graben structures and inversion structure.	194
8.8	Line drawing and interpretation of seismic line BP 091-110 showing horst and graben structures.	197
8.9	Bouguer anomaly map in the East Java Sea (Modified from Edcon 1991).	200

8.10	The geometry of the slab subduction of the Indo-Australian plate beneath the Sunda-Banda arcs to the effect of the gravity models in the East Java Sea.	201
8.11	Gravity model BEN 20	204
8.12	Gravity model RAMA 67	205
8.13	Gravity model BP 037	207
8.14	Gravity model MSN 14B	209
8.15	Gravity model MSN 14A	211
8.16	Comparison of bathymetry, free-air and Bouguer anomaly profiles of BEN 20, RAMA 67, BP 037, MSN 14B AND MSN 14A.	212

CHAPTER NINE

Figure 9.1	Geological and gravity survey area in the Flores Sea Islands.	217
9.2	Three major morphological units in SW Sulawesi; the Western Divide Mountains, the Bone Mountains and the Walanae Depression (Leeuwen 1981).	224
9.3	Simplified stratigraphy of Southwest Sulawesi with the special reference to the Biru area (Leeuwen 1981)	225
9.4	Location of gravity stations on islands of the Selayar group.	231
9.5a	Location of gravity stations on islands of the Bonerate group.	232
9.5b	Location of gravity stations on islands of the Kalaotoa group.	232
9.6	Geological map of Tanahjampea and Tanahmalala.	234
9.7	Geological map of Kalao (Modified from Koswara <i>et al.</i> 1991;1993).	245
9.8	Geological observation map in Kalao.	246
9.9a	Traverse map in Bonerate.	253
9.9b	Geological map of Bonerate (Modified from Koswara <i>et al.</i> 1991;1993).	253
9.10a	Traverse map in Kalaotoa.	255
9.10b	Geological map of Kalaotoa (Modified from Koswara <i>et al.</i> 1991;1993).	255
9.11	Summary of stratigraphy of the Flores Sea Islands.	257
9.12	G-286 gravimeter drift lines.	266
9.13a	Bouguer anomalies, Selayar group.	273
9.13b	Bouguer anomalies, Bonerate group.	274
9.13c	Bouguer anomalies, Kalaotoa group.	275

CHAPTER TEN

Figure 10.1	Bathymetric map of the Flores Sea Islands and vicinity.	278
10.2	Sequences of stratigraphy from single channel seismic reflection in the Flores Basin (Silver <i>et al.</i> 1986).	281
10.3	Seismic interpretation of line IND 116 showing basement faults, angular unconformity and intrusion of more basaltic rocks.	283
10.4	Seismic interpretation of line PAC 213 showing basement uplift	284
10.5	Correlation between single channel seismic reflection, bathymetry and gravity profiles of Mariana 09.	285
10.6	The Free-air anomaly map of the Flores Sea Islands and vicinity (Compiled from free-air anomaly map of Bowin <i>et al.</i> (1980); free-air anomaly map of Edcon (1991) and 1993 Flores Sea Islands gravity survey).	287
10.7	Gravity model Atlantis 07.	290
10.8	Gravity model MSN 13 showing crustal thinning beneath the Flores Low, suggesting the presence of oceanic crust.	291
10.9	Gravity model Silver 06 showing crustal thinning beneath the Flores Low, suggesting the presence of oceanic crust.	293

CHAPTER ELEVEN

Figure 11.1	Early Cretaceous reconstruction map and section showing the configuration of the junction between the East Java Sea microplate, the Pacific Plate and the Indo-Australian Plate. Subduction extends from Sumatra through Java, the proto Java Sea and SE Kalimantan, generating an accretionary complex. The boundary between the Indo-Australian and Pacific plates is probably a transform fault. In the east, the SW Sulawesi microcontinent was conveyed along the transform fault.	303
11.2	Late Cretaceous reconstruction map and section showing how, after collision the SW Sulawesi microcontinent with SE Kalimantan (emplacement of basement complexes), the passive margin changed to an active margin to accommodate continuing movement of the Pacific Plate.	304
11.3	Paleocene section showing the uplift and block faulting of the collision between SE Kalimantan and SW Sulawesi. The continuous magmatic	306

- activity in SE Kalimantan is interpreted to derive from this subduction.
- 11.4 Eocene reconstruction map and section showing increasing plate convergence due to vertical sinking of the subducting plate causing back-arc spreading in the Makassar Strait and Java Sea, generating horst and graben structures accompanied by deposition of rift sediments. 307
 - 11.5 Oligocene reconstruction and section showing the collision of the East Sulawesi ophiolite with SW Sulawesi, causing the formation of the Peluru Melange Complex and the emplacement of the Latimojong ophiolite in SW Sulawesi. 308
 - 11.6 Middle-Late Miocene reconstruction and section showing collision between the Banggai-Sula microcontinent and East Sulawesi followed by the opening of Bone Bay. Clockwise rotation of Java, Sumbawa and West Flores was followed by the opening of the Flores Sea. 310

LIST OF TABLES

CHAPTER THREE

Table 3.1	Seismic refraction and radiosonobuoy data from the East Java-Flores Sea	77
	(Sources; Ben-Avraham and Emery 1973 and Curray <i>et al.</i> 1977).	

CHAPTER NINE

9.1	Micropaleontological analysis at gravity station GS 040 (Kalao Island).	251
9.2	Calculation of average Gobserved on the subsidiary base stations with reference to the Hasanuddin Airport.	264

LIST OF PHOTOS

CHAPTER NINE

Photo 9.1	Outcrop showing unconformable contact between old volcanic breccia and bioclastic limestone (Location GS 065).	235
9.2	Outcrop of bioclastic limestone with vertical joints (Location GS 065).	235
9.3	Outcrop of granite showing very extensive vertical joints, which was intruded by andesite as dykes (Location GS 068).	238
9.4	Diorite xenoliths within the granite (Location GS 069).	238
9.5	Outcrop of rhyolite showing layering, jointing and folding (Location GS 066).	240
9.6	Outcrop of intercalation between volcanic breccia and tuff with calcite veins (Location GS 067).	243
9.7	Outcrop of volcanic sandstone showing minor faults and joints (Location GS 034, St 02 on Kalao).	248
9.8	Outcrop of conglomerate and intercalation between tuffaceous sandstone and claystone showing irregular contact (Location GS 040 on Kalao).	248

LIST OF APPENDIX

Appendix	9.1	Description of gravity base station at Hasanuddin Airport, Ujung Pandang (Adkins <i>et al.</i> 1978).	322
	9.2	Description of subsidiary base station 9381.9001 at Hotel Ramayana, Ujung Pandang.	324
	9.3	Description of subsidiary base station 93819002 at Lapee Harbour, Bulu Kumba.	325
	9.4	Description of subsidiary base station 9381.9003 at Benteng Harbour, Selayar.	326
	9.5	Description of subsidiary base station 9381.9004 at Hotel Berlian, Selayar.	327
	9.6	Description of subsidiary base station 9381.9016 at Bonerate.	328
	9.7	Description of subsidiary base station 9381.9021 at Kalaotoa.	329
	9.8	Description of subsidiary base station 9381.9044 at Benteng, Tanahjampea.	330
	9.9	Reduction of gravity data in the Flores Sea Islands.	332

ACKNOWLEDGEMENTS

The completion of this research has been contributed by the help of many people spiritually and financially. To these people I would like to express my sincere gratitude. Firstly, all the virtue should go to my supervisor Dr. John Milsom, for taking me in this research and for his great patience, tolerance, attention, valuable guidance, encouraging criticism and useful discussion. Honestly, this manuscript has been tremendously improved by his editorial work especially for the English usage. I would also like to thank him for his effort in finding extra resource when my grant finished a few month ago.

Dr. Bona Situmorang, my former lecturer at Trisakti University, who then became my senior colleague at the same university gave me support and recommendation for this studentship. I really appreciate and thank him.

The funding of this research came from British Petroleum Indonesia and I would particularly like to thank Mr. Gunther Newcombe for his support in this research. All staffs in the BP office Jakarta, especially Mary Suwandi, who previously helped me during my work in the BP office, Jakarta.

At Trisakti University, I have received invaluable help. I thank the Dean of Faculty of Mineral Technology, Bapak Ir. Sutan Asin, and former Head of Geological Department, Bapak Ir. M.H. Thamrin for giving me permission to study at University College London, and also to all my colleagues and staff at the department.

During my study at University College London, I also received many help from the staff. I would like to extend particular thank Dr. E.J.W. Jones and Prof. Robert Hall for global discussion in geophysics and geology. Ron Dudman and Celine for their help in administration work. Simon Baker for allowing me use of the computer in the regional geology room. Diane Cameron for her great help whenever I ask and for her hospitality, thank you Diane. I hope I can see you sometimes in Jakarta.

A special thank you goes to my fellow postgraduate students and my friends for being good companion through my study. Bapak Sarjono helped me in collecting gravity data in the Flores Sea Islands. I really appreciate the work you have done for me. Thanks to all people in the Flores Sea islands, who helped me during my fieldwork. Alit alias 'Pak Kumis' and his wife and Bapak Dwi and families for being very special friends and also thanks for your helps. Dr. Jeffrey Malaihollo and wife thank you very much for all your help, especially with the discussion and suggestion for my thesis.

To all my families in Indonesia; Guntoro families and Laksono families thank you very much for all your support in giving me good motivation, financial and spiritual supports. To my dearest mother and father to whom I dedicate all this my work. A very special thanks for my beloved wife for everything and I really appreciate for all your sacrifices for me and to my beloved son, Johnatan P. Steven Guntoro, and my daughter, Diana P. Guntoro.

CHAPTER ONE

INTRODUCTION

1.1 PREAMBLE

The Indonesian archipelago can be divided tectonically into two large geological provinces, the Eastern Indonesian Province and the Western Indonesian Province. The Western Indonesian Province is geologically simpler and its geological history is better understood. The Eastern Indonesian Province is geologically one of the most complex regions of the world, both structurally and stratigraphically. This is because it lies at the triple junction of three large plates; the Indo-Australian Plate, Eurasian Plate and Pacific Plate (Fig. 1.1). Since the Late Cretaceous the area has been subjected to varying phases of rifting, subduction, volcanism, collision, wrenching and rotation. Although many geologists have studied this area, evolution and histories are still subject to debate.

One of the most interesting features at the boundary between the Western and Eastern Indonesian provinces is the existence of outcrops of deformed pre-Tertiary basement in West and Central Java, the Java Sea, Southeast Kalimantan and South Sulawesi which are similar in age, lithology and structure (Hamilton 1979; Katili 1978; van Leeuwen 1981; Sikumbang 1990; Parkinson 1991). These authors suggest that these terranes are fragments of a microcontinent, the East Java Sea microcontinent, which accreted eastward and was dismembered in the Early Cretaceous. The eastward migration of a subduction system during the Late Cretaceous and Cainozoic is suggested by the eastward growth of melange terranes, by the position of the Neogene magmatic arc to the east of the Cretaceous one and by the separation of the Western Arc of Sulawesi from Kalimantan (Hamilton 1979). It is generally accepted that tectonic development during the Late Mesozoic to Early Tertiary caused changes in subduction zone direction, from NE-SW on the Java-Meratus trend to E-W in the south of Java.

The area between the supposed Cretaceous subduction zone passing through Java, Kalimantan and Sulawesi and the present subduction zone south of Java is characterised by an assemblage of crustal fragments and a number of deep sea basins of different origins which are poorly understood. The present study integrates geological and

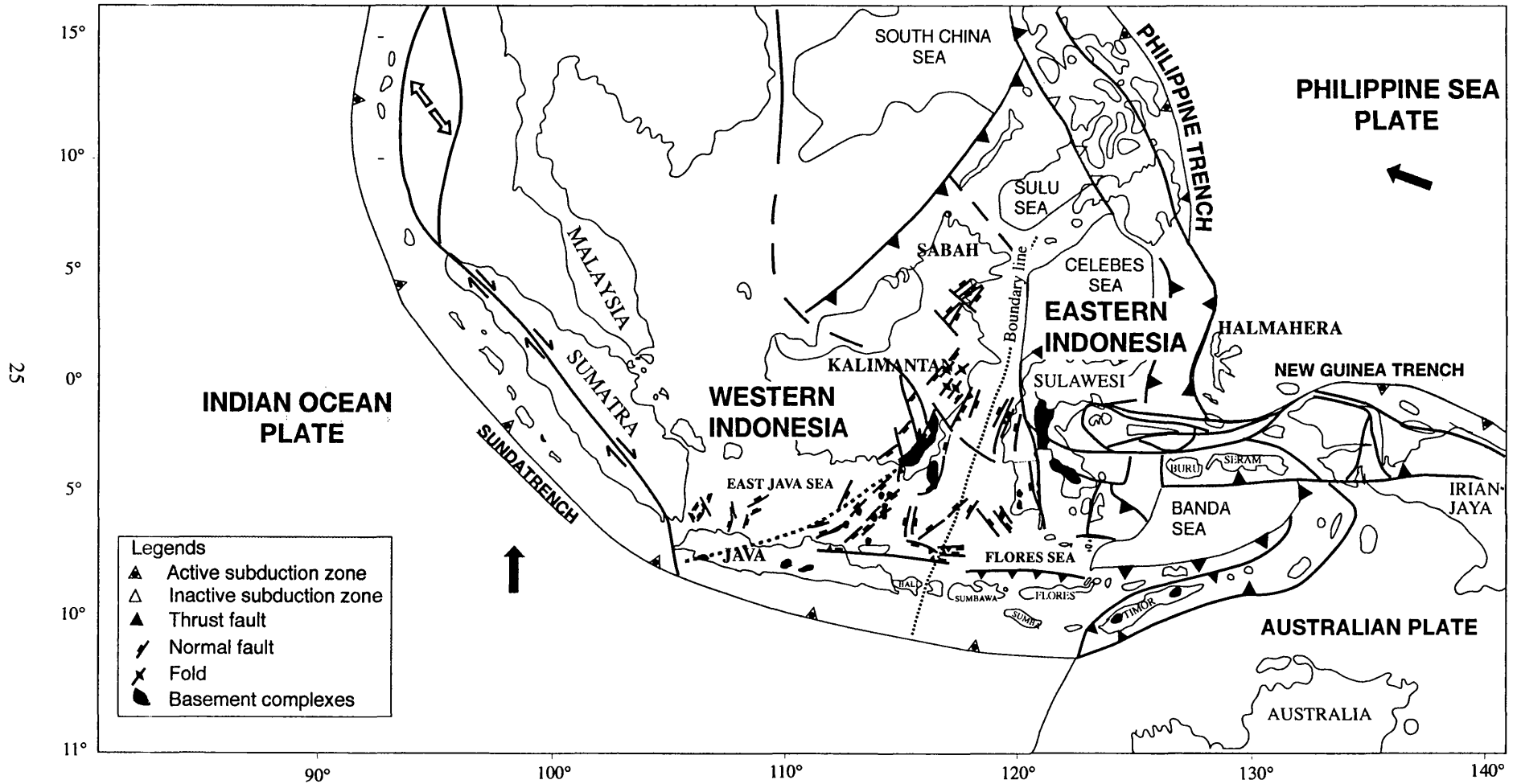


Figure 1.1: Present-day tectonic setting and the distribution of basement complexes around the boundary between the Eastern and Western Indonesian regions (Modified from Hamilton 1979; Parkinson 1991; Bransden and Matthews 1992).

geophysical data from a variety of sources which together provide significant constraints on tectonic models and palinspastic reconstructions of the area.

1.2 AIMS OF THE STUDY

The main objective of the present study is to define the distribution of fragments of the supposed Cretaceous-Palaeogene arc which linked Java, the Java Sea, Southeast Kalimantan and Southwest Sulawesi, and to relate their present locations to the evolution of the subduction zones, forearcs, magmatic arcs and back-arc basins which developed between the Sunda Platform (southeast margin of Eurasian Plate) and the Australian continental margin during the Late Mesozoic and Early Tertiary. To achieve this aim the following methods have been used:

- To make and interpret gravity models in the study area constrained by geological and other geophysical data, to re-examine the nature and extent of the supposed Cretaceous-Palaeogene arc.
- To analyse seismic stratigraphy in order to understand basin evolution in the region
- To determine the nature of the crustal structure in the study area by gravity modelling.
- To make a kinematic analysis of the development of East Java Sea microcontinent since the Cretaceous in relation to tectonic evolution in the Flores Sea islands.

1.3 AREA OF STUDY

The area chosen for this study is approximately between 50°S - 90°S latitude and 110°E - 123°E longitude (Fig.1.2). This area is referred to as Central Indonesian Region. Most of this area is under water, but there are some small islands (Flores Sea Islands) where geological and geophysical data can be obtained.

1.4 METHOD OF STUDY

The work can be divided into a pre-field work stage and a post field work stage. The pre-fieldwork stage included a literature study and also interpretation of existing geological and geophysical data. Since the data available from islands in the Flores Sea islands were

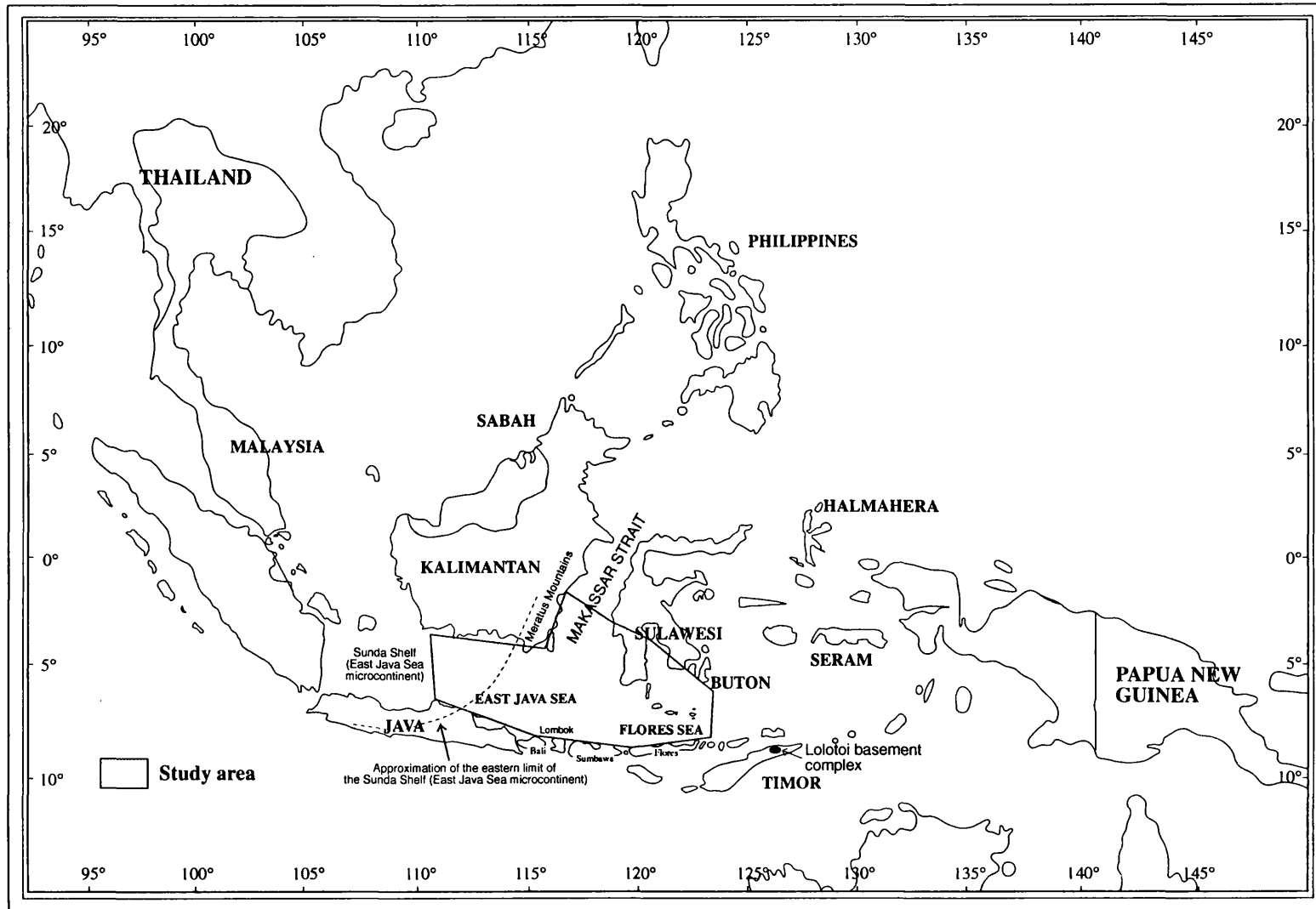


Figure 1.2: The Study area

rather limited, it was decided to visit these islands and obtain additional lithological, structural, tectonic and geophysical information. Following the field work, the data obtained from the islands was used to constrain modelling and test some hypotheses relating to tectonic development and basin evolution.

The present study is based principally on the interpretation of geophysical data from the Central Java Sea, the East Java Sea, the Flores Sea, Bone Bay and the Makassar Strait, since geophysical studies are very important to provide the key to understanding tectonic development and basin evolution in the Central Indonesian Region.

The main geophysical methods used in this thesis are seismic stratigraphic analysis and gravity modelling. Seismic stratigraphic analysis is intended to obtain information about depositional units and structural settings of the sediments in order to understand basin evolution of the region whilst gravity modelling is intended to obtain information about the crustal structure of the region.

1.4.1 Seismic stratigraphic analysis

Seismic stratigraphic analysis is an approach used to translate seismic reflection profile information into geological sense. There are two major methods; seismic sequence analysis and seismic facies analysis (Vail *et al.* 1977). In seismic sequence analysis, the section is subdivided into sequences of stratigraphic units bounded by unconformities or their relative conformities, indicated by reflection truncation, toplap, onlap and downlap. In seismic facies analysis, the section is analysed together with other parameters including reflection configuration, amplitude, continuity, frequency and interval velocity in order to interpret environmental settings and depositional processes and to estimate the lithologies of the strata involved.

1.4.2 Gravity modelling

The gravity models were generated using the GM-SYS interactive 2 D modelling program produced by Northwest Associates Inc. of Corvallis, Oregon, running on an IBM compatible 486-based microcomputer. The principle of the modelling program is to obtain an agreement between the observed gravity anomaly profile and the calculated

gravity anomaly profile obtained from geological models represented by polygons. The calculated gravity anomaly profile continuously changes as a polygon corner point is moved under cursor control.

As usual, quantitative interpretation of gravity field is ambiguous. Without other independent information an infinite number of models can be fitted to a given anomaly. In this thesis, seismic reflection, refraction and geological data are used to constrain models for crustal structure in the Central Indonesian region.

In the interpretation of combined gravity and seismic data, rock layers must be assigned density. Densities have been approximated from seismic velocities using the conversion curve of Nafe and Drake (1963). In the East Java and Flores seas, seismic reflection and radiosonobuoy velocities have been used to obtain densities in the shallow crust. Densities for the deeper crustal and mantle have been determined from P-wave velocities obtained from seismic refraction surveys by Ben-Avraham and Emery (1973) and Curray *et al.* (1977). A reference crustal density of 2.67 Mg/m^3 has been used with a thickness of standard crust of 30 km.

1.5 THESIS OUTLINE

The present understanding of the plate kinematics of the southeast Asian region is reviewed first to establish a plate tectonic framework (Chapter 2). The term "Central Indonesian Region" is then introduced as the basic concept underlying the research, and this is followed by discussion of the regional geology and geophysics of the region (Chapter 3). On the basis of gravity, magnetic and structural maps, the Central Indonesian Region is then divided into five major morpho-structural provinces (Chapter 4). The geology and geophysics of each province are discussed in detail in Chapters 5 to 10 and data from the geological and gravity surveys on the Flores Sea islands are then integrated to control gravity modelling. The geological evolution and crustal structure of the Central Indonesian Region as constrained by the available data are summarised in Chapters 11. Finally a palinspastic model and related plate tectonic framework are presented.

CHAPTER TWO

REVIEW OF TECTONIC EVOLUTION OF THE INDONESIAN REGION

2.1 RECONSTRUCTION OF PLATE KINEMATICS IN THE INDONESIAN REGION

The tectonic evolution of the Indonesian region cannot be separated from the tectonic evolution of Southeast Asia. As already noted, the Indonesian region lies at the junction of three large plates (Indo-Australian Plate, Eurasian Plate and Pacific Plate). The chronostratigraphic evolution of these plates with respect to the evolution of the Indonesian region is summarised from the works of Daly *et al.* (1987; 1991), and when necessary some additional information from other workers are also included.

2.1.1 Late Cretaceous (70 Ma) (Fig. 2.1a)

The relative positions and motions of India, Australia and 'mainland' Eurasia are well-constrained. India separated from Africa and moved NNW, converging on Eurasia. Oceanic crust of the Indian plate was being subducted to the north beneath Eurasia. At the southeastern corner of Eurasia, the Meratus Terrane of Southeast Kalimantan (the Java Sea microcontinent) was subducted beneath Southeast Kalimantan. This accreted terrane comprises a melange of blueschists and ocean floor fragments known as the Meratus thrust belt.

2.1.2 Late Paleocene (55 Ma) (Fig. 2.1b)

India continued to converge on Eurasia, and Australia began to move to the NW. The Meratus Terrane, the Schwaner Block of Kalimantan and western Sulawesi were already in place. Sumatra and Java are also envisaged as forming by progressive accretion of material, including the products of volcanism, along a subducting plate margin. During this subduction phase there was compression and uplift, as demonstrated by geological maps of pre-Eocene subcrop in the Kangean and surrounding areas (Scott and Atkins 1991)

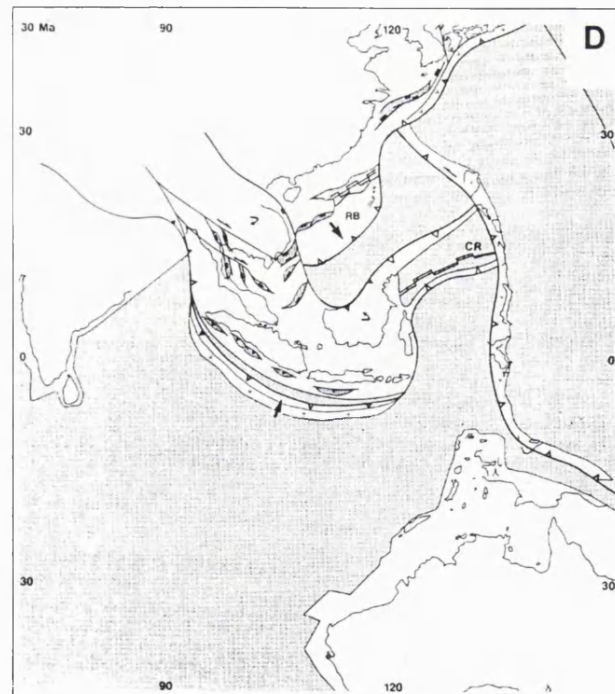
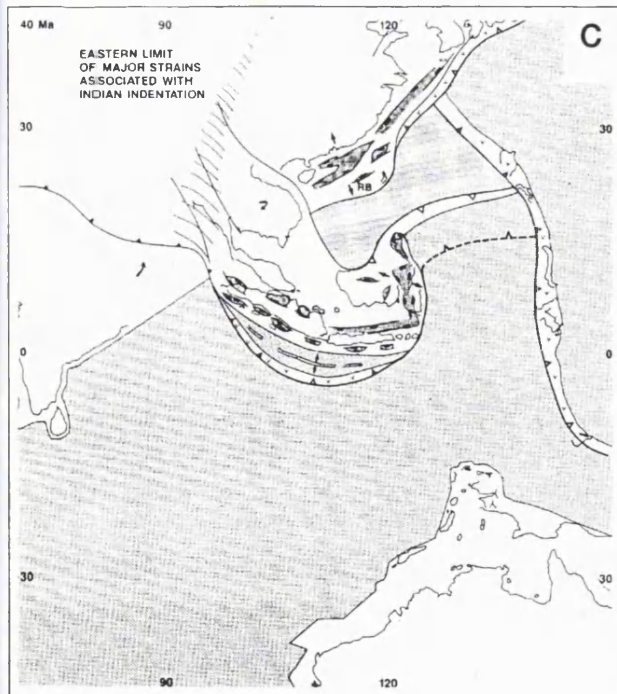
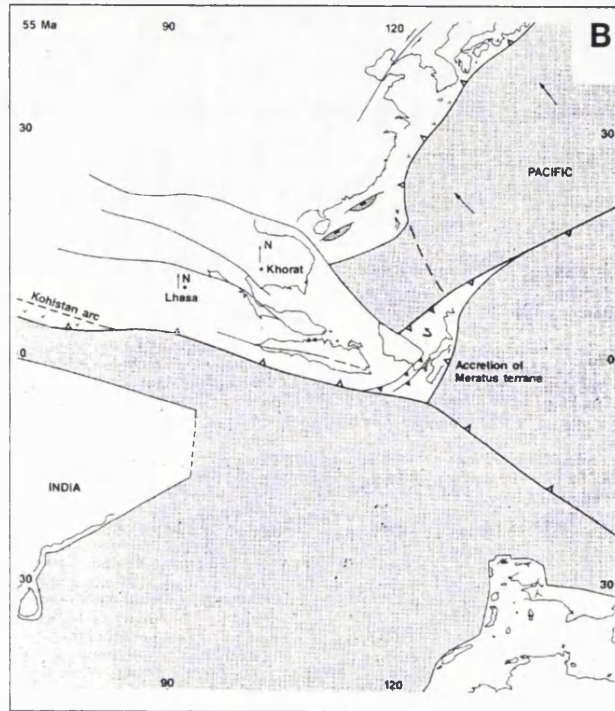
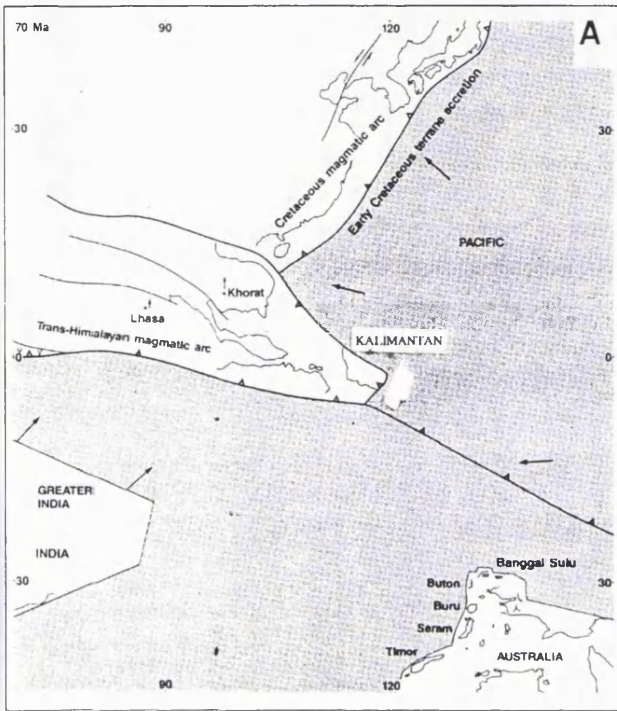


Figure 2.1a-d: Plate reconstruction in the Indonesian region in 70, 55, 40 and 30 Ma. (Daly et al. 1991).

2.1.3 Late Eocene (40 Ma) (Fig. 2.1c)

Continental India collided with the Eurasian margin and the rate of spreading between Australia and Antarctica increased. The Eocene collision between India and Eurasia also coincided temporally with the initiation of much of the basin evolution in Southeast Asia. A change in motion of the Pacific may have resulted in the generation of a number of micro-plates in the West Pacific by reactivation of transforms and fracture zones as subduction zones.

During the Eocene, and possibly as early as the Paleocene, the Tarakan, Kutei and Barito back-arc basins of Kalimantan were receiving sediments. Extension had also resulted in the formation of the deep basin of the Makassar Strait by Miocene time. The initiation of these basins has been interpreted as being related to reactivation of the earlier Meratus thrusts in SE Kalimantan. It is believed that subduction beneath the East Java Sea microcontinent ceased at this time and that subduction began to the south of Sumatra and Java. By the Early Eocene, most of the uplifted parts of the East Java Sea had been peneplaned (Scott and Atkins, 1991) and the products of erosion had been deposited in low areas around the East Java Sea. Some of these sediments are now exposed on Kangean, Bonerate and surrounding islands.

2.1.4 Oligocene (30 Ma) (Fig. 2.1d)

The back-arc basins of Sumatra and Java were placed under compressional stress that resulted in their inversion. In Sumatra and Java also a major contractional event is recorded in the present-day forearc region. This has been interpreted by Daly *et al.* (1991) as a result of reversal of the offshore arc and subsequent closure of the marginal basins with arc collision. The collided products may in part be preserved offshore Sumatra and Java today.

The Tarakan, Kutei and Barito back-arc basins were subsiding throughout this period, due to thermal relaxation.

2.1.5 Early Miocene (20 Ma) (Fig. 2.1e)

The collision of northern Australian with the Pacific and its buffer plates instigated the evolution of Eastern Indonesia as it is seen today. Probably the most important aspect of this collision was the commencement of the tectonic erosion of irregularities of the Australian passive margin by the oblique motion of the Philippine Sea Plate. This resulted in detachment of the Banggai-Sula and Buton microcontinental fragments (and perhaps others as well) in the form of tectonic flakes which were transferred from the Australian margin in New Guinea to the Philippine-Pacific Plate and were then transported westwards towards their present positions. Their westward motion caused the rotation of North Sulawesi and the choking of subduction in west Sulawesi.

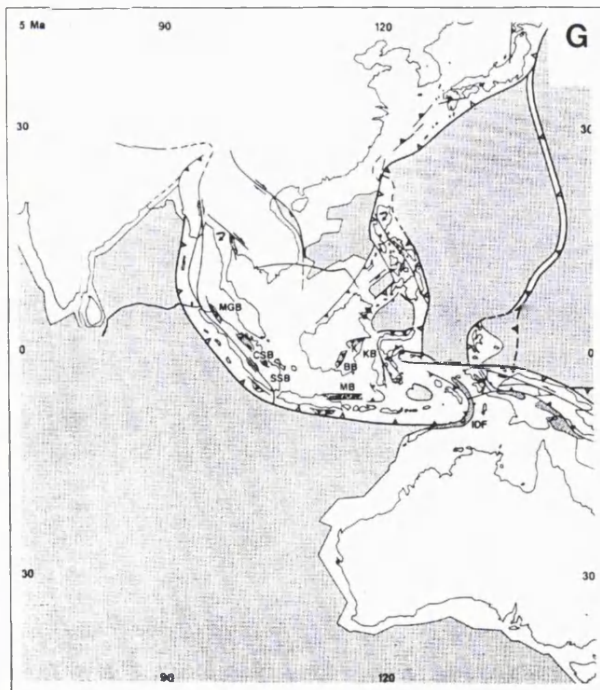
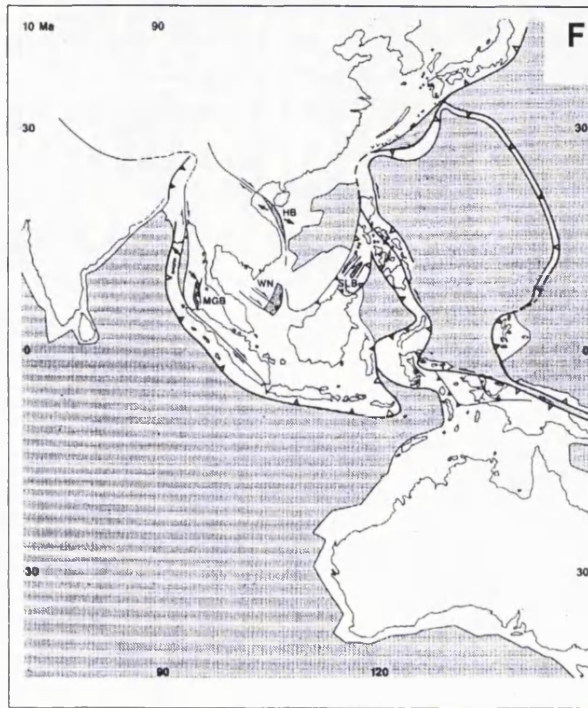
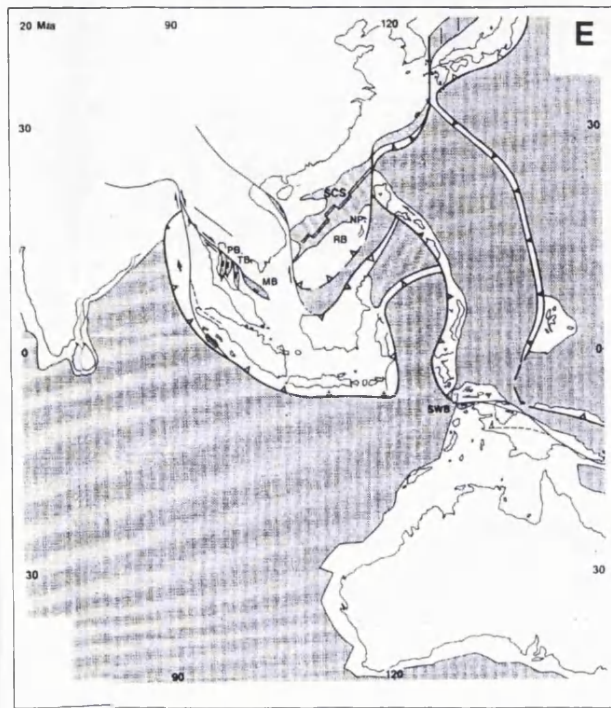
2.1.6 Middle Miocene (10 Ma) (Fig. 2.1f)

By the Middle Miocene, the Buton and Banggai-Sula fragments had collided with Eastern Sulawesi. The compressional regime that accompanied this collision must have been largely extinct by 15 Ma, as a large proportion of the thrust belt is overlain by undeformed Mid-Miocene sediments (Kundig 1956, quoted in Daly *et al.* 1991). However, following the thrusting, a phase of ENE trending sinistral strike-slip faulting occurred that cut the thrust belt and displaced Banggai-Sula to the NW.

In the reconstruction, East Sulawesi moves with the resolved velocity of the Pacific and Australian Plates. Halmahera at this time is envisaged as a part of the Philippine Sea Plate, possibly as an oceanic plateau. East Sulawesi continued its westward motion, subducting part of the trapped Indo-Australian oceanic crust as it went and North Sulawesi rotated clockwise in the process. The WNW-directed sinistral strike-slip motion between Buton and Banggai-Sula may have continued through to this time but appears to have ceased by the Pliocene.

2.1.7 Early Pliocene (5 Ma) (Fig. 2.1g)

An important tectonic event at about 5 Ma was the northward collision of the NW Australian passive margin with the Sunda trench and Banda forearc. The dynamic effects of the collision were to generate a SSW-directed thrust belt and fore deep basin on the Australian passive margin and NNW-directed thrusting to the north of Timor. The latter



LEGENDS

Fault systems			
	Extensional		Subduction zone
	Inverted extensional fault		Volcanic arc
	Strike-slip		Continental
	Compressional		Oceanic
	Basin outline		Convergence velocity mm/yr
	Anticline		
	Suture		

(BB) East Java Sea Basin; (HB) Hainan Basin; (KB) Kutei Basin; (MGB) Mergui Basin; (NP) North Palawan; (PB) Penyu Basin; (RB) Reed Bank; (SLB) Sulu Basin; (SSB) South Sumatran Basin; (SWB) Salawati Basin; (TB) Tarakan Basin; (WN) West Natuna Basin

Figure 2.1e-g: Plate reconstruction in the Indonesian region in 20, 10 and 30 Ma. (Daly et al. 1991).

is now represented by the Flores and Wetar thrusts. NNW-trending strike-slip shear zones developed north of the Banda Arc in South Sulawesi. This deformation cross-cuts the earlier thrusts and ENE-trending strike-slip faults and is expressed today as the Walanae and Palu Fault zones. These two anastomosing fault zones are associated with thrusts and extensional structures and control the locations of the centres of active volcanism in Sulawesi. The Walanae Fault is also responsible for the deformation of the Bone Basin and the Walanae depression of South Sulawesi (Daly *et al.* 1991).

The temporal and kinematic coincidence of NNW-directed displacement in Sulawesi and NW-directed inversion of the Kutei, Tarakan and Barito basins of east Kalimantan suggests that the inversion of the basins can be directly linked to the contractional tectonics of the Australian collision with the Banda Arc. The basins developed in response to rifting in the Makassar Strait during the Eocene and the Kutei Basin experienced a mild inversion during the Early Miocene. During the Early Pliocene, all three basins experienced major structural inversion by reactivation of the basin-forming extensional faults. The Early Pliocene age of the Kutei Basin inversion correlates temporally with the collision of Australia with the Banda forearc. This collision resulted in SE-SSE-directed thrusting of the arc onto the Australian foreland.

Contemporaneous back-thrusting generated the Flores and Wetar thrusts, and instigated NW-NNW strike-slip displacements in southern Sulawesi along the Walanae Fault system. A feature of this collision is that the associated contractional displacement dies out to the west, where the Australian margin is not yet in contact with the Sumatra-Java trench.

2.2 HYPOTHESES CONCERNING THE PLATE BOUNDARY IN THE EASTERN SUNDA SHELF

Various hypotheses have been put forward to explain the evolution and pre-Tertiary geometry of plate boundaries in the eastern Sunda Shelf. However, the mechanisms and reconstructions are still subjects of controversy. The common ground among many workers is that the formation and development of eastern Sunda Shelf subduction is a

result of the interactions of the three large plates since the Early Cretaceous. In the brief summary below, some of the different hypotheses are described.

Katili (1971, 1973) and Hamilton (1979) suggested that the Late Cretaceous and Early Tertiary volcanic arc passed from the southeast end of Sumatra across the Java Sea and through the Meratus Mountains of SE Kalimantan whilst the subduction zone lay seaward (southwards) from this trend (Fig. 2.2).

Audley-Charles (1976) made a reconstruction on the basis of the subduction zone and arc having been in its present position since at least the Late Cretaceous and probably since Permian or Triassic time, bringing the allochthonous rocks of Timor from a position south of the eastern half of Java. He suggested that this mass was removed from the front of Java by rifting or marginal basin extension at some time in Tertiary, probably during the Paleocene (Fig. 2.3).

Barber (1981) and Johnston (1981) suggested that the Lolotoi basement complex in Timor was part of the accretionary terrain at the SE Margin of Sundaland during the Cretaceous because of the similarity of the rocks to those in other terranes for which a similar origin has been suggested. However, the manner in which the Lolotoi could have reached its present position is a matter of controversy. Barber (1981) and Johnston (1981) proposed that the Lolotoi complex originally formed part of a microcontinental fragment rifted from the margin of the Australian craton in the Jurassic. This is supported by the similarities in sedimentary facies, structure and fauna, as noted by Audley-Charles (1968, quoted in Parkinson 1991). The fragment then supposedly migrated across the Tethys and entered and choked the subduction zone at the margin of Sundaland in the Early Cretaceous. Subsequent rifting and opening of the Banda Sea from Paleocene to Pliocene conveyed the Lolotoi fragment to collide with and overthrust the advancing Australian margin (Fig. 2.4).

Van Leeuwen (1981), in his investigation of the pre-Tertiary rocks in the Biru area of SW Sulawesi noted that these are very similar to those of Southeast Kalimantan. The similarity in the pre-Tertiary succession in SE Kalimantan and SW Sulawesi suggested

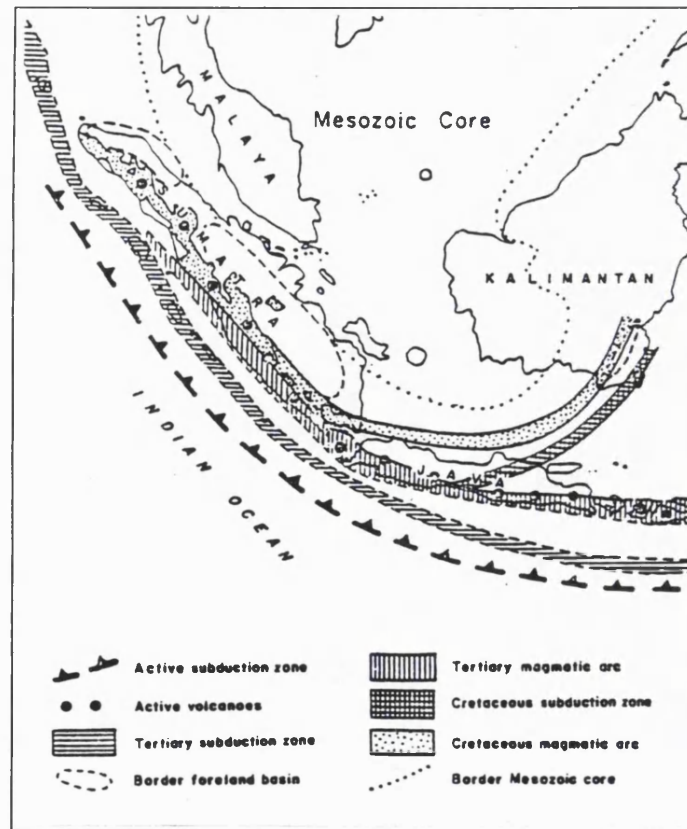


Fig. 2.2: Late Cretaceous reconstruction showing the Cretaceous magmatic arc and subduction zone passing from the southeast end of Sumatra across the Java Sea and through the Meratus Mountains of SE Kalimantan. (Katili 1971, 1972 and Hamilton 1972, 1979)

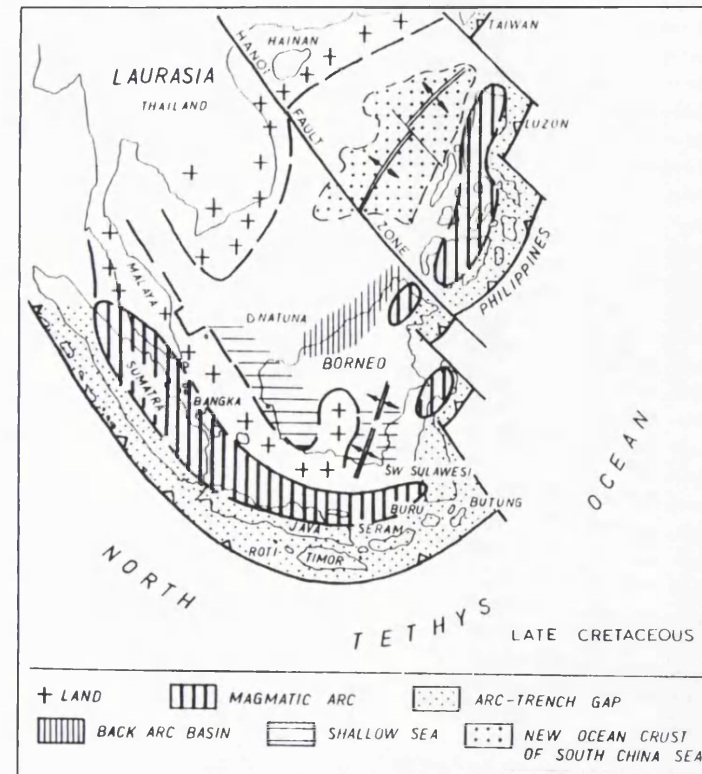


Fig. 2.3: Late Cretaceous reconstruction of Asian Indonesia showing the paleogeography of the Northern Tethys margin and the position of Timor south of East Java. (Audley-Charles 1976)

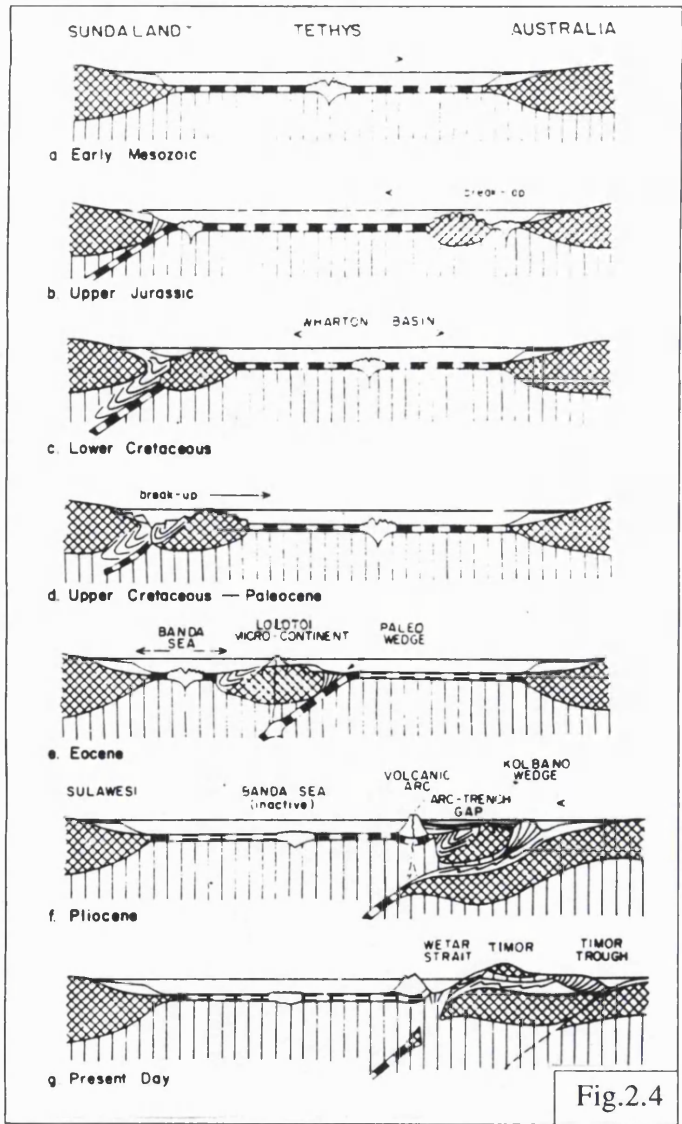


Fig.2.4

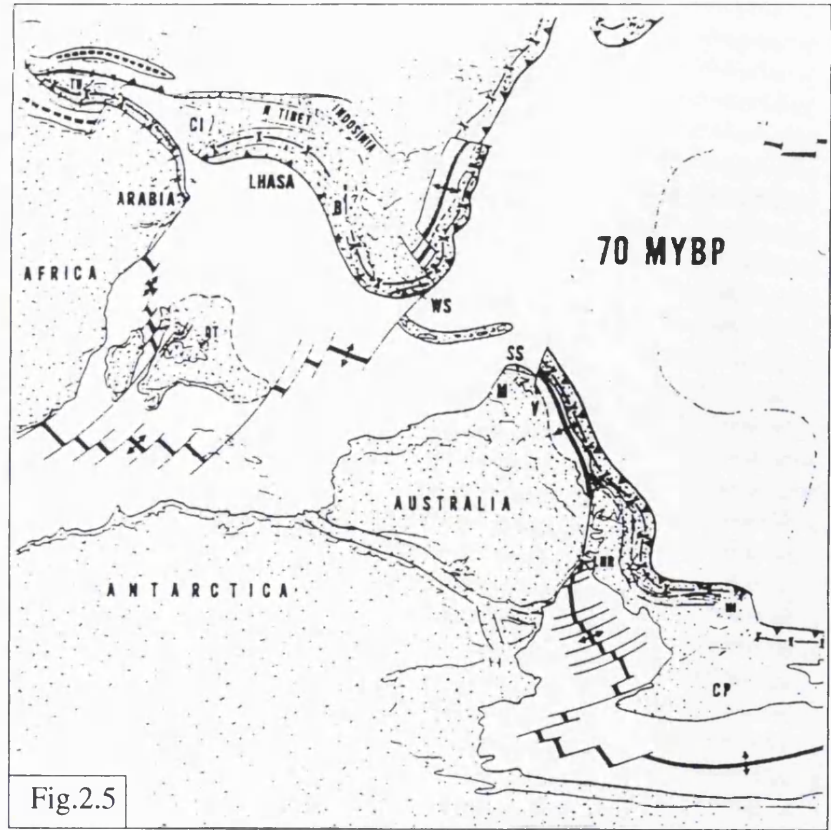


Fig.2.5

Fig.2.4: Cartoons showing evolution of the Australian continental margin, Sundaland, the Banda Sea and the island of Timor from the early Mesozoic to the present day (Barber 1981).

Fig. 2.5: Late Cretaceous reconstruction showing the position of the West Sulawesi (WS) microcontinent to the south of Borneo. The West Sulawesi (WS) microcontinent was interpreted to derive from the westernmost Banda Arc (Parker and Gealey 1983).

that these areas were joined together in the Mesozoic, as also proposed by Hamilton (1979).

Parker and Gealey (1983) suggested that in the Late Cretaceous West Sulawesi was situated southeast of Kalimantan and was an accreted microcontinental fragment from the westernmost Banda Arc. Their reason for postulating that the colliding fragment came from the Banda Arc was its proximity to Sumba and the fact that there appears to have been ample space to fit it onto the pre-rift margin of Australia (Fig. 2.5).

Sikumbang (1990) proposed that in the Early Cretaceous, Tethys oceanic crust was present at the SE margin of Sundaland during the deposition of the Late Barremian-Early Aptian Batununggal Formation. In the Late Cretaceous this oceanic crust was subducted beneath the SE margin of the Sundaland with the development of the Alino Island Arc (AIA) between the SE margin of Sundaland and the subduction zone (Fig. 2.6). Granitic rocks dated at 95.3 Ma intruded the Alino Group as a result of this subduction. In the early Late Cretaceous the western margin of the AIA collided with the SE margin of the Sundaland, leading to thrusting and ophiolite obduction onto the leading edge of Sundaland (Meratus ophiolite complex). Other tectonic events during or shortly after the collision included the formation of the Rimuh Plutonic Complex, strike slip faulting, and the formation of the pull-apart basins such as the Manunggul Basin. Later, the transcurrent movement changed its direction, due to oblique convergence, and slices of ophiolite and of the Lower Cretaceous Paniungan and Batununggal formations formed a sequence of imbricate structures and tectonic slices which were incorporated into the accretionary prism. Sikumbang (1990) also suggested that the final phase of magmatic activity in the Meratus Mountains was marked by igneous intrusion together with volcanic extrusion and explosions. These events suggest renewed subduction in the southeast during the Early Paleocene.

Shortly after the cessation of magmatic activity, probably in the Late Paleocene or Early Eocene, southeast Kalimantan was rifted and fragments moved east and southeastward. Fragments showing a strong affinity to the Meratus Mountains are now found in Sulawesi and in Timor and Sumbawa islands. The Makassar Strait is suggested to be a

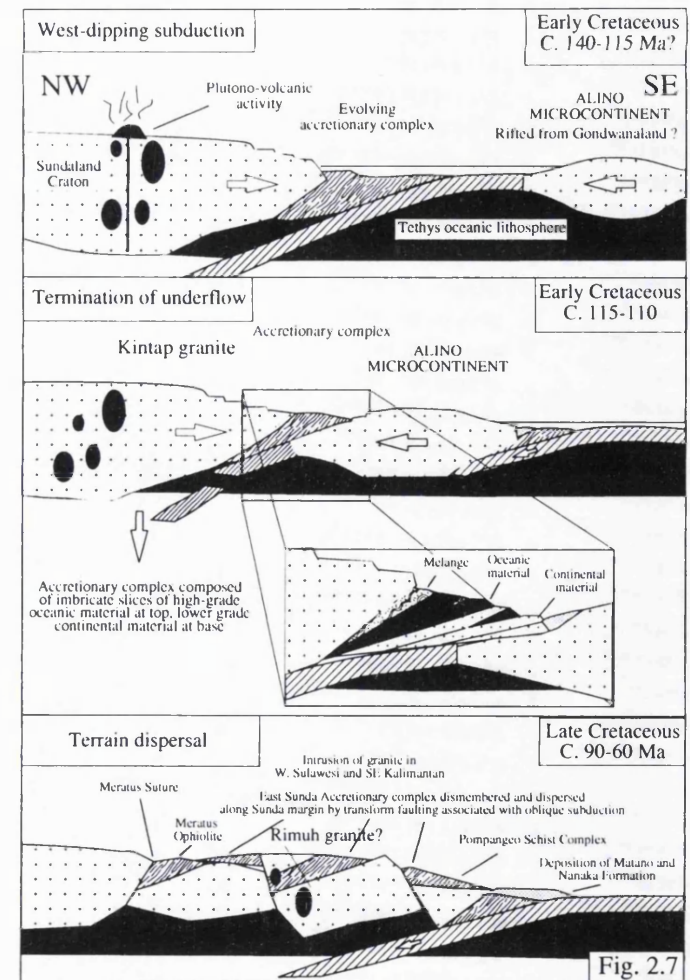
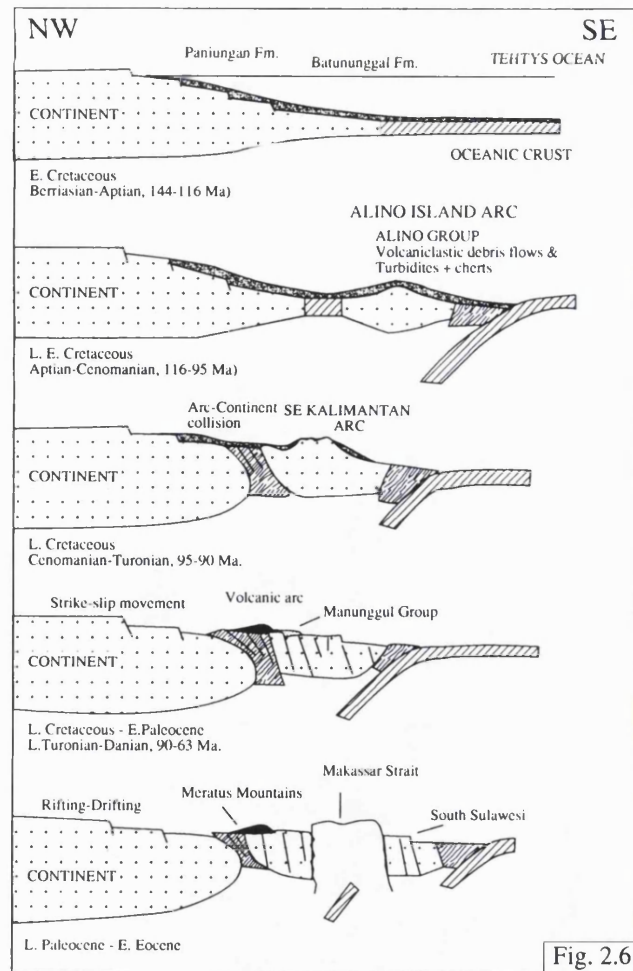


Fig.2.6 and 2.7: Cartoons of the tectonic evolution of SE Kalimantan and SW Sulawesi showing the main theories of the origin of present SW Sulawesi block. In Fig.2.6 (After Sikumbang 1990), the SW Sulawesi block is derived from oceanic crust subducted at the Alino Island Arc. In Fig. 2.7 (After Parkinson 1991) the block is derived from a microcontinental fragment rifted from Gondwanaland.

result of this rifting, as are basins in east Kalimantan (Barito, Asem-Asem and Kutei basins).

Parkinson (1991) discussed metamorphic processes in Central Sulawesi and suggested that metamorphic crystalline basement exposed in Central Sulawesi, the Southwest Arm of Sulawesi, the Meratus Mountains of Kalimantan, Central Java, and possibly the Lolotoi Complex of Timor are dismembered fragments of a single, extensive Early Cretaceous accretionary complex (Fig. 2.7). He showed that the parent rocks of the Pompangeo Schist Complex of Central Sulawesi were predominantly terrigenous clastics, which Barber (1981) interpreted as indicating that they had been derived from part of a microcontinental fragment. Bowin *et al.* (1980) speculated that the Pompangeo Schist might have been derived from continental crust that had been subducted, and is an example of what might be seen if Timor were to be uplifted sufficiently. The question of whether the parental rocks of the "Central Indonesian Accretionary Complex", which occupied the area between the Late Cretaceous subduction system passing from Java, Java Sea and Southeast Kalimantan and the Early Tertiary subduction system passing from Central Sulawesi to Timor(?), originated from the continental basement of Sundaland or the Australian craton in the Early Mesozoic or even Palaeozoic, is a critical one.

Of all hypotheses described above, the most plausible seems to be that presented by Parkinson (1991). However, some modification is needed in the light of other models, especially that of Sikumbang (1990). Differences between the two workers relate especially to the evolution of Southeast Kalimantan. In Parkinson's model, active subduction had already begun when the Alino microcontinent collided with the Sundaland platform (see Fig. 2.7) while in Sikumbang's model the Alino microcontinent was an island arc and the collision of that island arc with Sundaland began at the passive margin of the Sundaland platform (see Fig.2.6).

It seems more plausible to envisage, from the position of the Kintap Granite in southeast Kalimantan, i.e. to the north of the Cretaceous subduction complex, and also from its Cretaceous age, that subduction of the Alino microcontinent beneath SE Sundaland

produced this pluton. This subduction phase was followed by block faulting and the passive margin to the west of the Alino microcontinent was subducted westwards with the formation of the Rimuh Pluton. The rifting and dispersal of the Alino microcontinent occurred in the Paleocene-Eocene with the opening of the Makassar Strait.

CHAPTER THREE

GEOLOGY AND GEOPHYSICS OF THE CENTRAL INDONESIAN REGION

3.1 GEOLOGICAL REVIEW

3.1.1 Geological subdivisions

Geographically the Indonesian archipelago is often divided into eastern and western parts, the boundary between them being placed in the Makassar Strait and passing from there south through the Lombok Strait. Wallace's line, defined in 1863 and 1910, divided the Indonesian region into two on the basis of differences of flora and fauna (Figure 3.1). Audley-Charles (1975) suggested the Sumba Fracture (to the south of central Flores Island) as a major discontinuity between Eastern and Western Indonesia. Nishimura *et al.* (1981) proposed that a major tectonic discontinuity separates Eastern Indonesia from Western Indonesia between Sumbawa and Flores, this view being based on investigations of the differences in geophysical, geochemical and submarine morphological features. The regional Bouguer gravity anomaly patterns change considerably in the area between Sumbawa and Flores (Chamalaun *et al.* 1976). East of Flores Island, there are east-west gravity anomalies along the outer Banda Arc with high positive values in the north. West of Sumbawa Island there are also east-west gravity anomalies associated with the Java Trench system, but in the field decreases from high positive values to the south to low or negative values to the north. Between these two regions of opposite gradient is a region in which contour lines trend north-south. In geochemical studies, there are differences in the chemical characters of the Quaternary volcanic rocks of Lombok, Sumbawa and Bali on the one side and Flores on the other side.

In the present thesis a new subdivision is proposed, introducing a Central Indonesian Region which represents a transition between the largely Eurasian elements of Western Indonesia and the Pacific and Australian related elements of Eastern Indonesia (Fig.3.2). The boundary between the Western and Central Indonesian regions is thought to mark the location of a pre-Tertiary subduction zone at the southeastern Eurasian margin, whilst the boundary between the Central and Eastern Indonesian regions is at the

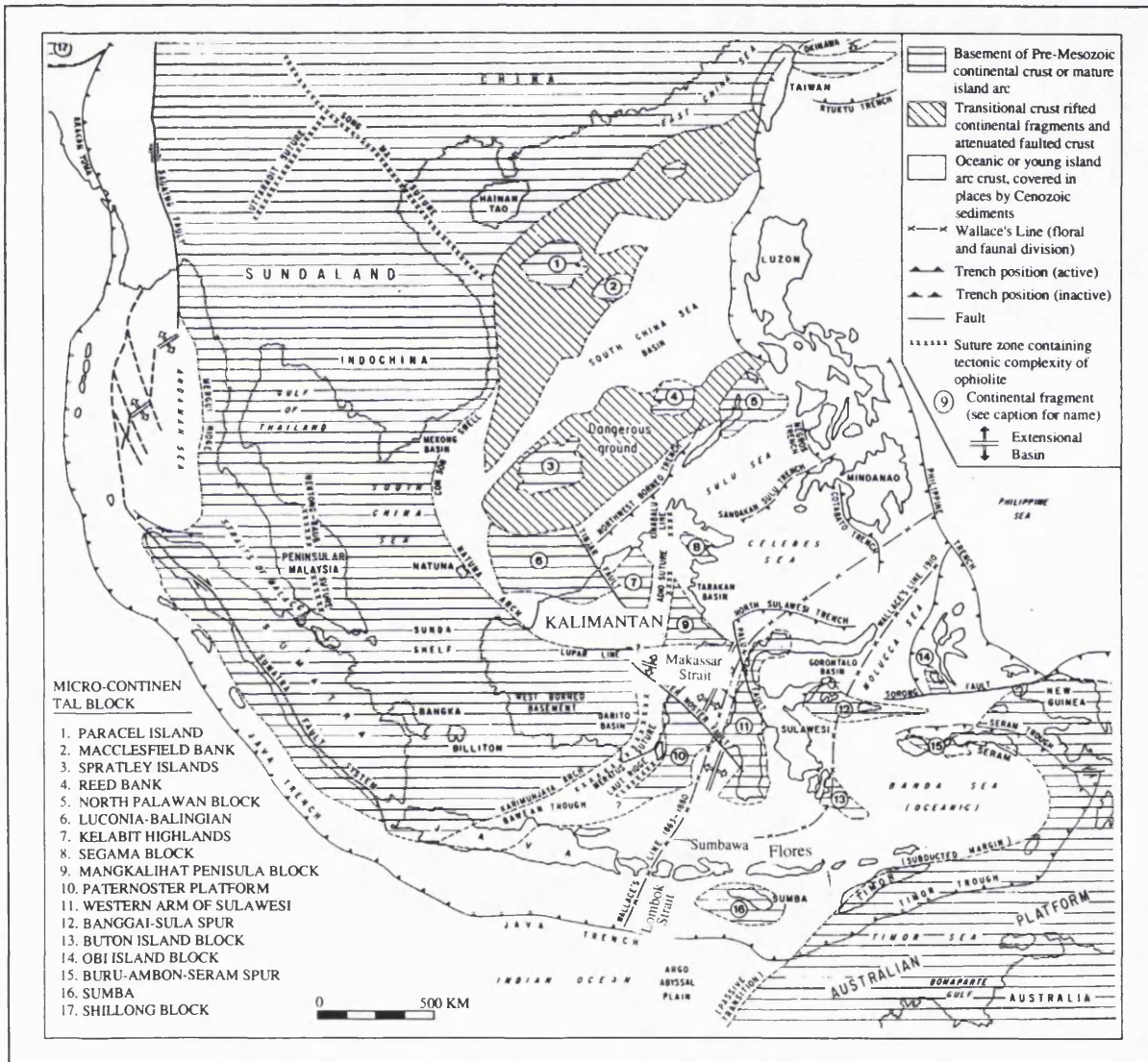


Figure 3.1: Location of the Indonesian region in relation to the Sundaland and Australian Platform (Hamilton 1979)

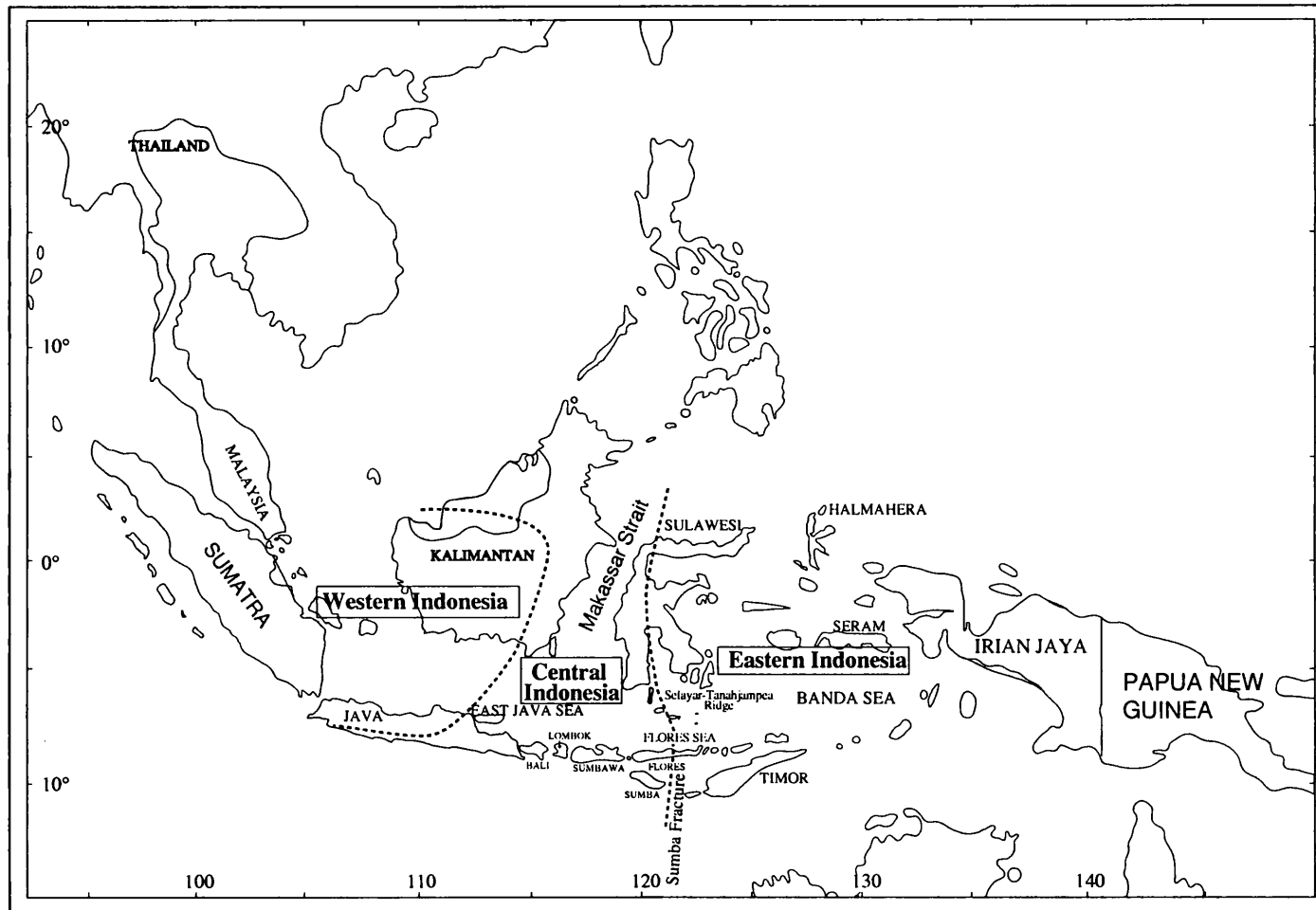


Figure 3.2: Proposed division Western, Central and Eastern Indonesia

location of a Palaeogene subduction complex accreted to this margin. The latter is marked by the Selayar-Tanahjampea ridge which separates the Flores Sea from the Banda Sea, the two areas being apparently different in their tectonic development.

The tectonic development of Western Indonesia has been largely controlled by the development of the Indian Ocean following the break up of the Gondwana supercontinent and the consequent northward drift of the Indian continental mass (PT. Trias 1989). The heart of the region is formed by the Sundaland craton which is thought to have been a stable area since the Late Mesozoic.

The present Central Indonesian region is situated in a back-arc tectonic setting. However, from the Cretaceous to the Eocene this area was the site of complex subduction, fore arcs and magmatic arcs. Central Indonesia now also represents the transition from a largely continental province to the more oceanic Eastern Indonesia Region. Its tectonic development has been determined by eastward accretion at Cretaceous and Palaeogene subduction zones and subsequently by the opening of the Makassar Strait. Most recently the structures have been modified as a result of the propagating collision of the Australian continent with the Banda Arc.

3.1.2 Pre-Tertiary Subduction in the Central Indonesian Region

The geometry of pre-Tertiary subduction in the Indonesian region is still controversial and various hypotheses have been put forward, as outlined in Chapter 2. It is generally accepted that the main indication of a former subduction zone is melange. Therefore the distribution of melanges in different regions having the same age and characteristics can be used as a sign that they originated in the same subduction zone. Using this assumption, combined with regional study, the geometry of pre-Tertiary subduction will be summarised in Chapter 11.

3.1.2.1 Definition of melange

Melanges are defined as mappable bodies of deformed rocks characterized by the inclusion of tectonically mixed fragments or blocks in a pervasively sheared, fine-grained, and commonly pelitic matrix (Hsu 1968). Blocks within the melange matrix are

fault-bounded, and the matrix itself consists of grains deformed by shearing and ductile flow (Hsu 1968; Hamilton 1979). Tectonic melanges are commonly thought to form in accretionary wedges at convergent margins. During subduction, fold and thrust packets are accreted at the toe of the wedge and are further deformed as accretion continues (Karig and Sharman 1975; Hamilton 1979).

3.1.2.2 Pre-Tertiary rocks in Java

The three areas in Java where pre-Tertiary rocks are exposed are Karangsambung, Ciletuh, and Bayat (Hamilton 1979) (Fig. 3.3). However, several wells which have penetrated basement rocks in northwest Java have also encountered complexes of igneous and metamorphic rocks (Tyrrel *et al.* 1986).

3.1.2.2.1 Karangsambung

In central Java melange is exposed beneath a folded cover of shallow-water and continental sediments, poorly dated to within the Eocene. According to Hamilton (1979) the melange includes widely varied intersliced rock types: greenschist, possibly glaucophane schist, amphibolite, eclogite, serpentinite, peridotite, gabbro, pillow basalt, red radiolarian chert and red pelagic limestone, scaly clay with sheared lenses of more resistant graywacke and siltstone, extremely sheared slate with resistant lenses, pebbly mudstone, quartz - pebble conglomerate, abundant crushed quartz porphyry, and others. Early Cretaceous foraminifera occur in limestones in the complex, and muscovite schist has yielded a potassium-argon age of 117 Ma. Sheared quartz porphyry has a fission-track age of 65 Ma (Ketner *et al.* 1976). Asikin (1974) found Paleocene nannofossils in sheared shale of the melange.

3.1.2.2.2 Bayat

Melange in the eastern part of Central Java, in the Jiwo Hills, consists mainly of varied greenschist, amphibolite, phyllite, slate, quartzite, limestone, radiolarian limestone, radiolarian chert, and serpentinite, all contorted and highly sheared (Hamilton 1979). The overlying strata are middle and upper Eocene marls and limestone.

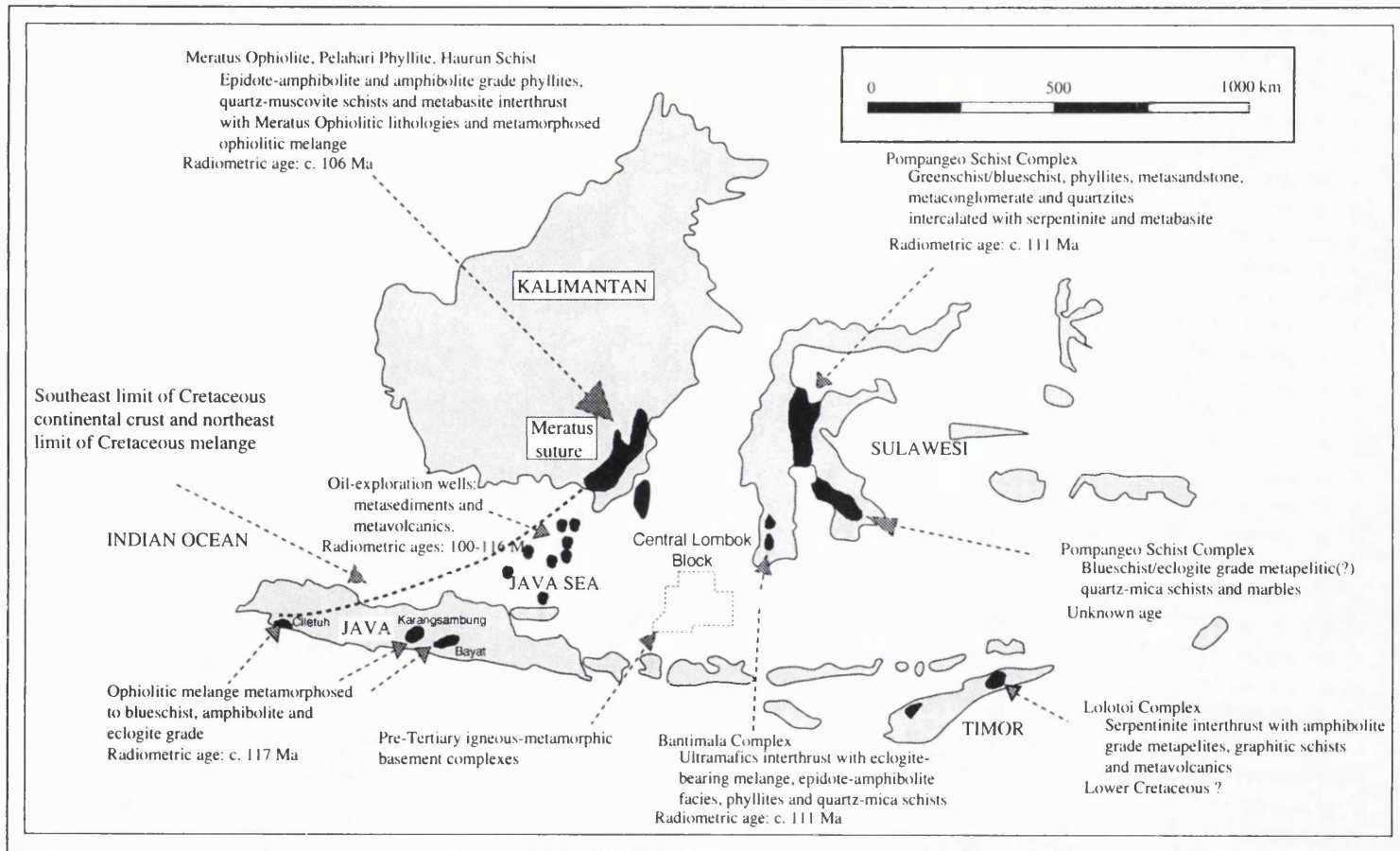


Figure 3.3: The distribution of the pre-Tertiary basement complexes in the Indonesian region
(Compiled from Hamilton 1979, Tyrrel et al. 1986 and Parkinson 1991)

3.1.2.2.3 Ciletuh

Melange probably occurs also in the southwest corner of Java, where there are outcrops of peridotite, gabbro, and albite-epidote amphibolite derived from basement complexes, and basalt outcrop, all variably altered and sheared (Thayib *et al.* 1977). Deformed upper Eocene and younger clastic rocks overlie these crystalline rocks.

3.1.2.3 East Java Sea basement complex

Magnetic anomalies in the southeast part of the Java Sea trend southwestward or west-southwestward, indicating that the general basement strike shown by the melange of Cretaceous or very Early Tertiary age in the Meratus Mountains of Kalimantan prevails over a large region to the south (Hamilton 1979). Basement rocks beneath Eocene, Oligocene or Miocene strata have been reached by many oil-exploration wells in the Java Sea (see Fig. 3.3), especially in its southern half (Ketners *et al.* 1976). The basement rocks in the north of western Java are mainly low-grade metasediments (slate, phyllite, quartzite and marble) but middle grade metasediments are also present. Large and small masses of granitic rocks (quartz monzonite more abundant than granodiorites, with gneiss, quartz diorite, and diorite all occurring locally) are widespread, as are mafic to silicic volcanic rocks. North of eastern Java, slaty metasediments, some of them extremely sheared, are dominant and are of either terrigenous or volcanoclastic origin, derived from basic to silicic volcanic rocks. Granitic rocks are also present in the northwest. Many K-Ar age determinations have been made on granitic, volcanic, and metasedimentary rock samples from wells and these mostly indicate Paleocene and Cretaceous ages of 58 - 115 Ma (Hamilton 1979; Katili 1991). Unmetamorphosed Late-Early Cretaceous limestones and clastic sediments unconformably underlie Eocene strata in one sector north of western Java.

Some geological data were obtained in the area of the Central Lombok Exploration Block by drilling during the 1970's (see Fig. 3.3). Of the four exploratory wells drilled in this area by Amoseas, three penetrated the pre-Tertiary igneous-metamorphic basement complex (Tyrell *et al.* 1986). Cities Service also drilled a series of Java Sea wells, five of which were located to the east of Kangean island, near the western boundary of the Central Lombok Block. For most part, these wells penetrated a Cretaceous basement

complex. These additional data provide more information on the limit of the continental shelf in the Cretaceous (see Chapter 2).

3.1.2.4 Pre-Tertiary rocks in Southwest Sulawesi and Central Sulawesi

In southwest Sulawesi, basement rocks of pre-Late Cretaceous age are exposed at two localities along the western flank of the Western Divide Mountains, at Bantimala and in the Barru area (van Leeuwen 1981), as well as in Central Sulawesi (See Fig.3.3). The so-called "Bantimala Tectonic Complex" in Southwest Sulawesi and "Pompangeo Schist Complex" in Central Sulawesi comprise metamorphic and ultrabasic rocks and a tectonic melange of radiolarian chert, shale, conglomerate, greywacke, clay, sandstone, basalt, diorite, granite, schist and serpentinite. The main structural features of this complex, such as foliations, faults and thrust planes, have northeasterly dip and suggest overthrusting in a westerly direction (Sukamto 1975; Sukamto and Simandjuntak 1983). Near Barru the basement is composed of schist, gneiss, radiolarian chert, silicified shale and ultrabasic rocks (van Leeuwen 1981).

The metamorphics are the oldest basement rocks. They comprise glaucophane schist, garnet schist, chlorite schist, amphibolite, muscovite + actinolite + tremolite schists, graphite schist, garnet gneiss, albite-orthoclase gneiss, quartz-feldspar gneiss and marble. The metamorphic grade increases westwards, from greenschist through blueschist to amphibolite facies (Parkinson 1991). Eclogite has been observed as large blocks. van Leeuwen (1981) suggested that the latest metamorphic event affecting these rocks took place at the end of the Early Cretaceous, based on a K-Ar date of 111 Ma on muscovite reported by Sukamto (1975).

3.1.2.5 Pre-Tertiary rocks in Southeast Kalimantan

Late Cretaceous-Early Palaeogene melange, characterized by highly deformed and disrupted ophiolitic, metamorphic and sedimentary rocks, occurs in several areas in southeastern Kalimantan (Sikumbang 1990)(see Fig. 3.3). These melanges are overlain by Eocene strata (Hamilton 1979), as in Java. The largest area of exposed melange is in the Meratus Mountains. This terrane consists of widely varied materials including polymict breccia, glaucophane schist, greenschist, peridotite, serpentinite, deep-ocean

radiolarian sediments, and clastic and carbonate sediments bearing pelagic Middle Cretaceous foraminifera, all chaotically intercalated at all scales from single outcrop to regional in a steeply dipping complex (Hamilton 1979). Farther east, on Laut Island at the southeast corner of Kalimantan, the presence of peridotite, serpentinite, gabbro, and basalt beneath Palaeogene strata suggests that melange is present there also (Hamilton 1979).

3.1.2.6 Summary

The data available from several authors who have studied the basement complexes in these areas (Asikin 1974; Katili 1978; Hamilton 1979; van Leeuwen 1981; Parkinson 1991) shows that the lithologies, metamorphic grades and deformational styles are strikingly similar. This is thought to indicate that during Late Cretaceous and Early Tertiary times an active subduction zone bounded Java, the Java Sea and SE Kalimantan. However, the limit and extent of this subduction boundary have still not been defined.

The Late Cretaceous and Paleocene K-Ar dates from the Java Sea basement suggest that the silicic magmatism records the same subduction system as does the melange of Late Cretaceous or very early Tertiary age farther east (Hamilton 1979). The low grade metamorphic rocks of SW Sulawesi can be correlated with metamorphic rocks in SE Kalimantan, Java and the Java Sea and are interpreted as fragments of a dismembered accretionary complex generated at the eastern margin of Sundaland in the Late Cretaceous (Parkinson 1991). The absence of Paleocene to Lower Eocene sedimentary rocks in those fragments reflects uplift during those periods, which was followed by rifting, regional subsidence and deposition of an Upper Eocene - Miocene transgressive sequence (Sikumbang 1990).

3.1.3 Volcanism in the Central Indonesian Region

Igneous activity in the Indonesian Archipelago occurred throughout its history, and the periods of activity probably were associated with major tectonic events (van Bemmelen 1949). Some of the most conspicuous magmatic features are the granitic belts which in some areas are very long and continuous and clearly mark the position of old tectonic belts. Such granitic belts have normally been associated with subduction-related

volcanism. The distribution of pre-Tertiary and Tertiary magmatism zones in the Indonesian region is shown in Fig 3.4 (Katili 1973).

3.1.3.1 Volcanism in the Java Sea and Southeast Kalimantan

Bathymetric maps show that the dominant ridge in the Java Sea is the Karimunjawa arc which strikes NE-SW and links the Meratus Mountains in the north to Central Java in the south. Ben-Avraham and Emery (1973) suggested that this NE-SW trending ridge was probably part of a remnant arc system.

There are four major volcanic formations in the Meratus Mountains of SE Kalimantan which can be correlated to the volcanic rocks in the Java Sea, each representing a different tectonic setting. These are the Alino Group, the Pitanak Formation, Benuariam Formation and Kayujohara Formation.

The Alino group is associated with the Kintap Granite and is divided into the Pudak and Keramaian formations (Sikumbang 1986). The Pudak Formation consists mainly of coarse volcanoclastic deposits with limestone blocks whilst the Keramaian Formation consists of volcanoclastic sandstone and mudstone and chert with or without radiolarian skeletons. The age of this group was based on K-Ar dating of the Kintap Granite at 95.5 Ma (Albian-Cenomanian or Early Cretaceous, Sikumbang 1986).

The Pitanak Formation is associated with the Rimuh Granite and consists of gabbro, diorite, granodiorite and granite. The age of this formation is considered to be Early Turonian, i.e. Late Cretaceous (Sikumbang 1986).

The Benuariam Formation, which is part of Manunggul Group, consists of very coarse pebbly volcanic breccia with interbeds of agglomeratic lapillistone and tuff, lava flows and associated volcanic breccias. The age of this formation is considered to be Santonian, i.e. Late Cretaceous (Sikumbang 1986).

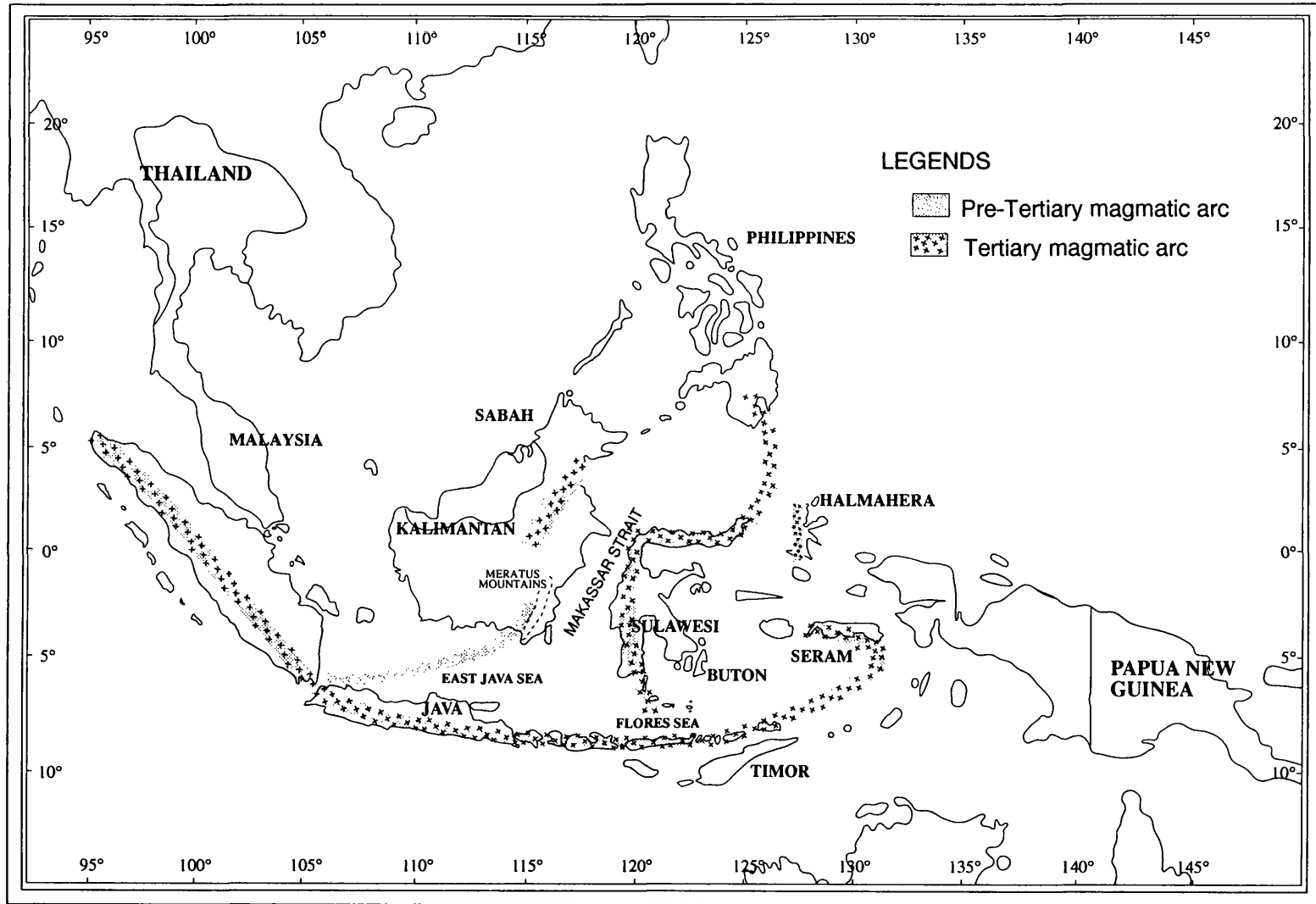


Figure 3.4: The distribution of pre-Tertiary and Tertiary magmatic arcs in the Indonesian region
(Modified from Hamilton 1979 and Katili 1991)

The Kayujohara Formation consists of massive lava flows together with intercalations of volcanic breccia. The age of this formation is thought to be Maastrichtian-Danian or Paleocene (Sikumbang 1986).

3.1.3.2 Volcanism in SW Sulawesi

Sulawesi consists of two main tectonic units, the Eastern Arc or Province, which is characterized by thrust tectonics associated with the emplacement of an ophiolite-metamorphic suite, and the Western Arc (Western Province) which displays folding in a sequence of Mesozoic to Tertiary metamorphics, sediments and volcanics intruded by plutonic rocks of acid and intermediate composition (van Leeuwen 1981). Southwest Sulawesi is located at the southern end of the Western Province. In general, the rocks present are predominantly of Cenozoic age, with minor outcrops of pre-Tertiary sediments and metamorphics.

3.1.3.2.1 Palaeogene volcanism in the SW Sulawesi

Hoehn and Ziegler (1917, quoted in van Leeuwen 1981) were the first to prove the existence of Early Tertiary volcanism in Sulawesi. They observed tuff bands below and within coal measures, and tuffaceous material in the overlying (Eocene) limestone. However, van Leeuwen (1981) has shown that this volcanism was much more intense and widespread than was first thought. In the Biru area, the Langi Volcanics, a thick series of propylitised andesitic rocks of Paleocene to Late Eocene age, can be traced south to near Banterihu, where they contain intercalations of Eocene limestone. A thick sequence of fractured and propylitised andesitic rocks similar to the Langi volcanics was observed by van Leeuwen (1981) in the Bone Mountains, east of Caming village.

At Bantimala a series of andesitic and basaltic rocks underlies the coal measures. A whole rock K-Ar analysis of a pillow lava yielded an age of 58.5 Ma (Sukanto 1975). A similar age (63 ± 2.2 Ma) was obtained for a tuff sample from Biru. These two dates suggest that the volcanism had begun by the Early Paleocene (van Leeuwen 1981). Palaeogene volcanics are known to continue from Southwest Sulawesi into the Java Sea (Hamilton 1979; Hutchison 1981; Katili 1991).

3.1.3.2 Neogene Volcanism in the SW Sulawesi

During the Neogene, large volumes of volcanic rocks were deposited in SW Sulawesi. An interesting feature of this Neogene volcanism is that besides andesites, basalts and some dacites, significant quantities of alkaline rocks were also produced. Van Leeuwen 1981 suggested that the Early Miocene through Pliocene rocks of the South and North Arms of Sulawesi are dominantly granitic magmatic rocks and calc-alkaline and alkalic volcanic and volcanoclastic rocks. The magmatic rocks form a belt 50-200 km wide, coextensive with the western arc of Sulawesi.

Calc-alkaline volcanism began during the main Middle Miocene orogenic event and continued afterwards (Sopo Volcanics). The Pamesurang Volcanics, which succeeded this volcanism, constitute a distinct alkaline phase which lasted till the end of the Middle Miocene. In the Late Miocene the andesitic Walanae Volcanics were deposited in a shallow marine environment. Towards the end of the Miocene, alkaline basaltic rocks were erupted, followed by the andesitic Lemo volcanics

3.1.3.3 Summary

The presence of pre-Tertiary and Tertiary volcanism in the Central Indonesian region points to the establishment of west-verging subduction to the east of these volcanics. The chronology of volcanism in terms of subduction was suggested on the basis of the information presented above.

The Early Cretaceous Alino Group, which is associated with the Kintap Granite, is considered to record the earliest volcanism in the Central Indonesian region and continues into the Karimunjawa and Bawean arcs where structural trends are similar. These arcs indicate the presence of a subduction zone to the east. The rocks of the Late Cretaceous Pitanak Formation, associated with the Rimuh Granite, were formed during or shortly after collision (Sikumbang 1986;1990). This leads to the conclusion that there was new subduction east of SW Sulawesi microcontinent after the collision. The volcanic products might be correlated with the Old Volcanic Breccia in the Java Sea and on Java.

The Paleocene Kayujohara Formation, associated with volcanic extrusions and explosions, has been considered to mark the final phase of magmatic activity in the Meratus Mountains (Sikumbang 1986;1990), which was followed by rifting and opening of the Makassar Strait. The Palaeogene volcanics in SW Sulawesi may be part of the Kayujohara Formation, formed before the opening of Makassar Strait.

The presence of Neogene volcanism in SW Sulawesi is considered to be the result of subduction which occurred after the collision of the eastern Sulawesi ophiolite with SW Sulawesi. Subduction in these areas was accompanied by intensive volcanism, the products of which are now exposed throughout Western Sulawesi and may continue through Selayar to the Bonerate islands. This interpretation is supported by the presence of volcanic rocks on Selayar (Sukanto and Supriatna 1982) and granitic rocks on Tanahjampea (Hetzl 1930). The probable Neogene granitic rocks on Tanahjampea, the largest of the Flores Sea Islands, are intruded in some places by Neogene basaltic-andesitic rocks. This phenomena can be also seen in the Biru area, south of Ujung Pandang, SW Sulawesi, whilst geophysical and bathymetric maps indicate that there is continuity from southwest Sulawesi to the Selayar-Bonerate islands. These observations suggest that Selayar and the Bonerate islands are part of a Neogene volcanic arc which stretched from the Philippines to a termination in the northern part of the Flores Sea Basin.

3.2 GEOPHYSICAL REVIEW OF THE CENTRAL INDONESIAN REGION

The purpose of this section is to review the available geophysical data, including published geophysical data, in order to obtain a rough idea about the relationship of deep crustal structure, as constrained by regional gravity and seismic variations, to shallow structures and lithologies as constrained by radiosonobuoy data and surface geological variations. The gravity signature apparently has sources in at least two distinct and independent realms: a deep crust/upper mantle transition, which involves a more or less uniform density contrast throughout the area, and upper crustal density contrasts, which vary greatly. Seismic reflection data provide the information necessary to understand the relationship between these realms.

3.2.1 Bathymetry

The bathymetric map in the Central Indonesian Region can be separated into two parts, with a boundary situated at the 200 m bathymetric contour, extending from the Makassar Strait in the north to the Lombok Strait in the south. To the west the water depths are less than 200 m whereas to the east water depths of as much as 5000 m occur. In this latter area the bathymetry has a segmented character which suggests structural control (Fig. 3.5). A number of features, such as the Doang Margin, Flores Depression, Selayar-Bonerate High, Selayar Deep, Selayar High and Bone Depression, may be distinguished from trends in the bathymetry and topography.

The Doang Margin is a name applied to the area to the southwest of Sulawesi where trends have a NE-SW orientation. It is the area with the shallowest water depth in the East Java Sea, ranging from 200-800 m (other areas are generally 2000-4000 m deep). The Doang margin has subsided since the Late Miocene and is associated with southward progradation of the Miocene carbonate shelf (Prasetyo 1992).

The Flores Depression, the most significant feature in the East Java Sea, is an E-W elongated depression where water depths are in excess of 5000 m. To the northwest it is bounded by the Doang Margin, to the north by the Selayar-Bonerate High and to the south by Flores Island.

The Selayar-Bonerate high is capped by a succession of islands separated by saddles which extend in an arc southwest from south Sulawesi. The geological surveys described in this thesis showed that these islands are mostly built up by volcanic rocks. They are interpreted as the back-arc belt of the Cretaceous-Early Tertiary subduction zone.

The Selayar Deep and the Bone Depression are separated by the Selayar high. The water depths in these depressions reaches about 3000 m. The Selayar Deep is cut by several NE-SW lineaments, and terminates to the north of Kalao.

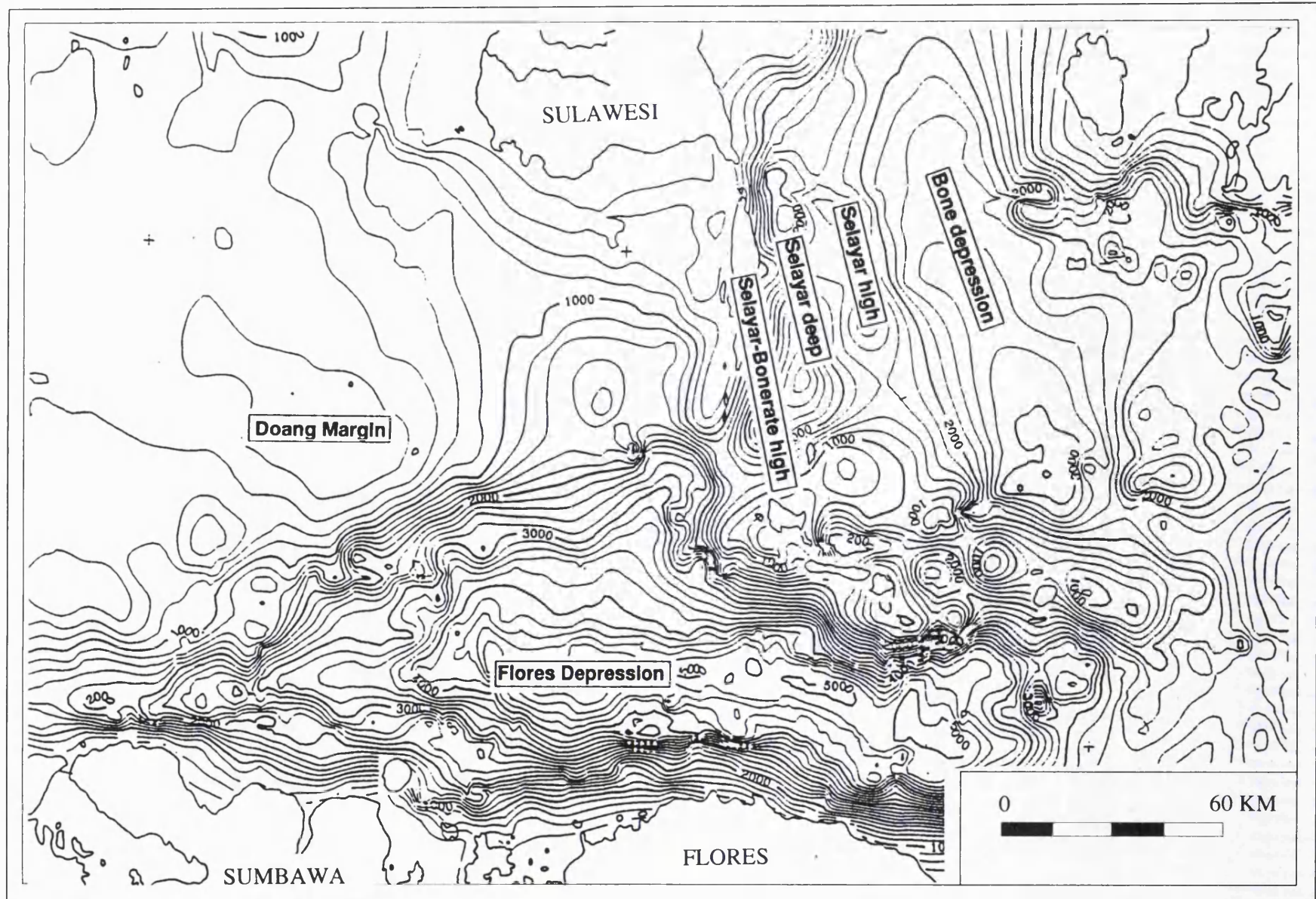


Figure 3.5: Bathymetric map in the East Java and Flores seas (Edcon 1991).

3.2.2 Earthquake data in the Central Indonesian Region

3.2.2.1 Introduction

The earthquake data were obtained from published reports. Fig. 3.6 is reproduced from seismotectonic map of Kertapati *et al.* (1992), and other information about earthquakes in the region was obtained from Cardwell and Isacks (1978), McCaffrey (1985) and Haryono and Prasetyo (1993).

3.2.2.2 Interpretation

Crustal deformation associated with release of energy is usually indicated by seismicity.

The distribution, magnitude and stress orientation of seismicity and orientation of stresses released during earthquake can provide information about plate boundaries.

Earthquakes normally occur along trenches, ridges and transform faults, the types of earthquake generated along each of the three types of boundary being distinctly different (Cox and Hart 1986). Small to moderate earthquakes are generated along ridges at depths of 10 km or less; large earthquakes are generated along transforms at depths up to 20 km; and the very largest earthquakes occur along subduction zones. Hamilton (1979) suggested that great earthquakes (magnitude greater than 8) occur primarily along subducting plate boundaries and, to a lesser extent in continental strike-slips and compressional terranes.

On the basis of active seismicity, the Indonesian region, which is a belt of active earthquakes (Fig. 3.6), can be divided into four major lithospheric plates (Ben-Avraham and Emery, 1973; Cardwell and Isacks, 1978), these being the Indo-Australian, Eurasian, Philippine Sea and Pacific plates. Figure 3.6 shows that the regions of most intensive earthquake activity are southern Sumatra, Java, Bali, the Banda arc and Sulawesi.

These belts of intensive earthquakes with great magnitude and depth are parallel to the active volcanic arcs, and are interpreted as marking the convergence zone where the Indian-Australian oceanic plate is subducted beneath Eurasian Plate. Cardwell and Isacks (1978) described the spatial distribution of intermediate and deep earthquakes which define inclined subducted lithospheric plates in the mantle (Fig. 3.7). The contours range

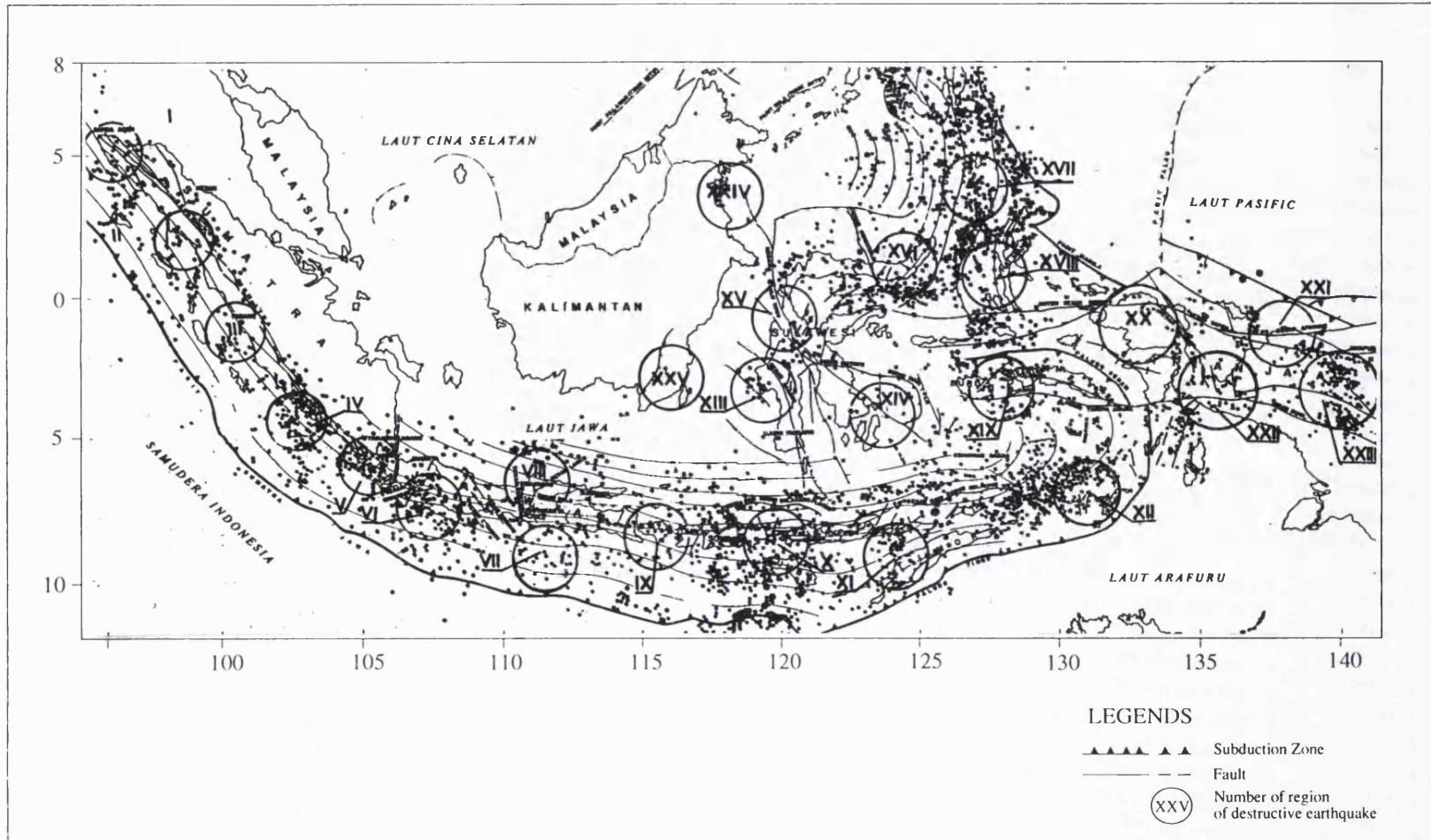


Figure 3.6: Seismotectonic map in the Indonesian Region showing the distribution of earthquakes (Kertapati et al. 1992)

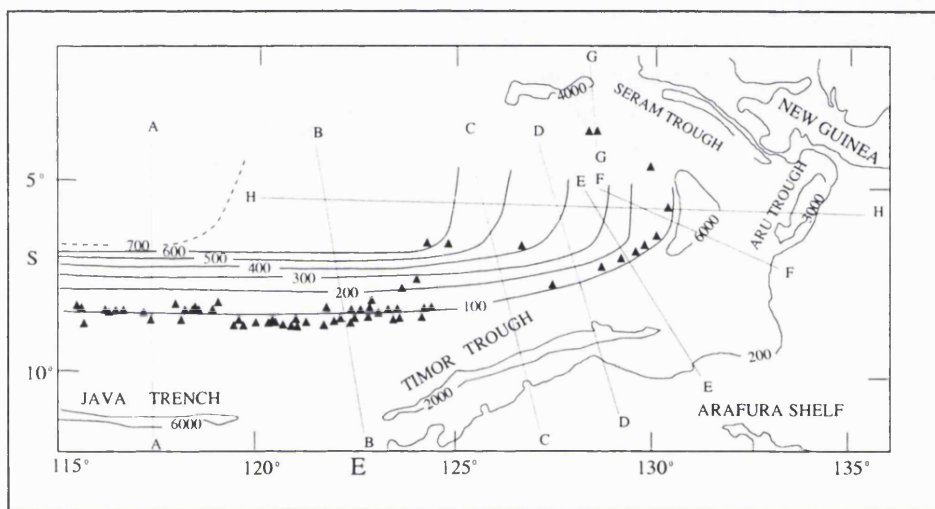


Figure 3.7: Map showing depth contours (in kilometers) to the top of the inclined seismic zone in the Central Indonesian Region (Cardwell and Isacks 1978)

from 0 - 700 km. A cross-section of the subducted lithosphere along the East Java, Flores and Banda seas is shown in Fig. 3.8

In the Central Indonesian region, seismicity varies. The Java Sea is nearly aseismic and therefore is interpreted as a stable tectonic area. The Makassar Strait is also aseismic except near the margin of western Sulawesi, where some earthquakes have been recorded. However, in the Flores Sea there is intense shallow earthquake activity superimposed on deep earthquakes, indicating active tectonics (McCaffrey, 1988). In 1978 and 1993 there were large earthquakes near Flores (McCaffrey, 1985; Haryono and Prasetyo, 1993). These earthquakes had magnitudes of 5.8 and 6.5 and depths of 11.5 km and 33 km, respectively. McCaffrey and Nabelek (1984) and Haryono and Prasetyo (1993) interpreted these earthquakes as associated with back-thrusts representing the initial stage of polarity reversal in the Eastern Sunda Arc.

3.2.3 Magnetic data

3.2.3.1 Introduction

A magnetic map of the Central Indonesian Region and its surrounding area was redrawn from Edcon (1991) using a 50 gamma contour interval instead of 20 gamma as in the original map. The accuracy of the contour lines is constrained by the data coverage, which is not systematic; spacing between lines is variable (Fig.3.9). The most comprehensive data sets are in the Kangean Island and Flores Sea areas. In contrast, in the Makassar Strait, Java Sea and in the vicinity of Selayar and Bonerate islands data are very scarce and in Bone Bay there is no data coverage at all. Contour patterns in the areas with low data coverage cannot perfectly reflect subsurface condition and the map can be used only for regional reconnaissance. To minimise misinterpretations, areas which have no data have been left blank.

The fact that the Central Indonesian region is situated near the magnetic equator influences the magnetic field, in that a body of sufficient magnetisation will give a prominent negative intensity anomaly.

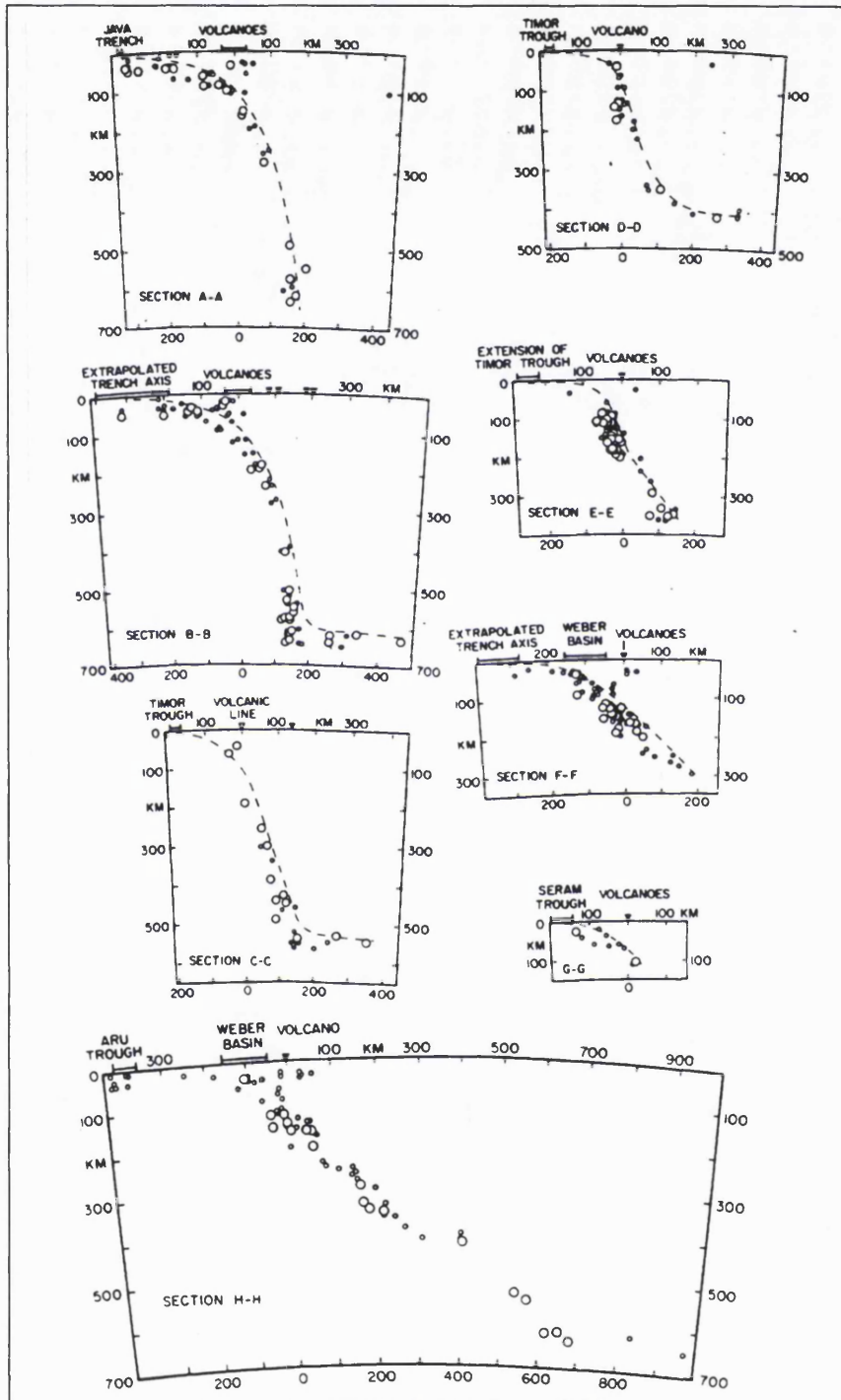


Figure 3.8: Composite vertical cross sections of earthquake hypocentres shown in fig. 3.7 in the East Java and Banda Seas (Cardwell and Isacks 1978)

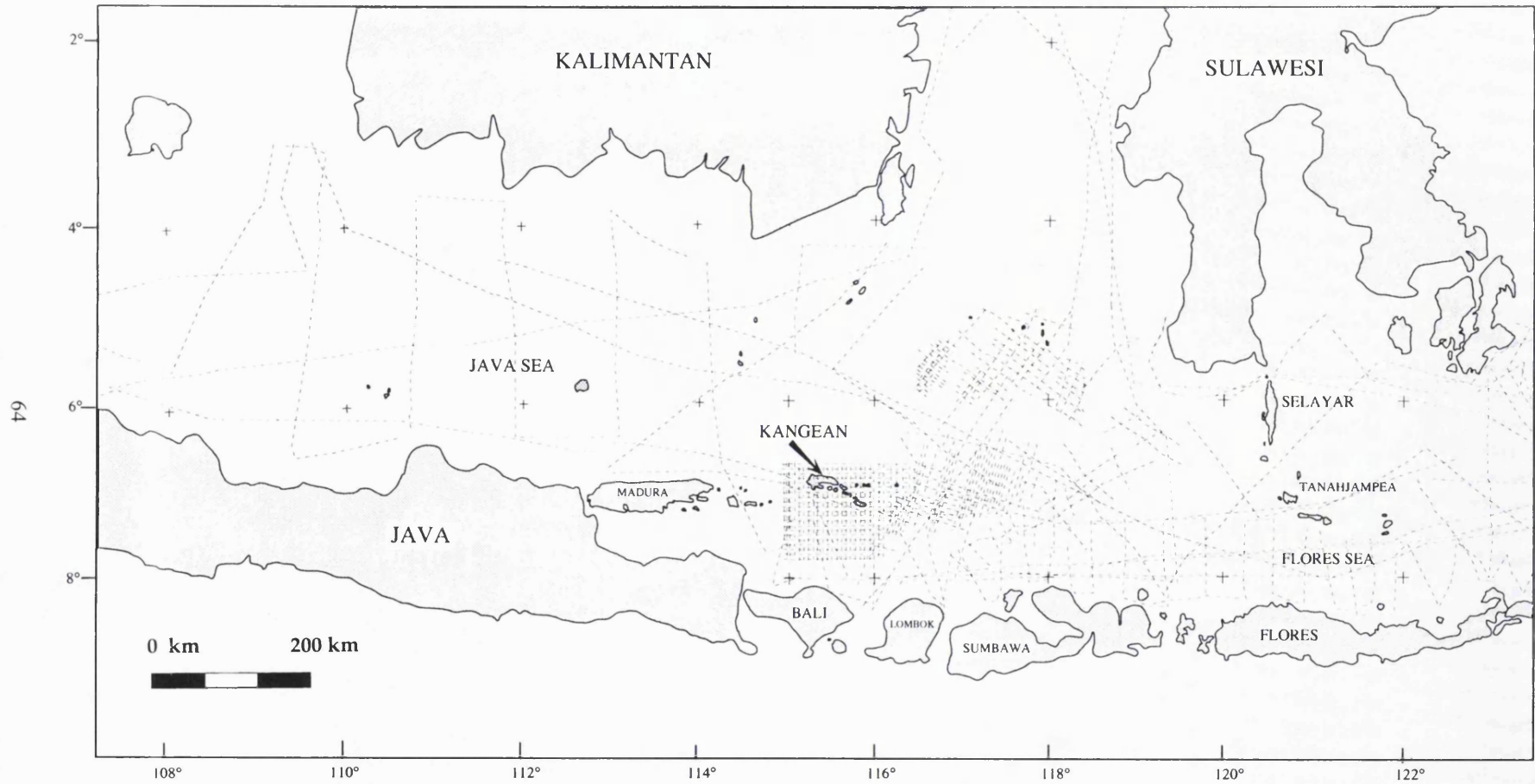


Figure 3.9: Magnetic data coverage in the Central Indonesian region (Edcon 1991)

3.2.3.2 Qualitative interpretation

The magnetic anomaly map of the Central Indonesian Region (Fig.3.10) shows a wide range of magnetic anomaly values (from -500 Gammas to +400 Gammas) having different wavelengths, amplitudes and trends. These various magnetic characteristics can be grouped into four major provinces, which may indicate differences of basement rocks, structures and tectonic settings. The four provinces are the Java Sea, Kangean, Flores Sea and Selayar-Tanahjampea.

Java Sea Magnetic Province

This province lies between Kalimantan and Java. It is characterised by broad isolated anomalies trending NE-SW with low amplitudes and short wavelengths. Figure 3.11 shows magnetic profiles in this province along some of the N-S lines of data coverage. Profiles 1-4 show series of nearly uniform high and low anomalies with amplitudes of between +100 gamma and -200 gamma and wavelengths of, on average, 10 - 20 km. The low amplitudes and wavelengths may indicate bodies of low magnetic susceptibility underlying the area. Some of the prominent local anomalies are associated with intrusive igneous bodies and others are believed due to metamorphic rocks. Geological data support the presence of granitic or metamorphic basement (Ben-Avraham and Emery 1973) with low susceptibility. Profile 5 shows a change in amplitude and wavelength. In the north of the profile the amplitudes increase in the range between +250 gamma to -400 gamma with short wavelength, suggesting the presence of high susceptibility magnetic bodies beneath the profile. This profile is situated south of Meratus Mountain and Laut Island, where ultramafic rocks occur.

Kangean Province

This province is situated in the area between Kangean and Bali-Lombok islands. An interesting feature is the fact that there is an E-W contour lineation in the west which changes gradually to NE-SW in the east. The E-W lineation corresponds to the regional trends of anticlinal axes on Java, which are young tectonic features, whilst the NE-SW lineation follows the older structures in the Java Sea. The amplitudes range between -200 gamma and +200 gamma with wavelengths of the order of 15 km. Figure 3.12 shows a profile along a line of data coverage in this province. The strong continuous

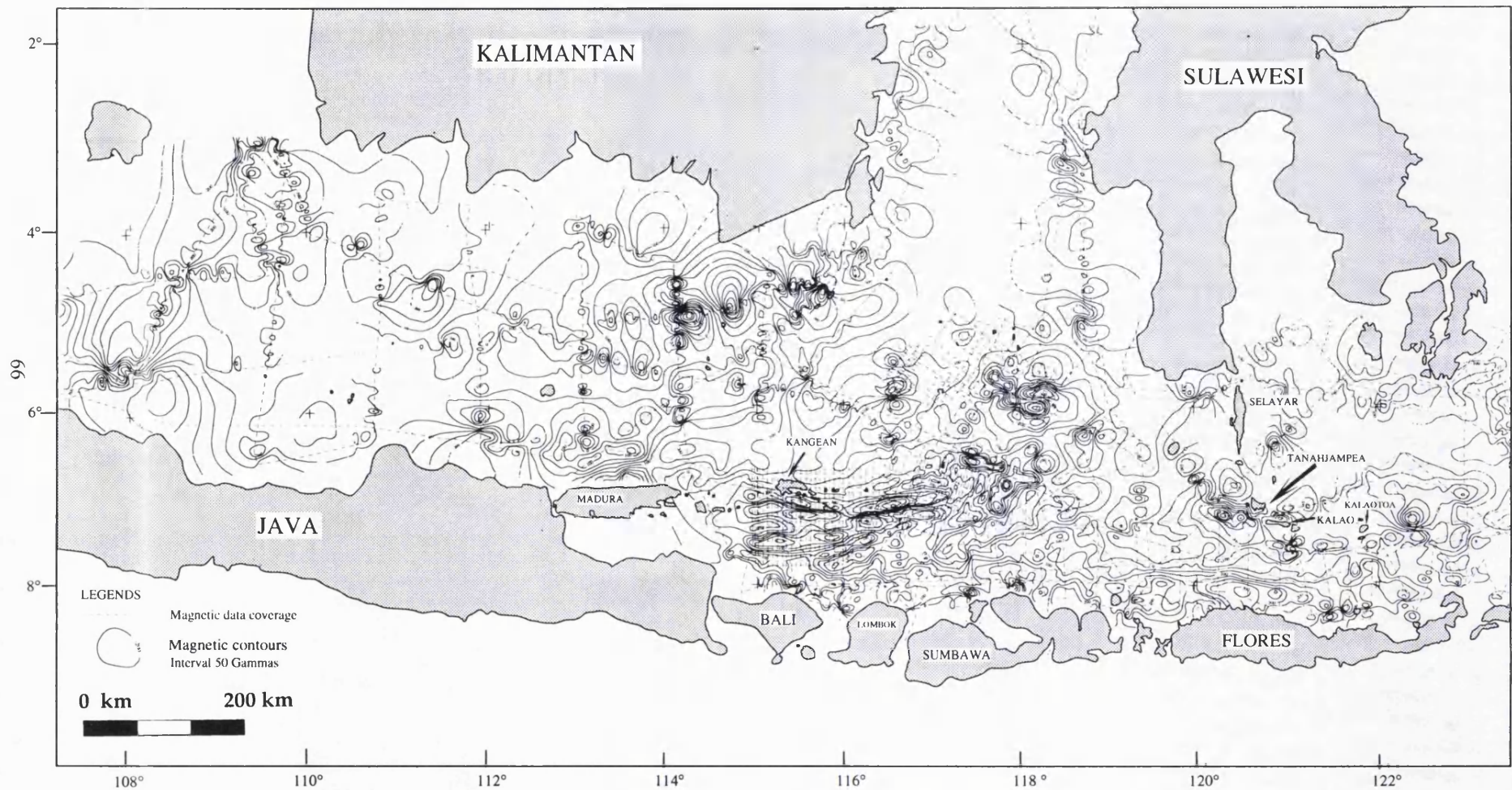


Figure 3.10: Magnetic anomaly map in the Central Indonesian region (redraw from Edcon 1991)

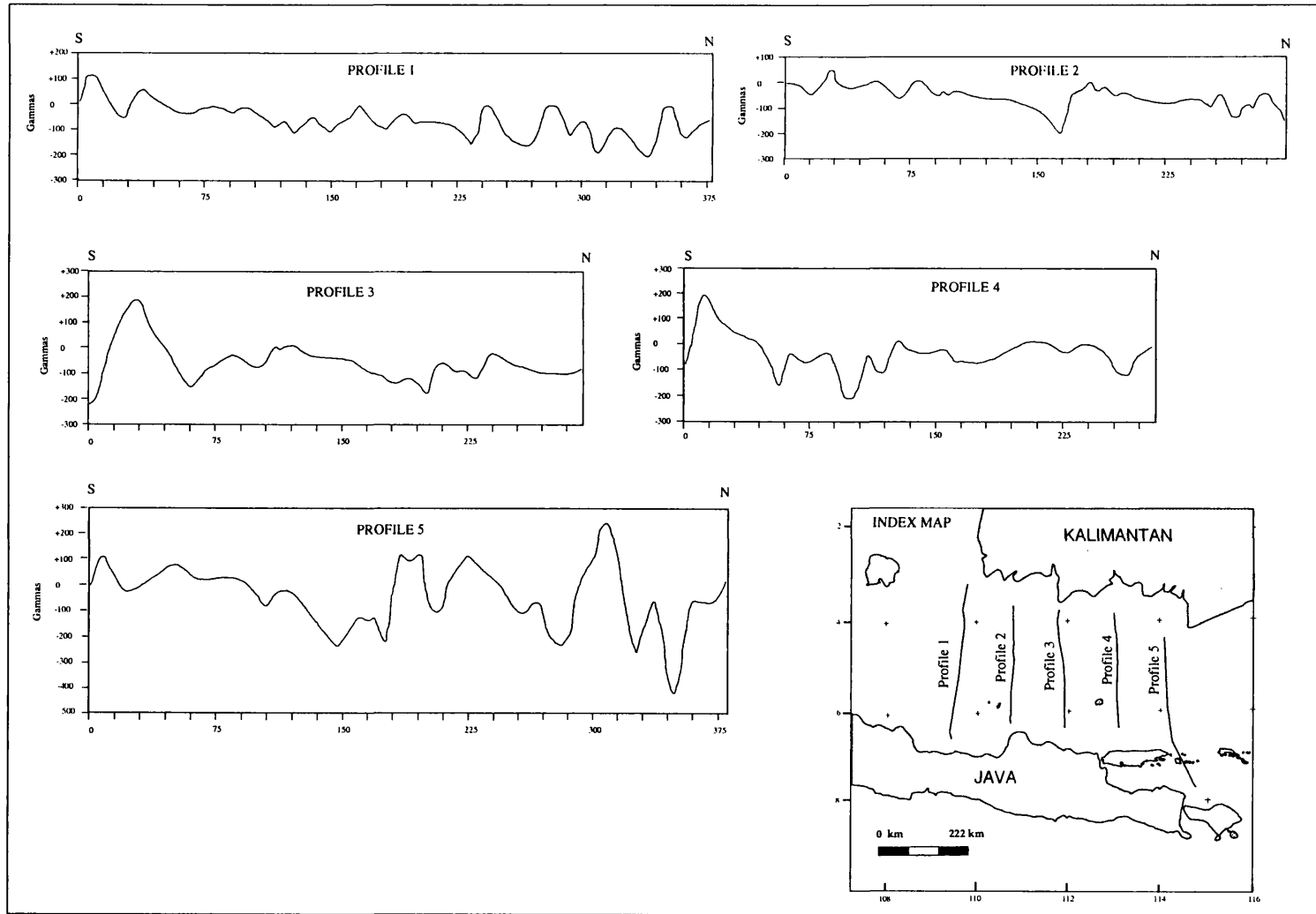


Figure 3.11: Magnetic profiles in the Java Sea Province

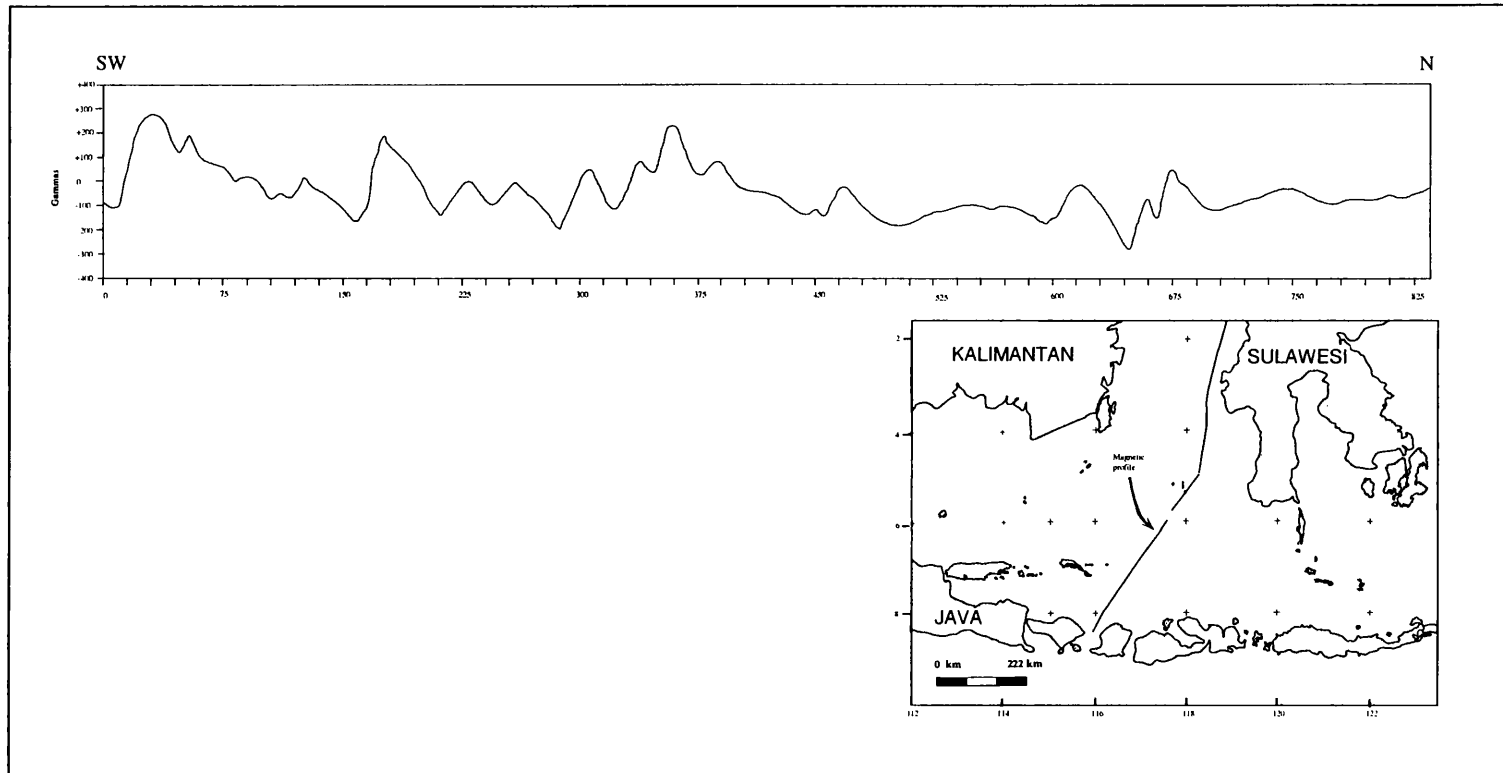


Figure 3.12: Magnetic profile in the Kangean Province

contour anomaly in E-W direction and steep gradient anomaly may indicate structural control influenced by uplifted basement.

Flores Sea Province

This province is situated in the Flores Sea and is separated from the Kangean Province by a NE-SW contour lineation in the area between Lombok and Sumbawa. It is characterised by E-W striking magnetic anomalies. The amplitudes range between -100 gamma and + 400 gamma with wavelengths averaging 25 km. Magnetic gradients are steeper to the south and anomalies are more positive. Figure 3.13 shows some magnetic profiles along lines of data coverage. Profile 3 runs diagonally from southwest of SW Sulawesi to the southwest of Tanahjampea and thence to the area north of Flores. The profile shows the steep gradient in the area between Tanahjampea and Flores which is interpreted as fault controlled, separating a non magnetic body in the south from a magnetic body in the north. The gradient is indicated by contours which run E-W from north of Flores to north of Bali which are thought to mark a major structure in the Flores Sea related to back-arc thrust indicating incipient subduction polarity reversal (Silver *et al.* 1983). To the south, off Flores, there are some isolated anomalies which have high positive amplitudes and are interpreted as due to volcanic intrusions.

Selayar-Tanahjampea Province

In this province the very scarce data coverage causes the orientation of anomalies to be unclear but it seems they have NW-SE and N-S directions. The amplitudes range between -500 gamma and +300 gamma. Figure 3.14 shows some of the magnetic profiles along lines of data coverage. Southwest of Tanahjampea there is a short wavelength anomaly, as shown in profile 2. This is interpreted as due to a magnetic body with high susceptibility very close the surface. On the map this strongly negative anomaly seems to continue to the north of Kalao before being interrupted by a NE-SW lineament. This lineament might be related to a structure which accommodated the displacement of basement rocks and the emplacement of ophiolite on Kalao and Kalaotoa islands.

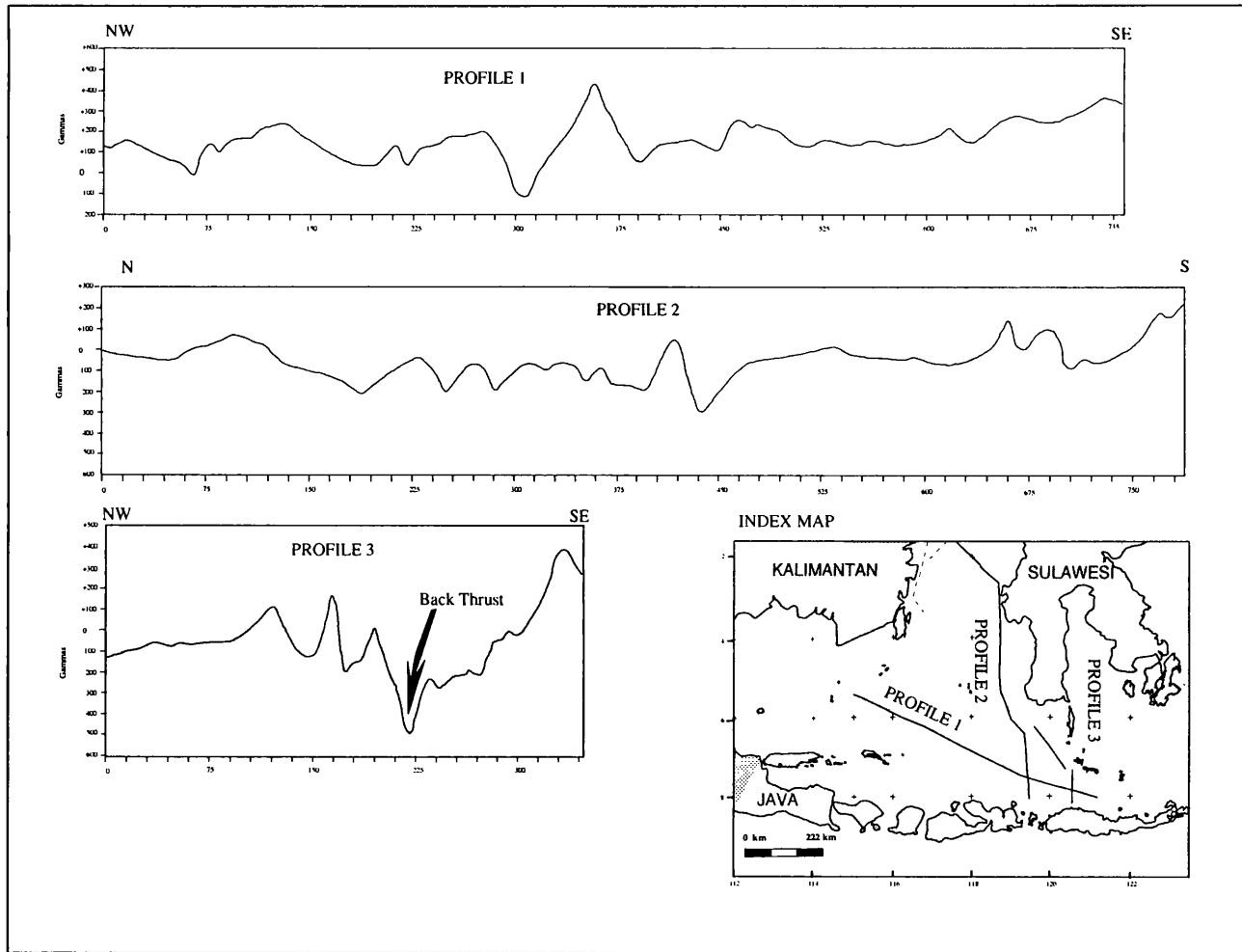


Figure 3.13: Magnetic profiles in the Flores Sea Province

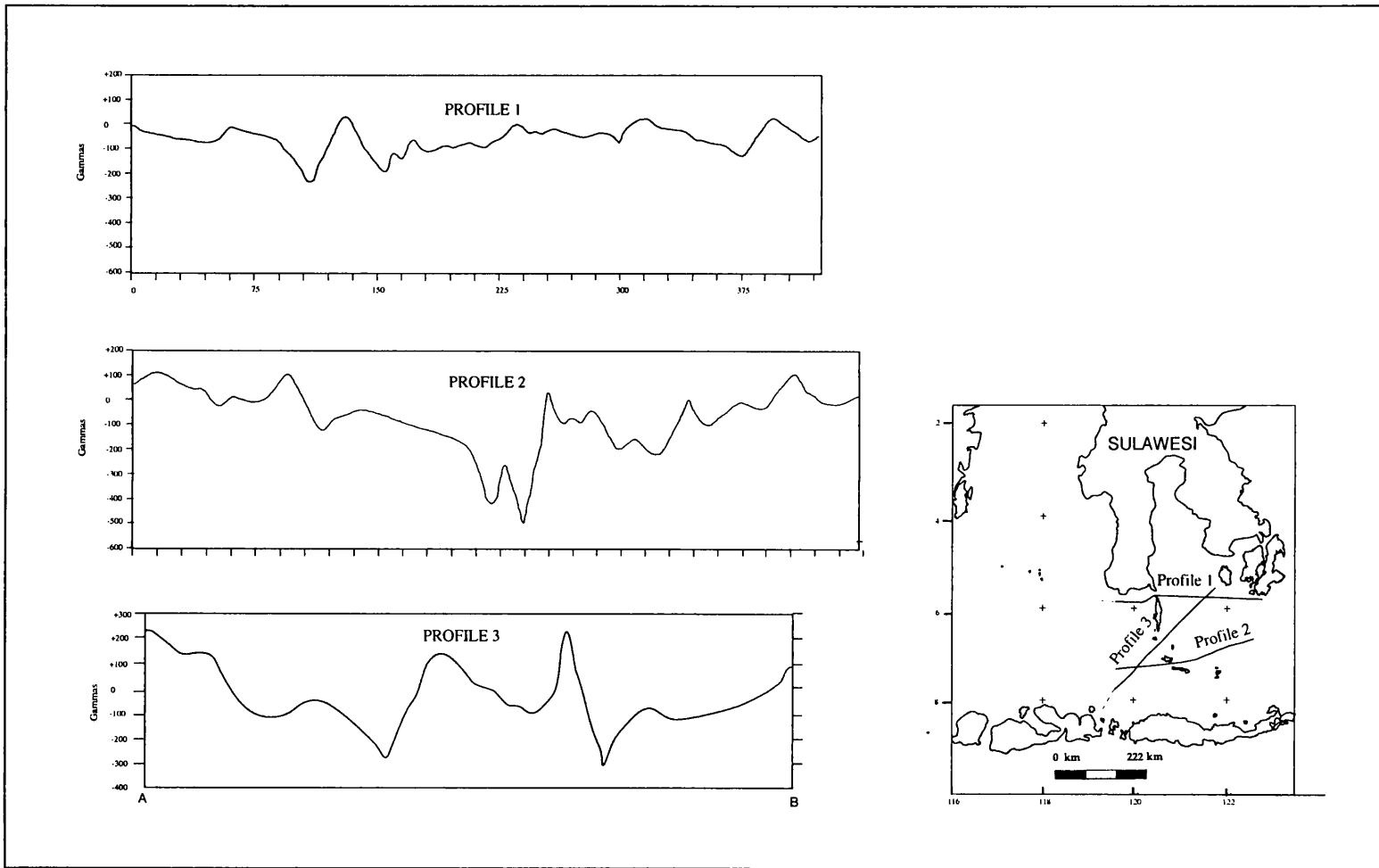


Figure 3.14: Magnetic profiles in the Selayar-Tanahjampea Province

3.2.4 Gravity Data

3.2.4.1 Introduction

The 1:1500,000 gravity data coverage in the study area is quite good, except to the east of the Selayar Island (Fig.3.15). North of Flores the data coverage is excellent.

3.2.4.2 Qualitative Interpretation

In the Central Java Sea, Bouguer anomalies range from +30 to +50 mGal, whilst in the East Java and Flores seas Bouguer anomalies range from +50 to +250 mGal (Fig. 3.16). The absence of negative Bouguer anomalies over the Java and Flores Seas is assumed to be due to the effect of downbowed lithosphere of the Indo-Australian oceanic crust beneath the Sunda and Banda arcs, as indicated by the contour lines on inclined subducted zone (Cardwell and Isacks 1978)(see Fig. 3.7). The increase in Bouguer anomaly from the Central Java Sea to the Banda Sea through the Flores Sea is interpreted as marking the transition from continental crust to oceanic crust. The high Bouguer anomaly in the Flores Sea is also interpreted as due to the presence of oceanic crust and thin sediments.

Anomaly trends can be categorized into three groups, these being E-W, NE-SW and NNW-SSE. The NE-SW trend is found in the Central Java Sea, from central Java to the Meratus Mountain. The E-W trend is found in the northern parts of the East Java and Flores seas and has steeper gradients than the other trends. The anomalies form closures characterized by E-W trend, with the highest values, of about 200 milligal, in the middle of the closures.

To the west of Selayar Island the trend of anomalies becomes NE-SW and to the east of the Bonerate and surrounding islands it becomes NWN-SES. The rest of the area is dominated by small circular contour anomalies, particularly offshore of Flores.

3.2.5 Seismic refraction in the East Java-Flores Sea

Preliminary results of the seismic refraction and radiosonobuoy investigations in the East Java-Flores Sea were reported by Ben-Avraham and Emery (1973) and Curray *et al.* (1977). Some of the seismic refraction and radiosonobuoy stations were within the study

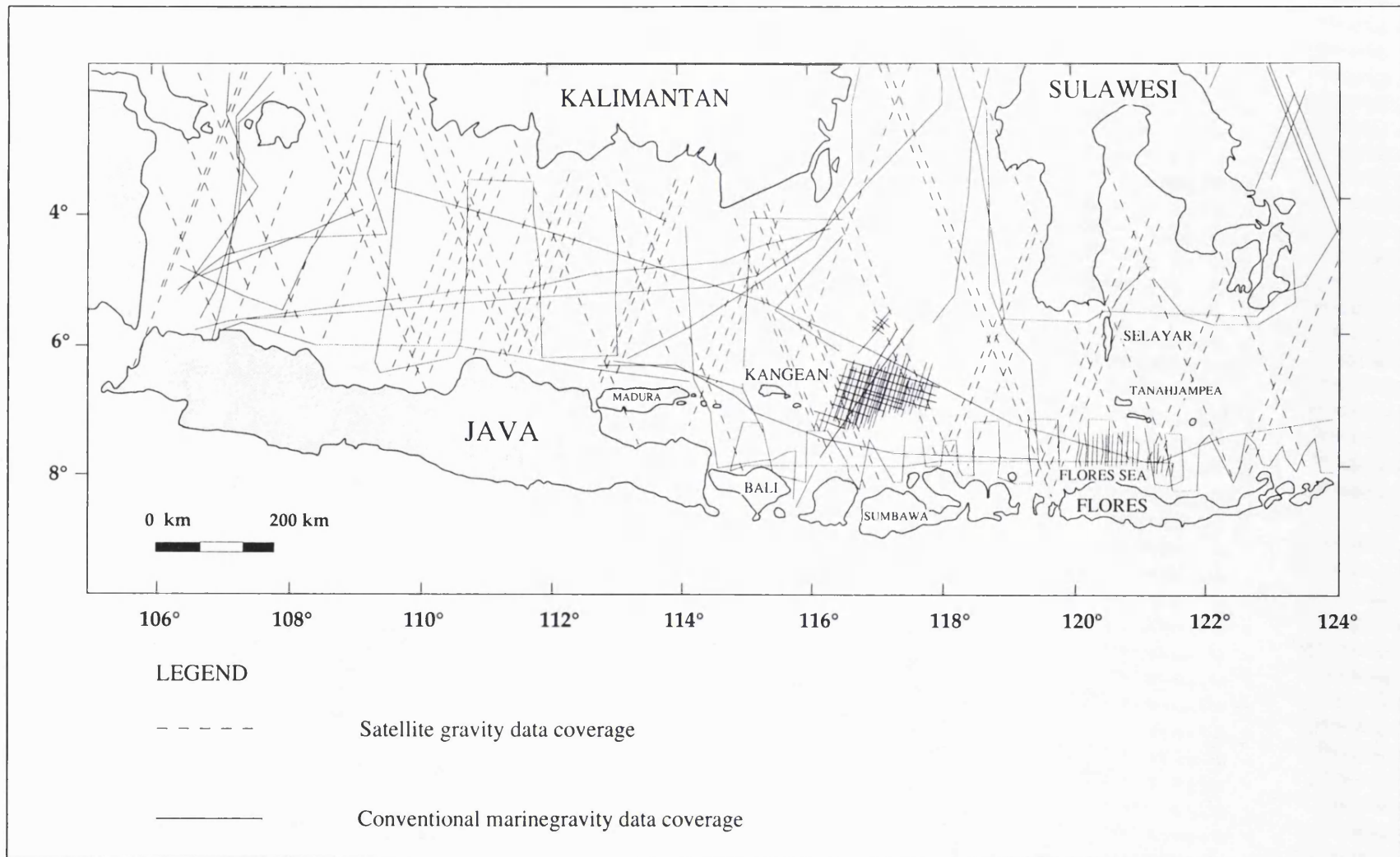


Figure 3.15: Gravity data coverage in the Central Indonesian Region (Edcon 1991)

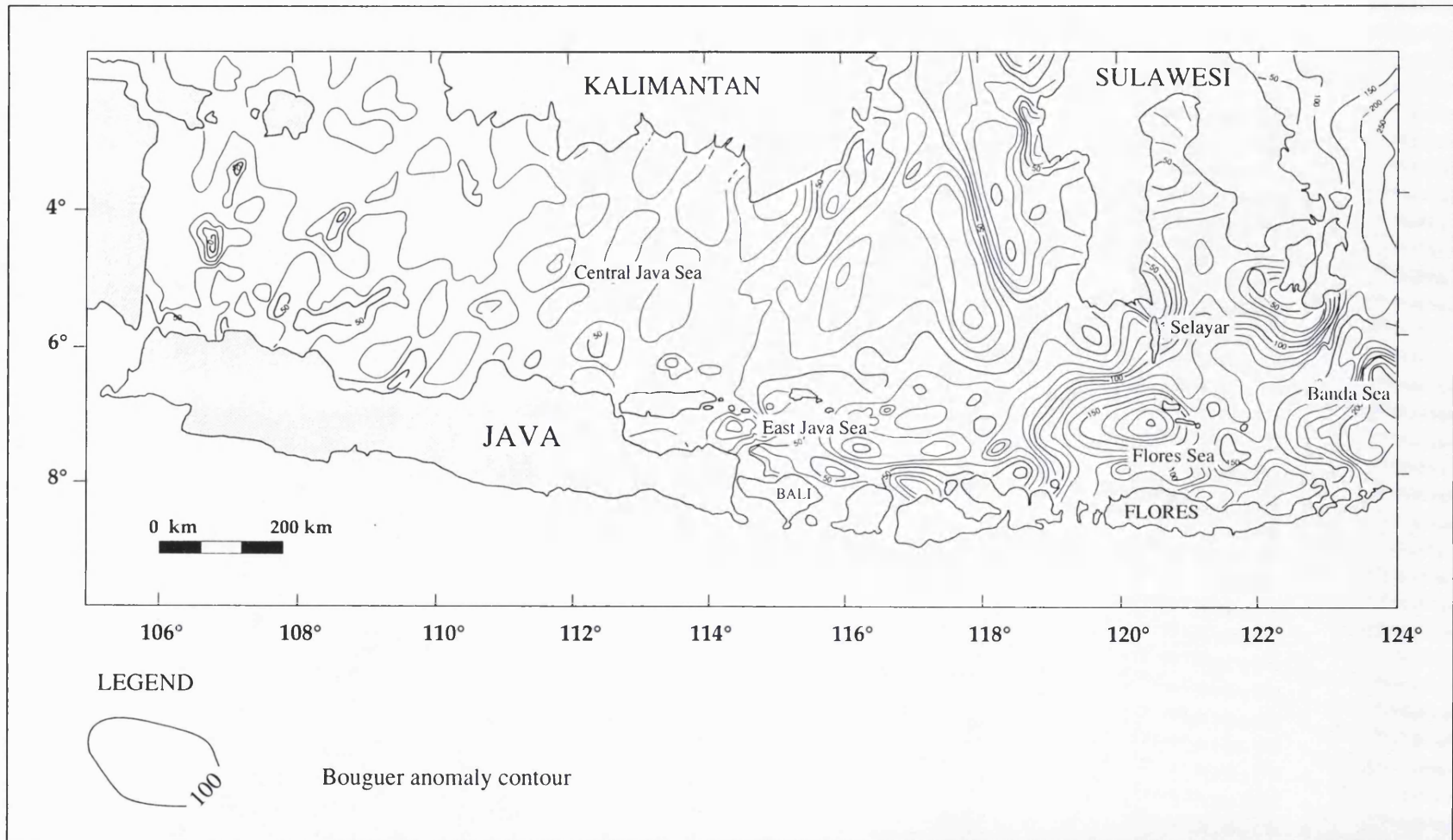


Figure 3.16: Bouguer anomaly map in the Central Indonesian Region (modified from Edcon 1991)

area (Fig. 3.17) and have been used to provide information on the depth to mantle and acoustic basement and also on the velocities of the various layers (Table 3.1).

The layering obtained from seismic refraction between stations MSN 12 (situated in the South Banda Basin), MSN 13 (situated in the Flores Sea) and MSN 14a&14b (situated in the Bali Basin, north of Sumbawa Island) was interpreted by Curray *et al.* (1977) (Fig. 3.18). Their interpretation indicates that crustal thickness increases from the Banda Basin to the East Java Sea through the Flores Sea. The crust at station MSN 12, in the South Banda Basin, was very thin (5.78 km, which is typically oceanic crust). The depth of mantle was recorded as 10.28 km in water 4.5 km deep. In the Flores Sea, the mantle was recorded at 14.3 km in the water 4.6 km deep. The crustal thickness was thus 9.7 km which is slightly greater than the average thickness of oceanic crust but significantly less than that of continental crust. Curray *et al.* (1977) suggested that the crust in this area was originally oceanic. Although oceanic crust was not detected, they suggested that it could have been masked. At stations MSN 14a and 14b, oceanic crust was detected but the depth of mantle was not determined. Curray *et al.* (1977) suggested that the mantle lay at considerable depth.

In the central Java Sea, no seismic refraction data are available, whilst radiosonobuoy data penetrated only down to the basement. The crustal thickness and depth of mantle are therefore not known. Average seismic velocities of the acoustic basement from radiosonobuoy velocity data are in the range of 4000-4500 m/sec. Over the Karimunjawa arc, at station R20, where the basement is underlain by a granitic body (as also suggested by Hamilton 1979), the velocity is 4830 m/sec. This might indicate that in the entire East Java Sea the basement is granitic and this is as a typical basement in continental crust.

Ben-Avraham and Emery (1973) suggested a structural section based on seismic refraction data across the Java Sea, the Java Trough, Java and the Java Trench (Fig. 3.19), showing that from south to north the crust increases in thickness. Although there are no data on mantle depth in the East Java Sea, the interpretation showed the crust getting deeper in that direction.

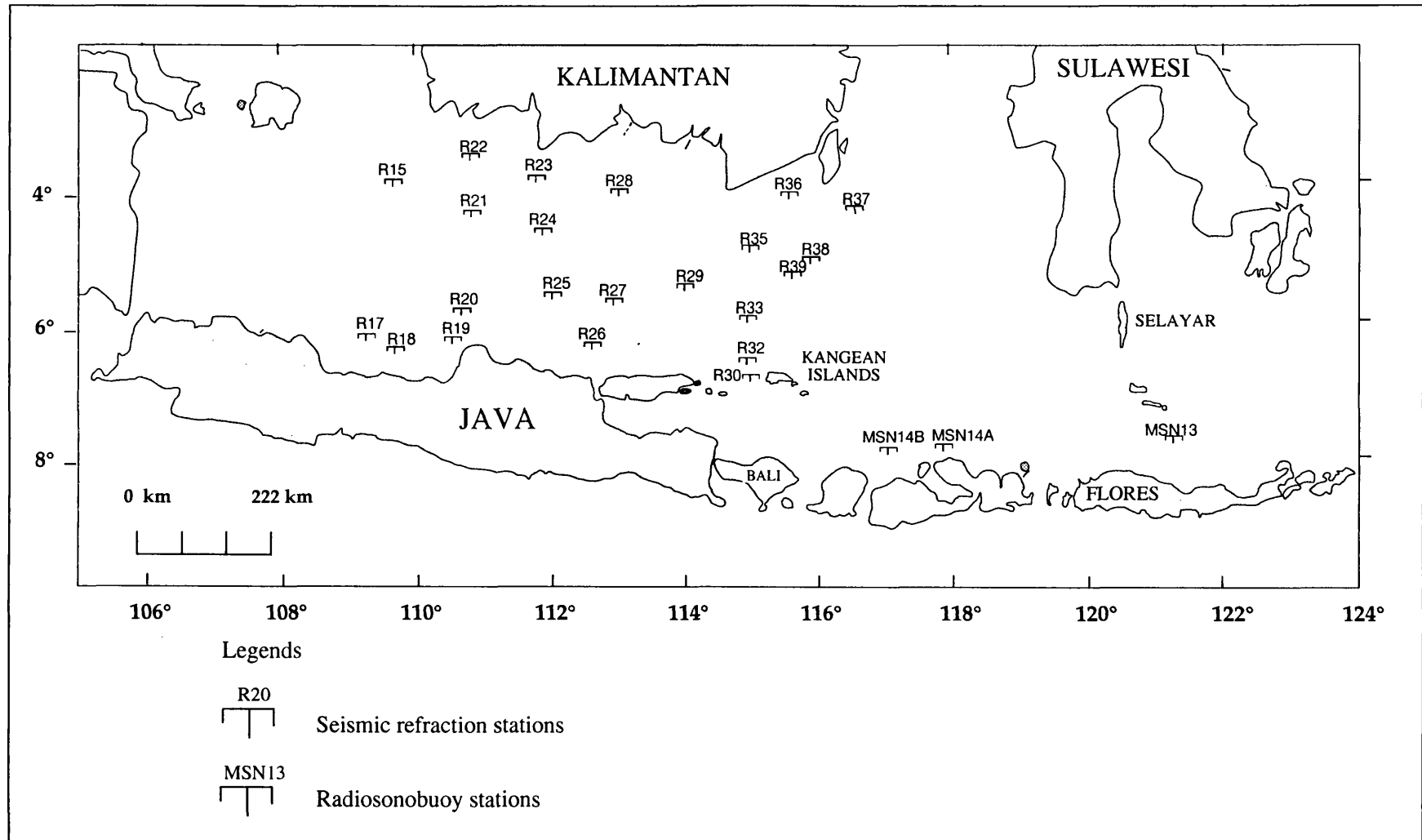


Figure 3.17: Locations of seismic refraction and radiosonobuoy stations in the East Java-Flores Sea (from Ben-Avraham and Emery 1973 and Curray et al. 1977)

Table 3.1: Refraction and radiosonobuoy data from the East Java-Flores Sea

Station	Latitude	Longitude	Water depth (metre)	Velocity (km/sec)								Thickness (km)					Moho dept (km)		
				V2	V3	V4	V5	V6	V7	V8	V9	H2	H3	H4	H5	H6		H7	H8
R15	-4.08	109.70	41.00	1.60		2.35			4.37	(6.04)	0.33		0.72				1.07		
R17	-6.29	109.34	45.00		1.71					4.72 (5.57)	0.25								2.03
R18	-6.49	109.71	45.00	1.60	2.10				4.26		0.14	0.16							
R19	-6.32	110.57	47.00	1.60	1.93	2.12	2.66		(4.75)	(5.95)	0.11	0.09	0.18	0.27					
R20	-5.93	110.69	49.00	1.60						4.83	0.09								0.12
R21	-4.52	110.78	51.00		1.78	2.18	2.26			5.32		0.19	0.10	0.62					
R22	-3.64	110.83	38.00	1.60	1.90		2.65	2.76	3.98	4.69	0.09	0.48		0.16	0.40	0.46			
R23	-3.81	111.78	30.00	1.60	1.94		2.58		(4.35)		0.19	0.17		0.36					
R24	-4.76	111.84	56.00	1.60					4.19		0.11								
R25	-5.95	111.88	66.00	1.60		2.18	2.47	3.18		5.35	0.23		0.09	0.56	1.27				
R26	-6.38	112.63	60.00	1.60	1.99	2.37	2.55				0.07	0.06	0.17	0.74					
R27	-5.81	113.02	71.00	1.60	2.03	2.17		3.26	3.59 (5.30)		0.15	0.08	0.33		0.54	0.70			
R28	-4.24	113.01	32.00	1.60	1.73	1.77	2.46	2.79	(4.12)		0.05	0.16	0.17	0.34	0.36				
R29	-5.69	114.13	66.00	1.60	1.66	2.14	2.53	3.03	(4.12)		0.10	0.06	0.31	0.33					
R30	-7.00	115.08	105.00	1.60		2.19			3.90		0.10		0.41						
R32	-6.82	115.02	73.00		2.14	2.45	2.88	3.12	3.29			0.17	0.06	0.09	0.37				
R33	-5.99	115.01	50.00	1.60	1.95	2.26			(5.40)		0.04	0.14	1.40						
R35	-4.99	115.07	30.00	1.60					3.64		0.12								
R36	-4.27	115.57	24.00	1.60					3.44	4.73 (6.29)	0.02							0.69	
R37	-4.54	116.56	58.00		2.03	2.41						0.25							
R38	-5.20	115.92	62.00	1.60	2.08	2.40			(4.10)		0.15	0.25	0.66						
R39	-5.44	115.69	58.00	1.60	2.06			3.05	3.69		0.13	0.30			0.52				
MSN 13	-7.47	121.17	4610.00	2.15	3.19				6.10	7.66	0.10	3.00					6.60		14.31
MSN 14a	-7.57	117.52	1540.00	2.32				5.03	6.29	6.75	1.83				1.64		6.10		
MSN 14b																			

Table 3.1: Seismic refraction and radiosonobuoy data from the East Java-Flores Sea (Souces; Ben-Avraham and Emery 1973; Curray et al. 1977)

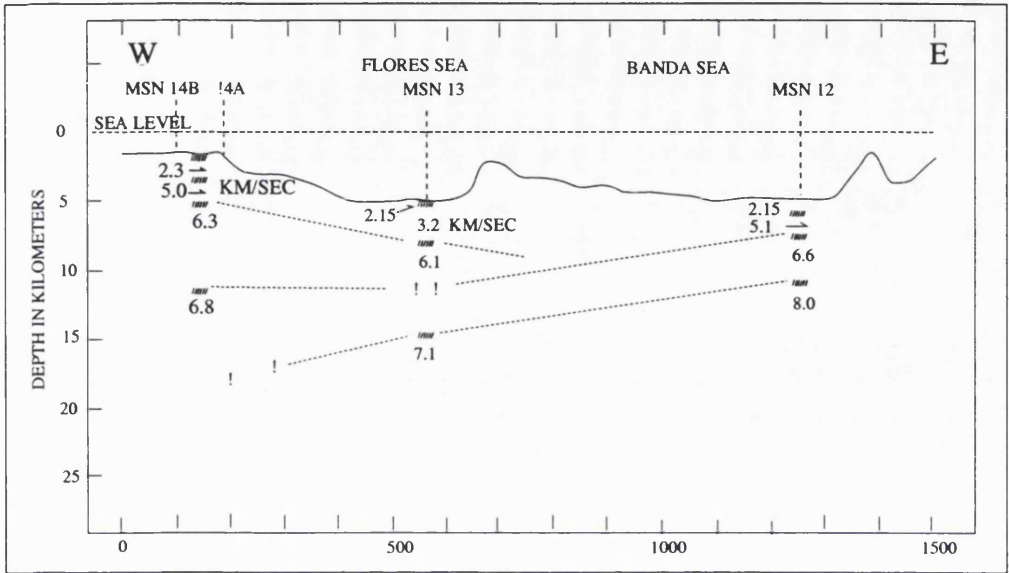


Figure 3.18: Correlation of layers obtained from seismic refraction between stations MSN 12, MSN 13 and MSN 14A&B showing the increase of crustal thickness from east to west (Curry et al. 1977).

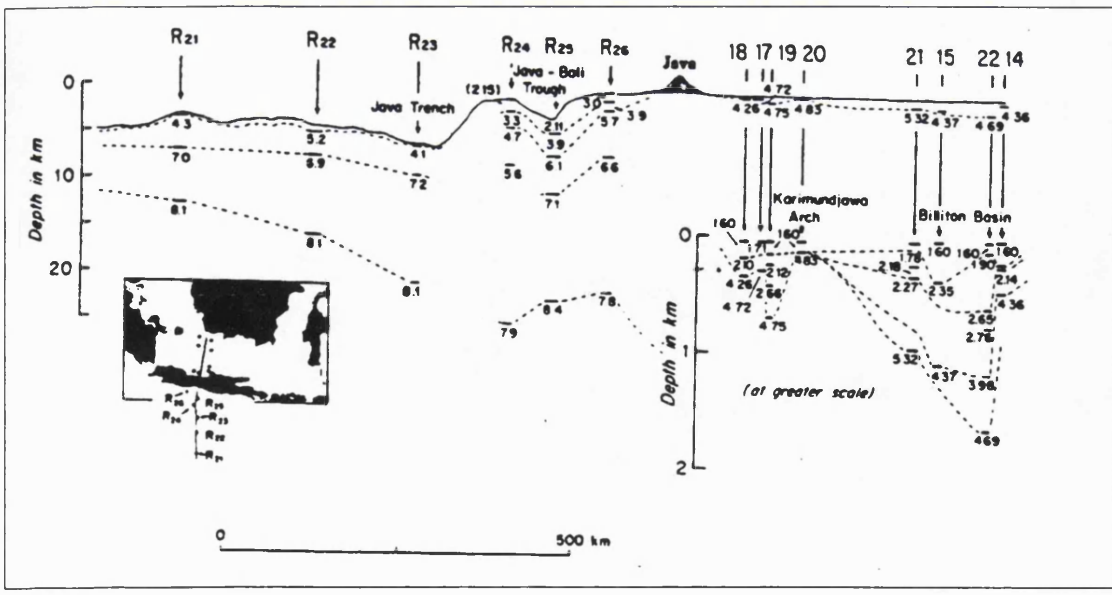


Figure 3.19: Seismic structure section across the Java Sea, Java Trough, Java and Java Trench showing the increase in crustal thickness from south to north which possibly continues into the Java Sea (Ben-Avraham and Emery 1973)

In conclusion, the crust in the East Java-Flores Sea changes gradually in thickness from East Java to the Banda Sea. This indicates that the type of crust changes from oceanic in the Banda Sea and the Flores Sea to continental in the west of the East Java Sea. Between these two regions, in the East Java Sea, the crust is of intermediate type.

CHAPTER FOUR

MORPHO-STRUCTURAL UNITS IN THE CENTRAL INDONESIAN REGION

4.1 INTRODUCTION

The Indonesian region is constructed of two major blocks of continental lithosphere (Fig. 3.1), these being Sundaland, which is part of the southeast Eurasian Plate, and the Australian platform which extends northwards into the Eastern Indonesian region. Between these two blocks lies a collection of landmasses or small continental fragments and a number of deep sea basins bounded by island arcs. The smaller continental fragments are interpreted as having been rifted either from the South China continental shelf or the northern Australian continental margin. They display a variety of tectonic styles and activity and sediment thicknesses, dictated largely by their proximity to arcs or continental margins (Prasetyo 1992).

4.2 GEOLOGICAL PROVINCES

On the basis of the magnetic contour patterns and values (Fig. 3.10) and the Bouguer anomaly map (Fig. 3.16), in addition to the structural map of the region, the Central Indonesia Region (CIR) and nearby areas can be divided into five major provinces (Fig. 4.1), these being;

1. Bone Bay Province
2. Makassar Strait Province
3. Central Java Sea Province
4. East Java Sea Province
5. Flores Sea Province

The geological and geophysical data available in each province will be examined in order to understand the tectonic styles and evolution. Subsequently, the evolution of each province will be related to the others in order to obtain a complete history of the evolution of subduction at the eastern margin of Sundaland since the Late Cretaceous.

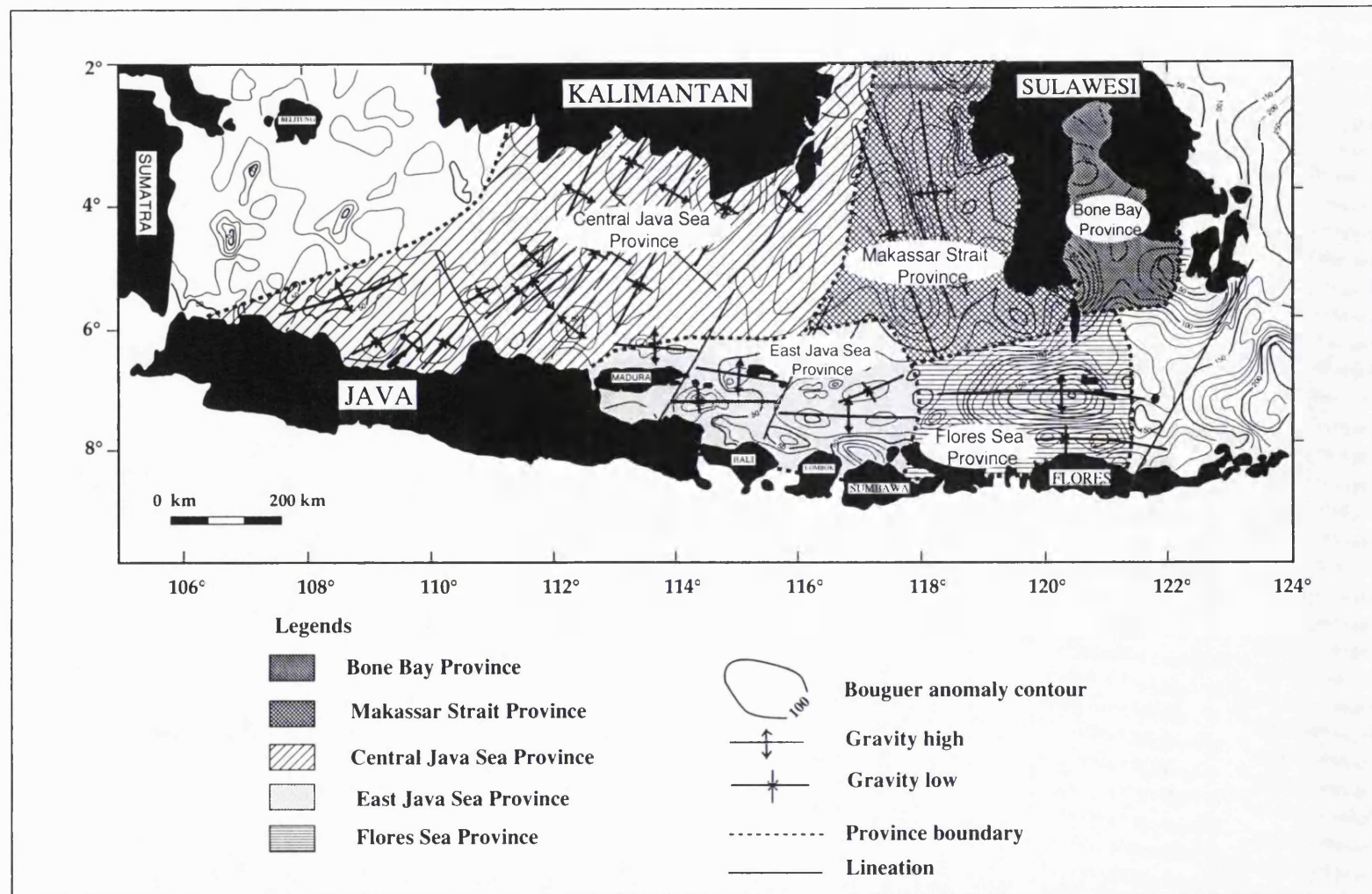


Figure 4.1: Morpho-structural units in the Central Indonesian Region based on gravity, magnetic and structural data.

4.3 SUBDUCTION ROLL-BACK

The Central Indonesian Region (CIR) is recently located in a back-arc region. Geology, gravity and seismic interpretation indicate that the region is occupied by deep basins which experienced crustal extension. Therefore, the term back-arc basin or marginal basin can be used in the CIR. However, the development and evolution of marginal basins are still poorly understood. Several hypotheses have been suggested (cf. Uyeda and Kanamori 1979) as follows;

1. Entrapment of a marginal part of a pre-existing ocean by the formation of an island arc
2. Back-arc spreading caused by or related to subduction
3. Opening related to a leaky transform fault
4. Opening related to the subduction of a ridge
5. Subsidence caused by oceanization of continental crust

Karig (1971) suggested that many marginal seas in the Southwest Pacific region have developed by crustal extension during subduction of oceanic lithosphere, usually called back-arc spreading.

The CIR is situated between Cretaceous-Early Tertiary basement complexes (see Fig. 3.3) and it is believed that basin formation has been associated with migration of subduction. The mechanism can be explained through the relationship between the age of the subducting slab and the gravitational instability of oceanic lithosphere (Molnar and Atwater 1978). Young lithosphere resists subduction, possibly causing compression behind the trench, while an old subducting slab may experience active roll-back of the trench axis and thereby cause back-arc spreading (Jarrad 1986). Dewey (1980) defined trench roll-back as the gradual seaward migration of a trench caused by the gravitational pull of the descending slab. This motion is greater for old, cold ocean plates than younger, warmer ocean plates. Several authors (e.g. Chase 1978; Molnar and Atwater 1978) have suggested that a back-arc basin occurs when the resultant of the velocities of the overriding plate and the trench roll-back motion has a component directed away from the trench, when viewed in a hot-spot frame of reference. Daly *et al.* (1991) described the mechanism of back-arc extension in relation to the relationship between the velocity of roll-back (V_t) and the velocity of the overriding plate (V_u) (Fig.4.2). If $V_u > V_t$, the

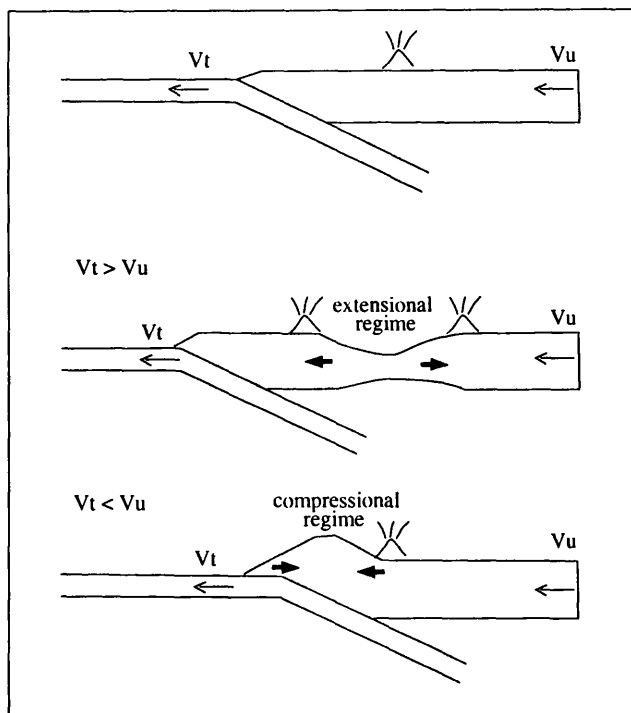


Figure 4.2: Sketch showing the relationship between the relative velocity of subduction zone rollback (V_t) and the velocity of the upper plate (V_u) in relation to extensional and compressional stress behind the arc (After Daly et al. 1991).

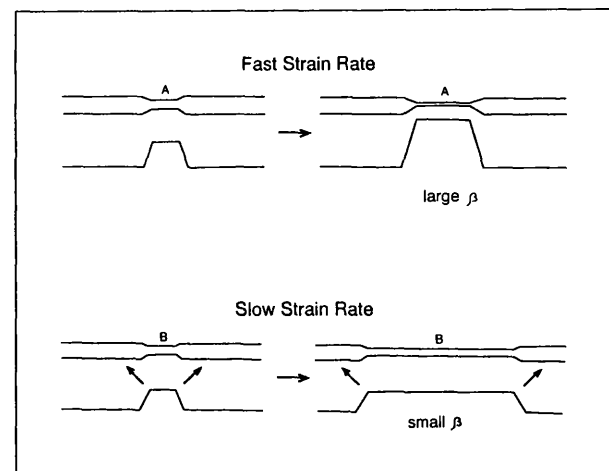


Figure 4.3: The two models showing the different styles of extensional deformation expected with fast and slow rates of lithosphere extension (Park 1988)

overriding plate advances over the trench line resulting in a compressive arc. If $V_u < V_t$, an extensional arc will be generated and may result in back-arc basin formation. The roll-back velocity (V_t) depends on the age of the slab since the older the slab the more dense it is and the faster it sinks. Therefore, subduction of an old slab is more likely to result in subduction roll-back.

Park (1988) pointed out two opposing effects resulted from the process of lithosphere extension; (i) steepening of the geotherm, brought about by bringing the hotter asthenosphere nearer to the surface, which weakens the lithosphere, and (ii) thinning of the crust, which will act to strengthen the lithosphere. Which of these two effects predominates depends on whether extension is slow or fast. Park (1988) presented two models showing the different styles of extensional deformation expected with fast and slow rates of lithosphere extension (Fig.4.3). The figure showed that fast extension rates are only possible for hot, thermally young lithosphere in which there will be locally intense extensional deformation, with strain softening, leading to large β values and ultimately, if the force persists, to the complete rifting of the continental crust and the formation of an ocean. The second model (slower extension rate) produced strain hardening and generated a β value of around 1.5. As each section of lithosphere hardens, intense deformation is localised along listric faults which would be expected to spread laterally to involve a much wider region of extensional deformation. This critical β value of 1.5 is in remarkable agreement with the estimated β values from a wide range of intra-continental extensional basins which show an average of β value of 1.4 - 1.5 (Park 1988). [Note: The β value is the lithosphere stretching factor of McKenzie (1978), equal to the ratio of the lateral extent of the stretched and unstretched crust. Thus a value of $\beta = 2$ corresponds to a doubling of the original width and a halving of the original thickness of the lithosphere (Park 1988)].

CHAPTER FIVE

BONE BAY PROVINCE

5.1 INTRODUCTION

The origin of Bone Bay, situated between Southwest and Southeast Sulawesi (Fig. 5.1), is still poorly understood and not many geological and geophysical data are available. It is believed that a better understanding of the geology and tectonics of Bone Bay will make an important contribution to explaining the complex geology and tectonics of Sulawesi.

5.2 PREVIOUS STUDIES

Hamilton (1979) suggested that the opening of Bone Bay was due to the separation of the South and Southeast arms of Sulawesi in the Middle Miocene and that the bay was underlain by more than 5000 m of sediments. In the northernmost part of the bay, a drill hole penetrated 3000 m of sedimentary rocks, of which the deepest were Middle Miocene. Daly *et al.* (1991) proposed that the opening of Bone Bay was caused by the collision of northern margin of the Australian Continent with the Banda-Sunda arcs.

In this study, the origin of Bone Bay will be discussed using seismic reflection and gravity data, as well as geological information from the Sulawesi region from many sources.

5.3 GEOLOGY OF SULAWESI

Sulawesi consists of four diverging arms named the South, North, East and Southeast arms, each of which records a very different and complicated geological history (see Fig. 5.1). The island is situated at the triple junction of the large Indo-Australian, Pacific and Eurasian plates which interact and collide one another.

The complicated geology of Sulawesi, consisting of various lithologies and structures with different histories and origins, leads to the conclusion that the island is composed of several different terranes and the terminology of Tectonostratigraphic Terranes can therefore be applied. Tectonostratigraphic Terranes are defined as fault bounded entities

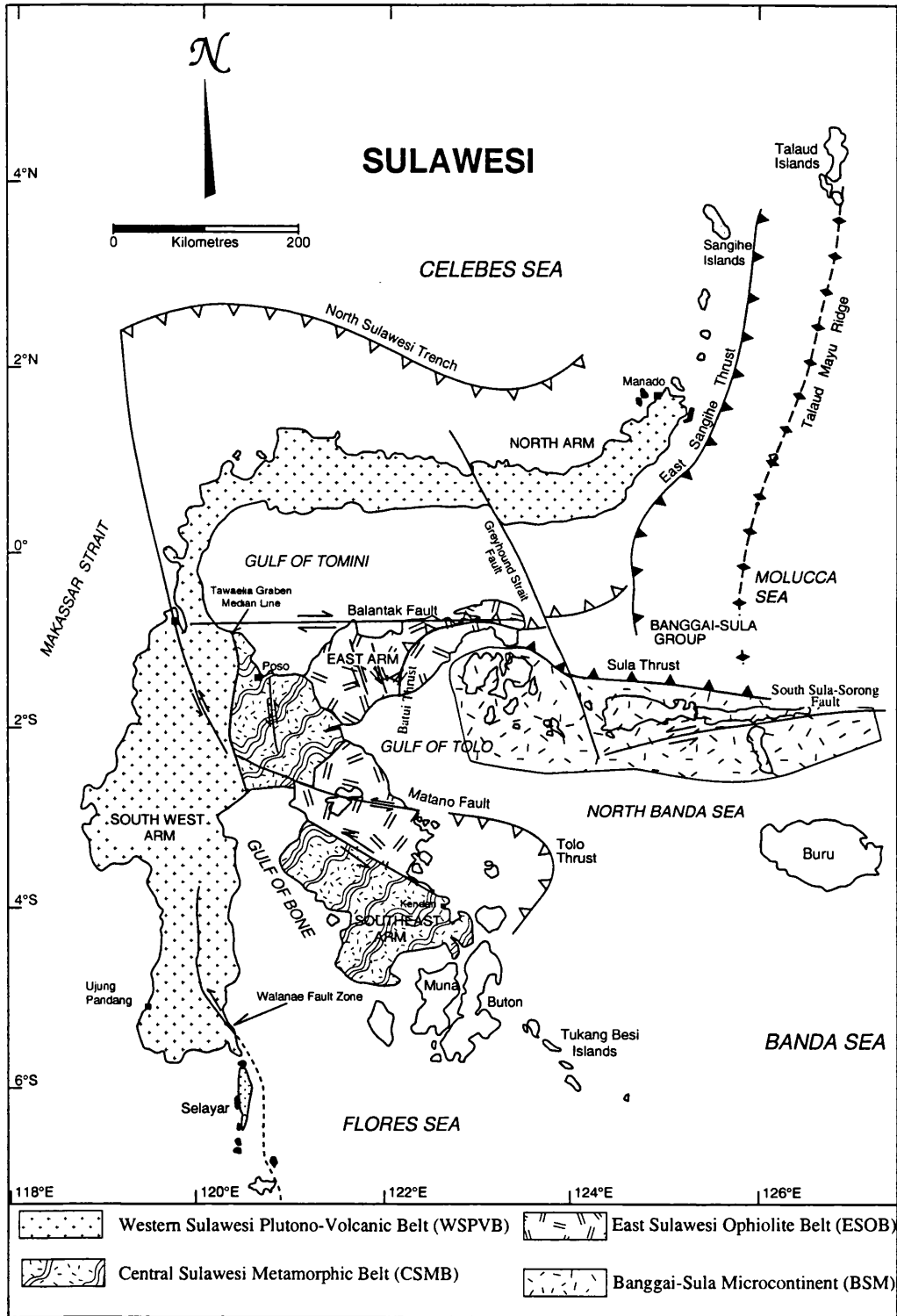


Figure 5.1: The four major belts and tectonic setting of Sulawesi (sources; Hamilton 1979; Silver et al. 1983; Simanjuntak 1990; Daly et al. 1987, 1991; Parkinson 1991)

of regional extent, each characterised by a geologic history that is different from the histories of contiguous terranes (Howell and Jones 1983, in Hartono and Tjokrosapoetro 1984). Although it is clear that Sulawesi can be described in these terms, the history of amalgamation of each terrane still remains subject to debate.

It is generally accepted that Sulawesi is divided into four major belts (see Fig.5.1) i.e., the Banggai-Sula Microcontinent (BSM); the Eastern Sulawesi Ophiolite Belt (ESOB); the Central Sulawesi Metamorphic Belt (CSMB) and the Western Sulawesi Plutono-Volcanic Belt (WSPVB). Hamilton (1979) divided Sulawesi into western and eastern arcs. The western arc includes the South and North arms and the western part of Central Sulawesi, where subduction complexes are overlain by sediments. The eastern arc includes the East and Southeast Arms and the eastern part of Central Sulawesi and consists of fragments of ophiolites and of subduction complexes. Bone Bay lies geographically between the Southwest and Southeast arms of Sulawesi, and in terms of the major belts listed above it lies at the boundary between WSPVB and CSMB. Brouwer (1949; in van Bemmelen 1949) considered the Palu Zone (equivalent to WSPVB) and the Poso Zone (equivalent to CSMB) to be separated by a distinct sub-zone named the Tawaelia Graben, defined by faults. The main fault of the Tawaelia Graben lies on the western side of the zone and was termed the Median Line (see Fig. 5.1). Along the Median Line a mylonitic zone is found which generally dips almost vertically, although westward dips of 45° are present. This has been interpreted by Hamilton (1979) as melange associated with the eastern arc. The location of the Median Line suggests that it continues southwards into Bone Bay. Brouwer (1949) also suggested that during the Late Neogene a strait separated the western and the eastern zones of Central Sulawesi and that thereafter the sedimentary deposits in this strait were folded and elevated well above sea level. Van Bemmelen (1949) described the Tawaelia Graben as being filled with strongly folded Late Neogene volcanics.

5.3.1 Western Sulawesi Plutono-Volcanic Belt (WSPVB)

This belt is characterised by crystalline schist rich in biotite, extensive massifs of granodioritic rocks, and sediments which were in general deposited closer to shore than those of the Eastern Ophiolite Belt (van Bemmelen 1949). Katili (1978) suggested that

this belt formed the magmatic arc related to the Tertiary subduction in the east. Van Leeuwen (1981) stated that the ages of the volcanic rocks varied from Palaeogene to Quaternary.

The basement of the province (the Bantimala Complex) crops out in two small windows (Bantimala and Barru). It consists of serpentinitised peridotites interthrust with highly deformed metaclastic greenschist and epidote amphibolites, and a tectonic melange of unmetamorphosed pelagic and terrigenous sediments, gabbros, amphibolites and blueschist (Parkinson 1991). Radiometric dating yielded a metamorphic age of 111 Ma. for the schist (Hamilton 1979).

5.3.2 Central Sulawesi Metamorphic Belt (CSMB)

This belt consists largely of epi to meso-metamorphic crystalline schist, rich in muscovite (van Bemmelen 1949). Helmers *et al.* (1989) conducted a survey of the metamorphic rocks in the Southeast Arm of Sulawesi and concluded, on the basis of structural and microstructural studies and determinations of mineral compositions, that these rocks had suffered HP/LT metamorphism during subduction-related fast burial to a depth of around 30 km. These metamorphic rocks have usually been regarded as uniformly metamorphosed and having a common genetic history (Hamilton 1979, Katili 1978, Silver *et al.* 1981). However Parkinson (1991) divided the CSMB into two different lithotectonic components, the Pompangeo Schist Complex (PSC) and the ophiolite and melange complexes

The Pompangeo Schist Complex (PSC) is a multiply and highly deformed but coherent basement of continental margin metasediments, which displays an intermediate to high P/T progressive field gradient from east to west. A K-Ar age determination on this rock yielded an age of 111 Ma (Parkinson 1991). The ophiolite and melange complexes are situated in eastern Central Sulawesi, where a wide variety of highly disrupted and metamorphosed ophiolitic and related rocks overlie the PSC. They comprise, from top to base; (i) Ultramafic tectonites at the base of the East Sulawesi Ophiolite. (ii) A metamorphic sole with an inverted metamorphic gradient (the Mowomba Metamorphic Sole). A K-Ar age determination on this rock yielded an age of 31.3 Ma (Late

Oligocene) (Parkinson 1991). (iii) An east-dipping ophiolite melange nappe (the Peluru Melange complex). A K-Ar age determination on this rock yielded an age of 30.9 Ma (Oligocene)(Parkinson 1991).

5.3.3 Eastern Sulawesi Ophiolite Belt (ESOB)

This belt is characterised by extensive outcrops of basic and ultrabasic igneous rocks and Mesozoic limestones and cherts, partly rich in radiolaria (van Bemmelen 1949). Silver *et al.* (1981) interpreted the ultramafic rocks as representing the lower part of an ophiolite suite. Parkinson (1991) described the ultramafic rocks as a dismembered ophiolite consisting of variably crushed, brecciated, sheared and serpentinitised fragments interspersed with smaller masses of Mesozoic and Tertiary sediments. Simandjuntak (1986) suggested that the ophiolites of eastern Sulawesi represented a substantial area of oceanic crust with segments dating from Cenomanian to Early Palaeogene or alternatively oceanic crust of Cretaceous age studded with Palaeogene seamounts. The way in which these ultramafic rocks were emplaced is poorly understood. Several different hypotheses have been put forward, these being (Silver *et al.* 1981); (1) obduction of oceanic crust along faults with dips opposite to the direction of subduction, (2) slicing of wedges of ocean crust during subduction along faults subparallel to the direction of subduction, (3) diapirism, (4) cold intrusion along vertical faults and (5) emplacement associated with changing motion along transform faults. Silver *et al.* (1981) favoured the second hypothesis because of the westward (arc-ward) thickening of the ultramafics, their apparent dip below the schist belt and their close association with melange. Recent studies (Simandjuntak 1990; Parkinson 1991) have shown that the age of ophiolite and the associated melange lies in the range from Cenomanian to Oligocene. It is possible that the ophiolites were not formed continuously throughout this period of time, and different parts of the complex may have had different histories.

5.3.4 Banggai-Sula Microcontinent (BSM)

This easternmost of the Sulawesi tectonic belts is situated off the eastern tip of the East Arm. The basement of the Banggai-Sula islands and adjacent offshore regions consists of Permo-Triassic medium-grade amphibolites, gneisses and schists intruded by granitoids (Parkinson 1991). Unconformably overlying the basement is a thick sequence

of Jurassic and Cretaceous shelf clastics and carbonate platform sediments which Hamilton (1979) noted as being similar to the sequence of rocks found in the Bird's Head region of Irian Jaya. Hamilton (1979) suggested that the Banggai-Sula Platform was a part of Irian Jaya which had been displaced westward to its present position in collisional contact with the ophiolite and melange belts of Sulawesi.

5.4 BATHYMETRY

The bathymetric map of Bone Bay (Fig.5.2) is characterised by N-S to NNW-SSE trending elliptical contours, with a maximum water depth in excess of 3000 m. The contours define a symmetrical shape, with the deepest water in the centre of the bay. To some extent, this bathymetry resembles that of many continental rift zones with a symmetrical depression of a median valley flanking the uplifted topography in each side.

5.5 SEISMIC INTERPRETATION

A structural interpretation of Bone Bay has been derived from seismic reflection data. Four seismic profiles have been interpreted which cross the bay in an east-west direction (Fig.5.2), i.e. approximately perpendicular to the structural trends. These are, from north to south, IND 07, IND 48, IND 97 and IND 116. All these profiles are multi channel seismic reflection with 60 fold coverage. Energy source used in the seismic survey is airguns. For reasons of commercial confidentiality, these sections are reproduced here as interpreted line drawings only.

5.5.1 Seismic interpretation line IND 07

This northernmost profile lies at a latitude of about 3°S and has a length of about 76 km. The line drawing with its interpretation are shown in Figure 5.3. Reflectors can be grouped into three units; acoustic basement, folded sedimentary units and flat-lying sedimentary units.

Acoustic basement

This lowest unit is characterised by the absence of reflections. The contact with the overlying sediments is difficult to see, especially between SP 1300 and SP 2700. From SP 300 to SP 1300 the depth is estimated to increase from approximately 3.1 seconds

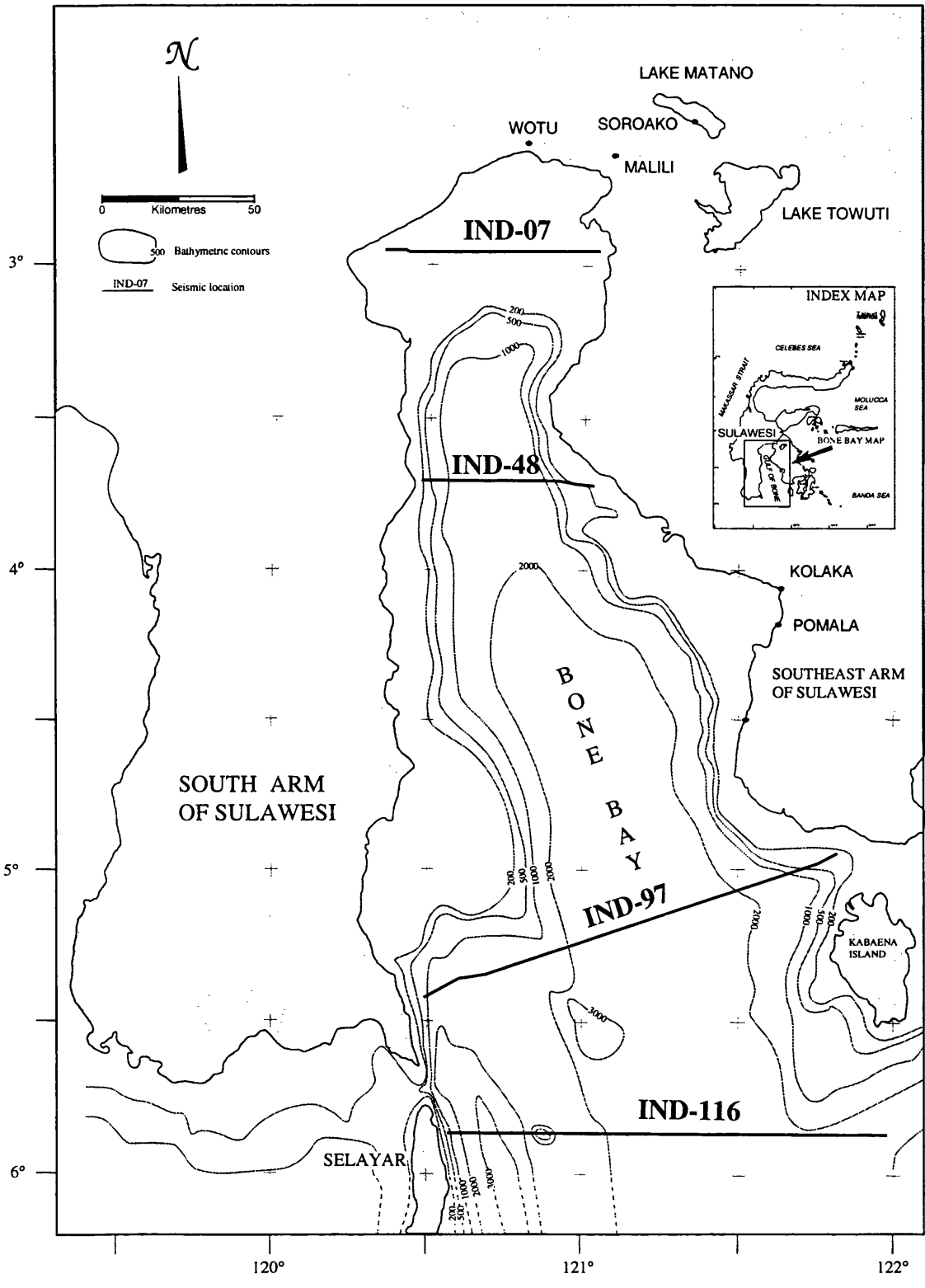


Figure 5.2: Bathymetric map and seismic location on Bone Bay

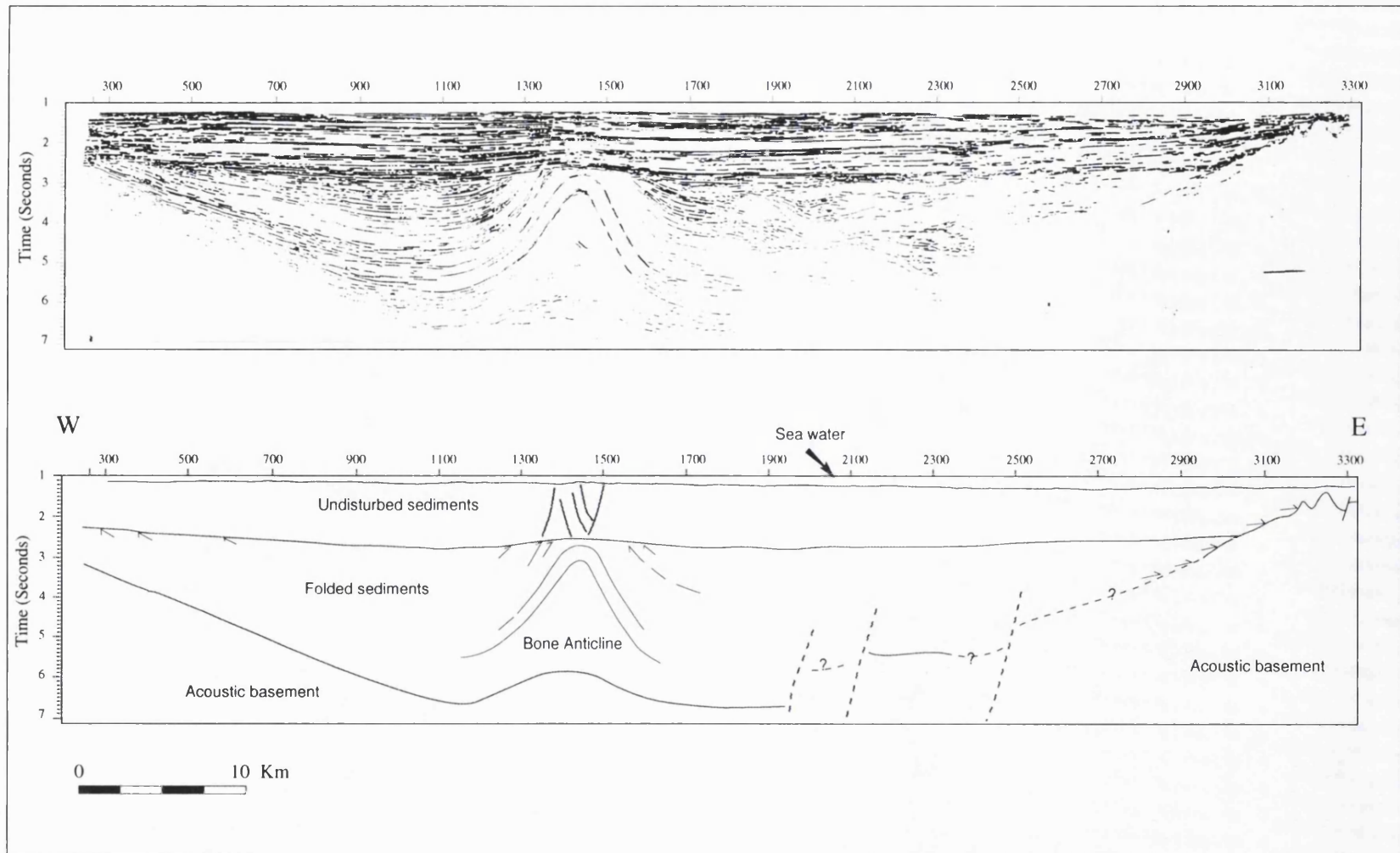


Figure 5.3: Seismic line drawing (above) and interpretation (below) of line IND 07 showing two major sedimentary units; folded and horizontal sediments in which the boundary between them marks the time of the collision between Banggai-Sula microcontinent and East Sulawesi. Arrows mark cycle terminations on onlap and toplap, which provide criteria for recognition of sequence boundaries.

TWT to 6.5 seconds TWT in the centre of the basin. From SP 2700 to SP 3300 the depth of acoustic basement decreases by faulting from 3.5 to 0.6 seconds TWT. Velocity analyses indicate that this unit has a lower velocity than the overlying sediments, which have a velocity in the range from 3000 m/sec to 4000 m/sec. The acoustic basement has an estimated velocity in the range 2000 m/sec and thus seems not to coincide with crystalline basement, being interpreted as consisting of low density material. There are several possible reasons for the presence of an apparent low velocity zone, ranging from errors in processing velocity data, multiples, over pressure zone, cracked layers, etc. The zone is seen along the whole profile and also on the other three seismic lines in Bone Bay. Considering that melange is exposed in the area surrounding Bone Bay, the low velocity material is interpreted as melange.

Folded sedimentary unit

This unit has been strongly folded into a symmetric anticline with flanking, asymmetric synclines. From SP 300 to SP 1900 the reflectors are continuous and have high amplitude and frequency but from SP 1700 to SP 2500 they are strongly disturbed, interpreted as associated with basement faults. The contact with the overlying sediments is clearly seen as an angular unconformity indicated by toplap of the upper folded sedimentary reflectors against the overlying sediments (SP 300 to SP 700, SP 1200 to SP 1700). Onlap of reflectors to the basement can be seen from SP 2700 to SP 3000. The strongly folded reflectors can be easily traced from SP 260 to SP 1600. The thickness of the unit varies from 0.8 seconds TWT to 3 seconds TWT.

Flat-lying sedimentary unit

This unit is characterised by undisturbed near-horizontal bedding with almost uniform thickness of about 1.5 km. From SP 1350 to SP 1500, i.e. in the axis of the anticline within the folded sedimentary unit, some small offsets of reflectors were observed which are not associated with disturbances to the underlying units. The offsets are interpreted as having occurred by reactivation of the axis of the anticline, representing a weakened zone.

The reflectors are characterised by parallel and continuous bedding with strong to medium amplitude, indicating marine deposition in a basin undergoing uniform and rapid subsidence (Vail *et al.* 1977).

5.5.2 Seismic interpretation line IND 48

This line is situated at latitude 3°45'S, and is 60 km long. It runs parallel to line IND 07 and approximately 80 km to the south. Unlike line IND 07, which shows the basin influenced by compression, line IND 48 shows a purely extensional feature. The line drawing and interpretation are shown in Figure 5.4. The reflectors can be divided into two major units, these being the acoustic basement and sedimentary units.

Acoustic basement

This unit is characterised by the absence of reflections. The contact with the overlying sediments is not clearly seen, probably because the density contrast between the two units is very low. A good contact can be seen in a few places such as at SP 150 - SP 250 and SP 2250 - SP 2500. Velocity analyses along the profile show that this unit has a velocity lower than that of the overlying sediments. The sediments have velocities in the range between 3000 m/sec and 4000 m/sec whilst the velocity in the acoustic basement is estimated to be about 2000 m/sec. If this estimate is correct, the unit is not crystalline basement but low velocity materials interpreted, as explained in Section 5.5.1, as melange.

Sedimentary units

Seismic sequence analysis using the procedures of Vail *et al.* (1977) suggest division of the sedimentary units into two seismic sequences. The boundary between the two is an unconformity or correlative conformity which can be recognised by onlap, downlap and toplap.

Seismic sequence 1

The reflectors are characterised by high amplitude reflections. Faults dip to the basement but do not reach the surface. The unit consists of sediments of variable thickness deposited in and over a complex system of tilted fault structures. The maximum

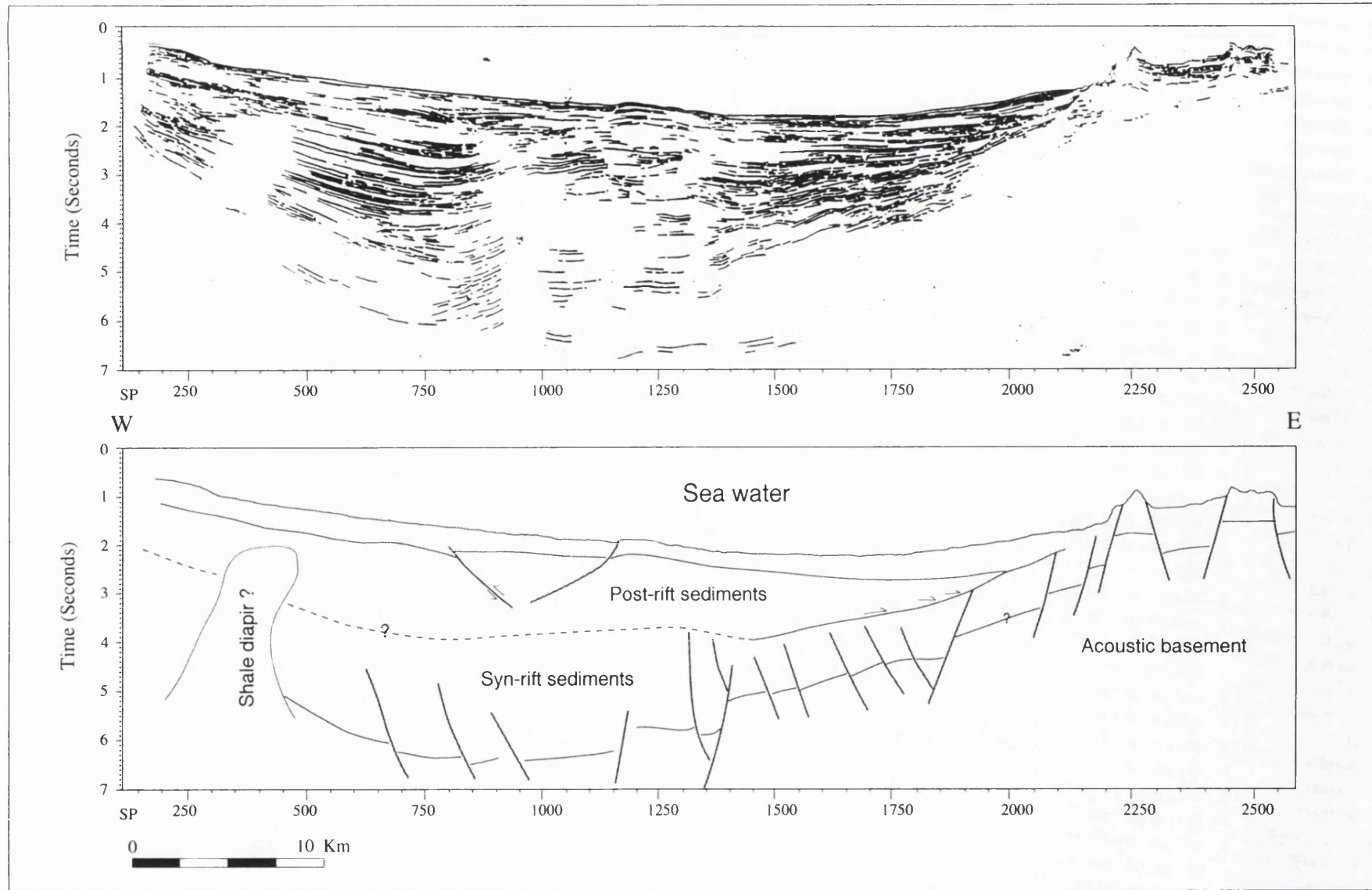


Figure 5.4: Seismic line drawing (above) and interpretation (below) of line IND 48 showing the presence of extensional basin in Bone Bay. Arrows mark cycle terminations on onlap, which provide criteria for recognition of sequence boundaries.

thickness is about 2.5 second TWT (approx. 3 km). Intrusion-like structures which can be seen from SP 300 to SP 450 are thought to be a shale diapirs because they occur where the sediment thickness is more than 6 km. Such a thickness can, under the right conditions, lead to shale diapirism at depth. The basin geometry is consistent with a horst and graben structure and is the basis for inferring that the sedimentary deposits can be classified as syn-rift.

Seismic sequence 2

This unit is characterised by sub-parallel reflections with fair continuity and medium-high amplitude. The sequence was deposited during a tectonically undisturbed period as the sediments are only rarely displaced by faults. The maximum thickness is about 2.5 seconds TWT (approx. 3 km). A few local faults are thought to date from the late rift phase. The unit is interpreted as post-rift sediments. The generally uniform spacing and lateral continuity of reflectors suggest deposition in a marine environment, in a rapidly subsiding basin (Vail *et al.* 1977).

5.5.3 Seismic interpretation line IND 97

This line runs NE-SW between about 5°S and 5°30'S, from east of the Southwest Arm to south of the Southeast Arm of Sulawesi, and is approximately 150 km south of Line IND 48. The length of the line is approximately 150 km. The geometry of basin is not much different from that on Line IND 48, showing the result of extensional processes. The maximum thickness of sediments, of more than 4 seconds TWT (more than 5 km), occurs in the centre of the basin in a water depth of more than 2 km. The line drawing and interpretation are shown in Figure 5.5. The reflectors can be grouped into two major units, these being acoustic basement and sedimentary units.

Acoustic basement

This unit is characterised by the absence of reflections. The contact with the overlying sediments cannot really be traced, except from SP 4500 to SP 6500. From SP 3150 to SP 4050 the basement lies deeper than the base of the seismic profile at 7 seconds TWT. Velocity analyses along this profile once again suggest that the velocities in this unit are about 2000 m/sec, i.e. lower than those in the overlying sedimentary unit, where they are

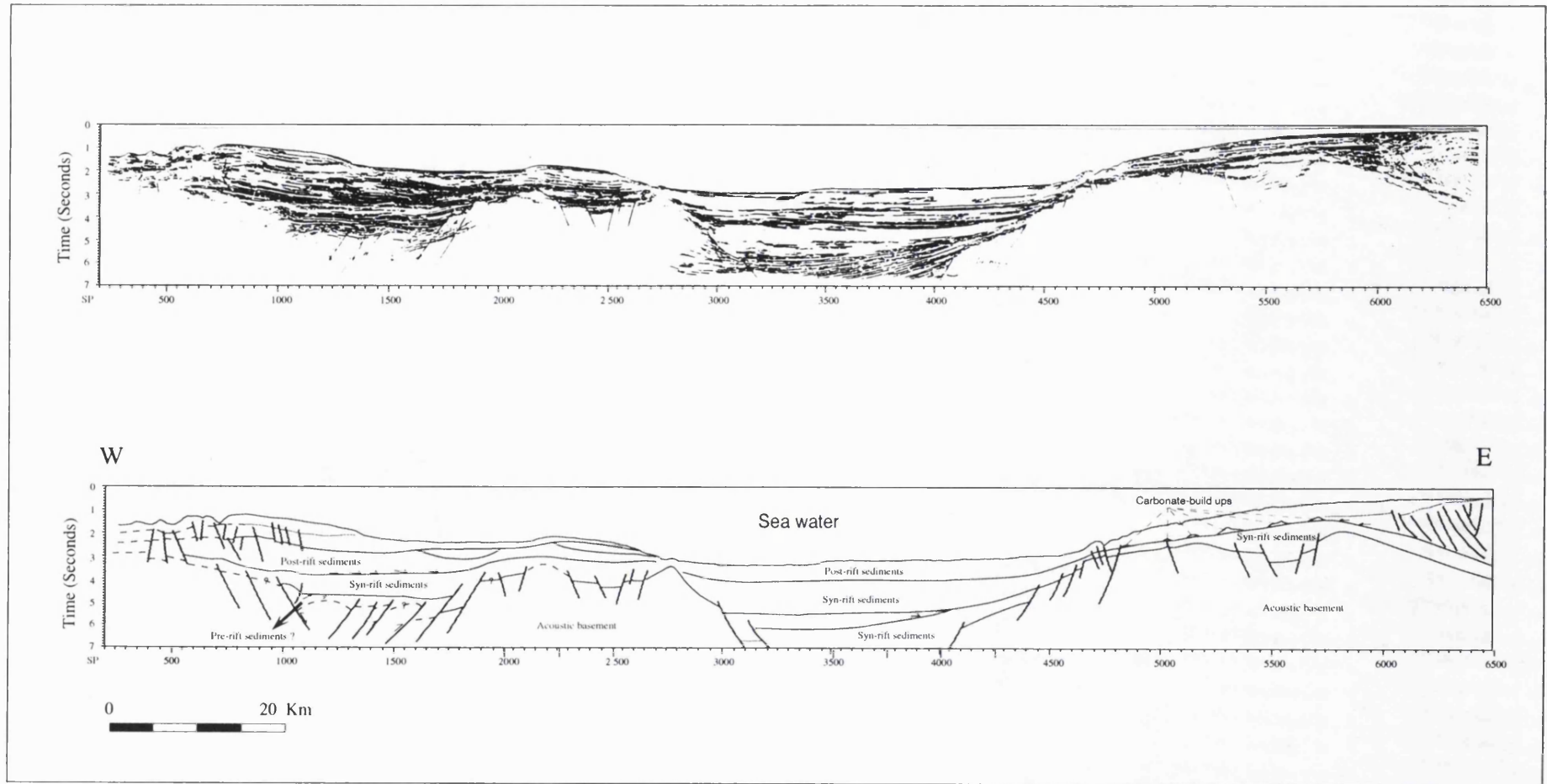


Figure 5.5: Seismic line drawing (above) and interpretation (below) of line IND 97 showing the presence of extensional basin in Bone Bay. Arrows mark cycle terminations on onlap and downlap, which provide criteria for recognition of sequence boundaries.

in the range between 3000 m/sec and 3500 m/sec. This is interpreted as indicating that the unit consists of low density melange.

Sedimentary unit

As on line IND 48, this unit is divided into two seismic sequences.

Seismic sequence 1

The sequence is characterised by extensive basement faults which define graben and half-graben structures filled with sediments. The reflectors within this unit are parallel to subparallel with high-medium amplitude. Divergent configurations occur from SP 3000 - SP 4050 with high amplitude, indicating rapid sedimentation in a fault controlled setting. There are two major depressions, the first from SP 900 to SP 1950 and the second from SP 2750 to SP 4550. In the first depression it appears probable, although the image is not entirely clear, that the pre-rift sediments(?) are bounded by east-dipping thrust faults between 4.8 sec and 5.8 sec TWT. In the second depression, the base of the sediments was not recorded as it lies deeper than the maximum time recorded (7 seconds TWT). This sequence is interpreted as syn-rift sediments.

Seismic sequence 2

This unit is characterised by parallel-subparallel reflectors with fair to good continuity and medium to high amplitude and has not been displaced by major faulting. Local effects can be seen from SP 350 to SP 1100 and are thought to have occurred after the late rifting phase. A complex thrust displacing the youngest sediments is observed towards the end of profile (SP 6000 - SP 6500), suggesting that compression took place after the deposition of the youngest sediments, which are probably Pleistocene in age. From SP 4800 to SP 5750, small carbonate build-ups can be observed, indicating a period of stable tectonics as required for the deposition of reef carbonate.

The generally uniform spacing and lateral continuity of the sedimentary layers suggest deposition in a marine environment, in a rapid and uniformly subsiding basin (Vail *et al.* 1977).

5.5.4 Seismic interpretation line IND 116

This is the southernmost of the four lines interpreted in Bone Bay. It is situated east of Selayar at latitude 5°57'S and is approximately 160 km long. The geometry of the basin is not very different from that seen on the lines to the north, which show a basin formed by extensional processes. The line drawing and interpretation are shown in Figure 5.6. This is the only interpretation of the four lines where the depth has been converted from time (seconds) into a depth (km) using an average velocity. The most prominent feature of this profile is the presence of a trough from SP 350 to SP 800, having a water depth of approximately 3000 m and bounded by normal faults in both sides.

The reflectors can be divided into acoustic basement and sediments. The boundaries between them are unconformities or correlative conformities which can be recognised by onlap, downlap and downlap of the reflectors.

Acoustic basement

This unit is characterised by the absence of reflections. The contact with the overlying sediments can be seen quite clearly between SP 2250 - SP 5750. However, it seems that this acoustic basement is not crystalline but merely low density material because velocity analyses along the profile show velocity decreasing from approximately 3000-4000 m/sec in the overlying sedimentary unit to 2000 m/sec. This low velocity material is interpreted as melange.

Sedimentary units

This sedimentary units are divided into two seismic sequences, using the same procedure as on lines IND 48 and IND 97.

Seismic sequence 1

This unit is characterised by parallel or subparallel reflections with fair to good continuity and medium to high amplitude. It was deposited in a complex system of tilted horsts and grabens, and ranges in thickness from 0.5 sec to 1.25 sec TWT. A possible intrusion is visible from SP 5850 to SP 6100. The unit is interpreted as syn-rift sediments.

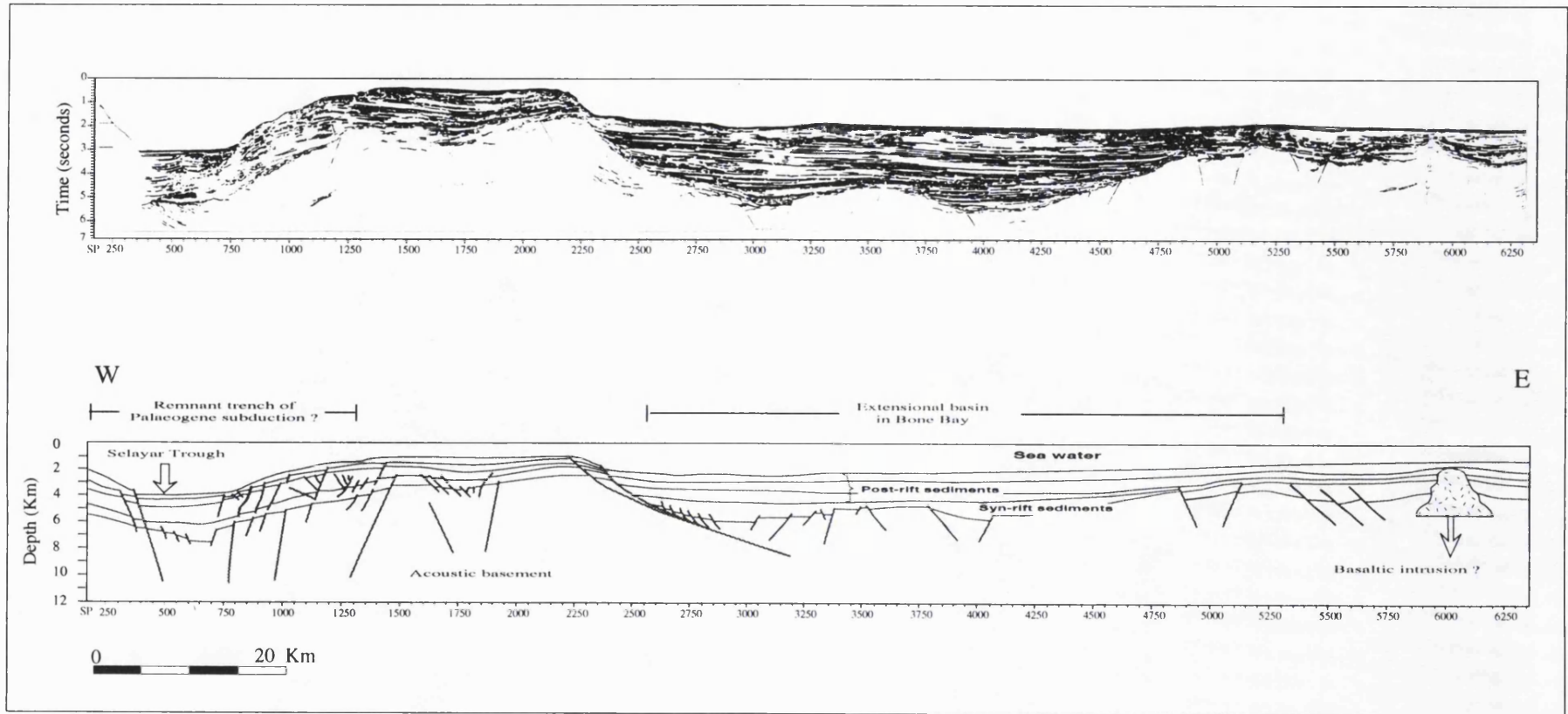


Figure 5.6: Seismic line drawing and interpretation of line IND 116E showing the presence of extensional basin in Bone Bay

Seismic sequence 2

This unit is characterised by parallel reflections with good continuity and medium-high amplitude. The unit was not affected by the block faulting, although there are some minor offsets from SP 750 to SP 1350, which are interpreted as reactivations of old basement faults. The generally uniform spacing and lateral continuity of the reflectors suggest deposition in a marine environment, in a uniformly and rapidly subsiding basin (Vail *et al.* 1977).

5.5.5 Summary

Of the four seismic reflection profiles interpreted in Bone Bay, three (IND 48, IND 97 and IND 116) show basins formed by normal faults that displace basement acoustic. They also show a later sedimentary section which is not displaced or significantly down-bowed over the basement faults. The flat sedimentary strata onlap and cover the basement, indicating that these strata were deposited after basement faulting had ceased and the graben had subsided. Such basins are obviously products of extensional processes. In terms of seismic stratigraphy the sedimentary reflectors can be divided into two major megasequences i.e., Seismic Sequence 1 which is interpreted as syn-rift and Seismic Sequence 2 which is interpreted as post-rift. Small faults displaced the post-rift sediments above the basement faults, indicating a minor late rifting phase, and some faults are associated with magmatic intrusions or shale diapirism.

Velocity analyses along the four seismic profiles confirmed the presence of low velocity (approximately 2000 m/sec) in the interpreted acoustic basement. The overlying sediments have velocities in the range 3000 m/sec to 4500 m/sec. This is interpreted as indicating the presence of low density material beneath Bone Bay which may be correlated with the melange in the Southeast Arm and Central Sulawesi (probably part of the Peluru Melange Complex in Central Sulawesi).

Seismic reflection line IND 07 clearly demonstrates the presence of a very strongly folded sequence which is unconformably overlain by a flat sedimentary sequence. In contrast, to the south of this strongly folded sequence is an area of extension, as seen on lines IND 48, IND 97 and IND 116. Although the age of tectonism is not well

constrained due to lack of data, it can be speculated that the major angular unconformity on line IND 07, indicating a major period of orogenesis in the whole region, can be correlated with the major orogenesis in the Sulawesi in the Middle Miocene.

It is also suggested that when the area in Line IND 07 experienced compression, the southern region experienced extension, as seen on lines IND 48, IND 97 and IND 116.

The Selayar Trough, seen on seismic line IND 116, clearly shows block faulting, which is probably continuous with the Walanae Graben of South Sulawesi.

5.6 GRAVITY DATA

5.6.1 Introduction

A gravity anomaly map of Bone Bay and the surrounding areas has been prepared by compiling gravity data from a number of sources (Fig.5.7). On the mainland of the South Arm of Sulawesi the data came from the GRDC Bouguer anomaly map (Simamora and Marzuki, 1990); on the coast of the Southeast Arm and Central of Sulawesi the data came from the Bouguer anomaly map of Silver *et al.* (1981); in Bone Bay the data came from the free-air anomaly map of Bowin *et al.* (1980); on Selayar Island the data came from the 1993 Flores Sea islands gravity survey and in the marine area between South Sulawesi and Selayar the data came from the Edcon free-air anomaly map (Edcon, 1991).

5.6.2 Qualitative gravity interpretation

The interpretation covers the area of Bone Bay extending between South and Southeast arms of Sulawesi and in the south approximately bounded in the east by Selayar at about latitude 6°S and longitude 122°E. This province is characterised by long N-S to NNW-SSE trending elliptical free-air anomaly contour closures. The trends are parallel to the main structures in Sulawesi. The contour values vary from -100 mGal to +150 mGal with the highest values in the eastern part of Bone Bay in isolated highs named the Wotu High, south of Wotu (maximum free-air anomaly +100 mGal), the Kolaka High, west of Kolaka (maximum free-air anomaly +150 mGal), and the Kabaena High, west of Kabaena Island (maximum free-air anomaly +100 mGal). It is possible that the latter

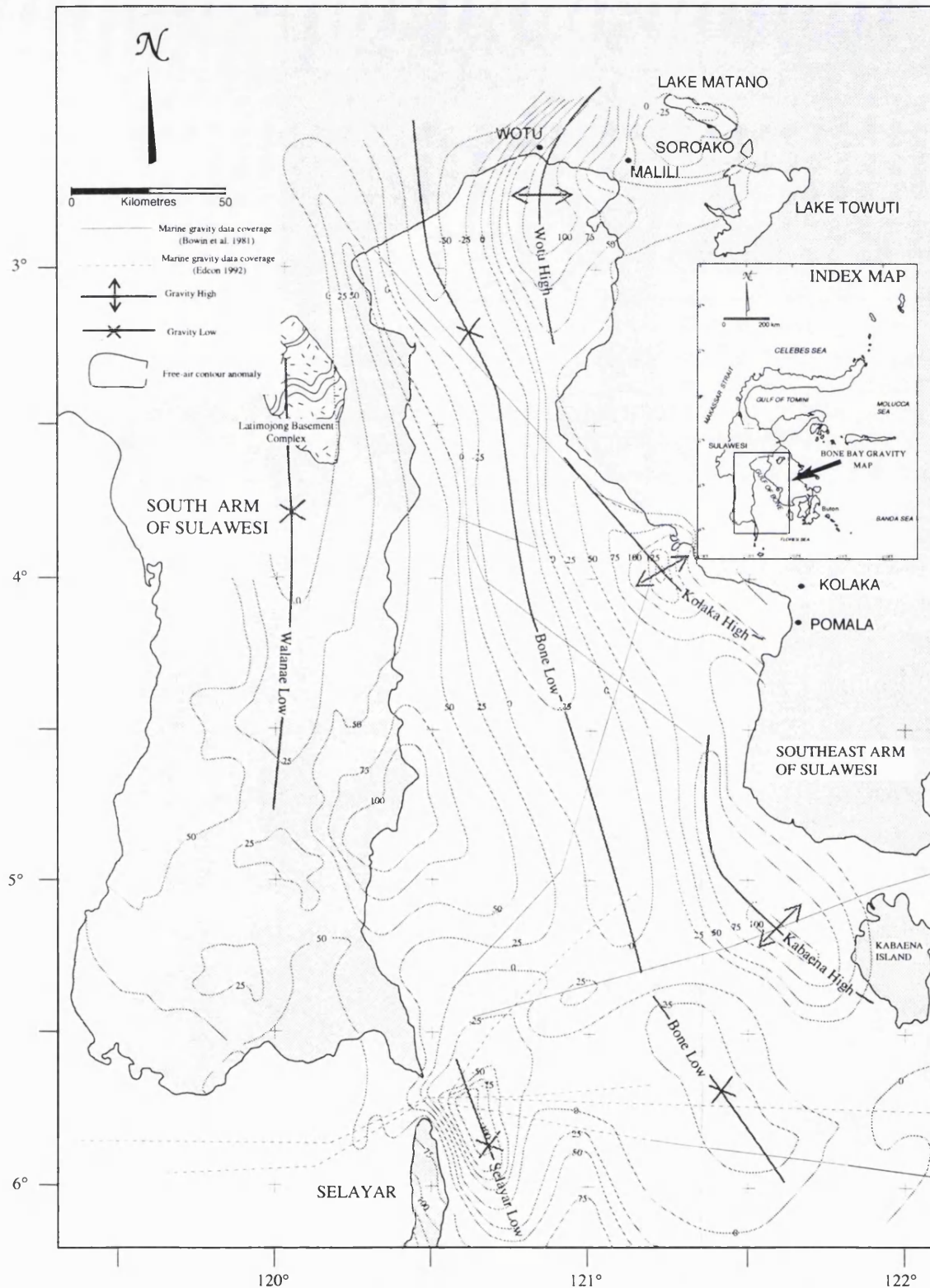


Figure 5.7: The free-air anomaly map of Bone Bay (Bouguer onland SW Sulawesi; modified from; Bowin et al. 1980; Silver et al. 1981; Simamora and Marzuki 1990; Edcon 1991; Flores Sea Islands Gravity Survey 1993)

high actually extends onto Kabaena Island, where no onshore data have yet been obtained but where ophiolitic rocks are known to outcrop (Milsom, pers. comm., 1995). The area around Malili and Soroako, approximately 30 km east of Wotu, is known to be covered by ultramafic rocks (Silver *et al.* 1981) and Bouguer anomaly values over this area vary between +10 and +35 mGal. Therefore the free-air anomaly highs in the Wotu, Kolaka and Kabaena are thought to be due not only to the presence of oceanic crust but also and mainly to significant uplift of mantle. This might be associated with the emplacement of ultramafic rocks and ophiolite in the Southeast Arm of Sulawesi.

A prominent free-air low in the middle of Bone Bay (Bone Low) reaches a minimum value of below -50 mGal. This low can be roughly correlated with the rifted basins containing thick sedimentary rocks which can be seen on the seismic sections. The axis of the low seems to continue the trend of the Poso Graben of Central Sulawesi.

The lowest free-air anomaly values, of less than -100 mGal, occur to the east of Selayar. The low may continue onto the South Arm of Sulawesi as the Walanae Low, which reaches minimum values below 0 mGal, and to the south into the Flores Sea. On the South Arm of Sulawesi the low is associated with the sinistral Walanae Fault which has formed a graben-like structure filled with Neogene sediments (van Leeuwen 1981). If the free-air lows are really continuous, they form a structural feature about 600 km long.

5.6.3 Gravity models

5.6.3.1 Introduction

Gravity models have been constructed using the two dimensional GM-SYS gravity modelling program along the IND 07 and IND 116 lines. The models were constrained using these seismic profiles.

5.6.3.2 Interpretation

5.6.3.2.1 Gravity model IND 07

Figures 5.8a and 5.8b show two possible models of the crustal structure in Bone Bay. The models relate to a line across the northernmost part of Bone Bay, which is perpendicular to the structure and Bouguer anomaly contours. Both models provide good

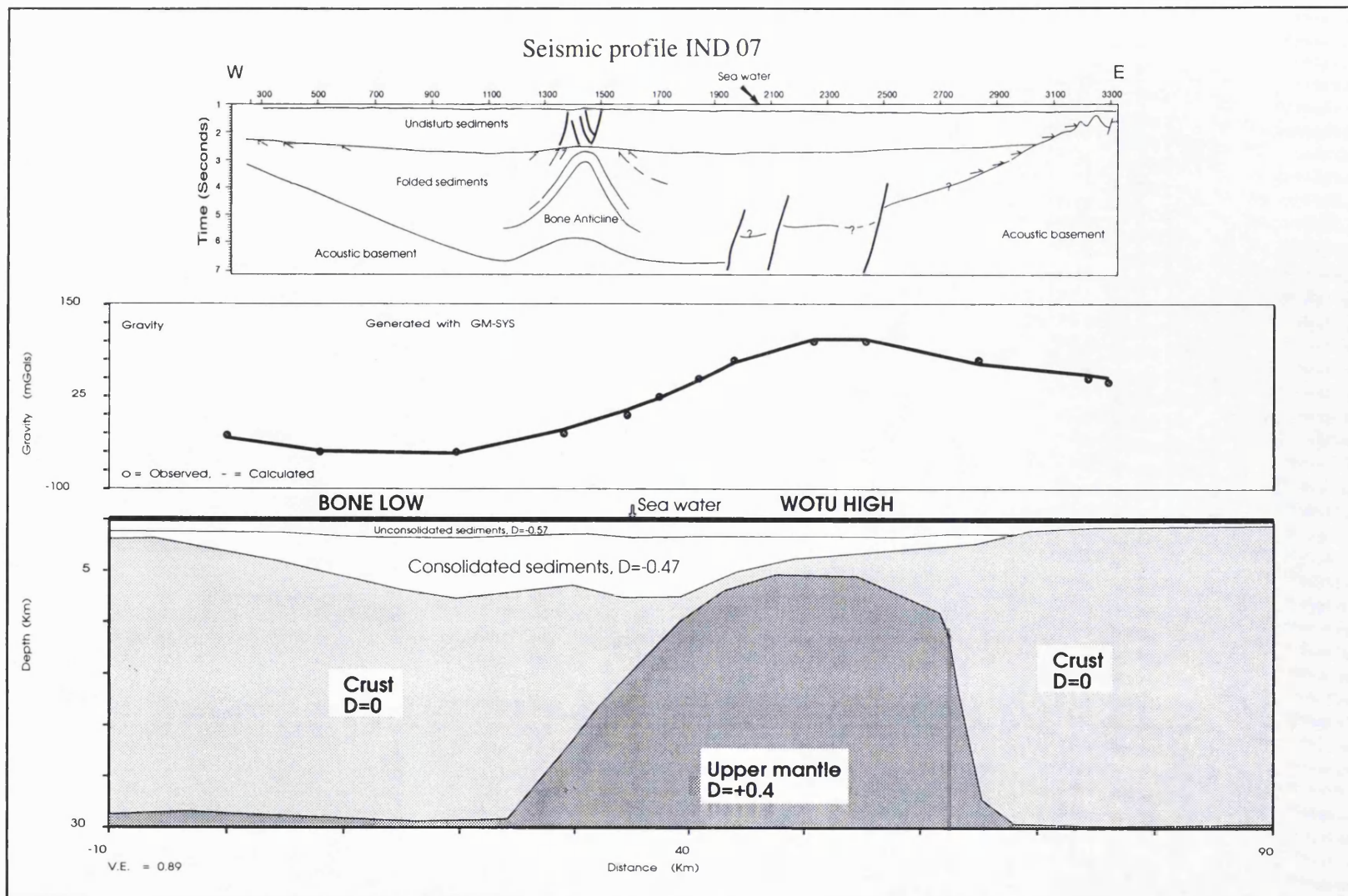


Figure 5.8a: Simplified gravity model of line IND 07 showing crustal structure in northern Bone Bay

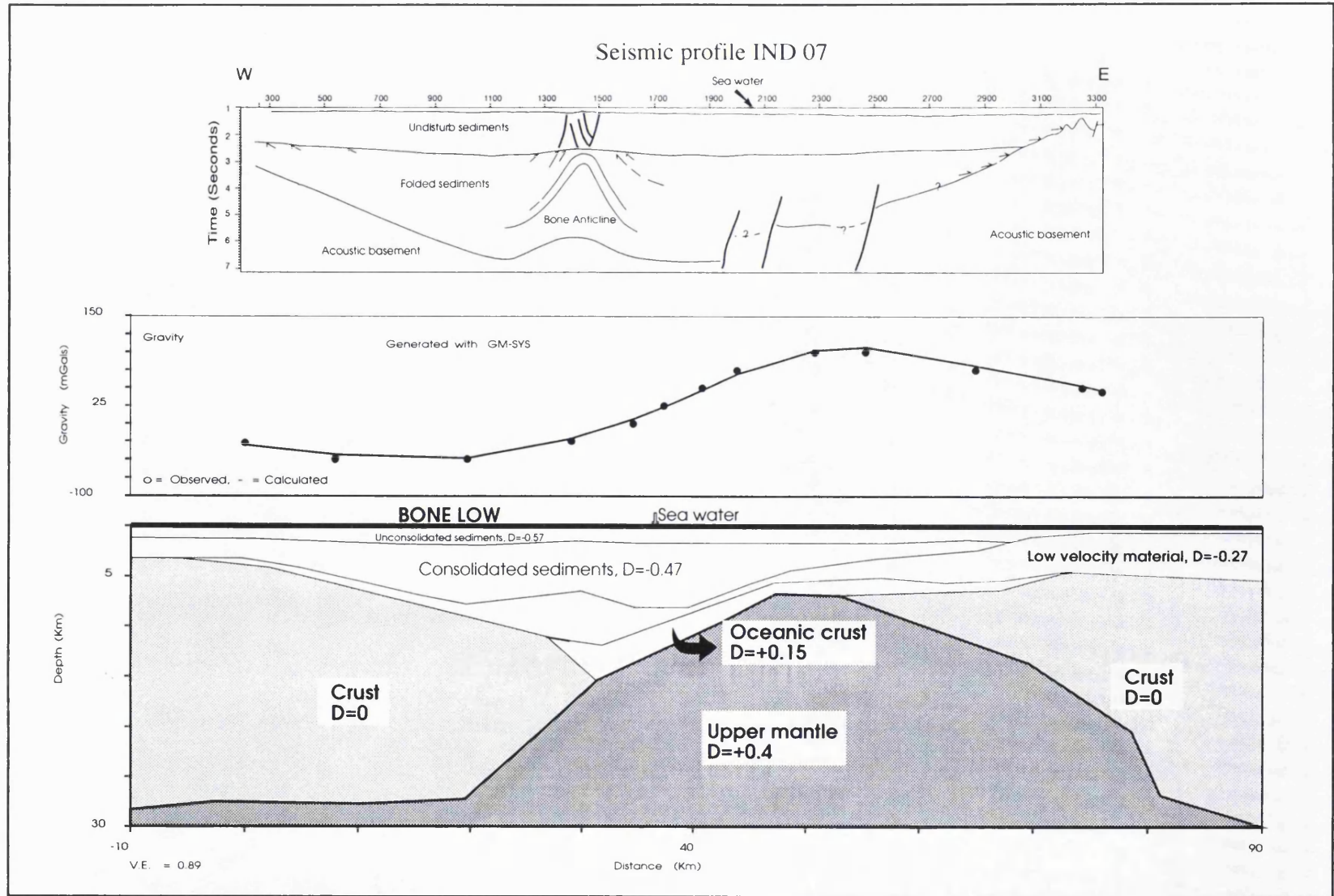


Figure 5.8b: Alternative gravity model IND 07 showing crustal structure in northern Bone Bay

matches between observed and calculated gravity anomalies and are in accord with the known geology.

The first model (Fig.5.8a) is a simple one constructed using four major layers, these being sea water (density = -1.64 Mg/m^3), sediments (geometry taken from seismic interpretation line IND 07 with assumed densities of -0.57 Mg/m^3 and -0.47 Mg/m^3 for unconsolidated and consolidated sediments, respectively), crust (no density contrast) and upper mantle (density contrast = $+0.4 \text{ Mg/m}^3$). In this model the Bone Low corresponds to the deepest basement, at about 7.7 km, and the thickest sediments. The depth of the Moho beneath this low is about 28 km, i.e. continental thickness. The Wotu High has a maximum value +100 mGal and in order to achieve these values it proved necessary to bring the upper mantle up to within 5 km of the sea surface.

In the second model (Fig.5.8b) it was assumed that the acoustic basement interpreted on seismic line IND 07 (see Fig. 5.4) was not crystalline basement but a zone of melange with a density contrast of -0.37 Mg/m^3 . This takes into consideration the fact that all velocity analyses along the profile show a decrease in velocity from about 3000-4500m/sec in the overlying sediments to 2000 m/sec. This model also suggests that Bone Bay is underlain by oceanic crust (with density contrast of $+0.15 \text{ Mg/m}^3$), which is supported by the presence of ophiolite and ultramafic rocks in the Southeast Arm and Central Sulawesi. The model shows that Bone Bay is flanked by two major blocks of continental crust to the west and east. The low velocity melange reaches a thickness of 12 km beneath the free-air low. The Wotu High still needs to be compensated by the large decrease in the depth of the upper mantle, bringing it up to 7.8 km beneath the sea surface. The model suggests that the crust thins toward the Southeast Arm of Sulawesi, whilst the melange becomes thicker.

5.6.3.2.2 Gravity model IND 116

Two possible gravity models (Fig.5.9a and b) have been proposed for the crustal structure of the southern part of Bone Bay. The models relate to a line which is perpendicular to structure and Bouguer anomaly contours. Both models produce good matches between observed and calculated gravity anomalies and the known geology. The

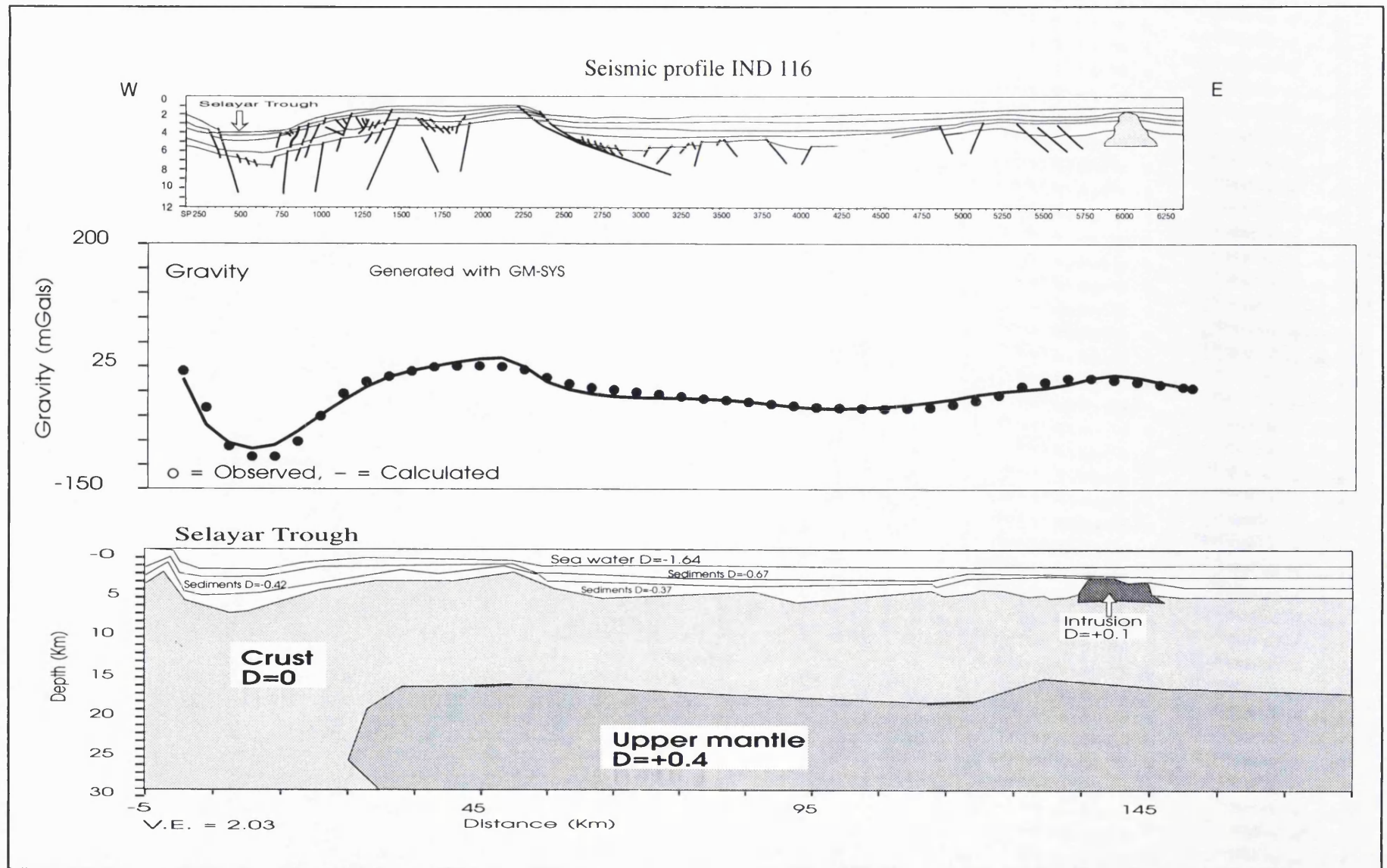


Figure 5.9a: Simplified gravity model IND 116 showing crustal structure in southern Bone Bay

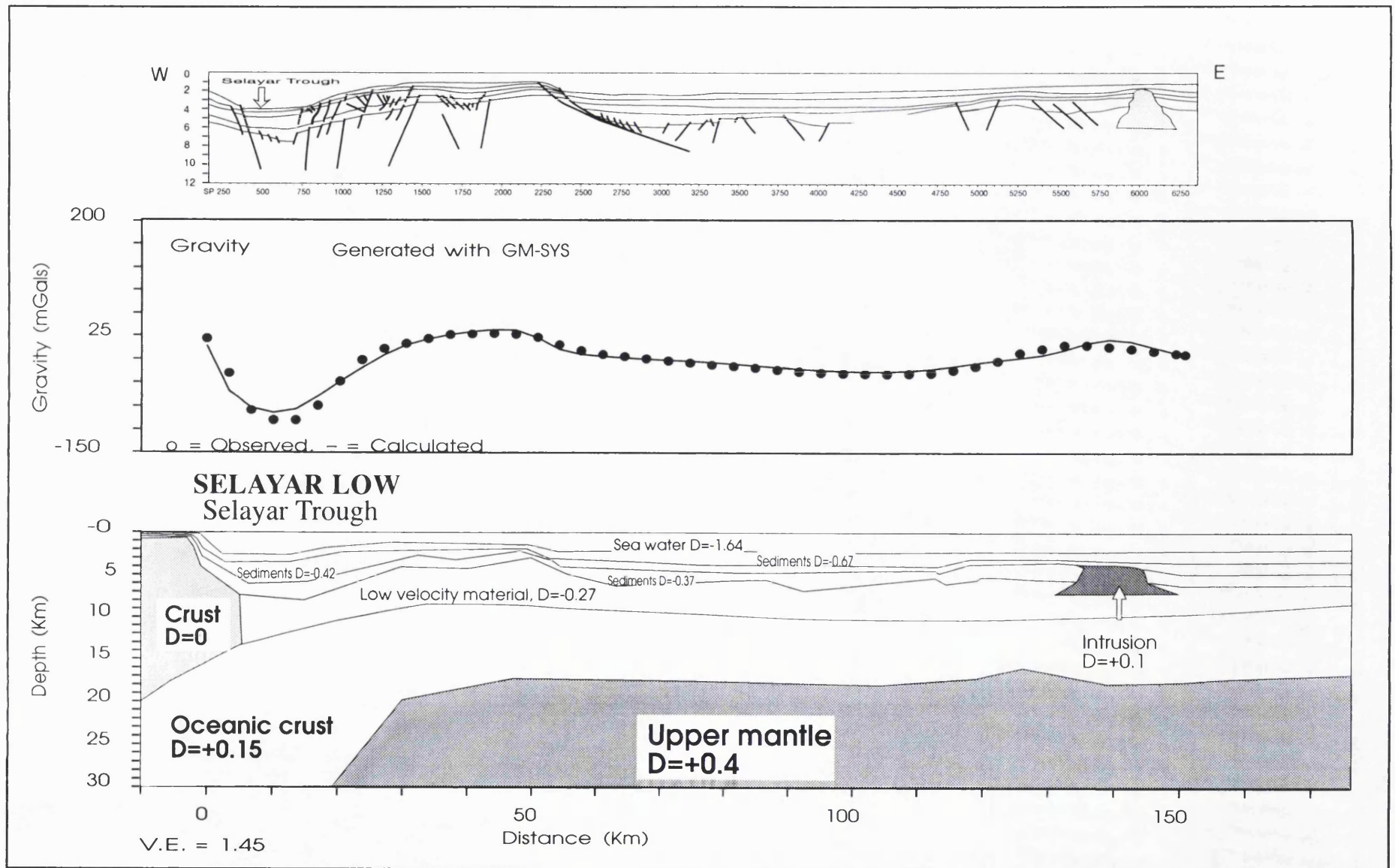


Figure 5.9b: Alternative gravity model IND 116 showing subducted oceanic crust beneath Selayar Island

greatest difficulty is in modelling the Selayar Low, which reaches -100 mGal east of Selayar Island.

The first model (Fig.5.9a) used the assumptions and modelling procedures of Fig.5.8a, with four major layers. The Selayar Low was modelled by taking the Moho down to a depth of 30 km. To the east of this low the depth of the Moho was decreased sharply, to between 16 to 19 km.

The second model (Fig.5.9b) used the assumptions of the model in Fig.5.8b, i.e. the acoustic basement was assumed not to be crystalline basement but low density melange, and the bay was assumed to be underlain by oceanic crust. The Selayar Low was modelled as due to subduction of oceanic crust beneath Selayar Island. The depth of the Moho beneath the Selayar Low was 30 km, and was decreased sharply to the east, to between 16 to 19 km.

5.7 CRUSTAL STRUCTURE

The two types of gravity models presented in Fig.5.8a & 5.9a (simple models) and Fig.5.8b & 5.9b (alternative models) do not show great differences in deep crustal structure. The simple models are compatible with the general information available on crustal structure. The alternative models, constrained by geological information in the adjacent regions, seem able to explain more of the details. The long and wide free-air low in the centre of Bone Bay is explained by a low density melange layer situated considerable deeper than the maximum depth of acoustic basement, at about 7.7 km. By introducing this low density layer the depth of true basement reaches about 12 km in the gravity models. The low density layer is interpreted as part of the melange belt exposed in the Malili-Soroako region about 25 km east of the end of the gravity model. The melange is in general in contact with the ophiolites along a low angle thrust with the ophiolites always forming the upper plate (Silver *et al.* 1981). The low (+10 and +35 mGal) Bouguer anomaly over the ultramafic rocks in the Malili-Soroako are thus explained by their being underlain by thick melange.

The gravity highs in the eastern part of Bone Bay are believed to be associated with the presence of ophiolitic and ultramafic rocks in the Southeast Arm and Central Sulawesi. In the gravity model IND 07 these highs are produced by raising the mantle to within almost 5 km of the sea surface but the same effect can be achieved by introducing thick oceanic crust beneath the high. However, towards the Southeast Arm of Sulawesi the oceanic crust has to be made thinner whilst the low density sedimentary layer has to be made thicker in order to obtain a good fit between the observed and calculated free-air anomalies. This implies that the ophiolite and ultramafic rocks in the Southeast Arm and Central Sulawesi are thin bodies overlying thick low density sedimentary rocks. The geometry of the mantle in model IND 07, where the Moho is uplifted suddenly and steeply, may derive from transpressional processes associated with oblique convergence which was in turn responsible for the emplacement of the ophiolitic and ultramafic rocks.

5.8 TECTONIC IMPLICATIONS

One of the most prominent features of Sulawesi is the presence of left and right lateral strike-slip faults. The left-lateral faults strike roughly NW-SE and dominate nearly all of Sulawesi (see Fig. 5.1). Some of the major examples are the Walanae Fault, the Palu-Koro Fault, the Matano Fault and the Poso Fault. Right lateral strike-slip faults occur mainly in the East Arm of Sulawesi and were called the Balantak Faults by Simandjuntak (1990). The major fault systems are not single fault traces but segmented networks of sub-parallel strands, each accommodating some displacement (Parkinson 1991).

The Palu-Koro and Matano fault zones form a transform system linking the North Sulawesi Trench to the Tolo Thrust (Hamilton 1979). They consist of a large number of splays, one of which has been interpreted as extending south into Bone Bay, but seismic reflection profile line IND 07 does not show the presence of this large fault in the young sediments. This might indicate that the fault is older than the sediments.

The Walanae Fault Zone transects the WSPVB and is divided into West Walanae Fault and East Walanae Fault. The 15 km wide region between these two faults is occupied by

sediments deposited in a graben-like structure. On the basis of gravity contours, the Walanae Fault seems to continue southwards for more than 600 km to the Flores Sea through the Selayar Trough. The seismic interpretation of line IND 116 (Fig. 5.6), combined with the gravity model of Fig. 5.9b, is consistent with the Selayar Trough being a remnant subduction zone. The free-air low of about -100 mGal implies that the trough is underlain by thick low density rocks and was formed on thick crust. In making a gravity model, the Moho has to be placed very deep in order to match observed to calculated free-air anomalies. Fig. 5.9b shows buried oceanic subduction beneath the Selayar Trough. Such subduction can be related to the subduction of Eastern Sulawesi beneath Western Sulawesi but the timing is not well constrained. Subduction can also probably be related to the rocks in Pegunungan Latimojong, north of the Walanae Graben (see Fig. 5.7 for location), which have been interpreted by Parkinson (1994) as a basement complex or to the Oligocene Peluru Melange Complex in Central Sulawesi. These two melanges may be of the same age, although Sukanto (1975) regarded the Latimojong rocks as Cretaceous and Daly *et al.* (1991) proposed that East Sulawesi has been in contact with West Sulawesi since the Early Tertiary.

The collision between East Sulawesi and West Sulawesi is here regarded as having occurred at the same time as the emplacement of the Latimojong basement complex in SW Sulawesi, i.e. in the Oligocene (Barber, pers. comm., 1995), and possibly relates to the presence of oceanic crust in Bone Bay as interpreted from gravity models. This collision also reactivated the Median Line as a thrust fault and emplaced the Pompangeo Schist Complex above the West Sulawesi Plutono-Volcanic Belt. This event is believed to be the main reason for the cessation of subduction between East Sulawesi and West Sulawesi.

It is generally accepted that movements of the Sorong Fault Zone displaced the Banggai-Sula Microcontinent westwards and caused the collision of the microcontinent with East Sulawesi. This collision was marked by the formation of the Kolokolo melange which contains fragments from both the ophiolite suite and the continental margin sequence (Simandjuntak 1990). The boundary between these two terranes is placed at the Batui-Balantak Faults. The Middle-Miocene is regarded as the time of this

collision (Hamilton 1979; Simandjuntak 1990; Silver *et al.* 1981; Parkinson 1991). Its effects are recorded as compression in the north of Bone Bay (line IND 07) and extension in the south of Bone Bay (line IND 48, IND 97 and IND 116), as shown in Fig. 5.10. The extrusion model of Tapponnier (1982), developed to explain the tectonic evolution of mainland eastern Asia, can be extended to explain the compression and extension in Bone Bay with respect to the oblique convergence between Banggai-Sula Microcontinent and East Sulawesi, and also in terms of the formation of the complex strike-slip faults of Sulawesi (Parkinson 1992). Figure 5.11 shows the analogy between the extrusion model of Tapponnier and the structural patterns produced in Sulawesi as a result of indentation. The ages of structures such as the Walanae and Palu-Koro faults are also correlatable with the collision between Banggai-Sula and East Sulawesi in the Middle Miocene. The Walanae Fault itself is interpreted as a reactivation of remnant subduction. The continuous movement of the Banggai-Sula Microcontinent westwards is thought to have caused displacement and rotation between the Walanae Fault and the Palu-Koro Fault (Fig. 5.12). The rotation of western arc of Sulawesi during the interval Middle Miocene to Recent was also supported by palaeomagnetic data suggesting that the western arc rotated of about 40° anticlockwise (Sasajima *et al.* 1981). The result has been extension along the zone of weakness forming the present Bone Bay.

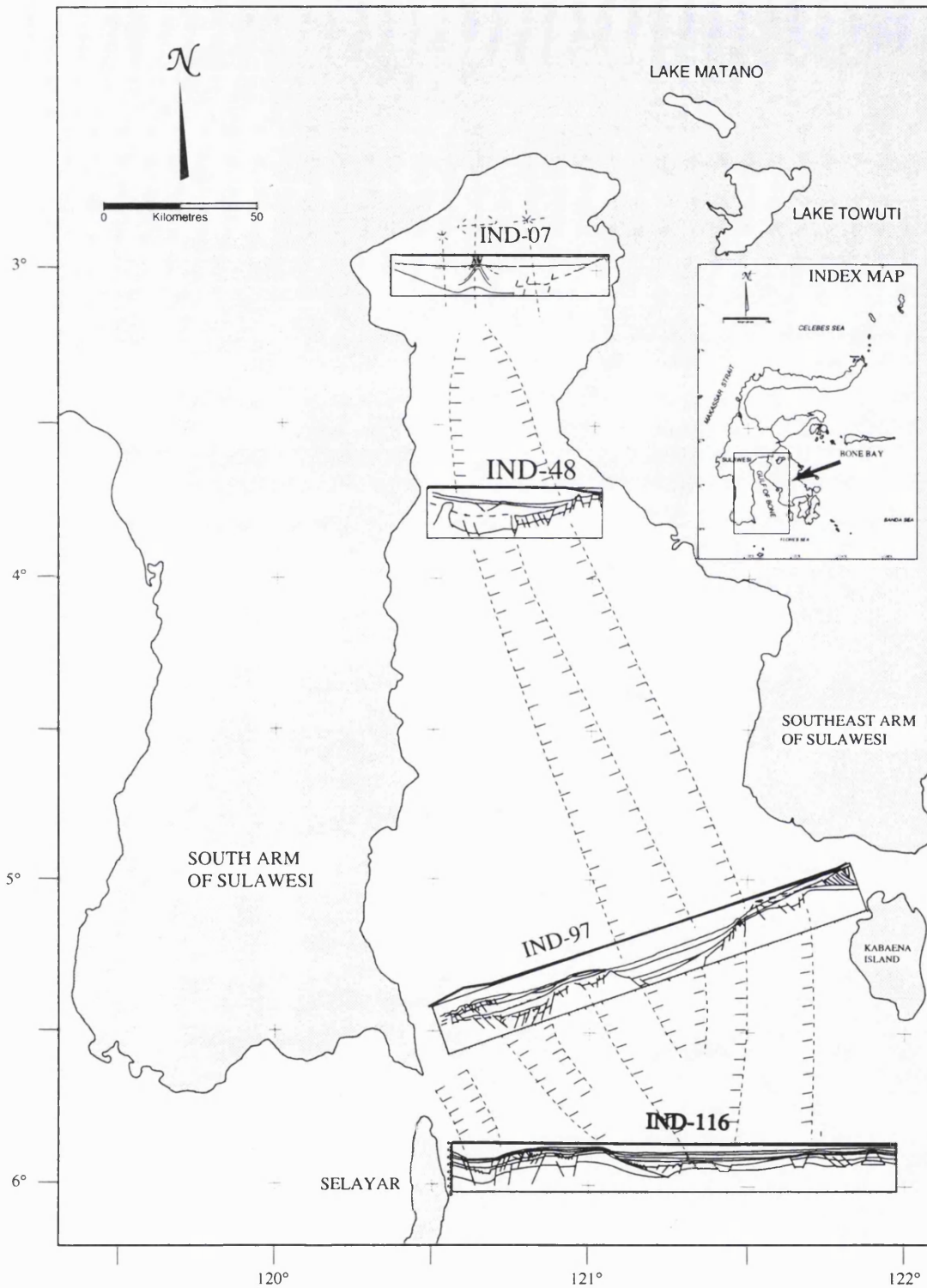


Figure 5.10: Possible correlation of seismic structures in Bone Bay constrained from gravity data

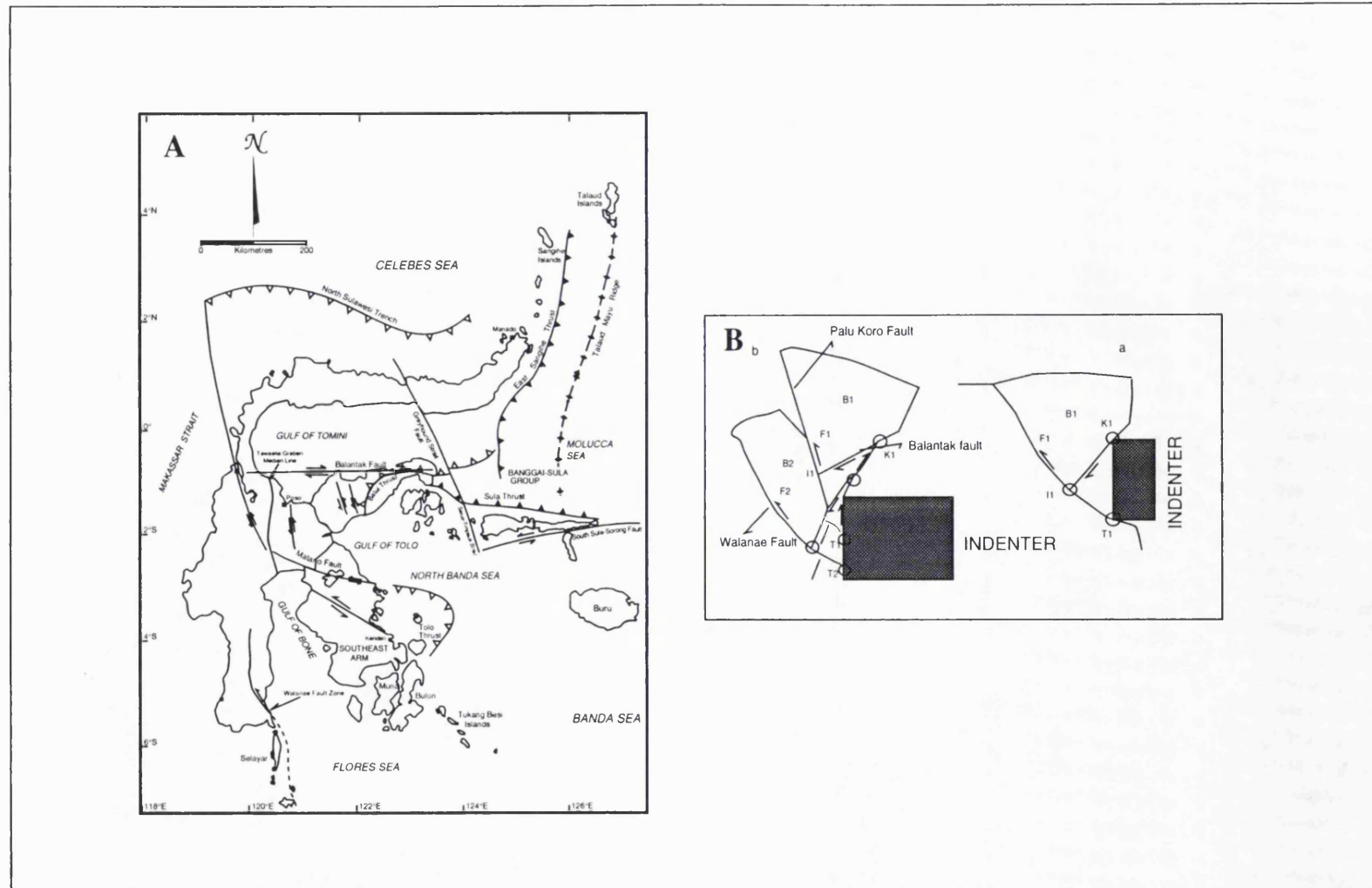


Figure 5.11: The comparison between strike-slip faults in Sulawesi (A) and the indentation model from Tapponnier (1982,1983) (B), showing the strike slip faults in Sulawesi are in agreement with the indentation model

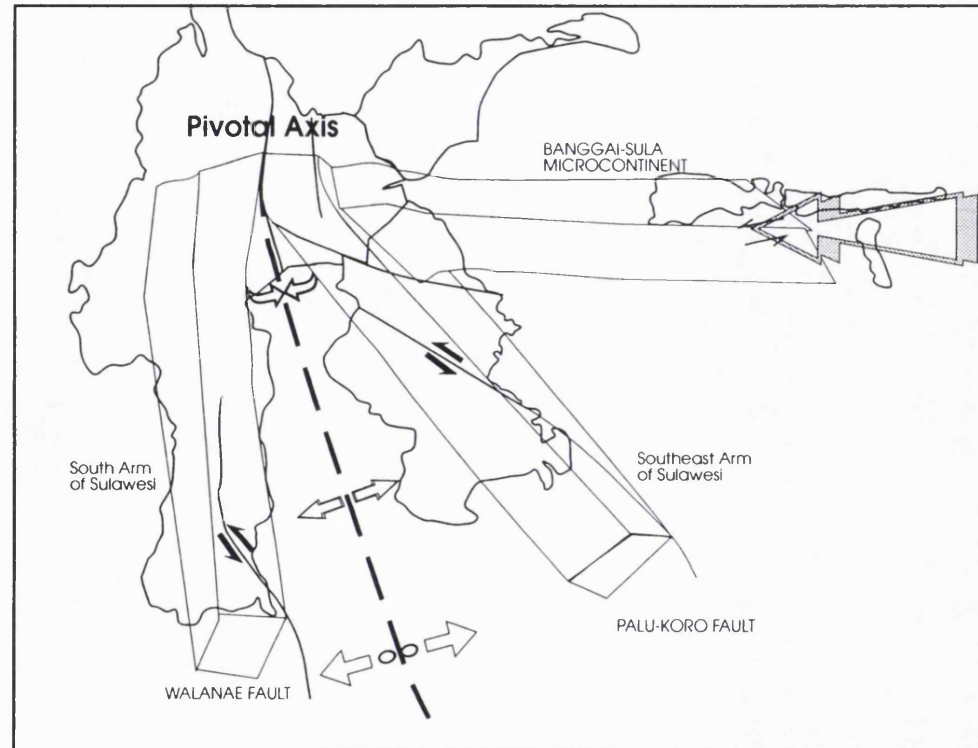


Figure 5.12: A Cartoon showing the effect of the Banggai-Sula collision to Sulawesi having caused displacement and rotation between two prominent strike-slip faults; the Walanae and Palu-Koro faults causing the opening of Bone Bay

CHAPTER SIX

MAKASSAR STRAIT PROVINCE

6.1 INTRODUCTION

The Makassar Strait is situated between Southeast (SE) Kalimantan and Western Sulawesi, and geologically separates the stable core of the Eurasian Plate to the west and the very active region of the triple junction of the three large plates to the east. To the north it is bounded by the Sulawesi Sea and to the south by the East Java Sea (Fig.6.1). The strait is roughly 100-200 km wide and 300 km long and geologically is usually divided into the North and South Makassar basins, separated by the Paternoster Fault (Katili 1973, Situmorang 1982). It is generally accepted that SE Kalimantan and Western Sulawesi once lay close together (Katili 1978; Hamilton 1979), the separation between the two being due to the opening of Makassar Strait. The age and driving mechanism for this opening are, however, still poorly understood.

The present study interprets the history of the Makassar Strait on the basis of seismic reflection profiles and gravity modelling, in addition to compilations of geological information. The implications for the origin of the rifting are also discussed.

6.2 PREVIOUS STUDIES

The origin and geological framework of the Makassar Strait have been considered by many authors, either in detailed studies of Makassar Strait or in compilations of the regional geology. It is generally agreed that the Makassar Strait formed as a result of spreading, but the details are uncertain. Katili (1978) proposed that the opening took place in the Quaternary along the Paternoster Fault, with the formation of oceanic crust. Rose and Hartono (1978) attributed the formation of the basin to counterclockwise rotation of Kalimantan during the Late Cretaceous and Early Palaeogene. Hamilton (1979) suggested that the Makassar Strait was formed by sea floor spreading in the Mid-Tertiary. Burrolet and Salle (1981) argued from the present depths of the Makassar Basin that it is a rhombochasm formed on rigid continental or intermediate crust. Situmorang (1982) explained the origin of Makassar Basin in terms of stretching from the Lower-Middle Eocene to Lower Miocene, and suggested that it is now underlain by

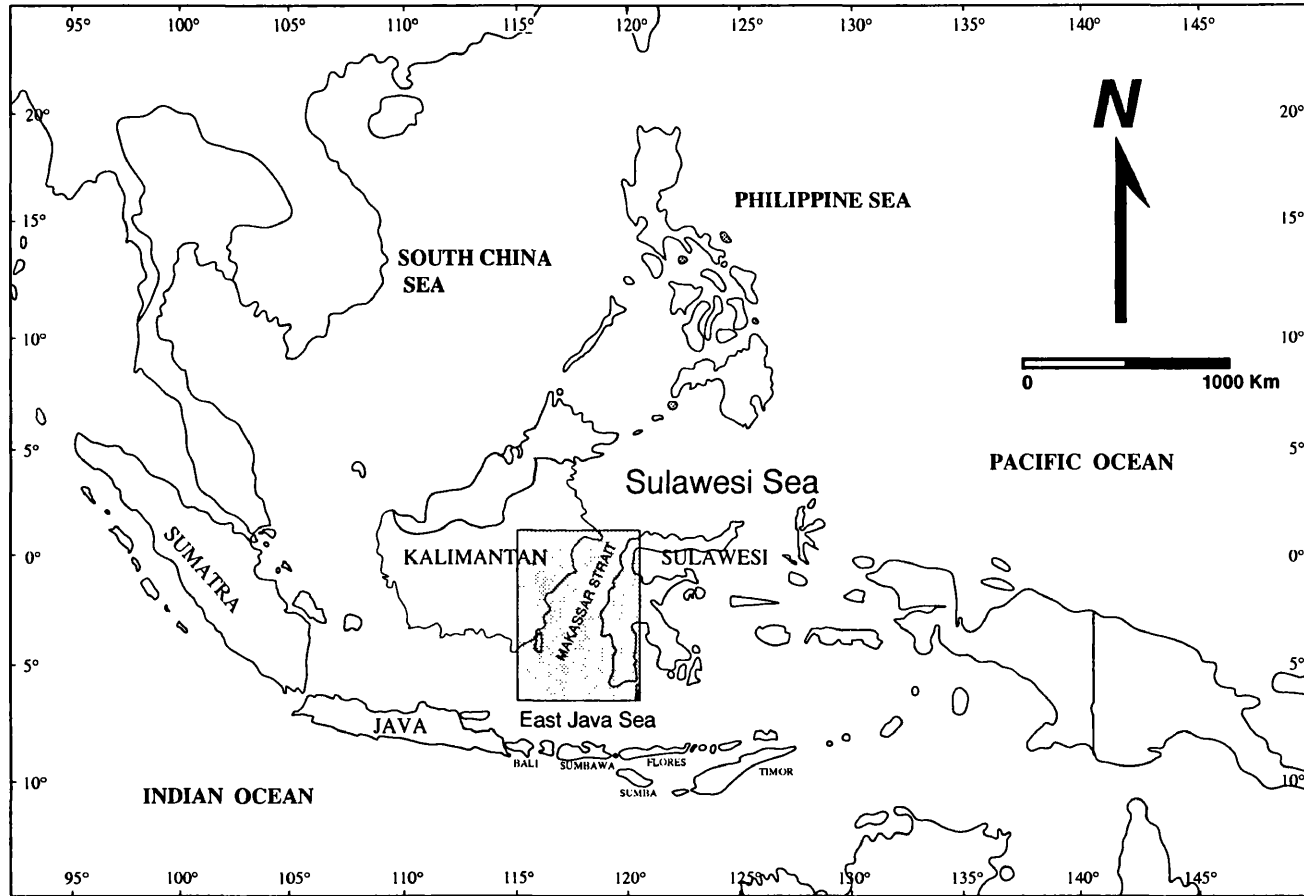


Figure 6.1: Location map of the Makassar Strait

attenuated continental crust. Daly *et al.* (1991) attributed the strait to back-arc extension along the Pacific margin, reactivating the earlier Meratus thrust terranes. Bergman *et al.* (1994) suggested that Makassar Strait is a foreland basin bounded on both sides by converging Neogene thrust belt.

6.3 BATHYMETRY

The Makassar Strait (Fig.6.2) resembles many continental rift zones in showing a symmetrical depression zone (median valley) flanked by uplifted topography in each side. It is flanked by the mountainous region of SE Kalimantan in the west and western Sulawesi in the east. Along the SE Kalimantan margin, the continental shelf is wide and gentle with water depth less than 200 m, and is referred to as the Paternoster Platform (Situmorang 1982) or more generally as the Sunda Shelf. Off western Sulawesi the shelf is narrow. Continental slopes are steep, descending to a maximum depth of more than 2000 m.

The bathymetry of the Makassar Strait shows several features interpreted to be structural controls. The strait can be divided into North Makassar Strait Depression (NMSD) and South Makassar Strait Depression (SMSD). These two depressions can be correlated with the North Makassar and South Makassar basins of Katili (1978) and Situmorang (1982), which are separated by the sinistral Paternoster Fault. The NMSD is 340 km long, 100 km wide and has water depths varying from 200 m-2000 m and a N-S to NNE-SSW trending axis. The deepest part is in the middle of the strait and the form is symmetrical. The SMSD is 300 km long, 100 km wide and has water depths varying between 200 m to 2000 m and a NE-SW trending axis.

Seismic reflection profiles show that the morphology of the main trough is commonly smooth compared to the continental shelf area to the east and west. Normal faults are abundant in the axial trough, indicating an extensional basin.

6.4 TECTONIC SETTING AND STRATIGRAPHY OF SE KALIMANTAN

The main tectonic control of Eastern Kalimantan and Western Sulawesi is believed to be a collision between the Eurasian Plate and Australian microcontinental blocks in the

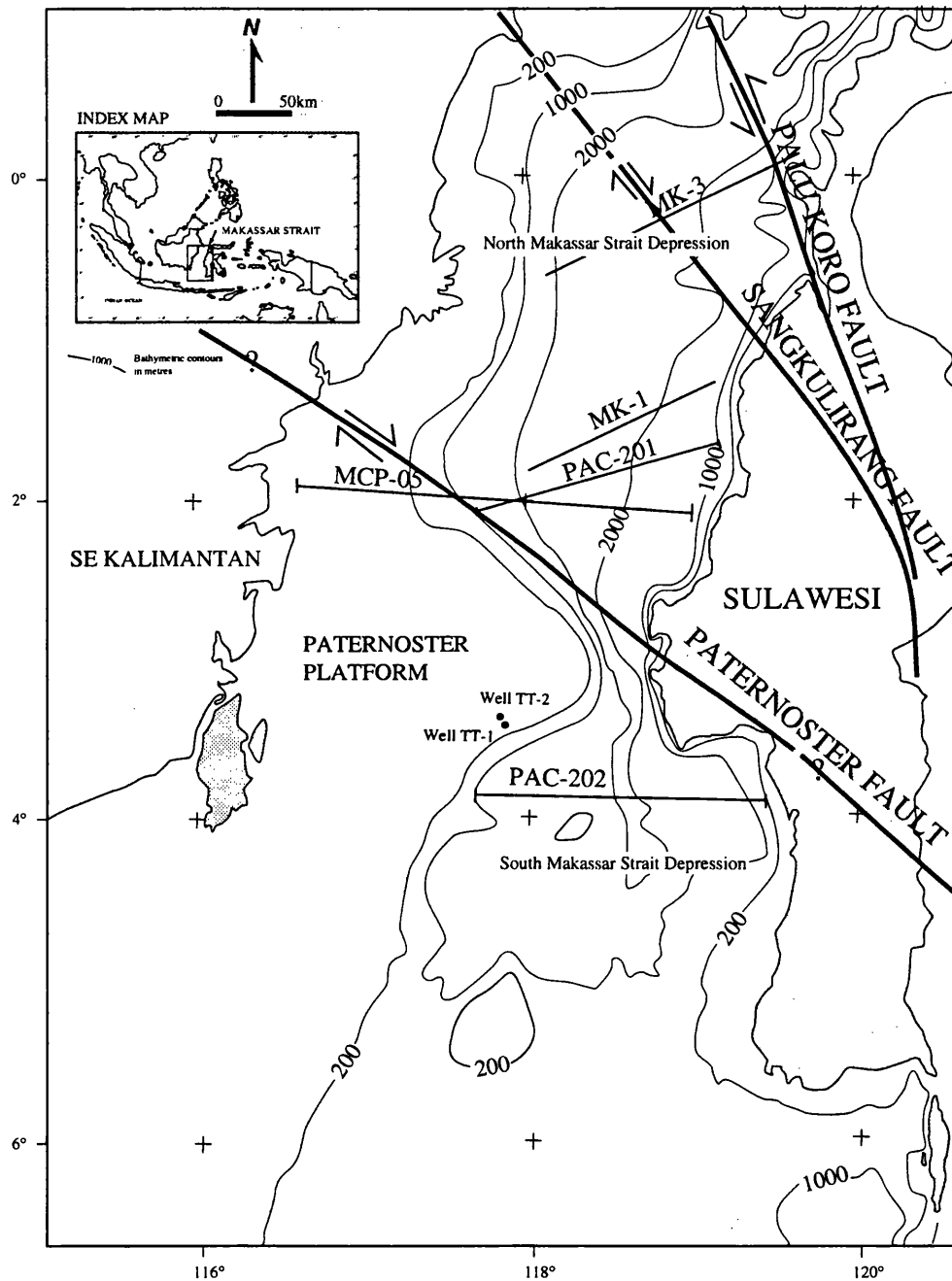


Figure 6.2: Bathymetric, structural and seismic location maps on the Makassar Strait (Fault data came from Biantoro et al. 1992).

Cretaceous (Sikumbang 1990). Kalimantan is usually regarded as having been a stable craton since the Middle-Late Cainozoic (Hamilton 1979), following formation by amalgamation of several unrelated terranes. Geologically, the area can be subdivided into five major units, namely West and Central Kalimantan, Southeast Kalimantan, Northeast Kalimantan, North Kalimantan and Northwest Kalimantan (van-Bemmelen 1949). The SE Kalimantan or Meratus Terrane consists of pre-Tertiary basement complexes which are similar to those of SW Sulawesi. The development of this area was influenced mainly by subduction and collision accompanied by basement complex emplacement. In SE Kalimantan, as in SW Sulawesi, pre-Tertiary basement complexes were covered by Tertiary sediments. The geology (Fig.6.3) and stratigraphy (Fig.6.4) of the Meratus region has been summarised by Sikumbang (1990), from whom most of the information below is taken.

6.4.1 Basement complexes

Pre-Tertiary basement complexes in the Meratus Mountains have a NE-SW structural lineation. They consist of the Meratus ophiolite and metamorphic rocks. The association of these rocks occurred in the subduction zone, forming melange.

Meratus Ophiolite

The ophiolite consists of ultramafic rocks, gabbroic rocks and plagiogranite and microdiorite. Ultramafic rocks are disrupted, sheared and serpentized, and locally exhibit boudinage structures. Sikumbang (1990) suggested an Early Aptian (116 Ma) age.

Metamorphic rocks

Metamorphic rocks in the Meratus Mountains can be divided into the Harun Schist and the Pelaihari Phyllite. The distinction between the two is made solely on the basis of grade since in both cases the age of metamorphism seems to have been Early Albian (108.4 ma).

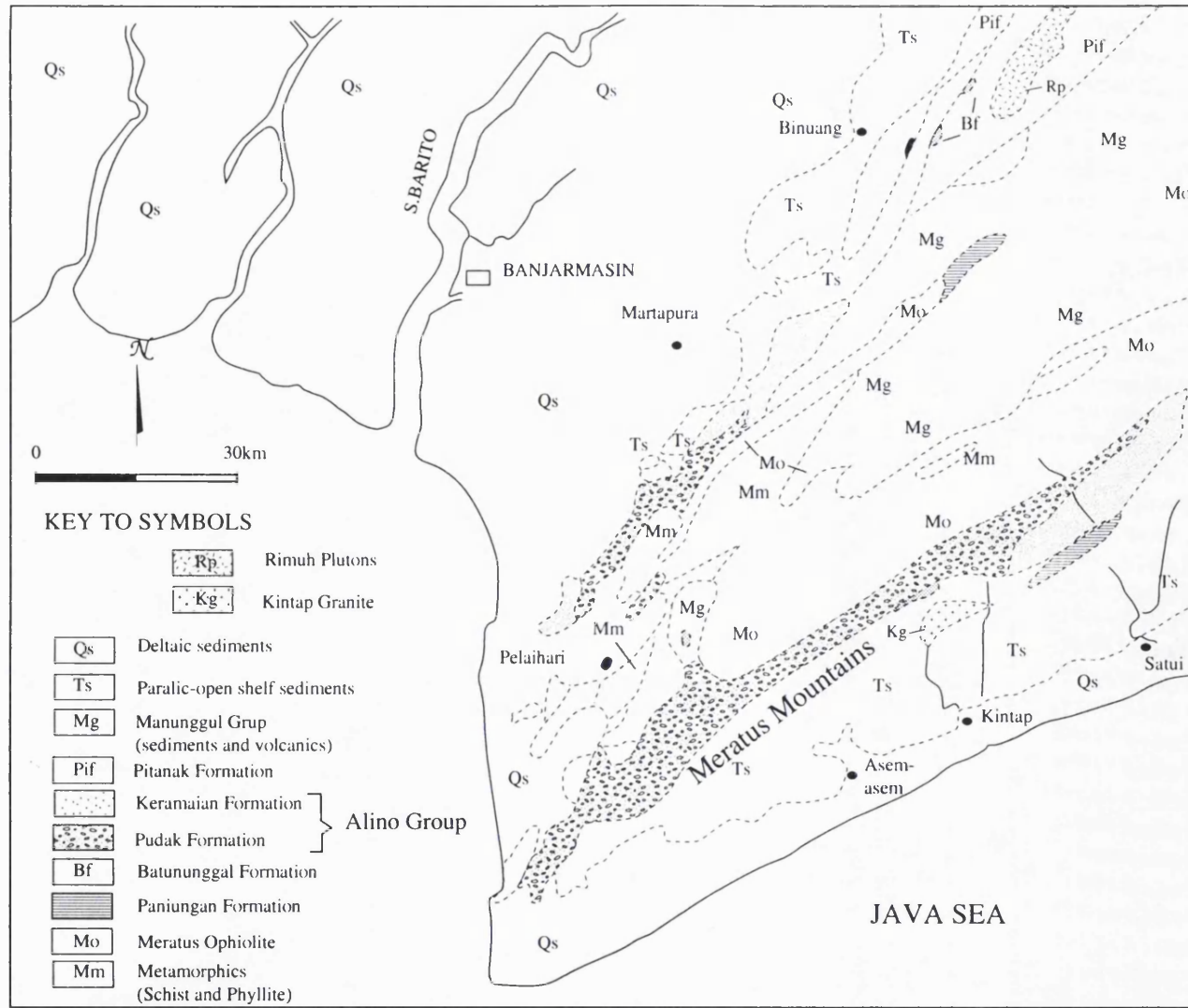


Figure 6.3: Distribution of stratigraphic and tectonostratigraphic units in the Meratus Mountains and adjacent areas (Sikumbang 1990)

PERIOD	EPOCH	AGE	Age(my)	DATED ROCK	ROCK UNIT		PALEO-ENVIRONMENT	VOLCANO PLUTONIC EVENTS	TECTONIC EVENTS					
					SEDIMENTARY AND VOLCANIC	IGNEOUS AND METAMORPHIC								
CRETACEOUS	EARLY	NEOCOMIAN	BARTONIAN	63	MANUNGGUL GROUP	TANJUNG FORMATION	Quartz, sandstone shale & coal	Deltatic	Down Warping Subsidence stretching of lithosphere					
			LUTETIAN							50.5				
			YPRESIAN							54.9				
			THANETIAN							60.2				
		DANIAN	65							Kayujohara Formation	Volcanic	Andesite microdiorite		
		LATE	MAASTRICHTIAN							73			Rantaulajung Formation	Conglomerate & sandstone
			CAMPANIAN							83			Tabatan Formation	
	SANTONIAN		87.5		Benuariam Formation									
	CONIACIAN	88.5	Pamali Formation		Conglomerate & sandstone & mudstone	Marginal marine to Submarine fan	Alluvial fan	ARC	Development of a pull apart basin Magmatism still active during deposition					
	LATE	TURONIAN	91							Pitanak Formation			Rimuh Pluton	Andesite to acid
		CENOMANIAN	95							Keramaian Formation			Kintap Granite	
		ALBIAN	108		Pudak Formation	Volcaniclastic & chert	ARC							
		APTIAN	113		Pelaihari Phyllite			Hauran Schist						
		BARREMIAN	116		Batununggal Formation	Meratus Ophiolite	Carbonate	Shelf to slope	MARGIN	Basalt-andesite	Subduction Strike-slip			
HAUTERIVIAN		125	PANIUNGAN FORMATION	mudstone & minor sandstone	Shallow shelf	CONTINENTAL						Ophiolite		
VALANGINIAN		131												
BERRIASIAN	138													
144								Stable						

Figure 6.4: Summary of stratigraphic framework and geological evolution of the Meratus Mountains (Sikumbang 1990)

6.4.2 Sedimentary and volcanic rocks

The oldest sedimentary rocks in the Meratus area are the Paniungan and Batununggal Formations of Berriasian-Barremian and Barremian-Aptian age, respectively. Both formations were deposited in a shallow marine to slope setting on the southeastern margin of the Sunda continent. The Paniungan Formation consists largely of mudstone with intercalations of sandstone and minor limestone. The Batununggal Formation is divided into three different units; autochthonous (intact limestone), para-autochthonous (thrust sheet) and allochthonous (exotic blocks). The formation occurs in the northeastern and southeastern parts of the Meratus Mountains (Fig.6.3). In the northeast it is largely covered by in situ and undeformed amygdaloidal lava flows.

The Alino Group, which is considered to derive from a volcanic island arc of Albian to Early Cenomanian age, can be divided into the Pudak Formation and the Keramaian Formation. The Pudak Formation consists mainly of coarse volcanoclastic deposits with limestone blocks. Most of the volcanic materials were derived from erosional disintegration and fragmentation of lavas. They are occasionally intermixed with pre-existing sedimentary material (i.e. limestone of the Batununggal Formation and sandstone of the Paniungan Formation) and with igneous material (e.g. mafic and ultramafic rocks of the Meratus Ophiolite).

The Keramaian Formation consists of alternating volcanoclastic sandstone and mudstone and chert with or without radiolarian skeletons. It overlies the Pudak Formation.

The Manunggul Group includes all the Upper Cretaceous sedimentary strata of the region, as well as andesitic lavas, rhyolitic volcanics and pyroclastics that occupy a trough-like basin in the central axis of the Meratus Mountains. The group is subdivided into the Pamali, Benuariam Volcanic, Tabatan, Rantaulajung, and Kayujohara Volcanic formations.

6.4.3 Plutonic rocks

There are two exposures of plutonic rocks in the Meratus Mountains. The first is the Rimuh Pluton, in the Tambak-Tamban Range, the second the Kintap Pluton about 10 km

north of Kintap. These plutonic rocks can be related to a west-dipping subduction zone in the Early Cretaceous-Early Tertiary. The early Upper Cretaceous or pre-Upper Turronian Rimuh Pluton is associated with volcanics of the Pitanak Formation. The Kintap Pluton is intrusive into both the Meratus Ophiolite and the Alino Group.

6.4.4 Implications

The pre-Tertiary rocks of SE Kalimantan are similar to those of SW Sulawesi (Hamilton 1979, Sikumbang 1990, Parkinson 1990). On the basis of the sedimentology, tectonic style and regional setting, Sikumbang (1990) suggested that the Manunggul Group was deposited in a pull-apart basin developed within a strike-slip zone initiated during or shortly after arc-continent collision. The group can be correlated with the Balangbaru Formation of SW Sulawesi (Hasan 1987), which suggests that the two regions lay close together in the Late Cretaceous.

6.5 SEISMIC INTERPRETATION

6.5.1 Introduction

Structural interpretations and seismic stratigraphy for the Makassar Basin have been derived from seismic reflection profiles PAC 201, PAC 202, MCP 05, MK1 and MK 3 (see Fig. 6.2 for location). PAC 201 and PAC 202 are multi channel seismic reflection with 24 fold coverage. The sections are displayed as line drawing interpretations.

Analysis is based on the procedures of *Vail et al. (1977)*.

6.5.2 Seismic interpretation line PAC 201

This line lies in the southern part of the North Makassar Basin, just north of latitude 2°S, trends WSW-ENE and is approximately 175 km long. It can be separated into eastern and western segments on the basis of structural regimes. The western segment (Fig. 6.5A) extends from SP 1200 to SP 4000 and displays thick sediments controlled by basement faults. In contrast, the eastern segment (Fig. 6.5b), from SP 0 to SP 1200, exhibits extensive thrust faulting and basement cannot be traced clearly due to widespread multiples and diffractions.

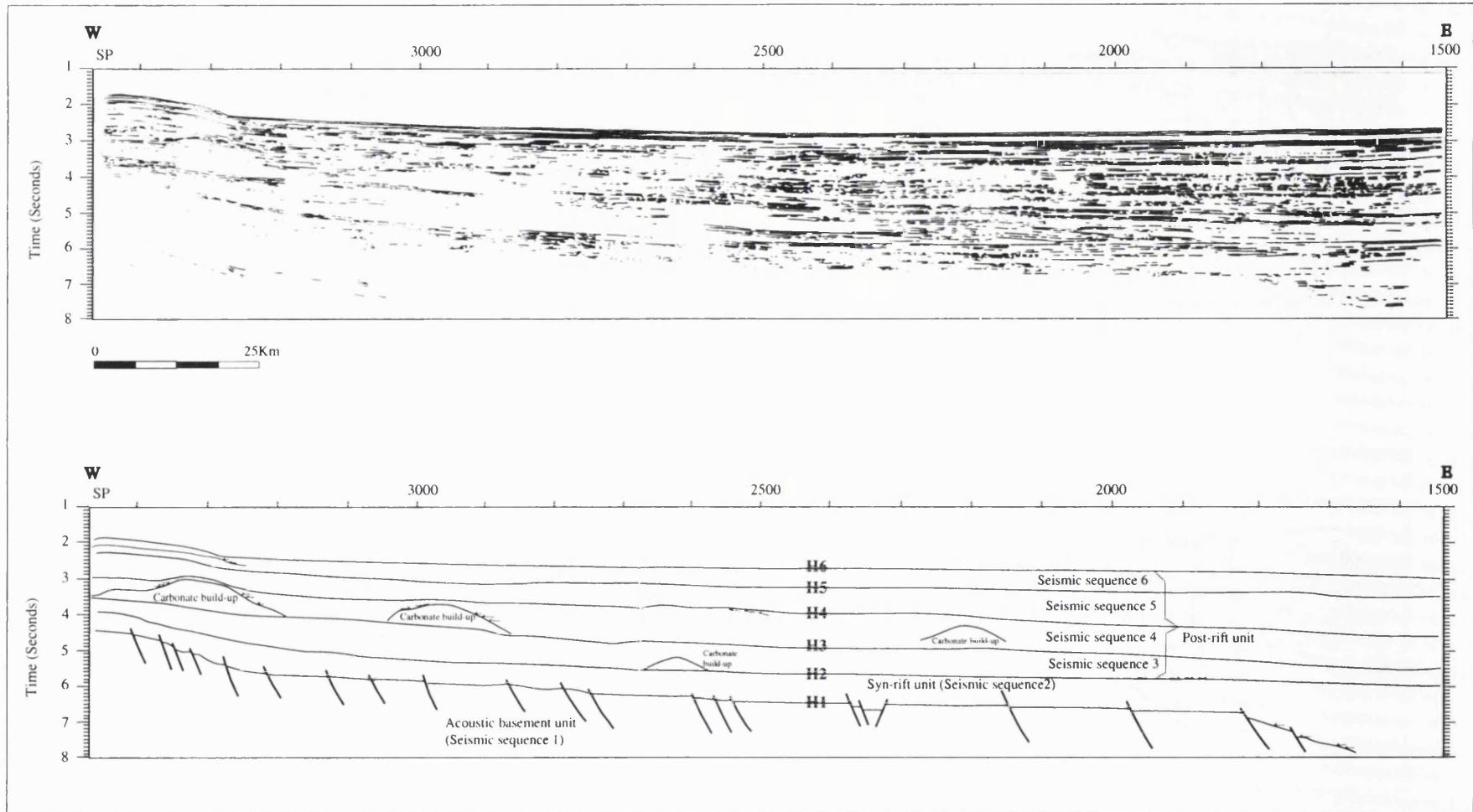


Figure 6.5A: Line drawing and its interpretation of western segment of line PAC 201 showing basement faults indicating extensional basin. Arrows mark cycle terminations on onlap, downlap and toplap which provide criteria for recognition of sequence boundaries. Letters H1-H6 designate seismic horizons.

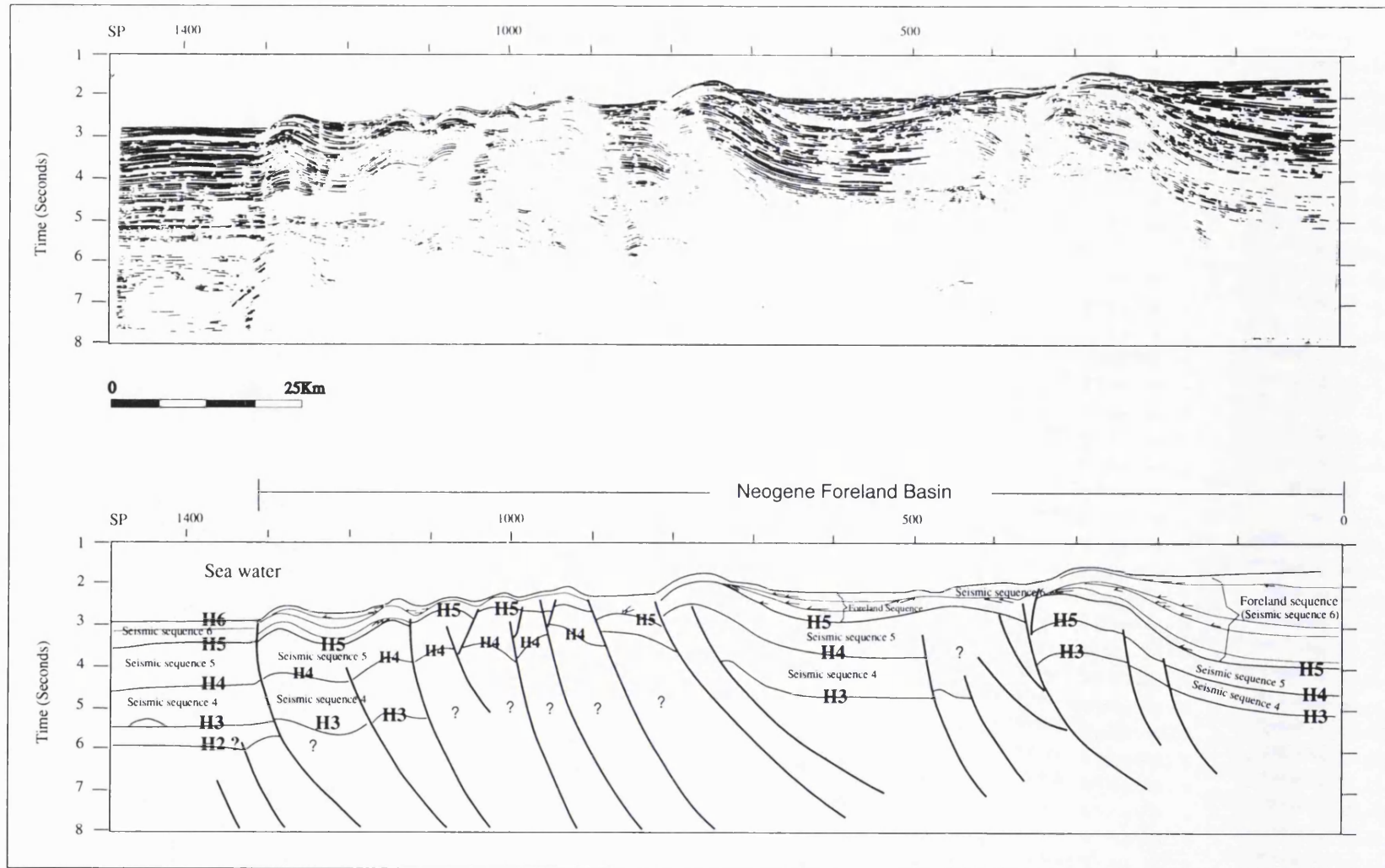


Figure 6.5B: Seismic line drawing and interpretation of eastern segment of line PAC 201 showing extensive thrust faults after the formation of horizons H5 forming Neogene foreland basin. Arrows mark cycle terminations onlap, downlap, toplap which provide criteria for recognition of sequence boundaries. Letters H1-H6 designate seismic horizons

Seismic sequence analysis, especially from the western segments (Fig. 6.5A) shows that the reflectors can be divided into six seismic sequences which can be grouped into three major units; acoustic basement (sequence 1), syn-rift sediments (sequence 2) and post-rift sediments (sequence 3-6). In the figures, the seismic sequence boundaries are shown as horizons H1-H6. The three units are described below.

6.5.2.1 Acoustic basement (seismic sequence 1)

The oldest recognised seismic sequence is characterised by an absence of reflections and is interpreted as acoustic basement. The contact with the overlying sediments is difficult to trace, especially in the eastern segments where it is obscured by diffractions and multiples. This contact is marked as H1 in the western segment of the line (Fig.6.5A) but even there it can only be identified at a few locations (e.g. SP 3400 at 4.6 sec TWT, SP 1650 at 7.5 sec TWT and SP 150 at 5.7 sec TWT). To estimate the basement depth, interval velocity data were used where available, the boundary between acoustic basement and the overlying sediments being placed at depths at which there was an extreme velocity contrast. The greatest depths are probably in the middle of the line, from SP 1470 to SP 1600, where horizon H1 was not seen as it lies deeper than the maximum time recorded (8 sec TWT). The horizon shallows to the west to 4.05 sec TWT (4 km) but is not seen further east. Where seen it is cut by normal faults, forming half-graben structures.

6.5.2.2 Syn-rift unit (seismic sequence 2)

Unconformably overlying seismic sequence 1 is seismic sequence 2. This sequence is characterised by parallel-subparallel reflectors with poor to fair continuity and low to medium amplitude. Reflection geometry suggests a concordant sequence boundary relationship at the top and onlap at the base against H1 (SP 1800 to SP 1650). Following the criteria of Vail *et al.* (1977), these reflection characteristics are interpreted as indicating a shelf depositional environment, whilst environmental facies interpretation indicates a near shore clastic deposit. In the western segment, the thickness of the sequence varies from about 0.4 sec TWT at the western and eastern ends of the profile to 2.2 sec TWT in the middle, suggesting infilling of a faulted and irregular basement. This is the basis for inferring that the sediments are rift-related. The faults cut the basement

but do not disturb the sea floor, indicating a limit to the period of tectonic activity. The top of the syn-rift sequences is designated H2. In the eastern segment, the sequence can be recognised only from SP 1490 to SP 1250 where the reflection configurations are subparallel and hummocky.

The top of this sequence appears as a strong reflector, indicating a large contrast in density and seismic velocity between the upper and lower rock units.

6.5.2.3 Post-rift unit

Overlying seismic sequence 2, which is considered to be a syn-rift unit, are seismic sequences 3-6, which have not been affected by normal faults and are therefore considered to be post-rift sediments.

Seismic sequence 3

This sequence is bounded by horizons H2 and H3, and exhibits parallel to sub parallel bedding with poor to fair continuity and high to medium reflection amplitude, except between SP 2600 and SP 2900 where amplitudes are low. The variation in amplitude and frequency may indicate a lithological facies change which could relate to a decreasing rate of subsidence. The lower boundary shows downlap to the top of seismic sequence 2 (Boundary H2) from SP 1700 to SP 2000, indicating sediment progradation from west to east. These reflector characteristics can be taken as indicating a shelf to shelf margin depositional environment (Vail *et al.* 1977).

In the eastern segment, this sub unit is dominated by diffractions and intensive thrust faults, and is difficult to define.

Seismic sequence 4

This sequence is bounded by horizons H3 and H4, and is dominated by parallel and locally subparallel reflections with fair to good continuity and medium to high reflection amplitude. The unit is characterised by the presence of local highs from SP 3400 to SP 3200, SP 3050 to SP 2850 and SP 2250 to SP 2150 which are interpreted as carbonate mounds. The upper boundary is marked by toplap to horizon H5 from SP 2450 to SP

2250. The reflector characteristics are classified as indicating a shelf to shelf margin depositional environment (Vail *et al.* 1977). The eastern part of this sequence is dominated by diffractions and intensive thrust faults, but it can still be defined from SP 0 to SP 350, SP 500 to SP 750 and SP 1250 to SP 1475.

Seismic sequence 5

This sub unit is bounded by horizons H4 and H5 and displays parallel configurations with fair to good continuity and medium to high reflection amplitude. Discontinuous reflectors are present from SP 3450 to SP 2150 with low to medium amplitude, whilst continuity is observed from SP 210 to SP 0 with medium to high amplitude. These reflection characteristics are typical of a shelf depositional environment and indicate a shallow marine shelf deposit (Vail *et al.* 1977). In the eastern segment, although this region is distorted by thrust complexes, the unit can still be recognised.

Seismic sequence 6

This sub unit is bounded by horizons H5 and H6 and shows parallel configurations with good continuity and medium to high reflection amplitudes. The reflection characteristics are classified as indicating a shelf depositional environment (Vail *et al.* 1977). In the eastern segment from SP 1300 to SP 0 the sequence can be subdivided into sub-sequences confined to local basins in which horizontal reflectors onlap to the top of Horizon H5. This sub unit is clearly not affected by thrust faults and was deposited as onlapping fill in a foreland basin.

6.5.3 Seismic interpretation line PAC 202

This line lies in the northern part of the South Makassar Basin and is approximately 200 km to the south of PAC 201. The line is situated at latitude 3°49'S, trends W-E and is approximately 200 km long. Unlike line PAC 201, where there is intensive thrust faulting in the east, sediments on this line have not been affected by thrust faults. The line drawing and interpretation are shown in Fig. 6.6. The section can be divided into six seismic sequences which can be grouped into three major units; acoustic basement (sequence 1), syn-rift sediments (sequence 2) and post-rift sediments (sequence 3-6). The sequence boundaries are shown as horizons 1-6 (H1-H6).

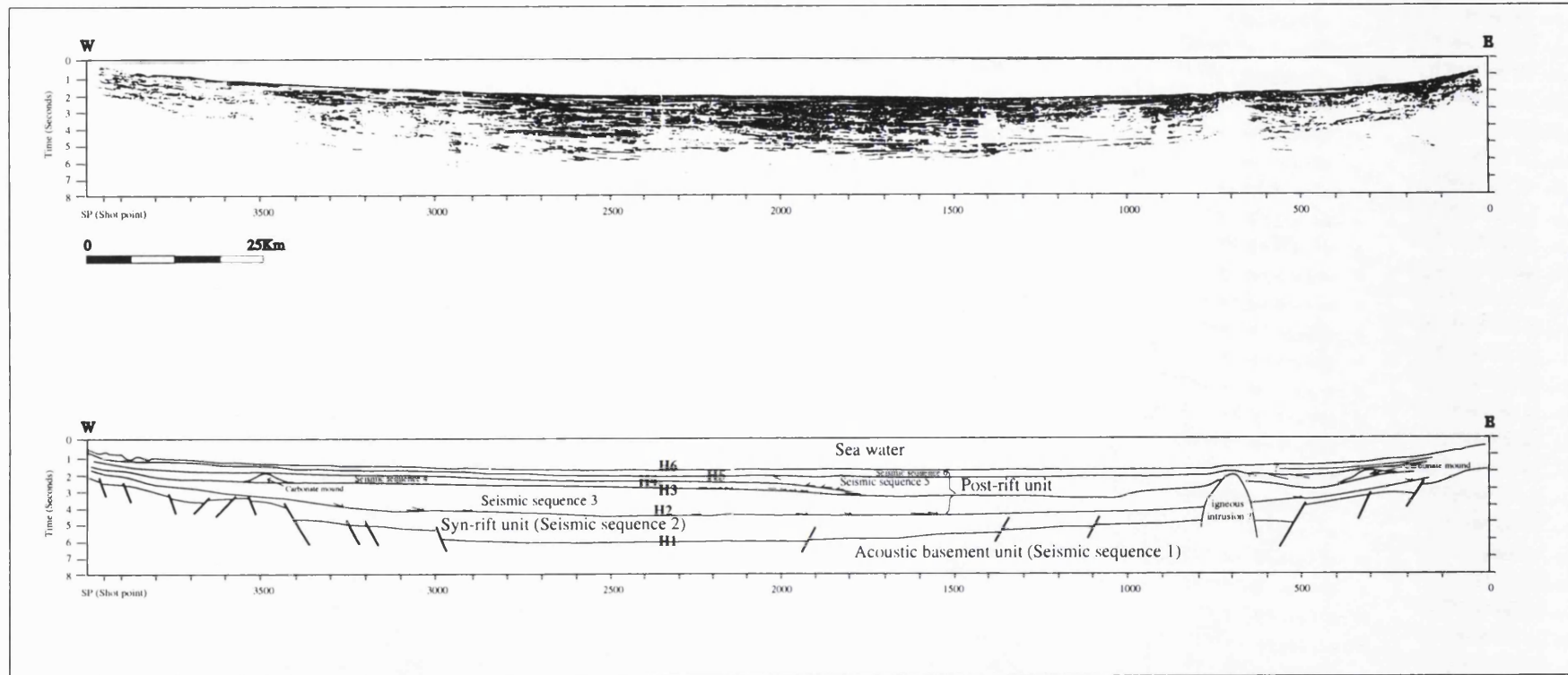


Figure 6.6: Seismic line drawing and interpretation of line PAC 202 showing basement faults, suggesting extensional basin. Arrows mark cycle terminations on onlap, downlap and toplap which provide criteria for recognition of sequence boundaries. Letters H1-H6 designate seismic horizons.

6.5.3.1 Acoustic basement (seismic sequence 1)

This sequence is characterised by the absence of reflections. The contact with the overlying sediments is very difficult to trace because it is obscured by intense multiples and diffractions. From SP 3270 to SP 3470, acoustic basement deepens towards the basin from 2.25 sec TWT to 5.45 sec TWT. This increase in depth is associated with normal faults. The same phenomena can also be seen at SP 2990 (6 sec TWT) and at SP 1900 (6 sec TWT). In the eastern part of the section (SP 0 to SP 1500), where interval velocity data were available, the boundary between acoustic basement and the overlying sediments was determined from the change in velocity. The depth of acoustic basement varies broadly but it is deepest in the middle of the line (SP 2000 to SP 2800) at 6.7 to 6.9 sec TWT (about 10 km) and rises to about 2.1 sec TWT (1.8 km) in the west and to 2.5 sec TWT (2.3 km) in the east.

6.5.3.2 Syn-rift unit (seismic sequence 2)

This sequence generally displays a parallel seismic configuration with medium to high amplitude, except from SP 3900 to SP 3650 where reflectors diverge, perhaps due to syn-tectonic deposition. These reflector characteristics point to a shelf environment, i.e. shallow marine deposition (Vail *et al.* 1977). The sequence was deposited in a complex system of tilted horsts and grabens. Thickness varies from 0.2 sec to 1.8 sec.

6.5.3.3 Post-rift unit

Seismic sequences 3-6 overlie seismic sequence 2 and have not been affected by basement faults. They are considered to be post-rift.

Seismic sequence 3

This unit is bounded by horizons H2 and H3 and reflectors are generally parallel to subparallel (SP 3650 - SP 3950) with moderate continuity and medium to high reflection amplitude. Hummocky (SP 3650 to SP 3850), parallel (SP 3850 to SP 2250) and complex sigmoid-oblique (SP 2250 to SP 1800) configurations are also seen, the latter indicating progradation with downlap to the top of the syn-rift unit (H 2). These reflection characteristics are classified as indicating a shelf to shelf margin depositional environment (Vail *et al.* 1977), with progradation of sedimentation from west to east.

This sequence is also affected by intrusion-like structures, as from SP 960 to SP 910 and SP 790 to SP 690.

Seismic sequence 4

This unit is bounded by horizons H3 and H4, and exhibits subparallel reflections which wedge out from west to east as they downlap to horizon H3 between SP 1800 and SP 2200. To the east of this point Sequence 4 was not developed, and Sequence 5 onlaps H4 at SP 1800. Reflection amplitudes in Sequence 4 are medium to high. Within this sequence, mounds, interpreted as carbonate, are observed from SP 3450 to SP 3550. These characteristics indicate a shelf margin depositional environment (Vail *et al.* 1977).

Seismic sequence 5

This sequence is bounded by horizons H4 and H5 and is characterised by parallel reflections with good continuity and medium to high reflection amplitude. Complex sigmoid to oblique configurations are also observed from SP 1800 to SP 2250. The lower boundary of this sequence is marked by downlap to Horizon 4 (H4) and there is toplap against Horizon 5 (H5) at the upper boundary (SP 2025, SP 650 and SP 600). These characteristics indicate a shelf margin and prograded slope depositional framework (Vail *et al.* 1977).

Seismic sequence 6

This unit is bounded by horizons H5 and H6 and is characterised by parallel reflections with continuous and strong amplitudes, characteristics which can be taken as indicating a shelf (shallow water) depositional (Vail *et al.* 1977). The sediments are probably neritic limestones.

6.5.4 Seismic interpretation line MCP 05

This line in the North Makassar Basin (Fig.6.7) has been interpreted and published as a line drawing by Katili (1978). It lies at about 20°S, trends E-W and is approximately 275 km long. It is crossed close to its centre by Line PAC 201. The line drawing produced by Katili did not show any detail of the reflectors and it is therefore difficult to correlate the interpretation in terms of sequence stratigraphy with PAC 201 and 202. However, the

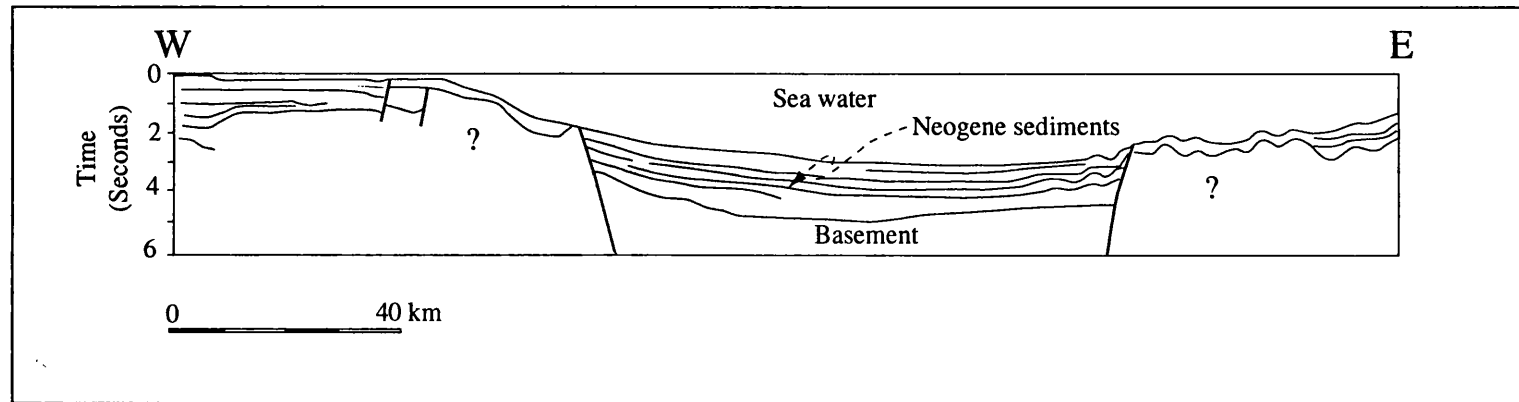


Figure 6.7: Seismic line drawing interpretation of line MCP 05 across the Makassar Strait showing the intracratonic rifting of the Makassar Strait causing separation between SE Kalimantan and SW Sulawesi (After Katili 1973)

section does show an extensional basin forming a graben structure. The reflection configuration within this graben is parallel and continuous, suggesting uniform rates of deposition on a uniformly subsiding base (Vail *et al.* 1977). The deepest basement occurs in the middle of the graben, at approximately 5 sec TWT (6 km); sediment occupies about 2 sec TWT beneath more than 2 km of water. The external form of this sequence appears to indicate onlapping infill. The sequence was deposited at a uniform rate on a uniformly subsiding basin floor (Vail *et al.* 1977). To the west of this graben is a basement high with depth varying between 2 sec TWT and 0.5 sec TWT, controlled by normal faults. It seems likely that the sequence shows parallel-divergent configurations with continuous reflectors over this high. To the east of the graben are folded sediments, suggesting compressional tectonics in this part of the line, as opposed to the central and western part which show extensional tectonics.

6.5.5 Seismic interpretation line MK1 and MK3

These lines (Fig. 6.8) in the North Makassar Basin have been interpreted and published as line drawings by Salle and Burrolet (1979). As with MCP 05, the interpretations were not drawn in detail and it is difficult to correlate the sequence stratigraphy with lines PAC 201 and 202.

Line MK 3 is situated in the northernmost part of the North Makassar Basin. In the east (SP 2200 to the end of the line at SP 3300), the basement is high and from SP 2950 to 3100 it forms the sea floor at approximately 2.5 sec TWT (1850 - 1900 m). Between SP 2300 and the western end of the line, basement is not shown but must drop sharply from 4 sec TWT to more than 6 sec TWT. The overlying sediments have generally uniform thickness of more than 3 sec TWT and display parallel configurations with moderate to good continuity.

Line MK 1 is parallel to PAC 201 and 25 km to the north. The compressional zone at the eastern margin which is dominant on PAC 201 is not observed. Acoustic basement was not detected continuously along the profile. It is present in the eastern part (SP 2400 to SP 2900) at about 4.5 sec TWT but in the western part, towards the axial trough, it is

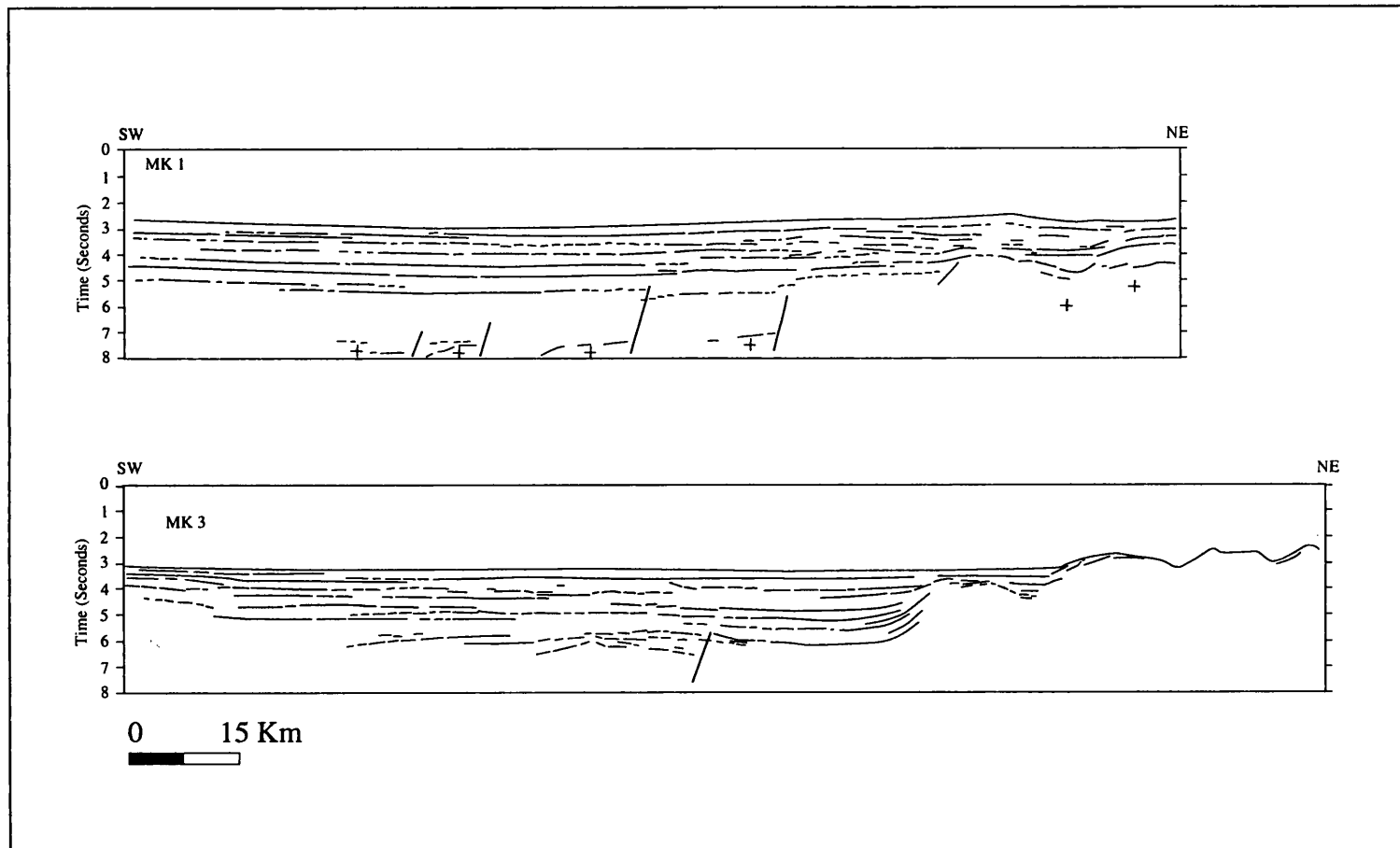


Figure 6.8: Seismic line drawing of line MK1 and MK3 showing deep basin of the North Makassar Basin (After Buroillet and Salle 1981)

seen only discontinuously, reaching a depth of 7.5 sec TWT in some locations. The sediments display parallel configurations, apparently with moderate to good continuity.

These interpretations of lines MK1 and MK3 suggest sedimentation similar to that seen on Lines PAC 201 and PAC 202, indicating that the whole Makassar Basin formed by rifting and was subsequently modified by thrust faulting along its eastern margin.

6.6 WELL DATA

Two wells, TT 1 and TT 2 (obtained from Situmorang 1982), have been used to correlate the seismic stratigraphy in the Makassar Strait. The following is the description of the wells.

6.6.1 Well TT 2

This well is located at 3°21'S latitude and 117°51'E longitude (see Fig. 6.2). The sedimentary section indicates continuous sedimentation throughout the Tertiary in fluctuating marine conditions. Basement, consisting of dolerites and gabbros, was encountered at 1598 m and the well was terminated at 1601 m. Unconformably overlying this basement were 106 m of Upper Eocene sediments consisting of argillaceous sandstones, sandy limestones and conglomerates with fragments of basement rocks. The unit is overlain by a Lower Oligocene - Lower Miocene carbonate reef with a thickness of 588 m and an interval velocity of 3750 m/sec. Middle Miocene sediments consisting of claystone interbedded with argillaceous carbonate and with a thickness of 200 m overlie the reef conformably. The interval velocity of this unit is 2270 m/sec.

Conformably above this unit were 624 m of Middle Miocene - Recent sediments consisting of shallow water limestones with rare intercalations of clay and occasional argillaceous limestones.

6.6.2 Well TT 1

This well lies approximately 7 km southeast of Well TT 2. The total depth was 3238 m although on seismic sections the basement was located at 2.9 sec TWT, where there is a

change in interval velocity from 4236 m/sec to 4879 m/sec, equivalent to a depth of 3560 m. As with well TT 2, the results from this well suggest continuous sedimentation during the Tertiary.

Basement consisted of undefined igneous rocks and was unconformably overlain by Eocene basal conglomerate, argillaceous sandstone with siltstone, claystone and argillaceous and conglomeratic limestone interbedded with claystone. These units had thicknesses of 39 m, 67 m, 163 m and 710 m, respectively.

Conformably overlying this rock unit was an Upper Eocene - Lower Miocene conglomeratic limestone with a thickness of 944 m. The interval velocity ranged from 3200 m/sec to 5334 m/sec. Lower to Middle Miocene sedimentary rocks conformably overlying this unit consist of claystones with intercalations of thin carbonates. The thickness of this unit is about 1046 m with an interval velocity of about 1796 m/sec from sonic data, or 2194 m/sec from seismic velocity analyses.

Conformably overlying this unit was a Middle Miocene - Pliocene shallow water limestone with a thickness of 184 m.

The thickness of sediments in wells TT 1 and TT 2 differs considerably. The Eocene unit in well TT 1 is ten times as thick as in well TT 2 and the carbonate reef was not developed in TT 1. This reflects a basin complexity with large facies and thickness changes within short distances.

6.7 CORRELATION OF WELL DATA WITH SEISMIC SEQUENCES

The age of the seismic units identified on lines PAC 201 and PAC 202 cannot be determined directly. However, the well data (TT 1 and TT 2) and regional studies provide some age and stratigraphic control (Fig. 6.9).

Regionally, the top of the carbonate reef has been used as an acoustic marker for the Early Miocene in the area to the south and also in the East Kalimantan basinal area (Situmorang 1982). On the basis of this knowledge, the carbonate reefs, recognised by

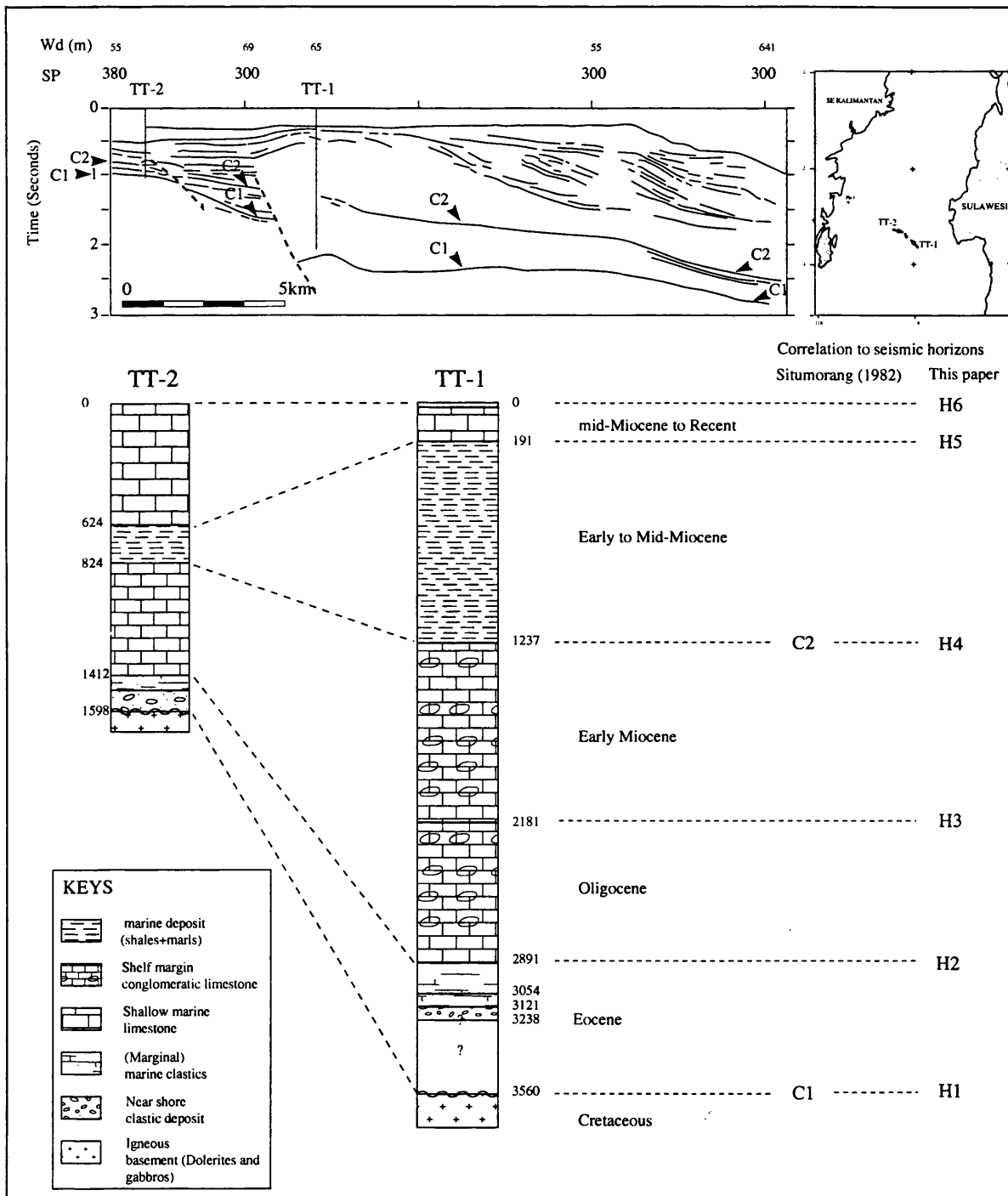


Figure 6.9: Lithologies of Well TT1 and TT2 and correlation to the seismic horizons (After Situmorang 1982)

their mounded external form in seismic sequence 4 on seismic section PAC 201 locate the top of the Early Miocene. Using this assumption, the other sequences can be correlated with the well data.

The top of sequence 1 (H1) is equivalent to horizon C1 of Situmorang (1982), which is the pre-Tertiary basement, consisting of gabbros and dolerites (Well TT 2). Sequence 2 (between horizons H1 and H2) is equivalent to the Late Eocene syn-rift sediments consisting of near shore clastic deposits. The top of this unit, designated H2, marks the end of the rifting phase, which was followed by basin subsidence and the deposition of post-rift sediments. The opening of the Makassar Strait can be related to the deposition of Sequence 2. Sequence 3 (between horizons H2 and H3) is equivalent to the Lower Oligocene conglomeratic limestone. The top of Sequence 4 (Horizon H4) is equivalent to horizon C2, the Early Miocene carbonate reef, of Situmorang (1992). Sequence 5 is equivalent to the Early to Middle Miocene deep marine shales and marls and Sequence 6 is equivalent to the Pliocene shallow marine limestone.

6.8 SUMMARY

A brief comparison between the North and South Makassar basins highlights similarities in stratigraphic framework and tectonic styles which can be explained by similarities in geological environments. Rift structures can be observed in both regions, characterised by basement faults forming horst and graben structures. A minor difference between these two regions is that there is, in the eastern part of North Makassar Basin, a compressional zone marked by thrust faults with associated folds affecting the young sediments. Basement in the eastern parts of lines in the south of the North Makassar basin cannot be identified due to extensive multiples and diffraction, but there are pronounced graben-like structures in their western parts. The compressional zone is observed in the eastern part of line PAC 201, MCP 05 and also in two other seismic lines located close to line PAC 201 interpreted by Situmorang (1982), namely P610 and P614, but not on other seismic lines to the north or south. Therefore, the thrust faults cannot be associated with a regional compressive regime. Since the zone of thrusting occurs between the Sangkulirang and Palu-Koro Faults (see Fig. 6.2), its presence might relate to the combined movement on these two faults.

In general, the seismic reflections within seismic sequences 2-6 in the North and South Makassar basins are parallel, suggesting uniform rates of deposition on a uniformly subsiding basement. Progradation of sediments occurs from west to east, suggesting the source of sediments came from the west (SE Kalimantan). The similarities in stratigraphic framework and tectonic styles between the North and South Makassar basins lead to the conclusion that initially the two were parts of a single basin formed by E-W rifting in the Eocene. In the post Middle Miocene (the time when horizon H5 was disturbed) they were separated by activity on the Paternoster fault.

6.9 GRAVITY DATA

6.9.1 Introduction

There are two different versions of the free-air anomaly map for the Makassar Strait. The first, produced by SIPM (Shell), was reproduced by Situmorang (1982) without any indication of the formulae used to calculate gravity values. The second map was produced by Edcon (1992), using the 1930 International Gravity Formula for gravity reduction. The two contour maps were based on different data, and the values of free-air anomaly also differ between the two maps. To find the magnitude of the difference, the two maps were overlapped and at every crossing point the free-air anomaly values were compared. The difference is approximately constant, the Edcon values being greater than the SIPM values by 50 mGal. This difference is thought to be related to the fact that the SIPM data was not tied to any international system (Milsom, pers. comm., 1994). In order to integrate the two maps (Fig. 6.10), 50 mGal were added to the SIPM values.

6.9.2 Qualitative gravity interpretation

The free-air anomaly map of the Makassar Strait is characterised by negative free-air anomalies along the axial depression and positive free-air anomalies towards the continental shelves of Kalimantan and Sulawesi. Free-air anomaly values thus reflect bathymetry. Major structural gravity trends have been named as follows; Laut High, Mahakam High, Paternoster High, Paternoster Lineament, North Makassar Low, and South Makassar Low.

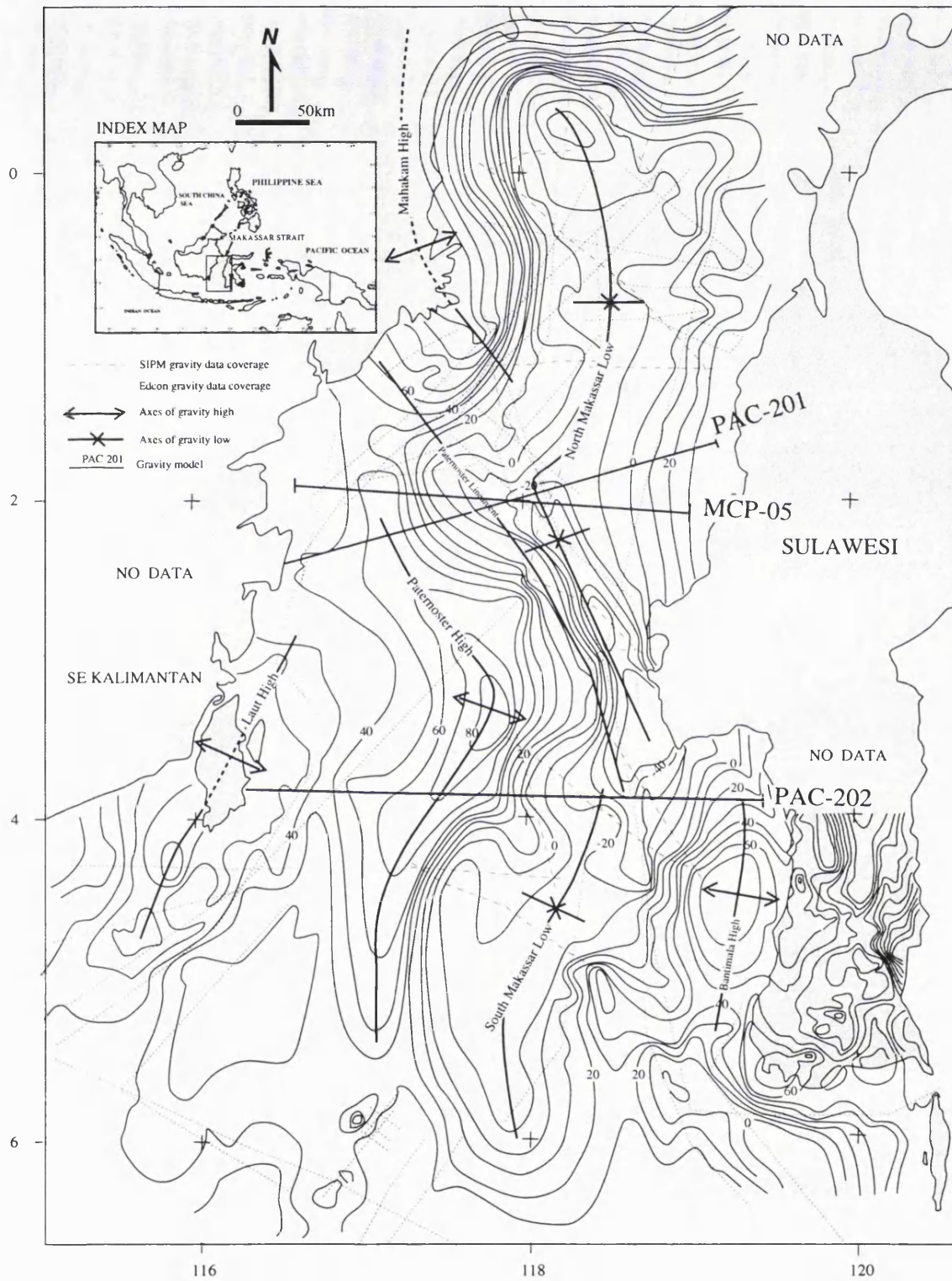


Figure 6.10: The free-air anomaly map of the Makassar Strait (Bouguer onland of SW Sulawesi) (Sources; Simamora and Marzuki 1990; SIPM, obtained from Situmorang 1982; Edcon 1991)

The Laut High is centred on Laut Island, close to the Meratus Mountains and trends NE-SW. The free-air anomaly ranges from +40 mGal to +70 mGal. This high is interpreted as indicating the presence of high density ultramafic rocks of the basement complex. Ophiolites are present on Laut Island and in the Meratus Mountains (Sikumbang 1990). To the northeast of the Laut High, the Mahakam High has a N-S trend which changes sharply to E-W at about 10°N. The free-air anomaly values range from +40 mGal to +120 mGal. The Laut High and Mahakam High are separated by a steep NW-SE gradient, the Paternoster Lineament. The Mahakam High is, therefore, thought to be a continuation of the Laut High, offset along this lineament.

Parallel and to the east of the Laut High, the Paternoster High forms an elliptical closure elongated in a NNE-SSW direction, in a region where the broad continental shelf of the Southeast Kalimantan margin lies in a water depth of less than 200 m. The free-air anomaly values range from +50 mGal to +70 mGal. Parallel and to the east of the Paternoster High is a long and narrow free-air anomaly low which trends roughly N-S. At about 30°S this is offset by the Paternoster lineament, dividing it into the South and North Makassar Lows. The North Makassar Low has free-air anomaly values ranging from 0 to -40 mGal in water depths of about 2000m, and the South Makassar Low has free-air anomaly values ranging from 0 to -50 mGal in water depths of about 2000m. These low free-air anomalies indicate the presence of thick low-density sedimentary rocks. The North and South Makassar lows are defined by steep gravity gradient, attributed to faulting, at the contacts with the Mahakam and Paternoster highs.

6.9.3 Gravity models

6.9.3.1 Introduction

Three gravity models of the Makassar Strait have been constructed using the GM-SYS Gravity modelling program. The models are constrained by the seismic reflection interpretation (PAC 201, PAC 202 and MCP 5) controlling the bathymetry and thickness of sediments. Densities have been assigned as follows: the density of sea water is taken as 1.03 Mg/m³. The average density of the sediments has been estimated using the average interval velocities from PAC 201 and 202 and radiosonobuoy data from Ben-Avraham and Emery 1973 at locations 38 and 39 close to Makassar Strait (see Fig.

3.17), converted using the density-velocity curve of Nafe and Drake (1963) found to be 2.3 Mg/m^3 . The density of the upper crust below the sediments is taken as 2.67 Mg/m^3 and density of the upper mantle is taken as 3.3 Mg/m^3 . The reference crustal model has a density of 2.67 Mg/m^3 and a thickness of 30 km.

6.9.3.2 Gravity modelling PAC 201

This cross section is taken across the Makassar Strait in a NE-SW direction along seismic reflection line PAC 201 but extends up to the coasts of Kalimantan and Sulawesi. The result of modelling is shown in Fig. 6.11. There is a good match between observed and calculated gravity values. In particular, the anomaly in the axial trough is simply explained by the sedimentary basin, indicating that the low is mainly caused by sediments on the down faulted blocks. The lowest free-air anomaly, of -30 mGal, occurs in the centre of the basin and has a symmetrical form. Towards the shelves off Kalimantan and Sulawesi the values increase sharply to about +50 mGal. The minimum free-air anomaly in the centre of the basin is due to the presence of approximately 8 km of low density (2.3 Mg/m^3) sediments. The depth to the upper mantle is 24 km towards Kalimantan and 15 km towards Sulawesi and decreases to 12.5 km in the centre of the basin.

6.9.3.3 Gravity modelling PAC 202

This model has been prepared along seismic line PAC 202, but is extended up to the coast of Laut Island on the Kalimantan side and to the coast of Sulawesi. The result of modelling is shown in figure 6.12.

The lowest free-air anomaly, of about -40 mGal, occurs in the middle of the basin, with steep gradients towards the continental shelves of Kalimantan and Sulawesi. The minimum free-air anomaly coincides with the centre of the basin, where the water depth is about 2 km and where there are about 8 km of sediments. The free-air anomaly increases to as much as +70 mGal towards Kalimantan and Sulawesi. The depth of the upper mantle beneath the shelves off Kalimantan and Sulawesi is about 25 km but in the centre of the basin is only about 15 km.

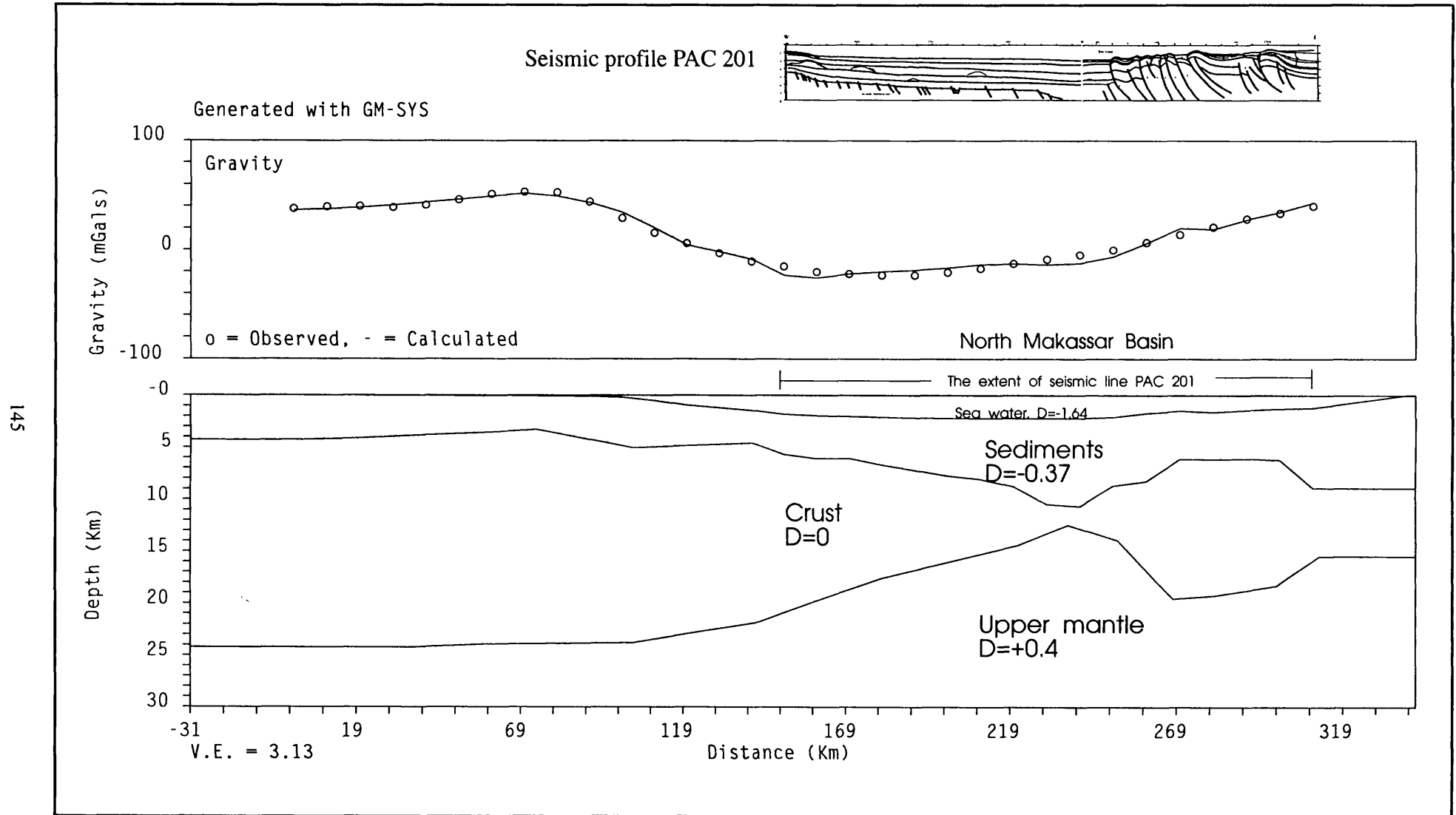


Figure 6.11: Gravity model PAC 201 showing crustal thinning over the Makassar Basin

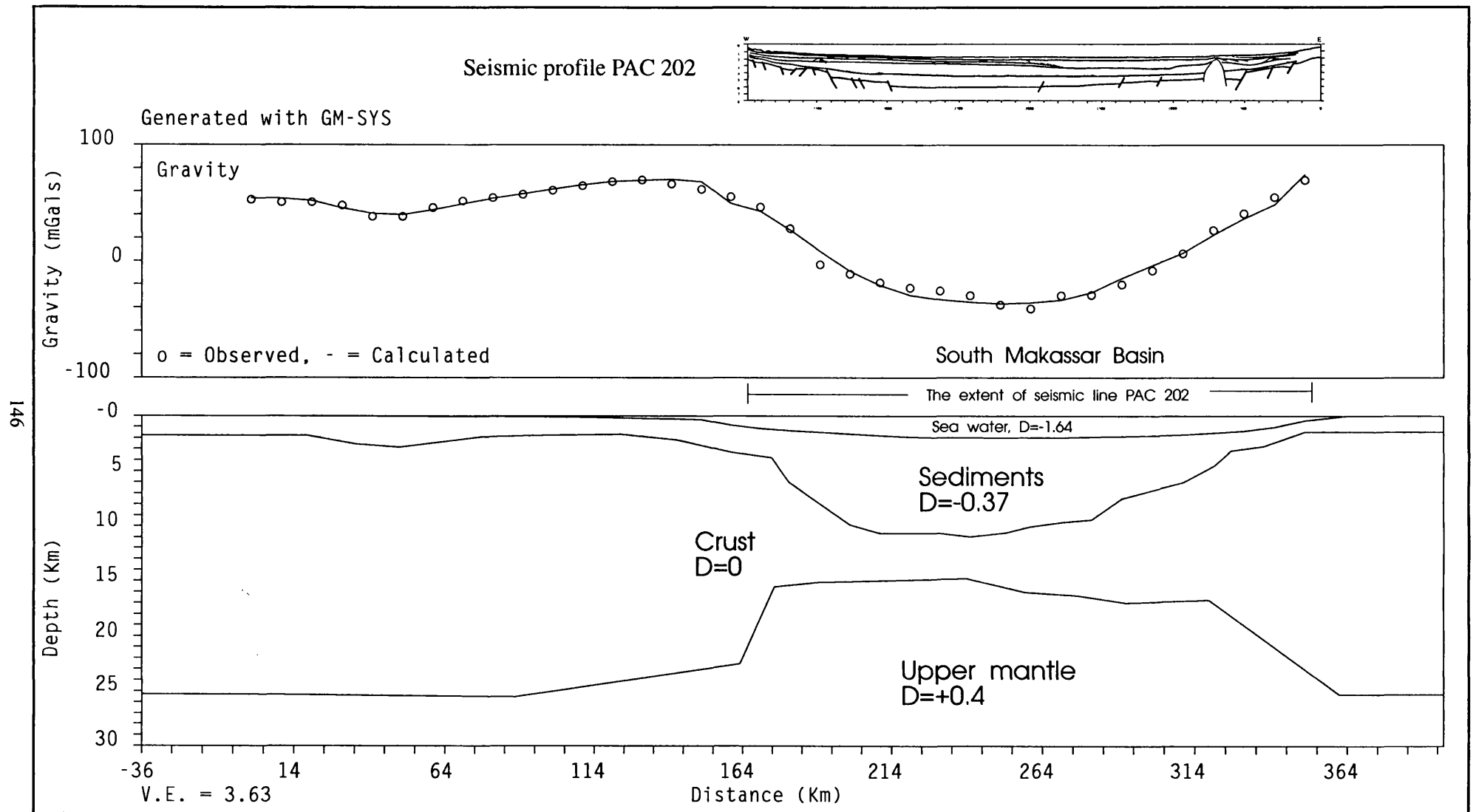


Figure 6.12: Gravity model PAC 202 showing crustal thinning over the Makassar Basin

6.9.3.4 Gravity modelling MCP 5

This model has been prepared along a line which crosses the Makassar Strait in a nearly E-W direction at latitude 20°S, i.e. along line seismic MCP 5, and is 275 km long. The thickness of sediments in the model was estimated using the average velocity from seismic line PAC 201, which was situated close to MCP 5. The result of modelling is shown in figure 6.13. The lowest free-air anomaly of -30 mGal coincides with the deepest water (2.1 km) and with the thickest sediments in the centre of basin (6.2 km). To the west, towards Kalimantan, the free-air anomaly increases sharply, reaching +50 mGal. This high free-air anomaly coincides with, and may be caused by, the basement uplift interpreted from the seismic profile. To the east of the axial trough, towards the shelf off Sulawesi, the free-air anomaly also increases sharply to +50 mGal. This increase is probably associated with a basement complex uplift.

The depth to the mantle is 28 km off Kalimantan and 25 km off Sulawesi; beneath the axial trough the depth decreases to 17 km.

6.10 CRUSTAL STRUCTURE

Deep water areas in the Makassar Strait correspond to areas of low free air anomalies, shallow bathymetry corresponds to areas of high free air anomaly. Gravity modelling shows, however, that the Moho is shallow beneath the axial trough and deepens towards the shelves (Fig.6.10-13) and that there is a change in the thickness of the crust, excluding the post-extensional sediments cover, from the continental shelf regions (25-28 km) to the axial trough (5-12 km). It is suggested that the crustal thickness changes are due to deformation by extensional thinning. The crustal thickness in the axial region indicates thinned continental crust. It is, however, still not certain whether the extension has generated oceanic crust. Seismic refraction data in the South Makassar Basin show basement velocities ranging from 3.56 to 5.69 km/sec (Prasetyo 1990), which are typical velocities for continental crust but could possibly be derived from the upper part of oceanic crust. Situmorang (1982) suggested that a stretching value of 2.9 is the lower limit for the formation of oceanic crust in the south Makassar Basin. Situmorang (1982) calculated that the Makassar Basin stretching factor was between 2 and 2.9 and that the basin had not yet developed oceanic crust. In contrast, the dolerites

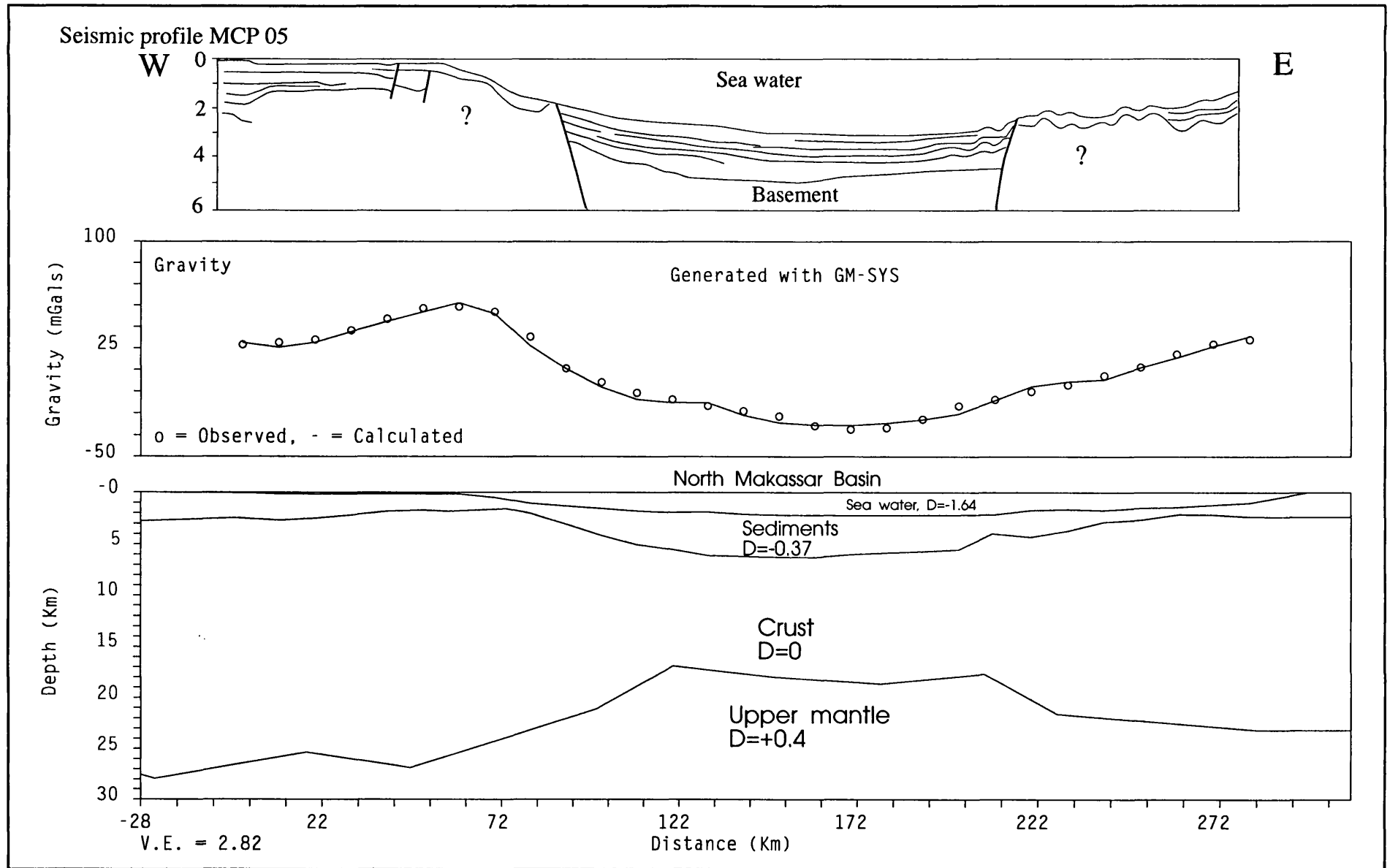


Figure 6.13: Gravity model MCP 5 showing crustal thinning beneath Makassar Basin

and gabbros in Well TT 2 in the Makassar strait are typical of an ophiolite sequence, suggesting the presence of oceanic crust. The present gravity models also suggest typical oceanic crust thicknesses. In view of the well data and gravity models, it is suggested that the central part of the Makassar Basin is underlain by oceanic crust.

6.11 TECTONIC IMPLICATIONS

Seismic reflection surveys and gravity modelling, as outlined above, support an Eocene extensional model for the Makassar Basin. Prior to extension the region is thought to have suffered compression due to the collision between SE Kalimantan and SW Sulawesi, which also produced the uplift of the Meratus range in the Late Cretaceous. This collision is thought to have thickened the crust, as normally happens in compressional regions.

From seismic reflection interpretation, the basement reaches a depth of 10 km and is overlain by sediments up to 8 km thick. The water depth in the axial trough reaches 2.2 km. Seismic stratigraphic analyses suggest that the Makassar Basin has subsided slowly and has experienced continuous sedimentation since the Eocene. This argument is supported by the depositional environment data from Wells TT 1 and TT 2, which showed continuous sedimentation during the Tertiary. The sediments were deposited in a near shore environment in the Eocene and a neritic to sub neritic environment in the Late Eocene to Middle Miocene. Shallow marine carbonates were deposited from the Middle Miocene to the Recent (Situmorang 1982). This observation leads to the interpretation that rifting was followed by thermal subsidence causing the basin to subside slowly and continuously.

The extension in the Makassar Strait can be explained by a sinking of the subducting plate east of western Sulawesi, leading to trench roll-back. This vertical sinking was accommodated by extension and rifting of the continental crust above the subduction zone at a previous site of collision, causing the opening of Makassar Strait. The time of this trench roll-back marks the cessation of subduction. Seismic reflection surveys (Figs. 6.5 and 6.6) rarely image effects of igneous intrusion, except on line PAC 202 at SP 600 - SP 800. Rifting was accompanied by the deposition of syn-rift sediments (Seismic

sequence 2, PAC 201 and PAC 202). In the Early Oligocene, the rifting may have terminated and have been followed by the deposition of post-rift sediments (Seismic sequences 3 to 6, seismic line PAC 201 and 202).

Young compressional zones (thrust faults) affecting strata up to horizon H5 (Mid-Miocene) formed a foreland basin as a crustal flexure in the eastern part of the Makassar Basin (Line PAC 201). This phenomenon can also be seen in the Kutai Basin (Biantoro *et al.* 1992), to the west of the Makassar Strait. The fact that the Makassar Basin is flanked by these two east-dipping thrust faults is difficult to understand because the basin is not disturbed at all, and on PAC 201 the thrusts die out from west to east, as in the Kutai Basin. Biantoro *et al.* (1992) suggested that anticlinorium and thrust faults in the Kutai Basin are due to the interaction of two major strike-slip faults; the Sangkulirang and Paternoster faults. The same explanation is also suggested for the formation of thrust faults in the eastern part of the Makassar Strait since the thrust faults observed on the seismic profiles also occur between these two major strike-slip faults. The collision of the NW Australian Continental margin with the Sunda Trench and Banda Arc is thought to be responsible for the formation of the major dextral strike-slip Paternoster and Sangkulirang faults.

CHAPTER SEVEN

CENTRAL JAVA SEA PROVINCE

7.1 INTRODUCTION

The Java Sea is normally divided into the West and East Java Seas. However using the structural grain, bathymetry and gravity data, the area can be divided into three major provinces; the West, Central and East Java seas. The West Java Sea is characterised by N-S structural trends, whilst the East Java Sea is clearly characterised by E-W structural trends; between these two structural provinces is a region marked by conspicuous NE-SW structural trends. This area, the Central Java Sea, extends approximately from north of Central Java to the Meratus region in SE Kalimantan. It consists of NE -SW structural lows and highs, i.e. basins with intervening uplifts, of pre-Tertiary age (Fig.7.1).

Physiographically it is situated in the Southeast Sunda Shelf where extensive Tertiary sediments are covered by shallow continental sea less than 100 m deep. The essential unity of the area is supported by magnetic and gravity maps (see Fig. 3.10 and 3.16) from Edcon (1991), which show the continuity of the structural patterns in these areas.

7.2 PREVIOUS STUDIES

The following are some of the results of workers in the Sunda shelf area. Earle (1845) and Molengraff (1919, quoted in van-Bemmelen 1949) suggested that the shelf seas were peneplains, submerged during marine transgression after the Pleistocene glaciation.

Koesoemadinata and Pulunggono (1971;1975) noted that the Sunda Shelf served as a source of sediments to the adjacent areas during the Tertiary. Hamilton (1979) summarised the results of exploration wells in the Sunda Shelf in terms of lithologies and age of the basement. Bishop (1980), summarising the structure, stratigraphy and hydrocarbon occurrences in the Java Sea region, considered the rocks below the pre-Tertiary angular unconformity to represent economic basement. Immediately above the unconformity the oldest strata are fluvial and lacustrine clastics, whilst the remainder of the Tertiary sedimentary interval consists largely of shallow marine calcareous shale with interbeds of fine grained quartz sandstone.

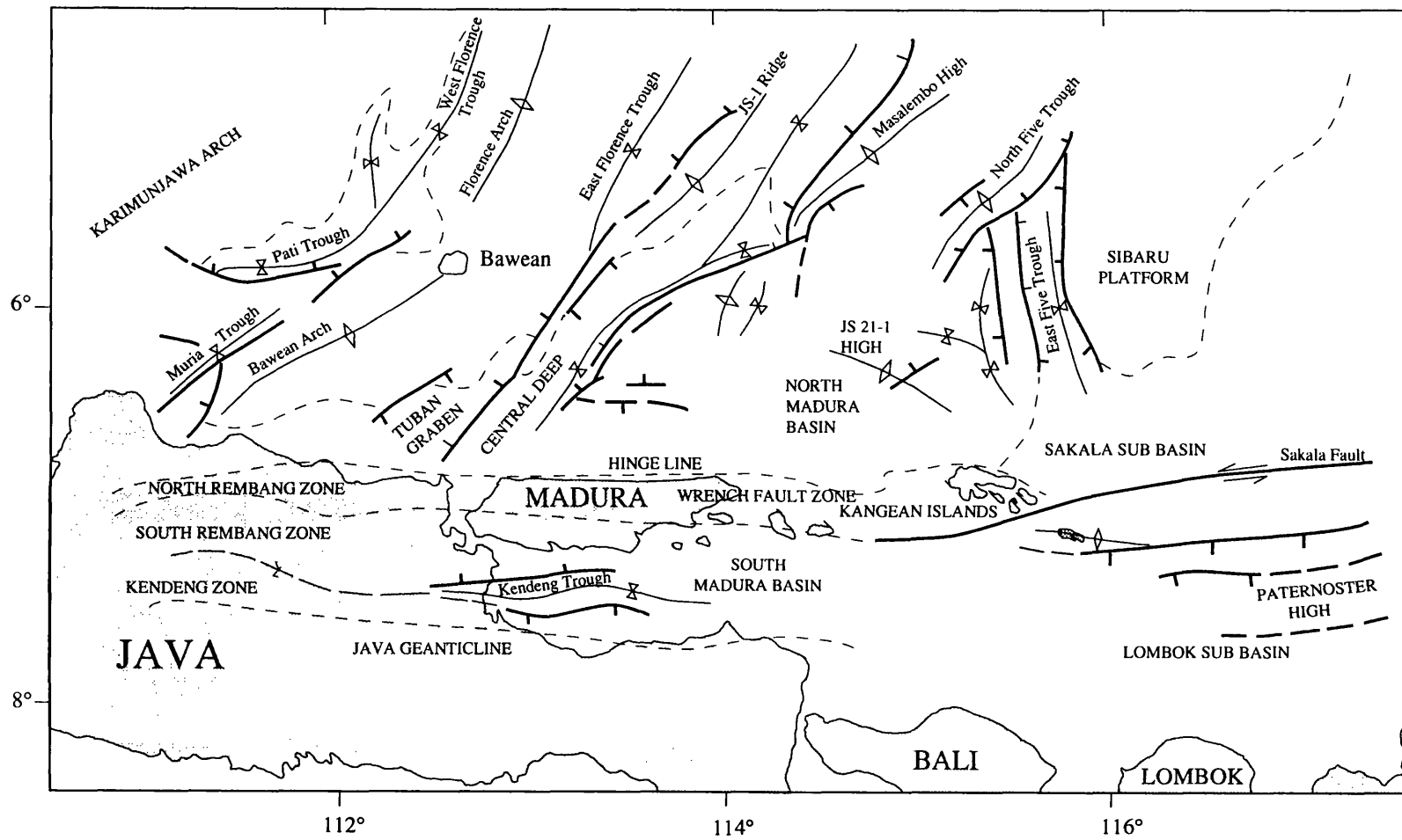


Figure 7.1: Structural setting of the Central Java Sea showing the NE-SW structural highs and lows (P.T Trias 1989)

7.3 BATHYMETRY

A bathymetric map of the Central Java Sea Province was obtained from Ben-Avraham and Emery (1973) and contoured at 20 m interval (Fig.7.2). The area is mostly covered by water less than 80 m deep and is generally flat-bottomed. Bathymetric trends have an E-W orientation in the west and then bend sharply in the east to NE-SW, towards the Meratus Mountain (SE Kalimantan) and the Makassar Strait. Circular closed contours mark basement highs, e.g. the Bawean and Karimunjawa islands. The shelf depth increases towards the East Java Sea, the easternmost boundary being marked by the 100 m bathymetric contour which separates the Central Java Sea Province from the East Java Sea Province.

7.4 TECTONIC SETTING AND STRATIGRAPHY

7.4.1 Subduction related region

The Central Java Sea Province is part of the Southeast Sunda Shelf, which is bounded to the west by the Western Java Sea, to the south by the Java Island Arc, to the north by the stable platform of south Kalimantan and to the east by the East Java Sea. Structural maps (Fig. 7.1) and seismic reflection profiles (Ben-Avraham and Emery, 1973; Silitonga and Hakim, 1990) show basement highs and lows which are thought to play a dominant structural role in the province. There are four major structural highs trending to NE-SW; the Karimunjawa Arch, the Bawean Arch, the Meratus High and the Laut Ridge (Fig.7.3). The structural patterns are closely related to island-arc systems. The presence of melange in the Meratus Mountains and in some part of central Java leads to the conclusion that these areas were close to subduction zones in the Early Cretaceous. The Karimunjawa arch represents the magmatic arc, whilst the volcanism in Laut Island and Bawean might be explained as a result of extension after collision at the southeastern margin of Sundaland in the Late Cretaceous-Early Tertiary. However Ben-Avraham and Emery (1973) suggested that the Bawean arch and the associated volcanism was due to eastward migration of subduction.

7.4.2 Basement rocks

Basement in the Java Sea includes metamorphic, granitic and volcanic rocks. Van-Bemmelen (1949) suggested that the oldest stratigraphic unit in the Sunda Shelf is a

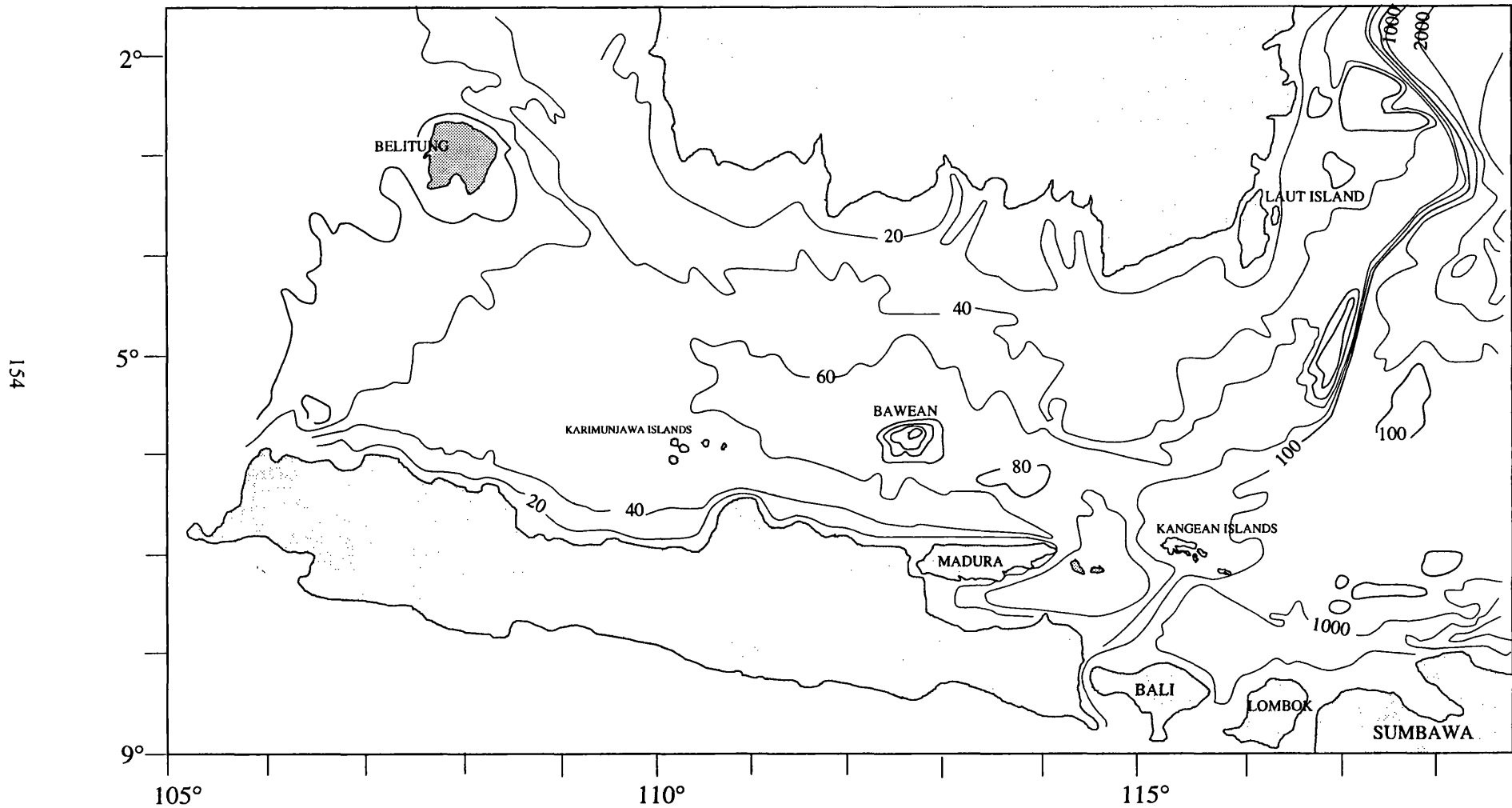


Figure 7.2. Bathymetric map of the Central Java Sea (Ben-Avraham and Emery 1973)

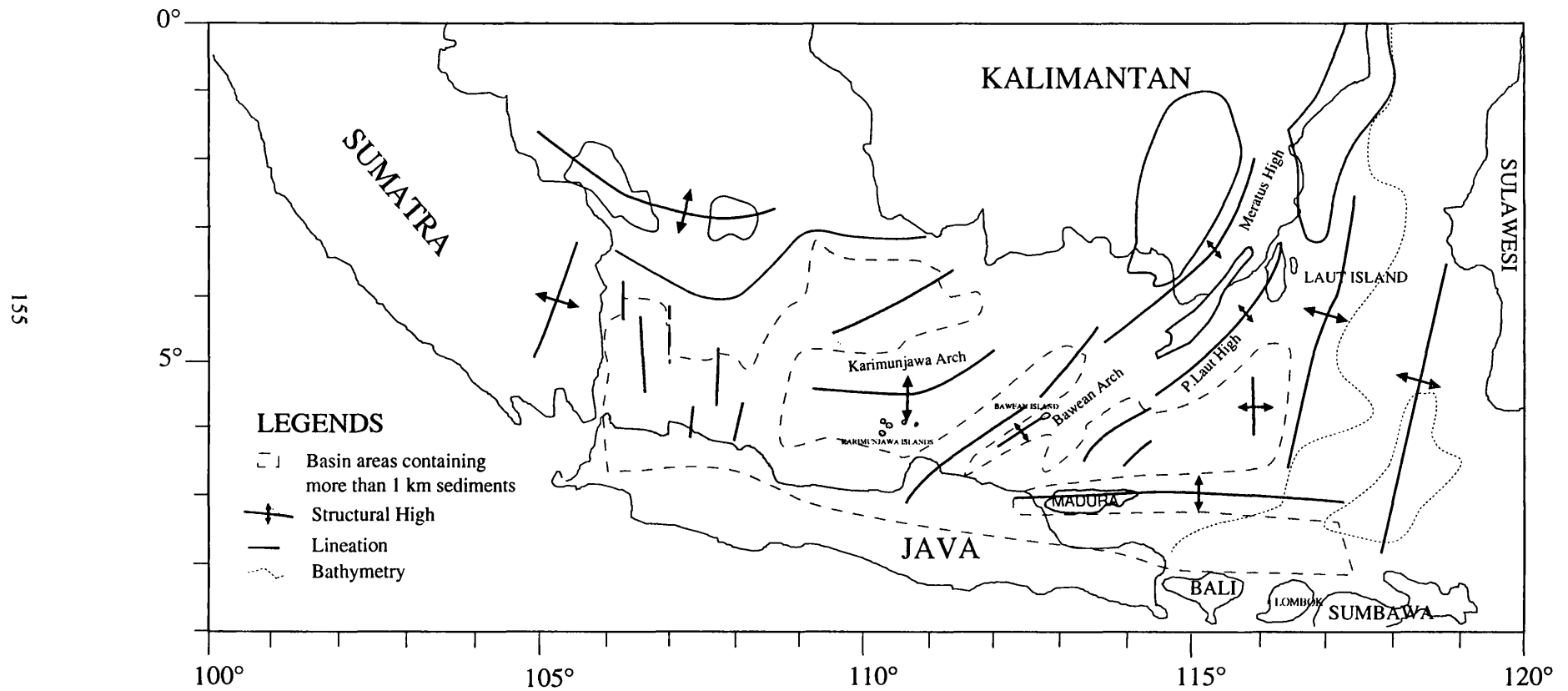


Figure 7.3: Tectonic elements in the Central Java Sea and vicinity showing four major structural highs in NE-SW direction (Simplified from Ben-Avraham and Emery 1973)

product of sedimentary deposits altered by regional metamorphism. The Meratus Mountains consist of ultrabasic rocks (serpentinized peridotites and gabbros), as well as radiolarian cherts, interpreted by Hamilton (1979) as subduction melanges of Late Cretaceous-Palaeogene age. Laut Island has a similar composition but contains some volcanic rocks. Bawean Island, atop the Bawean Arch, consists of alkaline volcanics of Tertiary age.

Ben-Avraham and Emery (1973) stated that the basement rocks of the Sunda Shelf consist primarily of low-grade pre-Tertiary metamorphics and Late Cretaceous igneous rocks. On the small Karimunjawa islands pre-Tertiary metamorphosed sediments are exposed. On the basis of the similarities between geophysical parameters across the Bangka-Belitung granite and the Karimunjawa arch, Ben-Avraham and Emery (1973) suggested that the arch may be underlain by a granitic batholith, though it just as well could be built up entirely of metamorphic sediments.

Hamilton (1979) noted that many oil-exploration wells have reached basement beneath Eocene, Oligocene or Miocene strata in the Java Sea. In the Central Java Sea Province, slaty metasediments, some of them extremely sheared, are dominant and are of either terrigenous or volcanoclastic origin; basic to silicic volcanic rocks and, in the northwest, granitic rocks are present. K-Ar age determinations on the granitic, volcanic and metasedimentary rocks have mostly indicated Paleocene and Cretaceous ages (58-115 m.y)(Hamilton 1979).

It seems probable that in the Java Sea the silicic magmatism records the same subduction system as does the melange of Late Cretaceous or very Early Tertiary age farther east.

7.4.3 Stratigraphy

The Central Java Sea consists of eastern and western basinal areas and the Karimunjawa arch can be considered as a boundary separating them. The two basins have different environmental history (Koesoemadinata and Pulunggono 1975, Nayoan 1975 and PT. Trias 1989). In general the western part was a non marine environment during all of the Oligocene and the Early Miocene, whereas the eastern part was marine during deposition

of the Oligocene and Early Miocene sediments. The differences in stratigraphy between the western and eastern parts can be seen in Figure 7.4 (PT. Trias 1989); the lithostratigraphy of the eastern part consists of the Ngimbang, Kujung, Poleng, North Madura and Prupuh formations, whilst the stratigraphy of the Western part consists of the Jatibarang Volcanics, which are considered to be of Cretaceous age and equivalent to the Manunggul Volcanic in the Meratus Mountains, followed by the Ciletuh, Bayah, Talang Akar and Rajamandala formations.

7.5 SEISMIC REFRACTION AND REFLECTION

The seismic profiles discussed here have been obtained from literature studies, in particular from Ben-Avraham and Emery (1973) and Silitonga and Hakim (1990).

7.5.1 Refraction data

7.5.1.1 Introduction

Figure 7.5 shows the oblique reflection-refraction coverage obtained using expendable AN/SSQ41 radiosonobuoys in the Central Java Sea and surrounding areas (Ben-Avraham and Emery, 1973). These data provided information on the depth to acoustic basement and the velocity of sound within it and at various depths in the overlying sediments.

7.5.1.2 Results and interpretation

From the radiosonobuoy data (see Table 3.1, in Chapter 3), eight groups of refraction velocities have been identified (Ben-Avraham and Emery 1973). In general, basement rock in the Central Java Sea has an average velocity of about 5 km/sec, which may indicate granite; at radiosonobuoy 20, over the Karimunjawa Arch, the basement, which is interpreted as granitic rocks, had a velocity of 4.83 km/sec. In the deep sedimentary basins, high velocities may be due to Lower Miocene Limestones (the Batu Raja Limestone in the western Java Sea and the Upper Kujung Limestone farther east). Velocities in group V7, with an average value of 4.09 km/sec, are also thought to be from the Lower Miocene Limestone. Velocities in groups V6 and V5, with average values of 3.04 and 2.59 km/sec, were found mainly in the Central Java Sea and were interpreted as indicating local distribution of shallow water glauconitic sands and clays

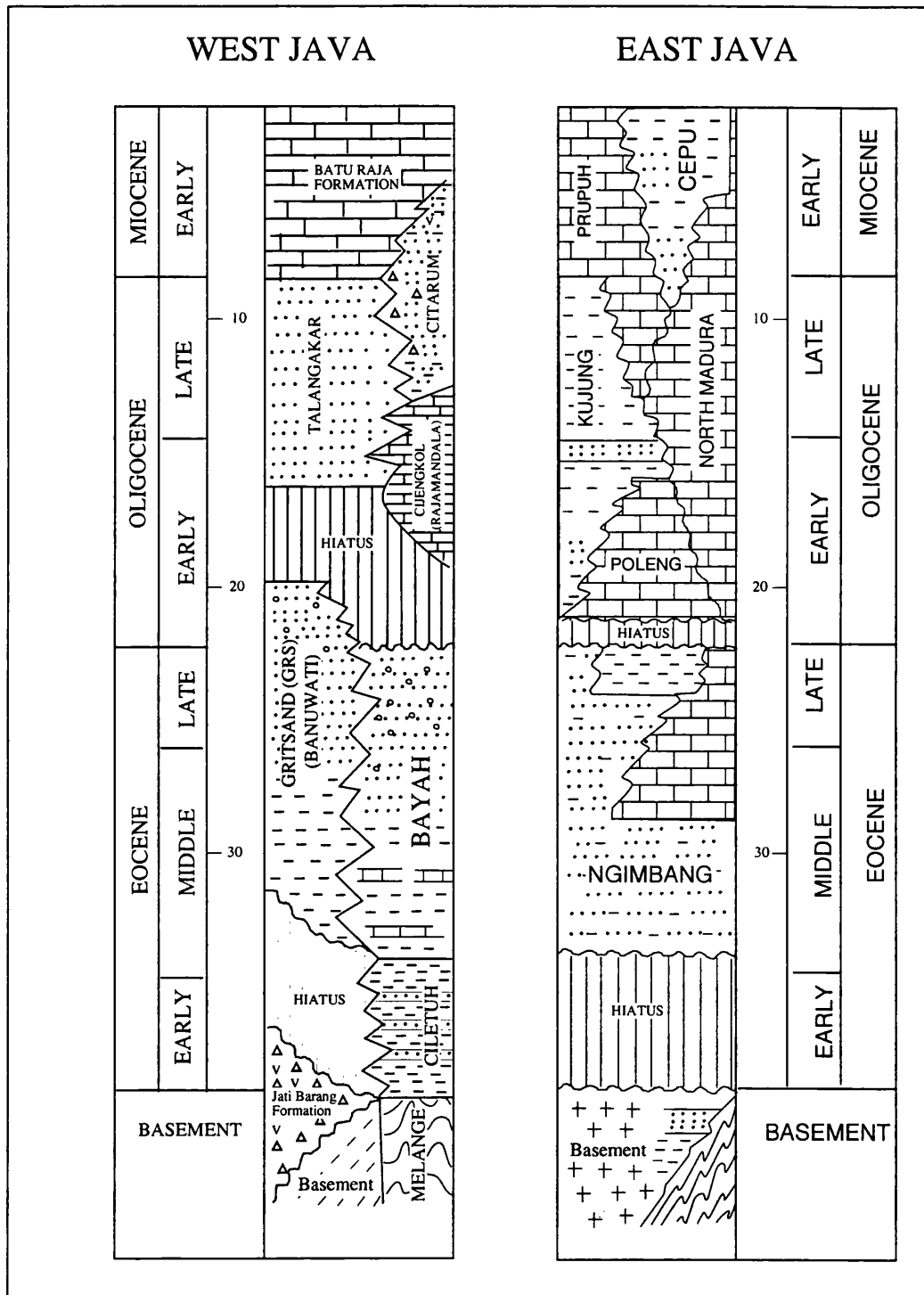


Figure 7.4: Stratigraphic correlation between Western and Eastern Java, which is comparable to western and eastern basinal areas (PT. Trias 1989)

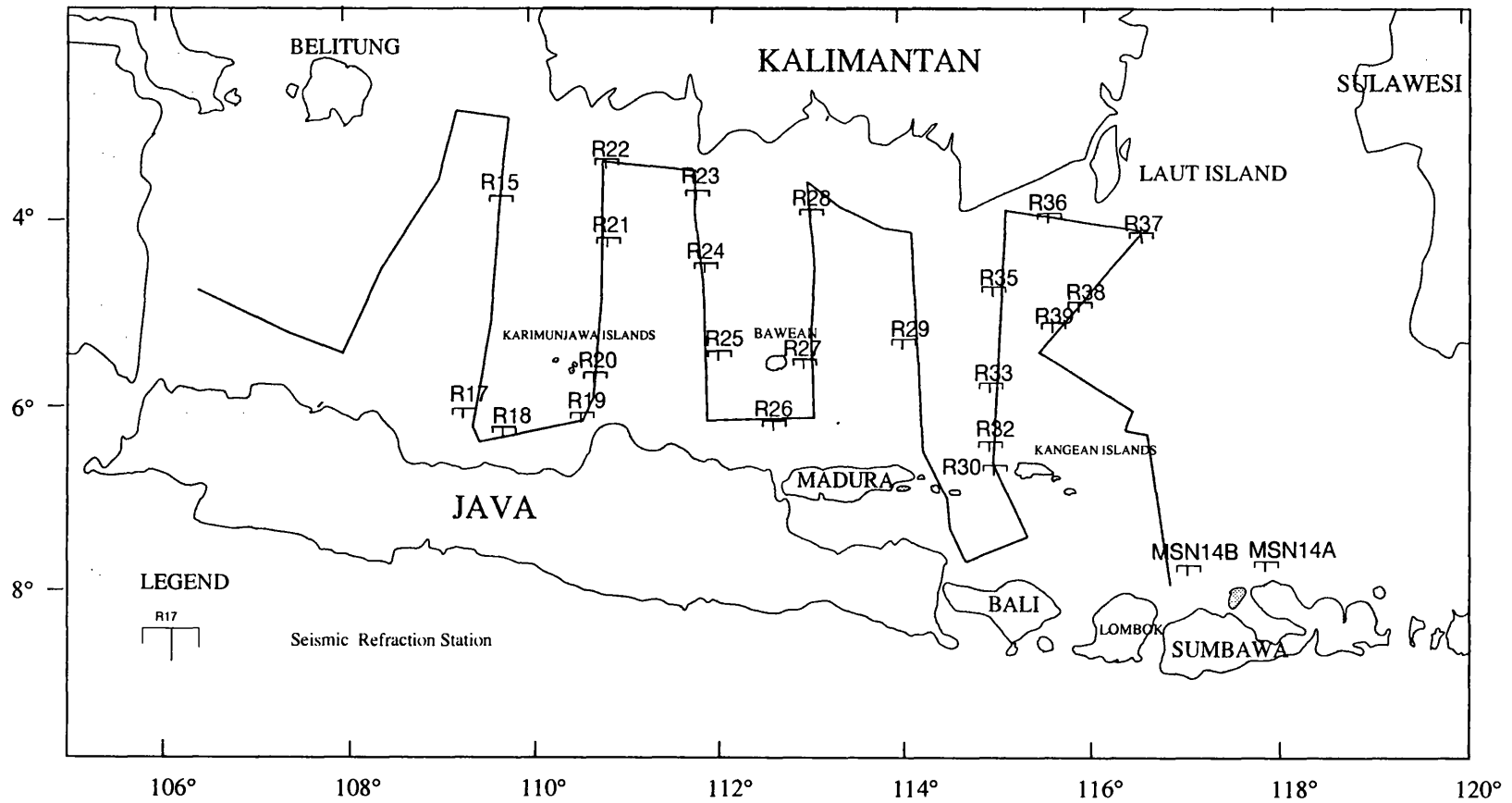


Figure 7.5: Location of oblique reflection-refraction data coverage in the Java Sea (Ben-Avraham and Emery 1973)

of Early Miocene age. Velocities V4, V3 and V2 (2.12, 1.93, and 1.60 km/sec, respectively) are abundant throughout the Java Sea and were interpreted as typifying sediments of Mio-Pliocene and Plio-Pleistocene age.

7.5.2 Seismic reflection

7.5.2.1 Introduction

Seismic interpretations in the region have been published by Ben-Avraham and Emery (1973) and Silitonga and Hakim (1990). All the profiles are shallow seismic reflection. Seismic profiles from Ben-Avraham and Emery were obtained from radiosonobuoy data which provide information on the depth to acoustic basement and the velocity of sound within it. Seismic profiles from Silitonga and Hakim were obtained using single channel of 300 Joules uniboom source, 700-1000 Joules sparker and 1750 PSI for airgun source.

7.5.2.2 Interpretation

Figure 7.6A shows a line drawing interpretation and associated free-air anomaly and magnetic anomaly profiles passing through the Central Java Sea in a N-S direction for approximately 300 km (Ben-Avraham and Emery 1973). The profile displays parallel bedded reflectors with moderate to good continuity. The basement was dominated by block faulting with the Karimunjawa Arch interpreted as uplifted basement covered by thin sediments. The arch corresponds to an area of high free-air anomaly, reaching +45 mGal, and a positive magnetic anomaly reaching 500 nT.

To the west and east of the Karimunjawa Arch, Horizon L (Lower Miocene Baturaja Formation) deepens sharply in both directions, probably due to faulting. The depth of the horizon ranges between 0.6 - 1.1 msec TWT. Some minor igneous intrusions were also indicated. The overlying sediments in general onlap the structural highs and have not been significantly deformed.

Figure 7.6B shows a line drawing interpretation and associated free-air and magnetic anomalies for a second section, about 200 km in length, across the Central Java Sea in a N-S direction (Ben-Avraham and Emery 1973). The reflectors are characterised by parallel bedding and a low degree of disturbance, whilst fluctuations in basement depth

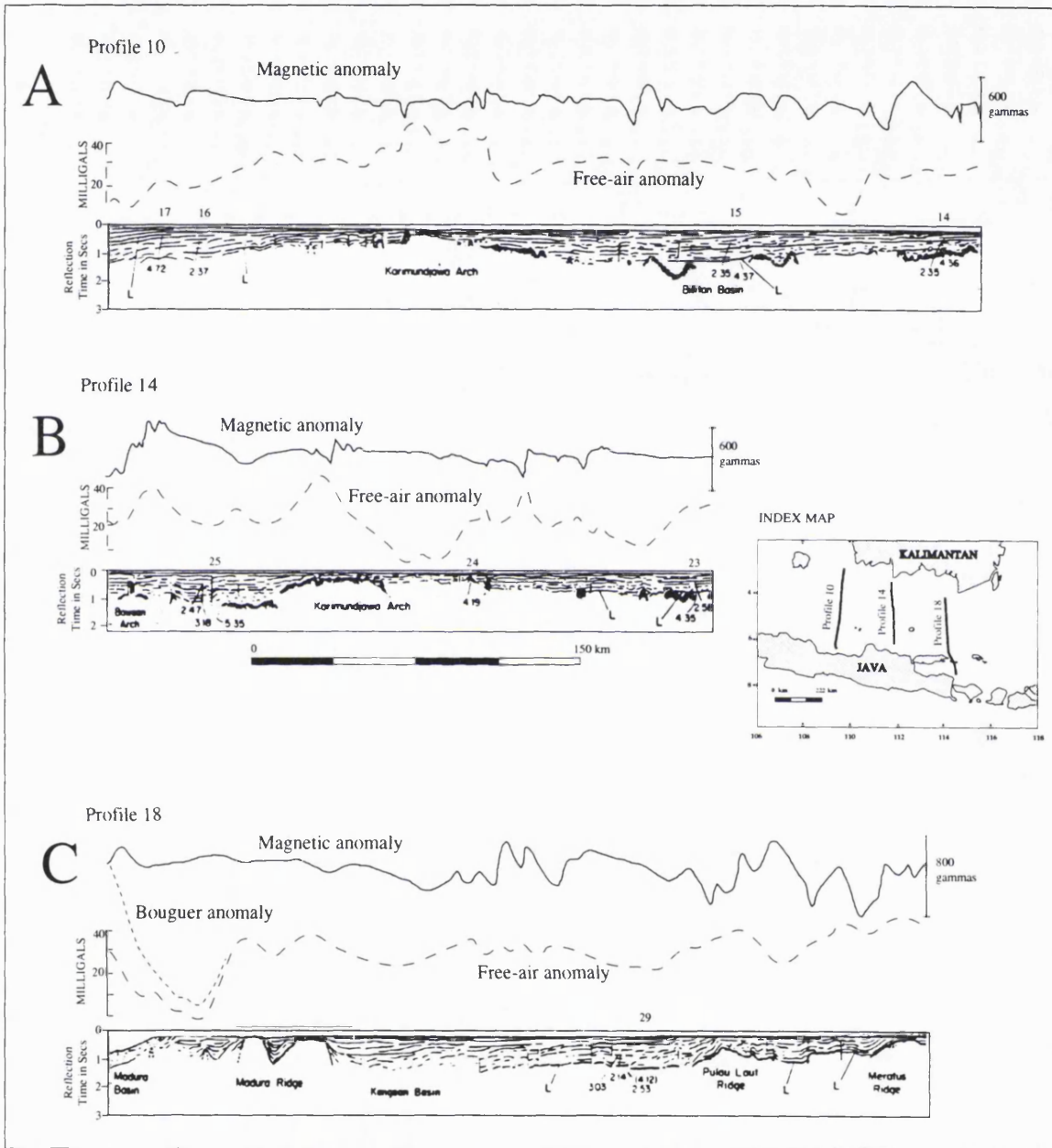


Figure 7.6A,B and C: Seismic line drawing interpretation with Bouguer, Free-air and magnetic anomaly profiles (Ben-Avraham and Emery 1973)

indicate block faulting. The interpretation shows two major highs; the Bawean and Karimunjawa arches. The Bawean arch on this profile is rather smaller in size and at a deeper level than the Karimunjawa Arch. The free-air anomaly over the Bawean Arch is about +40 mGal whilst over the Karimunjawa Arch it is +45 mGal. Between these two highs lies a deep basin with sediment thicknesses of approximately 1.2 Sec TWT.

Figure 7.6C shows a line drawing interpretation and associated free-air and magnetic anomaly profiles for a line crossing the Central Java Sea in the north and the East Java Sea in the south, in a N-S direction, a total length of about 300 km (Ben-Avraham and Emery 1973). The reflectors are parallel and not much disturbed. The interpretation shows three major structural highs with intervening basins; the Madura Ridge in the East Java Sea and the Laut Island and Meratus ridges in the Central Java Sea. The acoustic basement, at between 1 and 1.8 sec TWT and indicated by the letter L on Fig.7.6, probably corresponds to the Lower Miocene Baturaja Formation.

Figure 7.7 shows the results of shallow seismic reflection surveys near Karimunjawa Island by the MGI research ship “Geomarine” (Silitonga and Hakim 1990). The interpretation shows the area to be dominated by normal faults. Basement is shallow and covered by thin sediments.

7.5.3 Summary

The Karimunjawa arch is the dominant ridge in the Central Java Sea, extending from offshore West and Central Java to southern Kalimantan. The seismic line drawing interpretations discussed above and also a geologic model across the Java seas (Fig. 7.8) show a stratigraphy and structure of the Central Java Sea that can be summarised as follows; the basins in general are formed on down-faulted basement, with some major uplifts and intrusions. In some respects these characteristics are typical of rifted basins. The overlying sediments in general exhibit parallel bedding without much deformation and have thicknesses of less than 1.8 Sec TWT. Carbonate deposition was dominant in the Java Sea during the Neogene. All these observations indicate that the basins in the Central Java Sea were relatively stable after their formation by block faulting and that tectonic activity was not extensive.

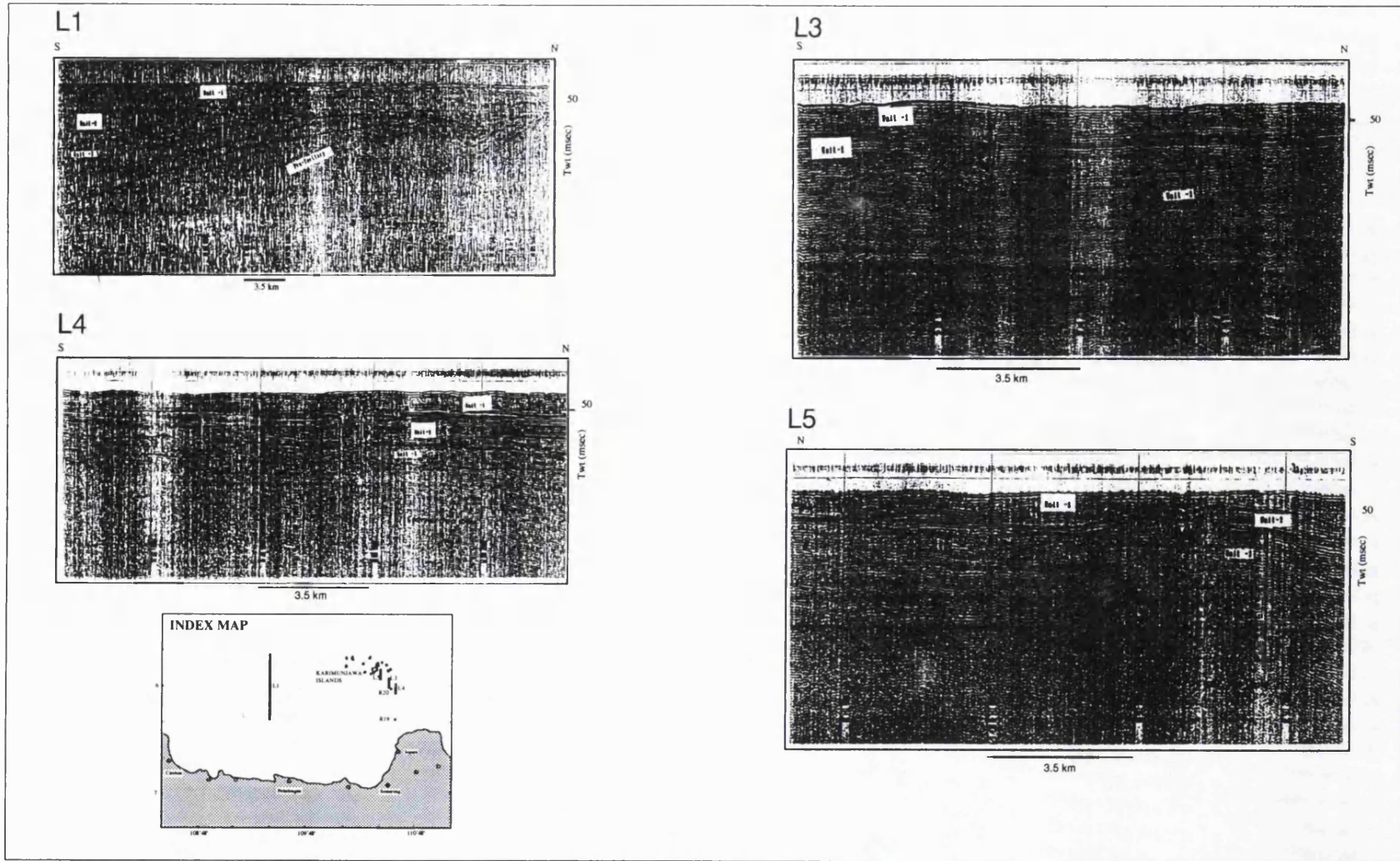


Figure 7.7: Shallow seismic reflection profiles in the Central Java Sea (Silitonga 1990)

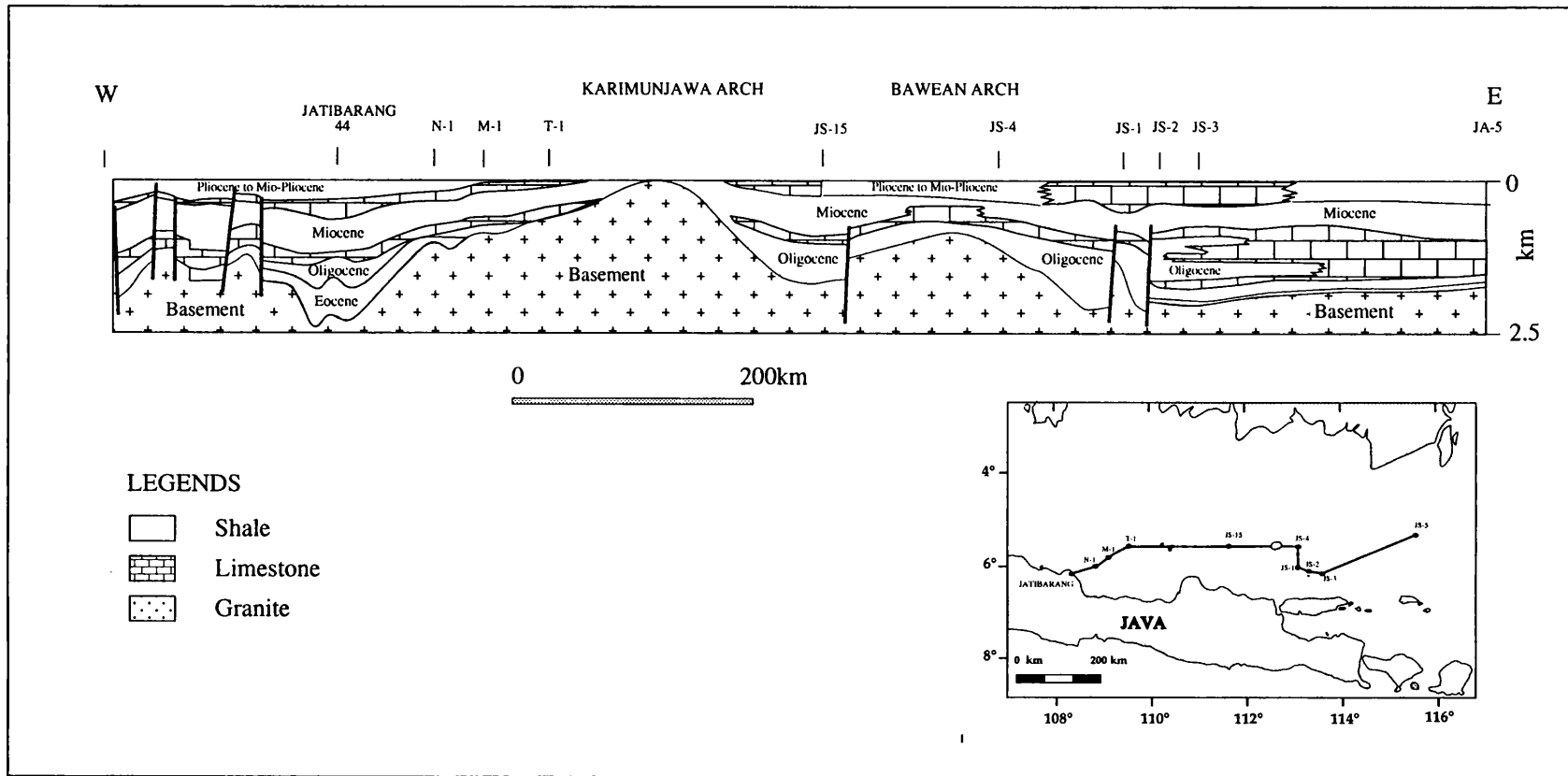


Figure 7.8: Geological cross section passing the Central Java Sea in E-W direction (After Koesoemadinata and Pulunggono 1971;1975)

Magnetic anomalies, as shown in Fig.7.6, have a wide range of amplitudes and wavelengths. They have been interpreted as the effects of various basement rocks (see Section 7.4.2, described as granitic, metamorphic and volcanic).

7.6 GRAVITY DATA

7.6.1 Introduction

The Bouguer anomaly map of the Central Java Sea was extracted and modified from the Edcon Bouguer anomaly map (1991). The modification was done by redrawing the contours without using the satellite gravity data because the accuracy of satellite data is not as good as the marine data. This modified map (Fig.7.9) was used to construct the gravity models. Edcon used a density for the Bouguer correction of 2.2 Mg/m^3 .

7.6.2 Qualitative Gravity Interpretation

The Bouguer anomaly map of the Central Java Sea is characterised by strongly NE - SW contour lineations and by broad isolated anomalies with amplitudes on average of +30 to +50 mGal and wavelengths of 10 - 250 km. The gravity gradients are the lowest of any province in the Central Indonesian Region, reaching only 0.5 - 1 mGal/Km. Water depths in this province are less than 100 m, whereas in the other provinces they are generally in the range 1000 - 5000 m. These differences reflect differences in crustal type and tectonic development. The broad distribution of isolated contours with gentle gravity gradients marks this area as dominated by basement faults. Low gravity values are possibly associated with deep basins filled with thick layers of sedimentary, whereas high gravity values are probably associated with basement uplifts with thin sedimentary cover. The four main gravity highs (see Fig. 7.9) are interpreted as marking the locations of uplift belts or structural highs; the Karimunjawa High, the Bawean High, the Meratus High and the Laut High (KH, MH, BH and LH), which run roughly NE-SW between Java and Kalimantan. The continuity of the trends is disrupted by ENE lineations which are interpreted as faults.

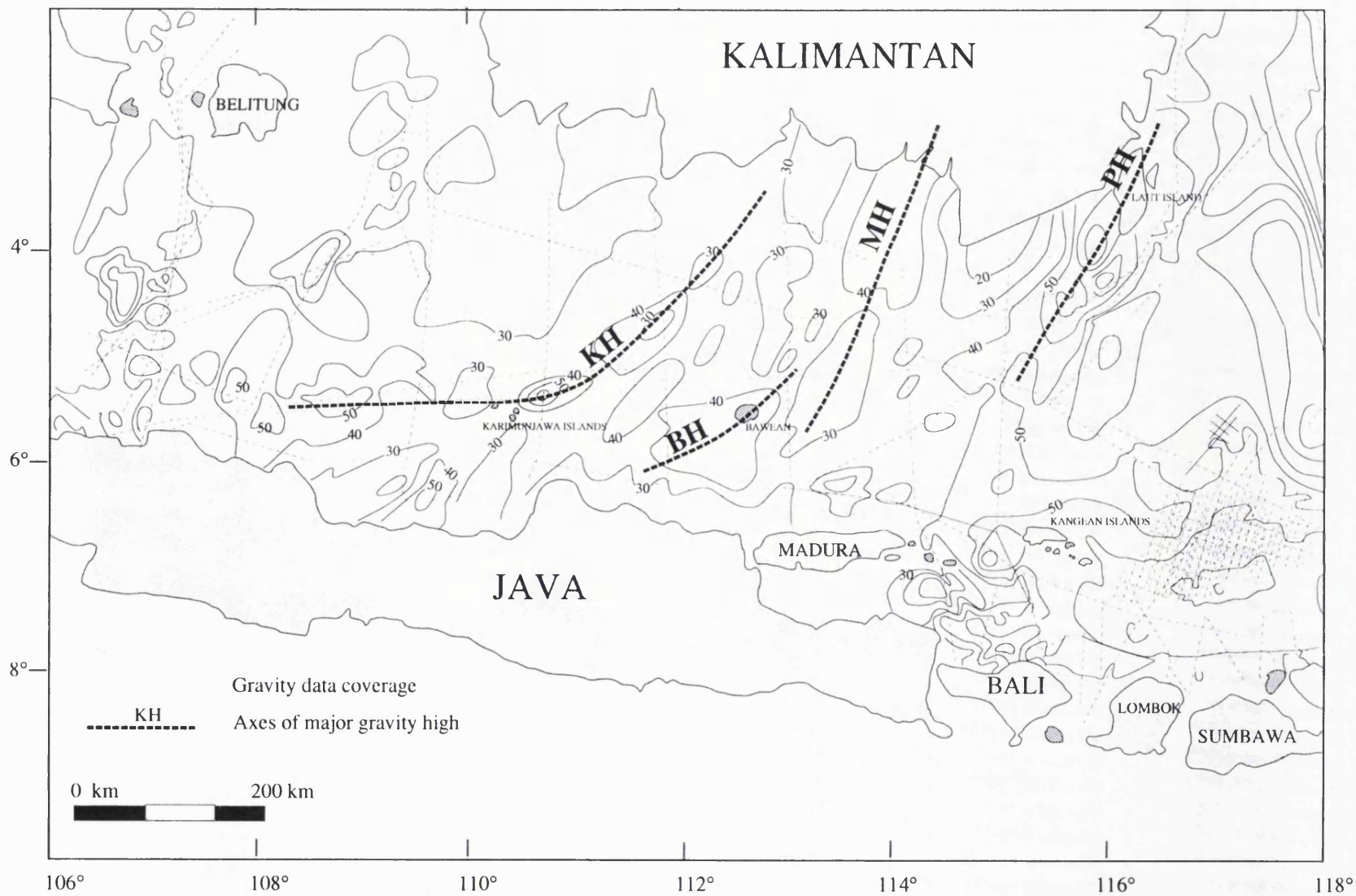


Figure 7.9: Bouguer anomaly map of the Central Java Sea and vicinity (modified from Edcon 1991)

7.6.3 Gravity models

7.6.3.1 Introduction

Three gravity models have been constructed using the GM-SYS gravity modelling program, these being, from south to north, the Java Sea 1, 2 and 3 models (Fig. 7.10). The Java Sea 2 and Java Sea 3 models were constrained using radiosonobuoy data whilst the Java Sea 1 model was constrained using the geologic cross-section of Koesoemadinata and Pulunggono (1975) as well as radiosonobuoy data.

The average density of the sediments was taken 2.1 Mg/m^3 , based on converting the average interval velocities from radiosonobuoy data (Ben-Avraham and Emery 1973) using the density-velocity curve of Nafe and Drake (1963). The density of granitic intrusions was taken as 2.72 Mg/m^3 , the density of upper crust as 2.67 Mg/m^3 and density of the upper mantle as 3.3 Mg/m^3 . The reference crustal density was 2.67 Mg/m^3 and the depth of standard crust was taken as 30 km.

7.6.3.2 Interpretation

7.6.3.2.1 Gravity model Java Sea 1

This model relates to a roughly E-W line across the Central Java Sea. Interpretation was primarily constrained by the geological section (see Fig. 7.8) constructed by Koesoemadinata and Pulunggono (1971;1975) and five sets of radiosonobuoy data (R20, R25, R27, R29 and R33), which gave information on the thicknesses and velocities of the sediments. The final model is shown in Figure 7.11. There is a good match between observed and calculated gravity anomalies and with the known geology.

There are two Bouguer anomaly highs which correlate with the structural geology; the Karimunjawa and Bawean highs. The Karimunjawa High, in the west, reaches +42 mGal and corresponds to the Karimunjawa arch on the structural map (see Fig. 7.3). This high was modelled by an igneous intrusion having a density contrast 0.05 Mg/m^3 at a depth below the surface ranging between 150-300 m and covered by sediments in a water depth of less than 50 metres. In the model this Karimunjawa High is flanked by deep sedimentary basins. To the west lies the Sunda Basin which has sedimentary thickness

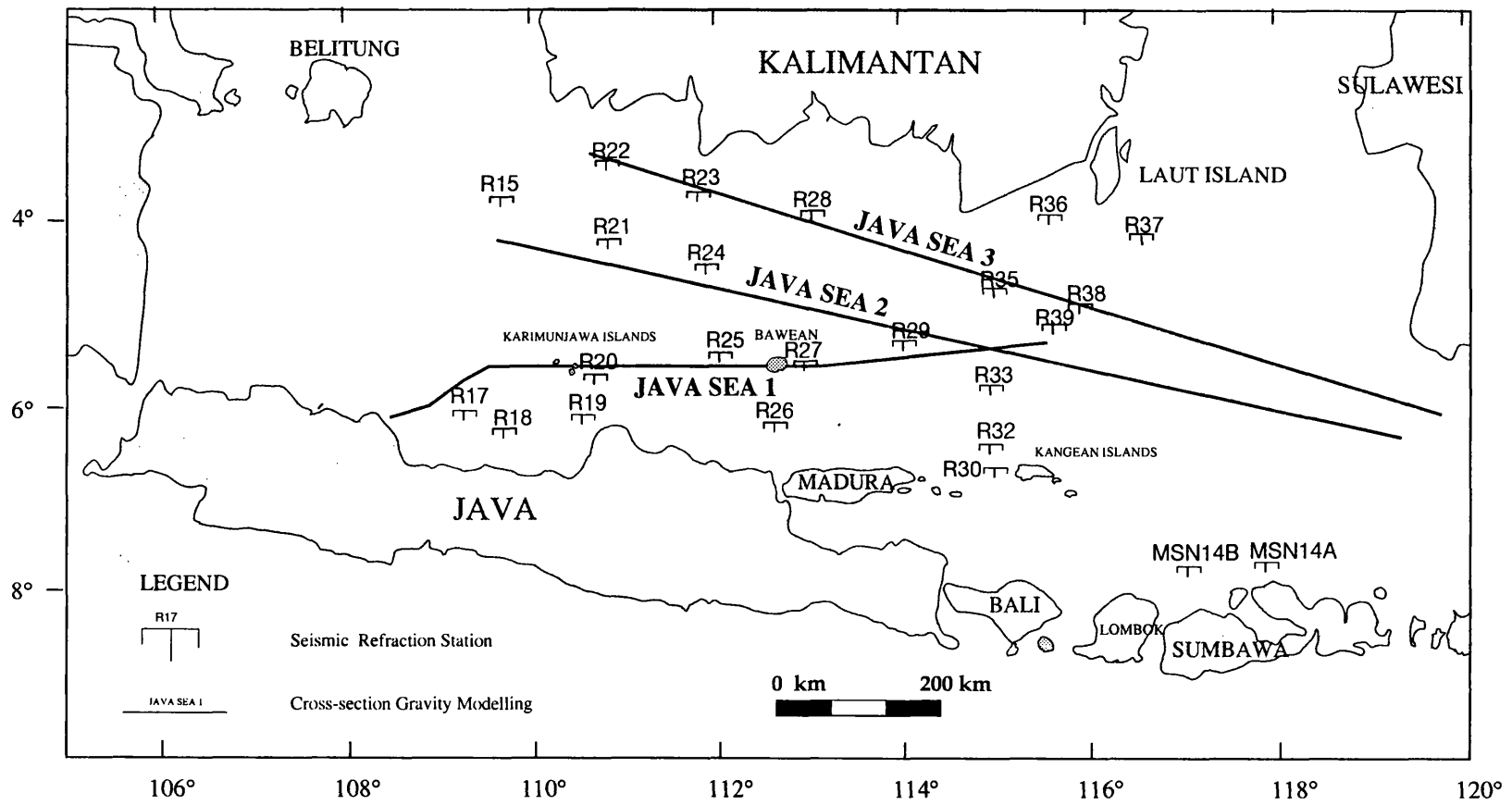


Figure 7.10: Location of gravity models and radiosonobuoy stations in the Central Java Sea

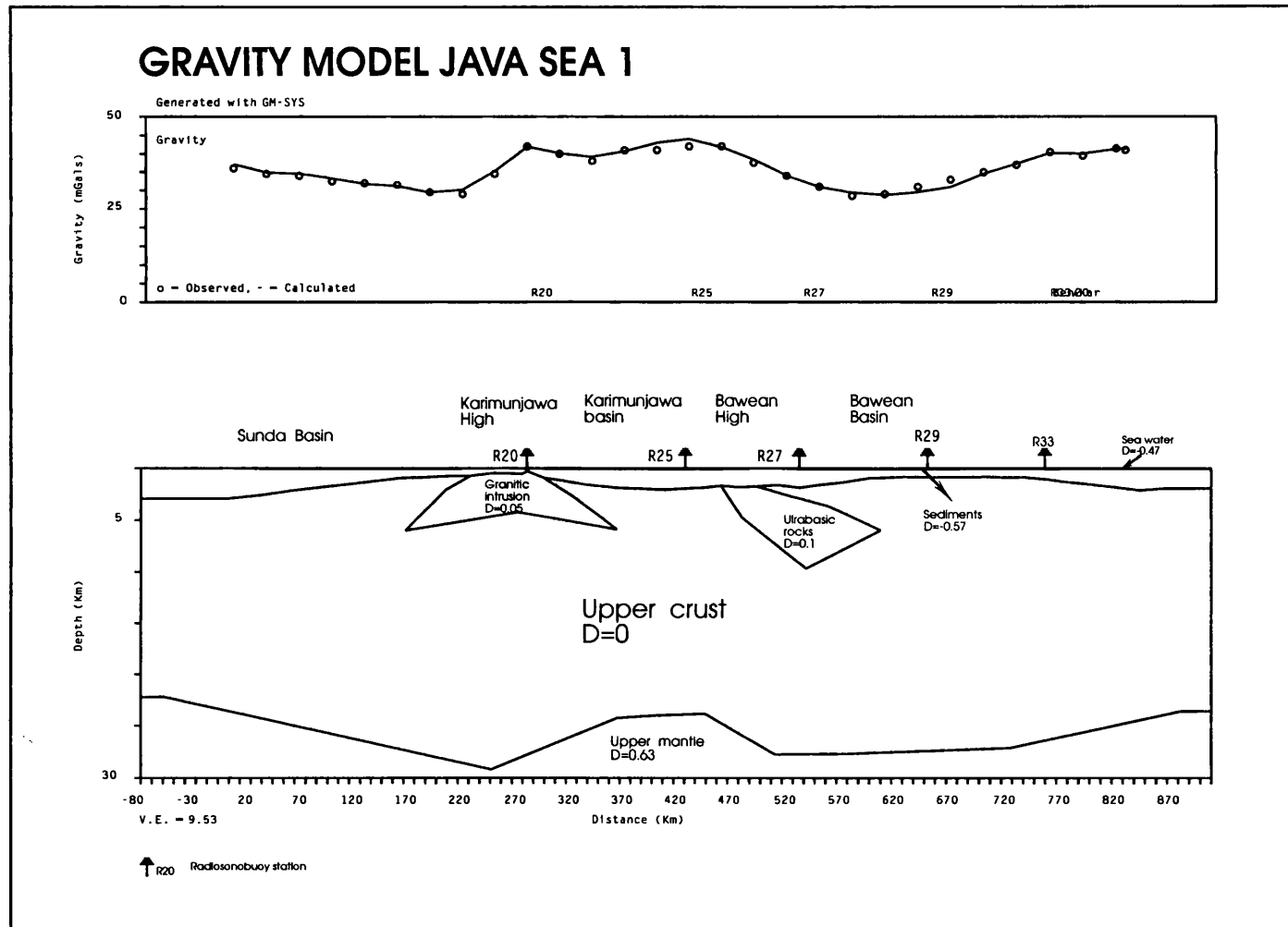


Figure 7.11: Gravity model Java Sea 1

up to 2.6 km, whilst to the east the Karimunjawa Basin has sedimentary thickness of up to 2 km.

The eastern Bawean High, reaching up to +40 mGal, corresponds to the Bawean arch of the structural map. This high was modelled as due to an intrusion of basic rocks having a positive density contrast of 0.1 Mg/m^3 with standard crust. In contrast to the Karimunjawa arch, which is underlain by a shallow intrusion, the intrusion beneath the Bawean arc is deeper (approximately 1.7 km). It is covered by sediments in a water depth of less than 50 metres. Although the depths of the intrusions are thus very different between the Bawean and Karimunjawa arches, the Bouguer anomaly values are nearly the same. This is explained by the fact that the Karimunjawa High is covered by very thin sediments in the model (less than 300 m) and is flanked by two deep sedimentary basins, causing the density contrast to be very high, which in turn causes a high Bouguer anomaly. On the other hand, the Bawean High was covered by thicker sediment (approximately 1.7 km) with density contrast -0.57 Mg/m^3 .

The reason for differentiating the type of intrusion between the Karimunjawa and Bawean highs is that they have extremely different magnetic associations, as can be seen in Fig.7.6. The Karimunjawa Arc has a low magnetic anomaly and an average seismic velocity from Radiosonobuoy data of 5 km/sec (R24 and R20), which is typical of granitic rocks. The Bawean arch has a higher magnetic anomaly although the intrusion lies much deeper than Karimunjawa arch; also, it has the same trend as the Meratus Mountains of South Kalimantan, where ultramafic rocks are exposed.

The crust thins towards the East Java Sea and West Java Sea, to about 23.5 km and 22 km, respectively. In the Central Java Sea, the depth of the Moho is in the range from 27 km to 29 km, with locally uplifted mantle in the centre, beneath the Karimunjawa Basin, reaching to 24 km. This suggests that basin formation in the Central Java Sea is associated with attenuated crust.

7.6.3.2.2 Gravity model Java Sea 2

This model relates to a line across the Central Java Sea, drawn roughly perpendicular to the structure and Bouguer anomaly contours. The model was constrained by five sets of radiosonobuoy data (R21, R24, R29, R33 and R39) which gave information on the thicknesses and velocities in the general area, although only R 29 actually lay on the line of section. The final model (Fig.7.12) produces a good match between observed and calculated gravity anomalies. There are four main Bouguer anomaly highs, these being, from west to east, the Karimunjawa, Laut, Paternoster and Makassar highs. In the case of the Makassar High, only the southern gradient is covered by the profile.

The Karimunjawa High, with a maximum Bouguer anomaly of +51 mGal corresponds to the Karimunjawa Arch. The source of this anomaly was modelled by an igneous intrusion with a density contrast +0.05 Mg/m³. The intrusion is covered by approximately 170 metres of sediments, as is confirmed by data from Radiosonobuoy R24 located on the High. The structural high alone seems insufficient to explain the positive gravity anomaly; locally denser rocks seem to be required with the basement.

The Laut High, reaching up to +40 mGal, occurs where the profile crosses the structural trend from Laut Island. The source of this high was modelled as an igneous intrusion having a density contrast of +0.1 Mg/m³. Ophiolitic rocks are exposed on Laut Island and probably underlie the whole of the Laut structural trend.

The Paternoster High, reaching up to +50 mGal, was modelled by uplifted basement flanked by deep sedimentary basins. The minimum depth of the basement on the Paternoster High is approximately 1.5 km. To the west the Laut Basin contains of 3 km sediments and to the east the Makassar basin contains 2.3 km of sediments.

The Makassar High reaches a maximum Bouguer anomaly of +85 mGal at the end of the profile, where values are still increasing. This increasing Bouguer anomaly occurs in a region where the water depth is increasing from 200 metres to more than 600 metres. The high values are largely caused by the application of the Bouguer correction; the implication is that the crust is thinning beneath the Makassar Strait.

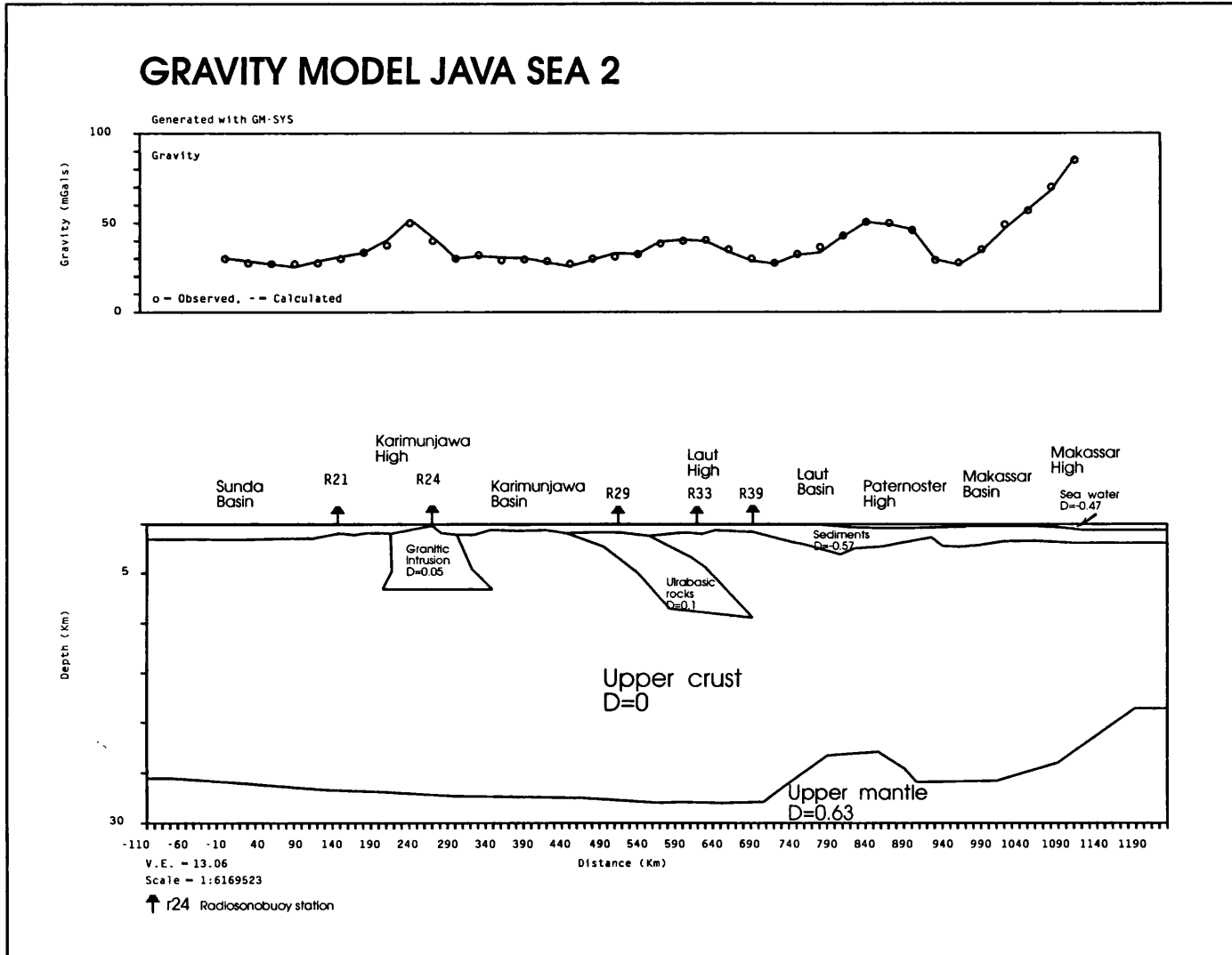


Figure 7.12: Gravity model Java Sea 2

Gravity interpretation suggests that the thickness of sediments in the Central Java Sea segment of this profile reaches as much as 1.6 km, whilst in the East Java Sea segment thicknesses are up to 3 km.

At the easternmost margin of the Central Java Sea the crust thickens to 28 km, and towards Sulawesi the Moho level decreases up to 18.5 km. Between these two areas is the Makassar Basin, filled with sediments of about 3 km thick, where the Moho is locally uplifted to 23 km. This suggests that the basin is formed on attenuated crust.

7.6.3.2.3 Gravity model Java Sea 3

This model relates to a line across the Central Java Sea and the northern part of the East Java Sea which is roughly perpendicular to structure and Bouguer anomaly contours. The model was constrained by five sets of radiosonobuoy data (R22, R23, R28, R35 and R38) which gave information on the thicknesses and velocities of the sediments. The final model is shown in Figure 7.13. There are five Bouguer anomaly highs which correlate to structures, these being, from west to east, the Karimunjawa, Meratus, Laut, Paternoster and Makassar highs.

The Karimunjawa High has a maximum Bouguer anomaly value of +32 mGal. On the structural map this high corresponds to the Karimunjawa arch. As in the previous model, the high was modelled as due to an igneous body with a density contrast of +0.05 Mg/m³. In this area, the depth of the top of the intrusion is 1000 metres and it is covered by sediments.

The Meratus High has a maximum Bouguer anomaly value of +42 mGal and was modelled as due to an igneous body with a density contrast of 0.1 Mg/m³. The depth of the intrusion ranges from 0.7 to 0.8 km and it is covered by sediments.

The Laut High has maximum Bouguer anomaly value of +52 mGal and was also modelled as an igneous intrusion, with a density contrast of 0.1 Mg/m³. The body is covered by approximately 150 to 1500 metres of sediments.

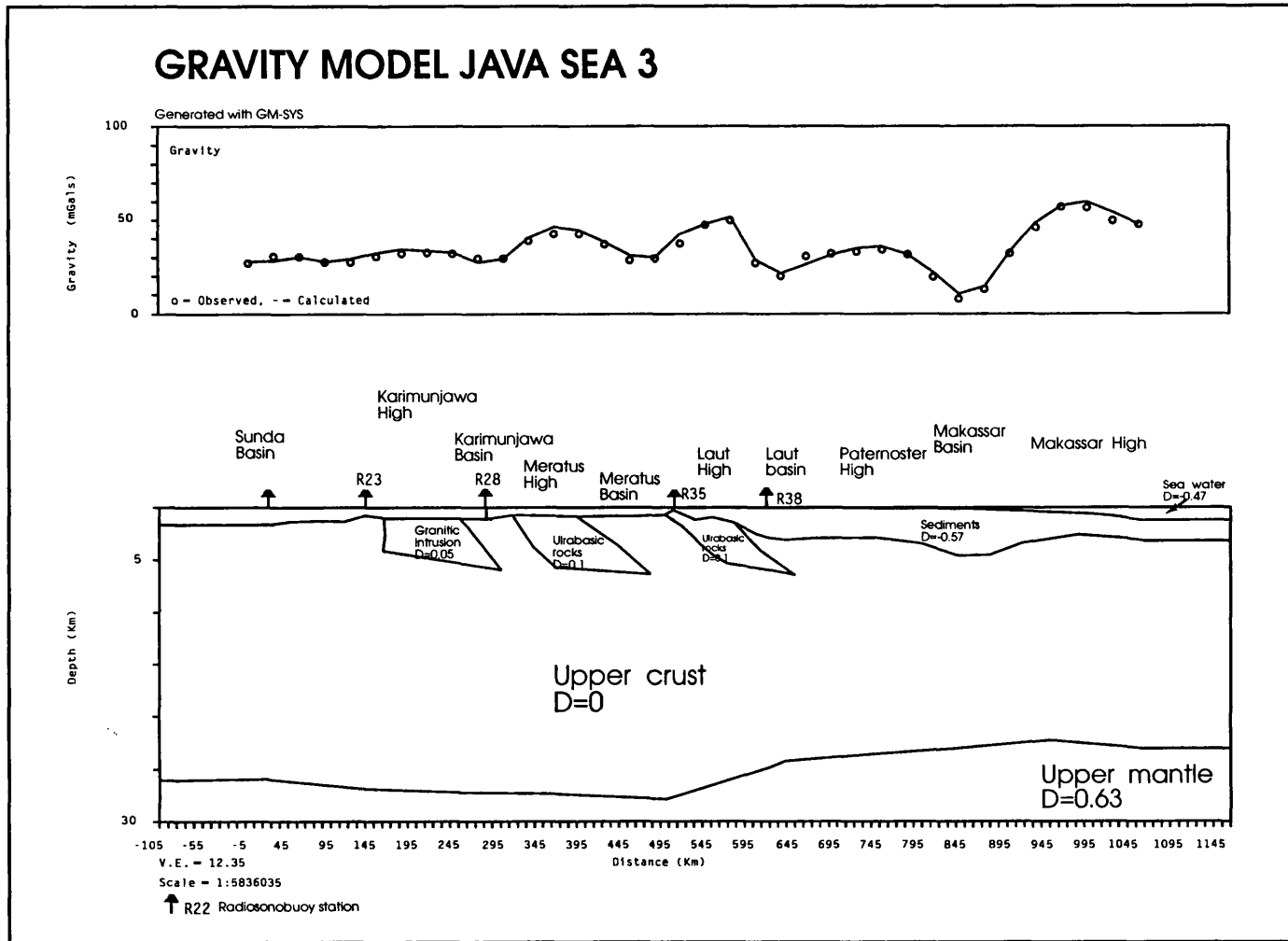


Figure 7.13: Gravity model Java Sea 3

The Paternoster High has a maximum Bouguer anomaly value of +32 mGal and was modelled as due to a basement uplift. The depth to basement is approximately 2.8 km, compared to 4.6 km to the east in the Makassar Basin.

The Makassar High has a maximum Bouguer anomaly value of +57 mGal. In the model the increase in Bouguer anomaly towards the Makassar High corresponds to an increase in water depth from 100 metres to 1250 metres. The Bouguer anomaly high in the Makassar High is thus mainly caused by the application of the Bouguer correction; the implication is that the crust is thinning beneath the Makassar Strait.

Gravity interpretation suggests that the thickness of sediments along the Central Java Sea segment of this transect ranges from 700-1600 metres, whilst in the East Java Sea sediment thicknesses are up to 4.6 km.

The depth to the Moho at the easternmost margin of the Central Java is up to 28 km, but it decreases sharply towards the East Java Sea, to about 22 km.

7.7 CRUSTAL STRUCTURE

The three Bouguer anomaly profiles discussed above all show a series of localised maxima and minima with amplitudes ranging between +10 to +80 mGal and wavelength ranging between 10-250 km. The long wavelength anomalies have been interpreted as being due to the thinning of the crust, involving mantle uplift, whilst the short wavelength anomalies have been interpreted as due to variations in the structure of the upper crust, e.g. intrusions, basement faults and variations in basement rock type.

Superimposed on the relatively high Bouguer anomalies between the Karimunjawa and Bawean highs is a short wavelength Bouguer anomaly low which coincides with the Karimunjawa Basin, indicating the effect of the basement faults forming the rifted basin.

Short wavelength gravity highs are interpreted as deriving from the upper crust and not from the upper mantle and some gravity highs in the Central Java Sea were modelled as being due to igneous intrusions. The Karimunjawa High was modelled as due to a granitic intrusion, as suggested by the velocities from radiosonobuoy data. The Meratus,

Bawean and Laut highs were modelled by basaltic bodies since they are situated on the same trends as the Meratus Mountains and Laut island, both of which include ophiolitic rocks. The models show the bodies dipping to the east. They are interpreted as slices of ultramafic rocks emplaced when collision occurred at the margin of the Sunda Shelf during the Late Cretaceous and Early Tertiary.

Gravity models suggest that the thickness of sediments in the Central Java Sea reaches 3 km in the south and decreases gradually to the north over the Karimunjawa High. Sediment thickness also increases steadily eastwards to up to 4.6 km in the Java Sea.

In general, the depth of the Moho beneath the Central Java Sea ranges between 27 and 29 km. Crustal thinning occurred mainly beneath the Sunda and Karimunjawa basins, where the crust is only 24 km thick. Crustal thickening at the boundary between the Central and East Java seas is marked by a change in water depth from less than 100 m to more than 2000 m.

7.8 TECTONIC IMPLICATIONS

Geologically, the Central Java Sea is situated on the Sunda Platform, which is considered to have been a stable core since the Tertiary, underlain mostly by pre-Tertiary metamorphics which have been intruded by granitic rocks of various ages (Hamilton 1979). Figure 7.1 shows that the Central Java Sea contains several basins bounded by normal faults trending in NE-SW, i.e. parallel to the structural elements in the area. Seismic profiles (Figs. 7.6 and 7.7) and geological cross sections (Fig. 7.8) indicate basement faults which are thought to control basin formation. The basins and faults shown in Fig. 7.2 have an en-echelon arrangement, suggesting wrench movements along a NE-SW shear. Some authors (Koesoemadinata and Pulunggono 1975; Ben-Avraham 1978; Hamilton 1979) have already suggested that strike-slip motions are the most important structural elements on the Sunda Shelf, that they control the basin distribution and that most are now inactive.

The Central Java Sea contains four major Bouguer anomaly highs, the Meratus High (MH), Laut High (LH), Karimunjawa High (KH) and Bawean High (BH), which are

thought to relate to major structures and evolution in the East Java Sea. If superimposed on the structural map (see Fig. 7.3), the Karimunjawa High corresponds to the Karimunjawa Arch which geological data and gravity models (Fig. 7.11) suggest that it is built up of granitic rocks of the Early Cretaceous age (Ben-Avraham and Emery 1973). The Meratus High corresponds to the Meratus Mountains of SE Kalimantan, where ultramafic rocks and chert outcrop (van-Bemmelen 1949). The Bawean High corresponds to the Bawean Arch which is a structural continuation of the Meratus High. Geological data suggests that Bawean Island, on the Bawean Arch, consists of alkaline volcanics of Tertiary age. The Laut High corresponds to Laut Island, where rocks similar to those in the Meratus Mountains outcrop, together with some volcanic rocks (Ben-Avraham and Emery 1973).

The evolution of the Central Java Sea can be summarised as follows. In the Early Cretaceous, a subduction zone ran from the Meratus area to Central Java through the Central Java Sea and was accompanied by volcanism. In the Meratus Mountains the igneous activity is now recorded by the Rimuh Granite, in the Central Java Sea it is represented by the Karimunjawa Arch and in Central Java by the Old Volcanic Breccia. The collision in the Late Cretaceous was associated with compression which resulted in crustal thickening; the three gravity models showing crustal thickening at the eastern margin of Central Java Sea. Collision was probably accompanied by uplift of the Meratus Mountains, Laut Island and the Bawean High, accompanied by the emplacement of slices of ultramafic rocks. The collision is believed to have been oblique, leading to the formation of pull-apart basins and accompanied by basic intrusion. On the basis of sedimentology, tectonic style and regional settings, Sikumbang (1990) suggested that the Late Cretaceous-Early Tertiary Manunggul Group accumulated in a pull-apart basin formed after the collision of the southeastern margin of Sundaland with the Alino Island Arc. At this time most of Central Java Sea was above sea level and therefore no sediments were deposited, as can be seen in the stratigraphic column of Fig.7.4.

In the Early Tertiary, crustal extension occurred causing attenuation of the crust (gravity model Java Sea 1) followed by regional subsidence along basement faults which

reactivated old strike-slip faults, forming low and high areas. The low areas later became sedimentary basins. The Karimunjawa Arch was the major high area separating deposition in the west and east. Koesoemadinata and Pulunggono (1975) suggested that early sedimentation took place under non-marine or at least paralic conditions but that in the early Miocene most of the basement highs in the Java Sea were submerged with exception such as Karimunjawa Arch.

CHAPTER EIGHT

EAST JAVA SEA PROVINCE

8.1 INTRODUCTION

In the published literature the Java Sea is divided into the West and East Java Seas; the East Java Sea being defined as lying approximately between the longitudes of Cirebon, in central Java, and Flores (Fig. 8.1). However, in this thesis the term is applied only to the area from the longitudes of Madura to western Sumbawa, where structural, bathymetric and Bouguer anomaly contour trends appear to be dominantly E-W. Recently, the East Java Sea has been studied intensively by oil companies exploring for hydrocarbons.

8.2 PREVIOUS STUDIES

The nature and crustal structure of the region is still poorly understood. Hamilton (1979) suggested on the basis of water depth and the assumption of isostatic equilibrium that the crust of the Bali Basin is transitional in thickness between oceanic and continental crust. In contrast Ben-Avraham and Emery (1973) inferred that oceanic crust is present beneath the Bali and Madura basins because of their positions in line with the Flores Basin, and McCaffrey and Nabelek (1987) suggested that the Sunda Shelf and the Bali Basin are genetically identical.

8.3 BATHYMETRY

Bathymetric contours in the East Java Sea are oriented E-W (Fig.8.2). The most prominent phenomena is the symmetrical Lombok Trough, where the water depth exceeds 1500 metres. Towards the volcanic arc, the continental shelf is narrow and very steep, suggesting structural control.

8.4 TECTONIC SETTING AND STRATIGRAPHY

Physiographically, the East Java Sea Province is an eastward extension of the Rembang-Madura and Kendeng anticlinorium of East Java, which have E-W structural orientations. It is bounded to the north by the Makassar Strait, to the south by the active volcanic arc of the lesser Sunda islands, to the west by the Tertiary Madura and Java sedimentary basins and to the east by the Flores Sea. From structural and gravity maps, the East Java Sea

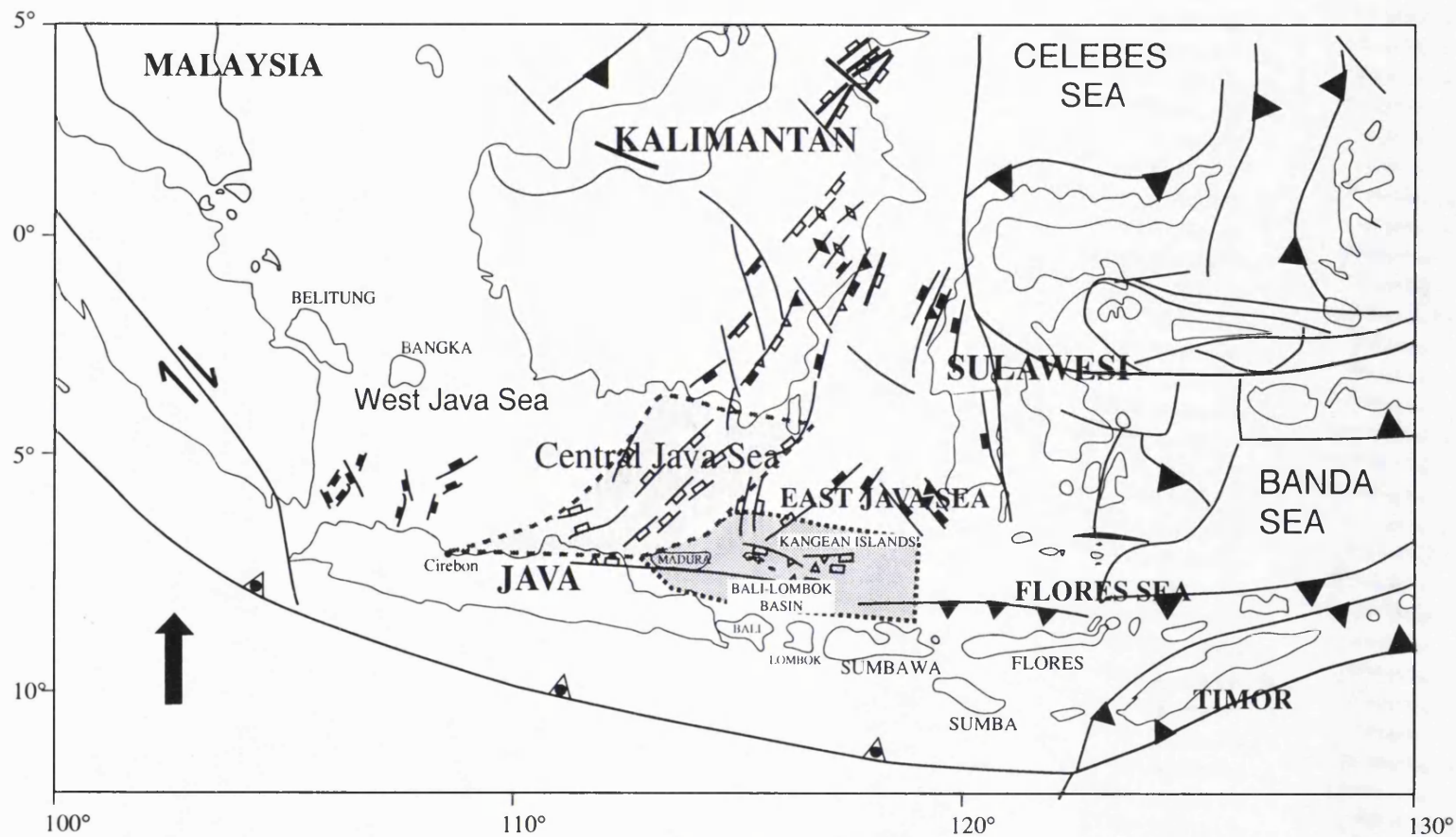


Figure 8.1: The new division of the East Java Sea into the Central Java Sea and East Java Sea on the basis of structural and Bouguer anomaly countour patterns (Note: the new East Java Sea extends only from north of Madura to north of Sumbawa).

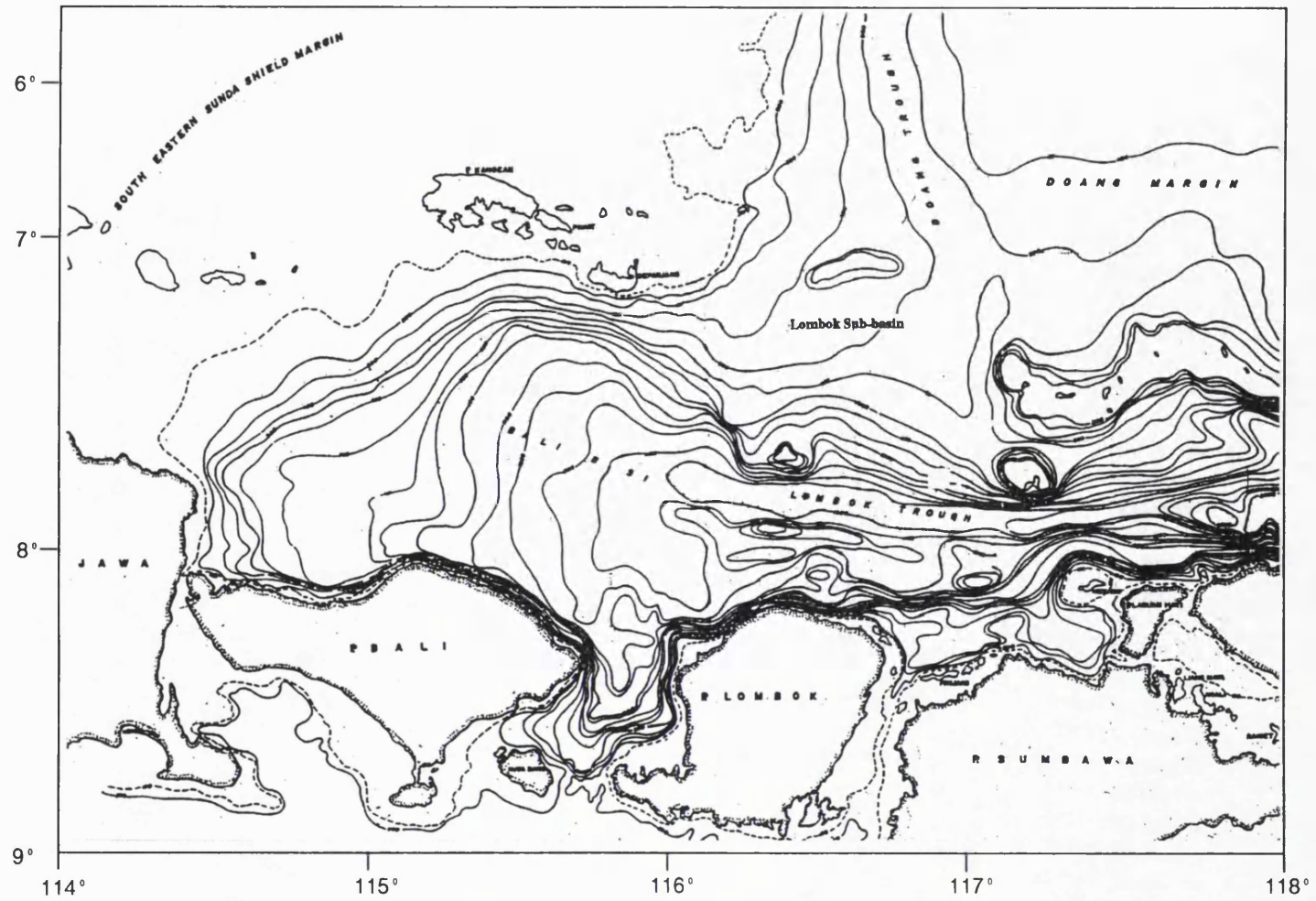


Figure 8.2: Bathymetric map of the East Java Sea showing E-W countour orientations and towards the Makassar strait the countours suddenly change into N-S directions.

Province can be divided into three major morphostructural units; The Madura zone, the Kangean-Sapudi islands and the Bali-Lombok Basin (see Fig. 8.1).

8.4.1 Madura zone

The E-W oriented Madura zone is a continuation of the Rembang Zone in the East Java, and the two have been grouped together as the Rembang-Madura zone (van-Bemmelen 1949). The geology of Madura Island has been summarised by van-Bemmelen (1949). On Madura, there is no sedimentary exposure older than Lower Tertiary. The oldest sediments found in cores are marine Oligocene sediments of the Rembang Beds, consisting of foraminiferal limestone, clay and marl. These were first deformed and folded in the Middle Miocene and again during the Pleistocene when Madura Island and the Rembang anticlinorium emerged from the sea (Ben-Avraham and Emery 1973). Upper Tertiary and Quaternary formations cover more than 90% of the surface of the island and dominantly consist of marine limestones, marl and clay. The youngest Pleistocene sediments are slightly arched up, and the Plio-Pleistocene sediments have been gently folded. In the southwestern part of the island, the anticlines are asymmetric with the southern flanks steeper than the northern flanks. It seems that the Madura Ridge basement uplift was due to compression only and there is no indication of either a magmatic arc or an allochthonous terrane. Duyjes (1938, quoted in Van-Bemmelen 1949) suggested that the compressive force was directed from the elevated centre of the island towards the subsiding area of the Strait of Madura, that is from north to south.

8.4.2 Kangean Island

The area was mapped by Sutisna *et al.* (1986) as showing continuous sedimentation from the Oligocene to the Pleistocene. The oldest sediments deposited in the basin were limestone which have been both folded and faulted. Fold axes are generally E-W and the plunges of the folds are steeper on the north (about 30°) than in the south (about 15°), indicating the major stress derived from the south. Normal faults and wrench faults are mainly NE-SW and NW-SE, in response to the N-S stress. The island is simply interpreted as a continuation of the Rembang-Madura Zone.

8.4.3 The Bali and Lombok seas

Geological investigations, mainly by drilling, in the East Java Sea have shown that the oldest sedimentary rocks overlying the basement are variously of Eocene to Middle Miocene age (Tyrrel *et al.* 1986). The Early Oligocene to Early Miocene rocks are generally shelf and reef carbonates overlain by deep water sediments. Seismic profiles in the Kangean and Central Lombok areas show the distribution of carbonate facies which prograde from northeast to southwest (Tyrrel *et al.* 1986). Coarse conglomerates of Eocene or younger age are common close to fault-bounded highs. The late Neogene sediments appear to be mainly of deep water origin although there are Recent coral reefs in some areas, indicating shallow water deposition.

Some geological data have been obtained in the area of Central Lombok Block (CLB), which is situated to the north of Lombok Island (Fig.8.3). During the 1970's, Amoseas drilled four exploratory wells, three of which penetrated Tertiary shallow water platform carbonates and thin basal clastics overlying the pre-Tertiary igneous-metamorphic basement complex (Tyrrel *et al.* 1986). During the late 1970's, Cities Service drilled a series of Java Sea wells, five of which were located to the east of Kangean Island, near the western boundary of the Central Lombok Block (see Fig. 8.3). Three wells penetrated Lower-Miocene, Oligocene, and Upper Eocene deep-water strata overlying Eocene shallow water carbonates and basal clastics above a Cretaceous basement complex. These results support Hamilton (1979), who considered the area to be underlain by Cretaceous melange and oceanic crust.

The lithology and stratigraphy of the area, as derived from the Amoseas L 40-1 and JS 25-1 wells (Tyrrel *et al.* 1986 and Kohar 1985), are shown in Figs. 8.4A and 8.4b, and Fig. 8.4C. It seems that in the Eocene most of the area was covered by shallow water, providing an environment for the deposition of carbonate rocks. Since the Late Neogene, deep water conditions appear to have prevailed over the entire area.

8.5 WELL L46-1

This well lies at 7^o20'18.52" Latitude and 116^o36'37.23" Longitude. The well reached 3451 m in a water depth of 481 m. Basement, encountered over the interval 3445-3451

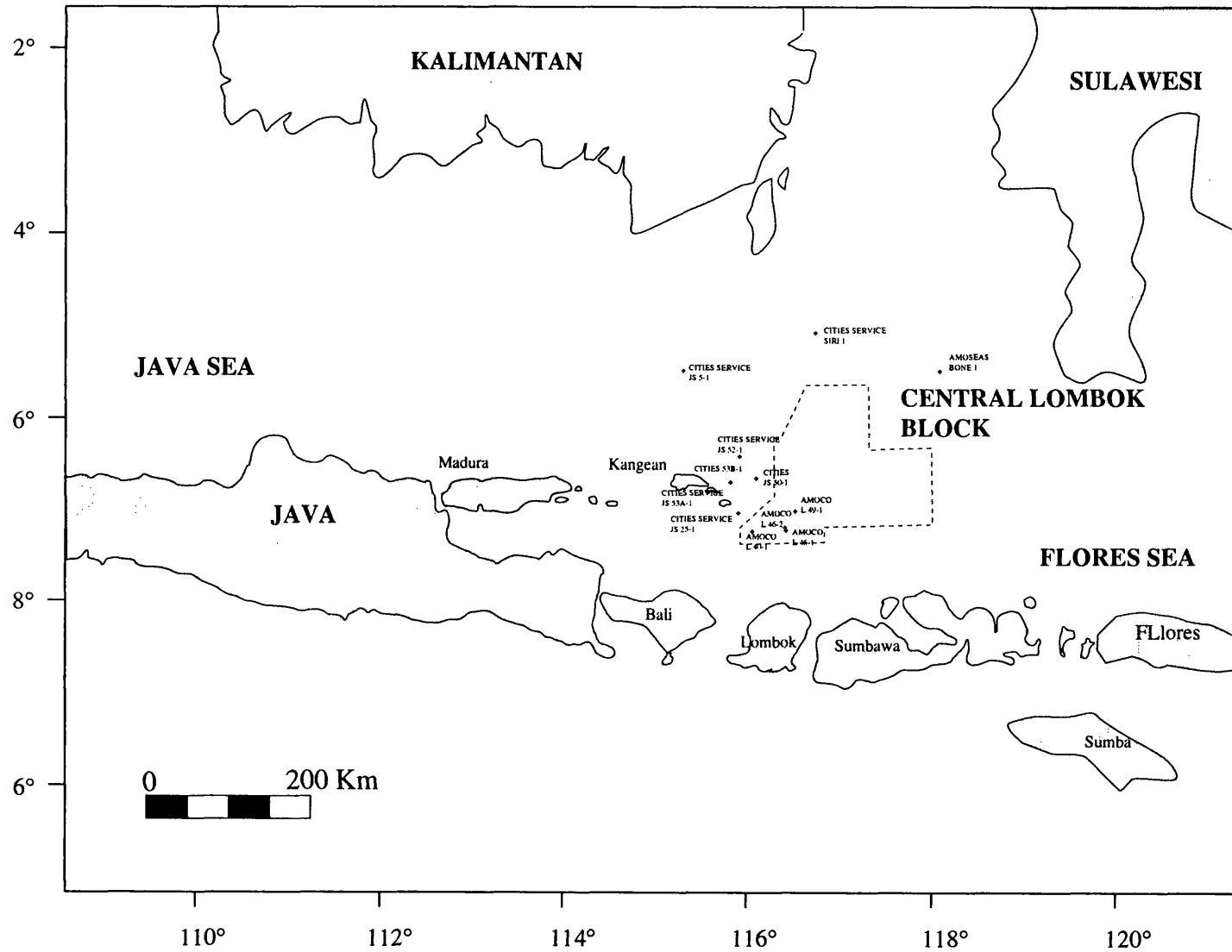
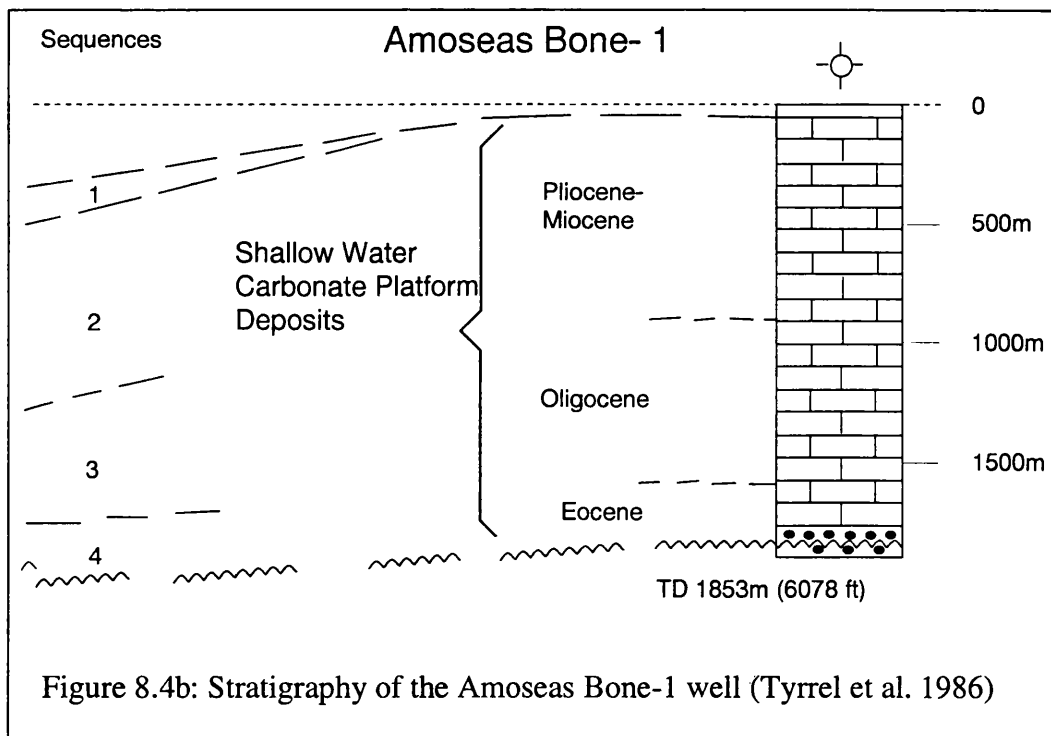
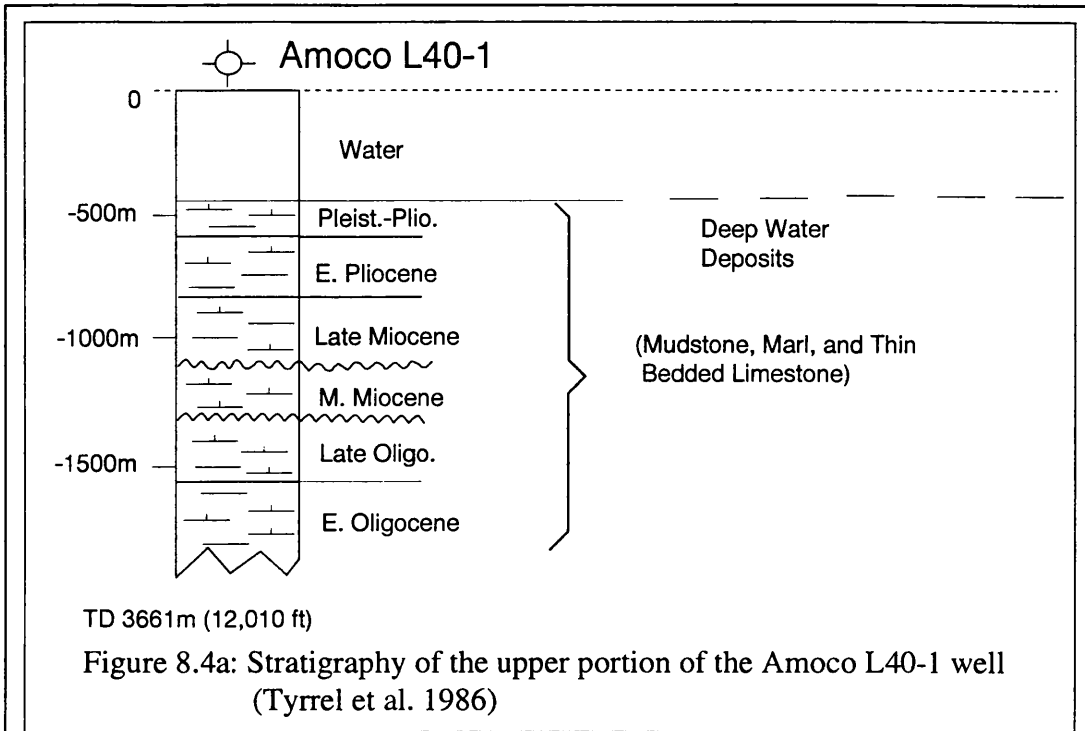


Figure 8.3: Location map of wells and the Central Lombok Block in the East Java Sea.



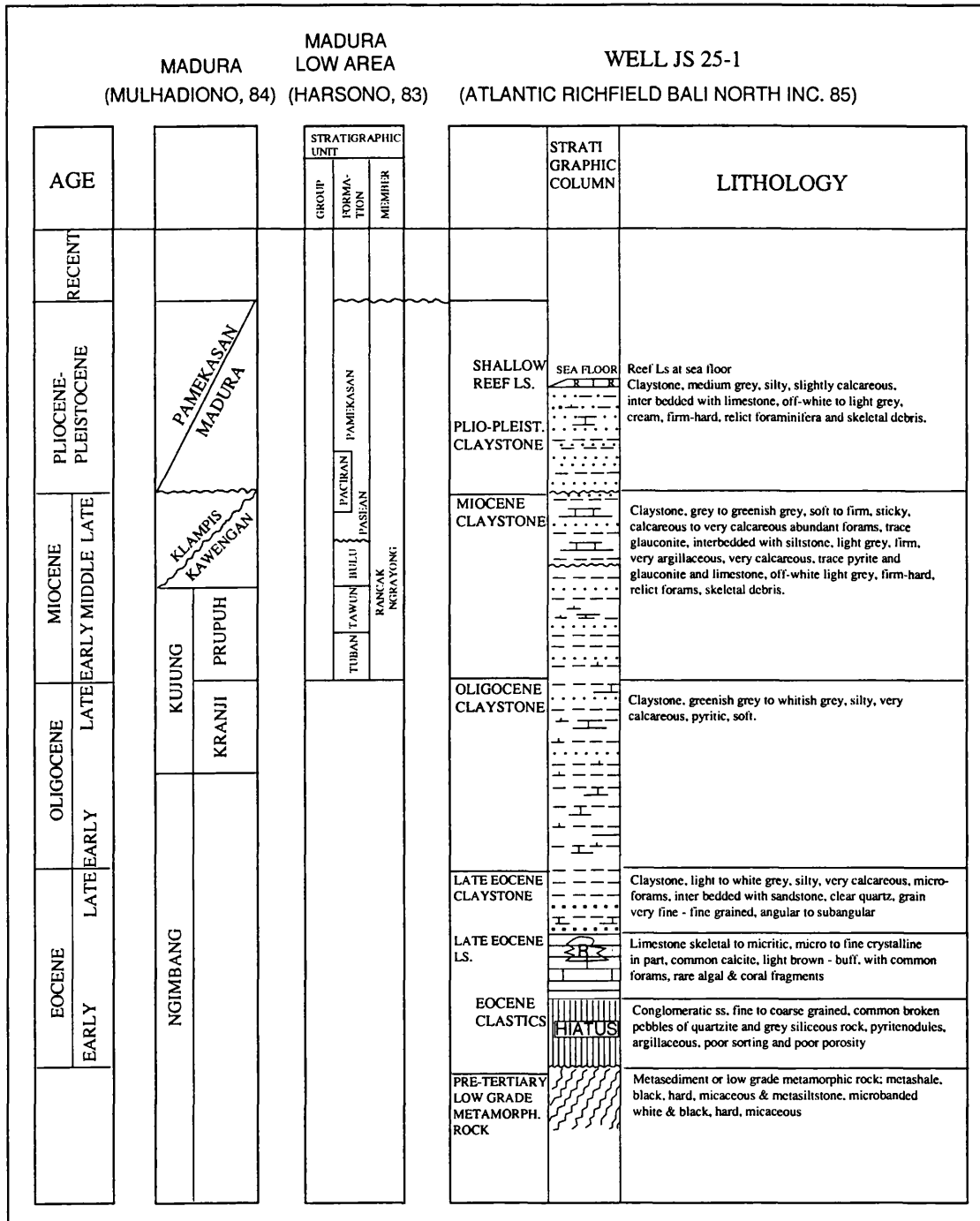


Figure 8.4C: Stratigraphy of JS 25-1 Well close to Kangean Island (Kohar 1985)

m, consisted of metamorphosed graywacke. Unconformably overlying the basement were Cretaceous sediments, considered to be the oldest sedimentary rocks in the eastern Sunda Shelf, consisting of sandstone, siltstone and claystone. The thickness of this unit was 236 m, but the sedimentary environment was not defined.

Unconformably above the Cretaceous were Paleocene(?) and younger sediments. No definite evidence exists for the Paleocene and on the basis of palynostratigraphy the oldest rift fill sediment in L 46-1 has been identified as Lower Eocene (Matthews and Bransden 1993). This consists of intercalated claystone, siltstone, sandstone and conglomeratic overlain by intercalated shale and coal or lignite. The thickness of this unit is 676 m, and the sedimentary environment was deltaic/marginal marine (tidal flat?).

Unconformably above this unit were Middle Eocene sediments consisting of intercalated shales and sandstones. The thickness of this unit was 137 m and the sedimentary environment was a shallow marine outer shelf.

Conformably above this unit were Late Eocene sediments consisting of claystone, siltstone, sandstone and limestone. The thickness of this unit was 97.5 m, and the sedimentary environment was bathyal.

Unconformably above this unit were Late Oligocene (P20-P22) to Early Miocene (N5-N4) sediments consisting of claystones and limestones. The thickness of this unit was 286 m and the sedimentary environment was bathyal.

Conformably above this unit were Middle Miocene sediments consisting of intercalated claystones and limestones. The thickness of this unit was 121 m and the sedimentary environment was bathyal.

Unconformably above this unit were Middle Miocene (N12-N14) sediments consisting dominantly of claystone and limestone. The thickness of this unit was 146 m and the sedimentary environment was bathyal.

Unconformably above this unit were Early Pliocene (N18-N19) sediments consisting dominantly of claystone and marlstone. The thickness of this unit was 146 m but the sedimentary environment was not defined. Rocks younger than Early Pliocene were not encountered.

8.6 SEISMIC INTERPRETATION

8.6.1 Introduction

The stratigraphic and structural framework of the East Java Sea has been derived from correlation of interpretations of three seismic profiles; BP 91-037, BP 91-010 and BP 91-110. All these profiles are multi channel seismic reflection with 66 fold coverage. The energy source is airgun with 2000 PSI. The locations of the profiles is shown in Fig. 8.5. For reasons of confidentiality, the profiles are displayed as line drawings only.

Applying the methods of seismic stratigraphic analysis outlined by Vail *et al.* (1977) as well as correlation with well L46-1 (on Line BP 91-037 at SP 3205), the stratigraphic acoustic units within the province can be divided into four major units; basement unit, pre-rift sediments, syn-rift sediments and post-rift sediments. Since the three lines intersected one another, the horizons defined on line BP 91-037 were used as marker horizons and were tied across to the other two profiles.

8.6.2 Seismic interpretation line BP 91-037

This line is situated to the north to Lombok Island, runs N-S, i.e. perpendicular to the regional structure and Bouguer anomaly contours, and is approximately 200 km long. A small scale reproduction and a line drawing interpretation are shown in Fig. 8.6.

8.6.2.1 Stratigraphic framework

8.6.2.1.1 Basement unit

This is the lowest seismic unit which represents acoustic basement and is characterised by the absence of reflections. It can be correlated with the metamorphosed graywacke encountered in well L46-1. The base is poorly imaged seismically. The top of the unit is marked by Horizon A on the profile; the contact with the overlying sediments can only be

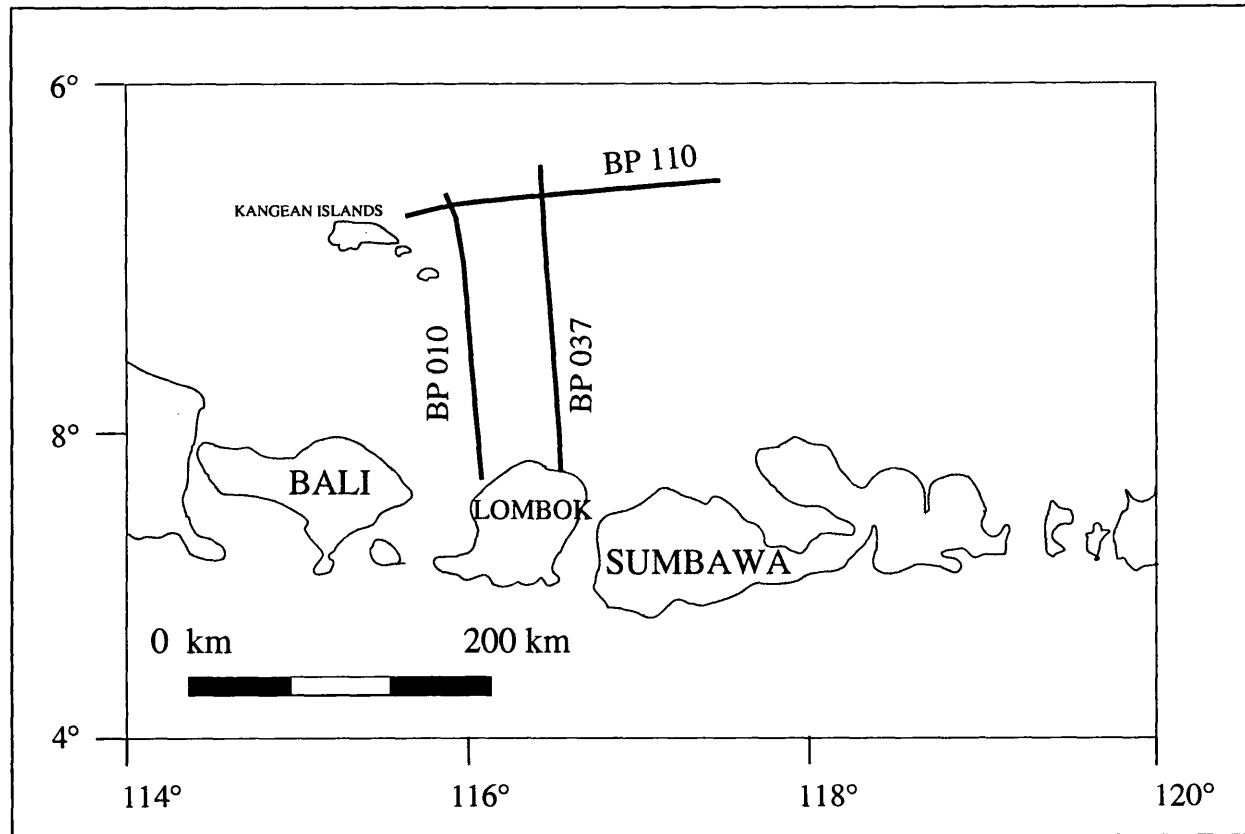


Figure 8.5: Location of seismic interpretation on the East Java Sea

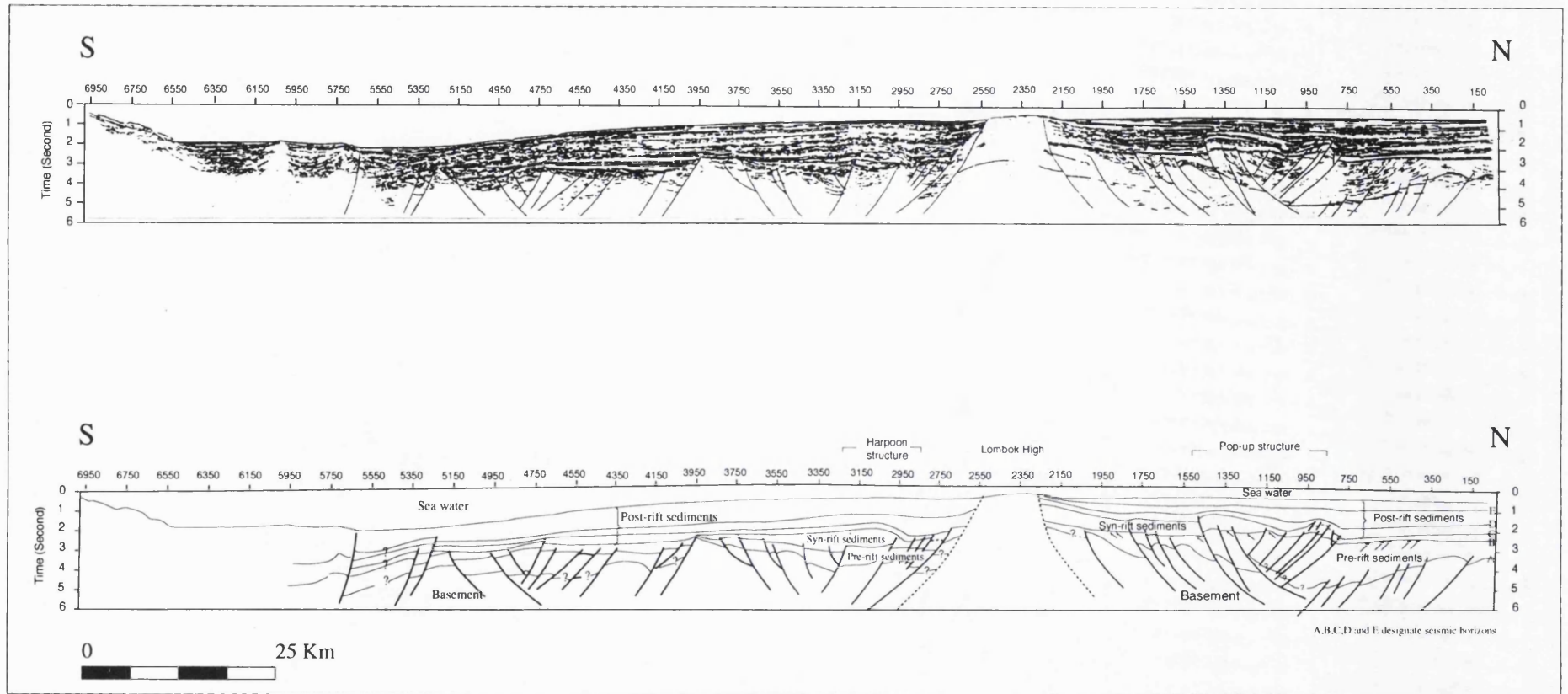


Figure 8.6: Line drawing and interpretation of seismic line BP091-037 showing horst and graben structures and inversion structure

seen clearly from SP 790 to SP 101, being difficult to see and sometimes is obscured by multiples in the rest of the section.

8.6.2.1.2 Pre-rift sediments

The pre-rift sediment unit, which is regarded as the oldest sedimentary unit at the eastern margin of Sunda Shelf, can be correlated with the Early Cretaceous sediments from well L46-1, which consisted dominantly of mudrock with interbedded siltstone and sandstone. On the seismic section at Well L46-1 (SP 3205) the base of the unit (i.e. the top of the basement) was picked at 3.97 sec TWT, which was converted to a depth of 5171 m using an average velocity of 2605 m/sec; the base of this unit was not encountered in the well. The reflection configurations strongly suggest folding and thrusting, indicating a compressional regime.

The top of the unit is marked by Horizon B and the contact with the overlying sediments is an erosional truncation (angular unconformity), clearly visible from SP 390 -SP 750, SP 1150 - SP 1270, SP 1470 - SP 2110, SP 3310 - SP 3590, SP 4230 - SP 4630 and SP 5390 - SP 5510, indicating a period of uplift followed by erosion before the deposition of the younger sediments.

8.6.2.1.3 Syn-rift sediment unit

This unit can be correlated with the Early Eocene-Late Eocene sediments from well L46-1. On the seismic section at the location of the well, the bottom of the unit was picked at 2.96 sec TWT, which was converted to a depth of 3197 m using an average velocity of 2157 m/sec, compared to a depth in the well of 3461 m. The unit is characterised by parallel-subparallel reflections with moderate continuity and medium to high reflection amplitude. Following the criteria of Vail *et al.* (1977), these reflection characteristics are interpreted as indicating a shelf depositional environment, whilst environmental facies interpretation typically indicates deposition in a shallow marine shelf area. The unit was deposited in a complex system of tilted horsts and grabens. The faults cut the basement but do not reach the surface. The thickness of the sequence ranges from 0.1 to 1 sec TWT. This is consistent with a horst-graben structure, and is the basis for inferring that the sedimentary deposits are rift related. Well L46-1 indicated that the lower part of the

sequence was deposited in a deltaic, changing gradually to bathyal in the upper part, again consistent with rift sedimentation.

The top and bottom of this unit are bounded by strong reflections which correspond to the Late Eocene and Cretaceous unconformities. The top of this unit is marked on the profile as Horizon C.

8.6.2.1.4 Post-rift sediments

This unit can be correlated with the Upper Eocene to Lower Pliocene sediments from well L46-1. On the seismic section at Well L46-1, the base of this unit was picked at 2.36 sec TWT, which was converted to a depth of 2330 m using an average velocity of 1975 m/sec, compared to a depth of 2261 m in the well. The unit consists of several seismic sequences and is characterised by parallel-subparallel bedding, in some parts wavy (e.g. SP 3750 to SP 4470), with low-medium amplitude and fair to good continuity. From SP 2990 - SP 5630 this unit presents a lateral change in seismic facies with the reflection configuration becoming wavy-subparallel, the continuity of the reflectors becoming poor and the reflection amplitudes becoming low. These reflector characteristics are classified as indicating a shelf to shelf margin depositional environment and suggest uniform rates of deposition on a uniformly subsiding or stable basin plain (Vail *et al.* 1977).

8.6.2.2 Structural framework

This seismic section can be described in terms of two major depressions (north and south), separated by the Lombok High, and igneous intrusion, thrust faults and block faulting.

Igneous intrusions can be observed from SP 5550 to SP 6150. The area of intrusion is bounded to the north by thrust faults which might have controlled the movement of intrusion. Folding and thrusting of the pre-rift sediments indicate a period of compression followed by uplift in the Late Cretaceous-Early Paleocene.

The extensional process which is marked by the formation of horsts and grabens in the Paleocene-Eocene was accompanied by deposition of syn-rift sediments. Later, the block

faults were reactivated as thrust faults. Inversion structures can be observed from SP 3310 to SP 2820 (harpoon structure), and from SP 1470 - SP 790 (pop-up structure in which the Cretaceous syncline was reactivated along its flanks which became uplifted along thrust faults).

Two major periods of flexure followed by subsidence can be recognised from the configurations of the Tertiary reflectors. The first (SP 710 to SP 1550 and SP 2830 to SP 3470) shows flexure up to Horizon D (post Middle Miocene) followed by subsidence and deposition of younger sediments which onlap the deformed sediments. The second (SP 2550 to SP 2150), shows flexure up to Horizon E (Pliocene) followed by subsidence and deposition of younger sediments which again onlap the deformed sediments. These flexures are associated with thrusting which reactivated the Paleocene normal faults.

8.6.3 Seismic interpretation line BP 91-010

8.6.3.1 Stratigraphic framework

This line is parallel to Line BP 91-037 and approximately 50 km to the west. The seismic horizons were tied to those of Line BP 91-037 via Line BP 91-110. The seismic stratigraphic units are therefore similar to those of BP 91-037. The line drawing interpretation is shown in Fig. 8.7.

8.6.3.1.1 Basement unit

This unit is characterised by absence of reflections. Its top is marked by Horizon A and the contact with the overlying sediments can only be seen in a few locations, e.g. from SP 5790 - SP 6750, SP 3270 - SP 4270. Multiples make identification of the contact between acoustic basement and the overlying sediments more difficult.

8.6.3.1.2 Pre-rift sediment unit

This unit is well-developed in the northern part of the line (SP 5670 to SP 6750), showing parallel bedding with moderate continuity and medium amplitude. The reflection configuration from SP 3350 to SP 4230 clearly shows folding associated with thrusting. The top of this unit is marked by Horizon B and the contact with the overlying sediments

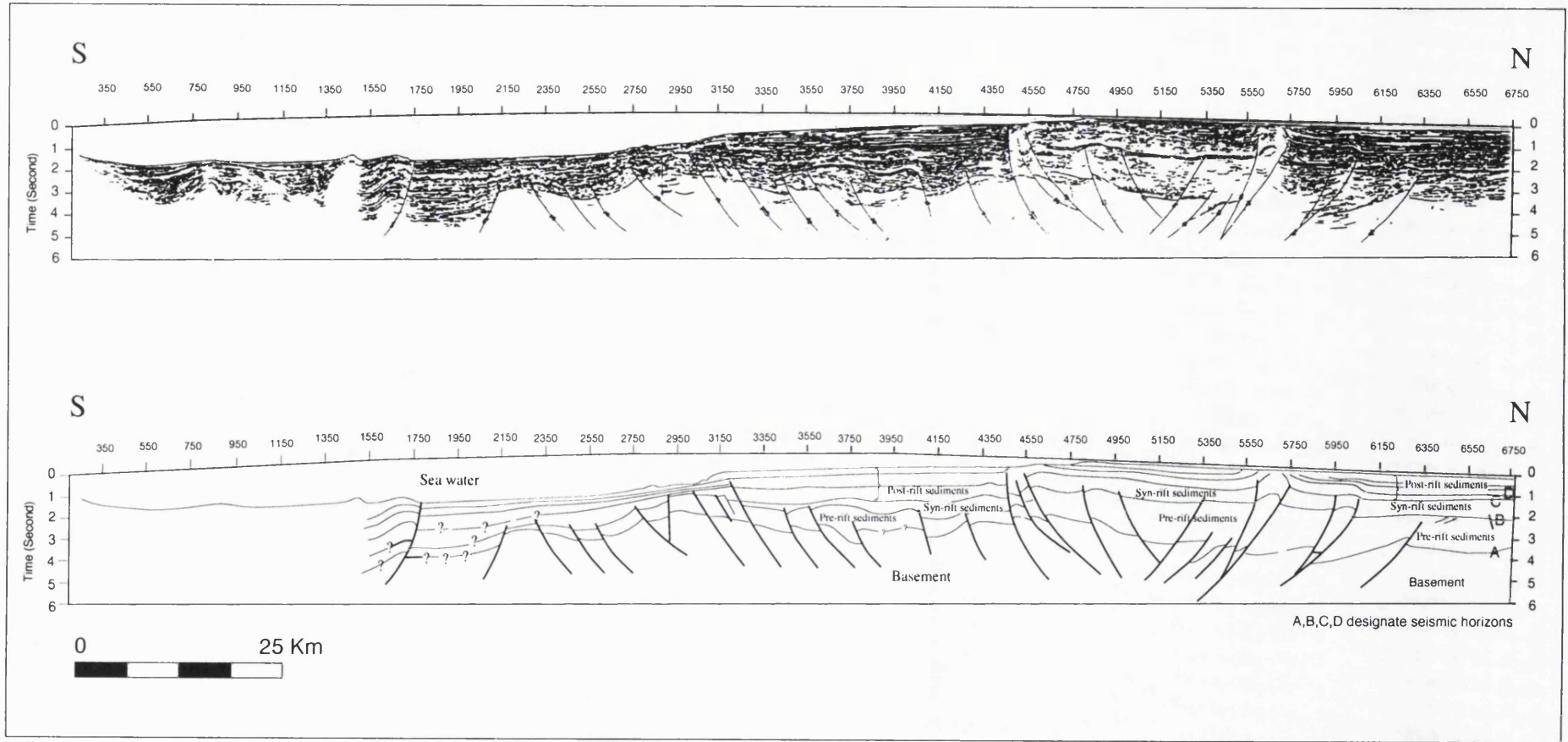


Figure 8.7: Line drawing and interpretation of line BP 91-010 showing horst and graben structures and inversion structure

is along an erosional truncation (angular unconformity) which can be seen from SP 6430 to SP 6510 and SP 4510 to SP 4030.

8.6.3.1.3 Syn-rift sediments

This unit is characterised by parallel-subparallel reflection configurations with fair to good continuity and medium to high amplitude. From the reflection characteristics, the depositional environment of this sequence can be interpreted as shelfal (Vail *et al.* 1977). The unit was deposited in a complex system of tilted horsts and graben and ranges in thickness from 0.2 to 0.9 sec TWT. The faults cut the basement but do not reach to the surface.

8.6.3.1.4 Post-rift sediments

This unit consists of several seismic sequences with parallel bedding, good continuity and high reflection amplitude. Onlap of sediments can be seen from SP 5750 - SP 6230, SP 5550 - SP 5430 and SP 4510 - SP 6230. Reflection configuration patterns suggest uniform rates of deposition on a uniformly subsiding basin plain (Vail *et al.* 1977).

8.6.3.2 Structural framework

The section images two major depressions, separated by the Lombok High. Structures can be recognised as due to folding, thrusting and diapiric intrusion.

Igneous intrusions can be observed from SP 710 - SP 1590 and are bounded to the north by thrust faults. Normal faults which form horst and graben structures involved the Paleocene-Eocene sediments; these normal faults were reactivated as thrust faults in the Middle Miocene-Pliocene.

The flexural reflectors observed in the profile (SP 4470 - SP 5750) can be roughly correlated to those seen in line BP 037, suggesting a period of compression when older normal faults were reactivated.

8.6.4 Seismic interpretation line BP 091-110

8.6.4.1 Stratigraphic framework

This line is situated north of Bali and Lombok islands, runs E-W and is approximately 190 km long. It lies parallel to the E-W regional structure. The seismic horizons were tied at SP 3512 to Line BP 91- 037 at SP 802. The line drawing interpretation is shown in Fig. 8.8.

8.6.4.1.1 Basement unit

This is the lowest unit on the section and is characterised by the absence of reflections. Its top is marked as Horizon A and the contact with the overlying sediments can only be traced at a few locations. e.g. from SP 3490 - SP 6370. Over the rest of the section the contact is obscured by multiples or is a weak reflector.

8.6.4.1.2 Pre-rift sediments

This unit is well developed from SP 3490 to SP 6370 and is characterised by parallel reflectors with fair continuity and low to medium amplitude; in the remainder of the section the unit is difficult to trace due to poor continuity and low amplitude. Its top is characterised by Horizon B and the contact with the overlying sediments shows an apparent erosional truncation (angular unconformity) as observed from SP 6370 - SP 5170 and SP 4530 - SP 4370, indicating a period of uplift and erosion.

8.6.4.1.3 Syn-rift sediments

This unit is characterised by parallel to subparallel reflections with poor to moderate continuity and low amplitude. It was deposited in a complex system of tilted horsts and grabens. The faults cut the basement and clearly do not reach the sea floor, indicating past tectonic activity. The thickness ranges from 0.5 - 1 sec TWT, consistent with deposition during faulting. There is an indication of a carbonate build-up from SP 3090 - SP 2530. Basin subsidence can be recognised by the onlapping of horizontal younger sediments onto the carbonate build-ups which are interpreted as having been deposited on a relatively stable platform.

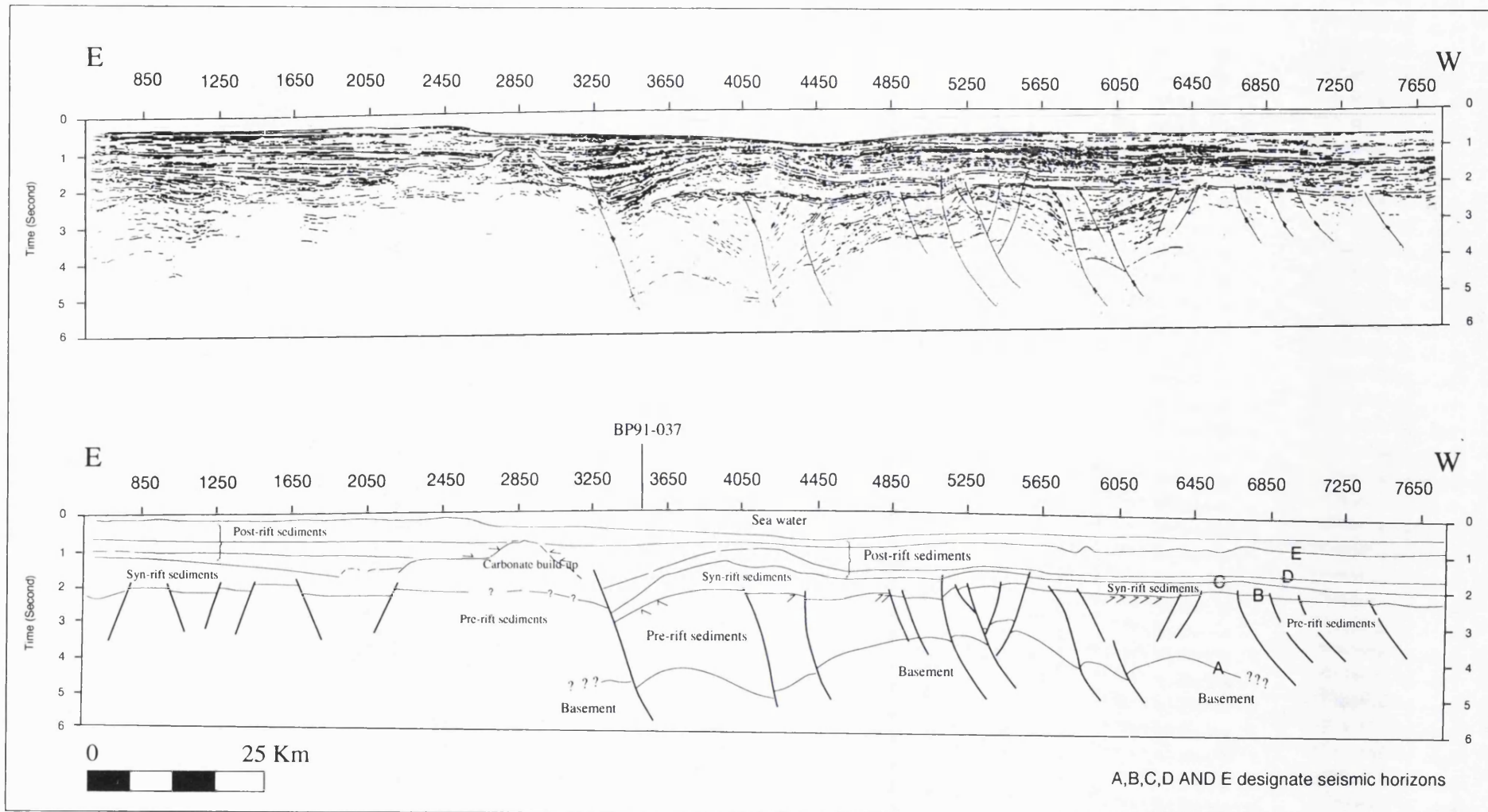


Figure 8.8: Line drawing and interpretation of seismic line BP 091-110 showing horst and graben structures

8.6.4.1.4 Post-rift sediments

This unit consists of several seismic sequences and is characterised by parallel and wavy reflections with fair to good continuity and low to medium amplitude. In some places the reflectors are distorted above a horizontal layer (SP 7170 - SP 3010), interpreted as a result of faulting.

8.6.4.2 Structural framework

The structures seen on the line involved thrust faults, normal faults and folding. Thrust faults are both old and young. The old thrusts occur only in the pre-rift sediment unit and are associated with folding, marking compressional activity in the Cretaceous. Normal faults form horst and graben structures, marking a period of extension in the Paleocene-Eocene. The young thrust faults, which displace the post-rift sediments, occur along previous normal faults, indicating inversion structure in the Neogene.

8.6.5 Summary

In summary, the stratigraphic framework in the East Java Sea Province can be described in terms of four major units, these being metamorphic basement, pre-rift sediments, syn-rift sediments and post rift sediments. In some places diapiric intrusions reach up to the post rift sediments. The movement of diapirs was associated with Neogene compression which resulted in the formation of thrust faults.

The older thrust faults, extending from basement through the pre-rift sediment units, were associated with Cretaceous compression which caused uplift of the region which was followed by erosion. Normal faults, extending from basement through the syn-rift sediments, were associated with the Paleocene-Eocene extension which produced horst and graben structures. Younger thrusts, extending from basement into the post-rift sediments, were associated with the reactivation of normal faults. The timing of inversion can be deduced from flexures observed in seismic sequences identified as post Middle Miocene to Pliocene.

8.7 GRAVITY DATA

8.7.1 Introduction

The Bouguer anomaly map produced by Edcon (1991) was used to construct crustal models of the region (Fig.8.9). Data coverage is good and the Bouguer anomaly contours are suitable for interpretation. In reducing gravity to Bouguer anomaly, Edcon (1991) used a rock density of 2.2 Mg/m^3 .

8.7.2 Qualitative gravity interpretation

Interpretation covers a province extending from west Madura to the Bali and Lombok seas through Kangean and the Sapudi islands. The province is characterised by generally E-W Bouguer anomaly contours, cut in some places by NE-SW lineations, and is considered to be a transition zone between the Central Java Sea Province (continental crust) and the Flores Sea Province which is underlain by oceanic crust. Bouguer contours are dominated by rather long and narrow anomalies with amplitudes of between +40 mGal and +100 mGal, with rather steep gravity gradients (2 to 5 mGal/km). The steep gravity gradients and short wavelength anomalies indicate that the sources are relatively shallow. Gravity lows may be associated with thick sedimentary rocks, steep gradients with faults and local and circular gravity highs with intrusions.

The two main Bouguer gravity highs in this province are the Kangean High (KH) to the south of Kangean Island and the Lombok High (LH) to the north of Lombok and Sumbawa islands. The Lombok High plunges to both east and west. The two highs are separated by a NE-SW lineation which may be a strike-slip fault. To the north of the Lombok High there are many circular Bouguer gravity lows which are also regions of low magnetic fields, and which are interpreted as marking diapiric intrusions.

8.7.3 Gravity models

8.7.3.1 Introduction

Five two-dimensional gravity models were constructed using the GM-SYS gravity modelling package, these being Ben 20, Rama 67, BP 037, MSN 14B and MSN 14A (Fig. 8.10). The models were constrained by radiosonobuoy data and by seismic refraction and seismic reflection interpretations. Densities were estimated from seismic

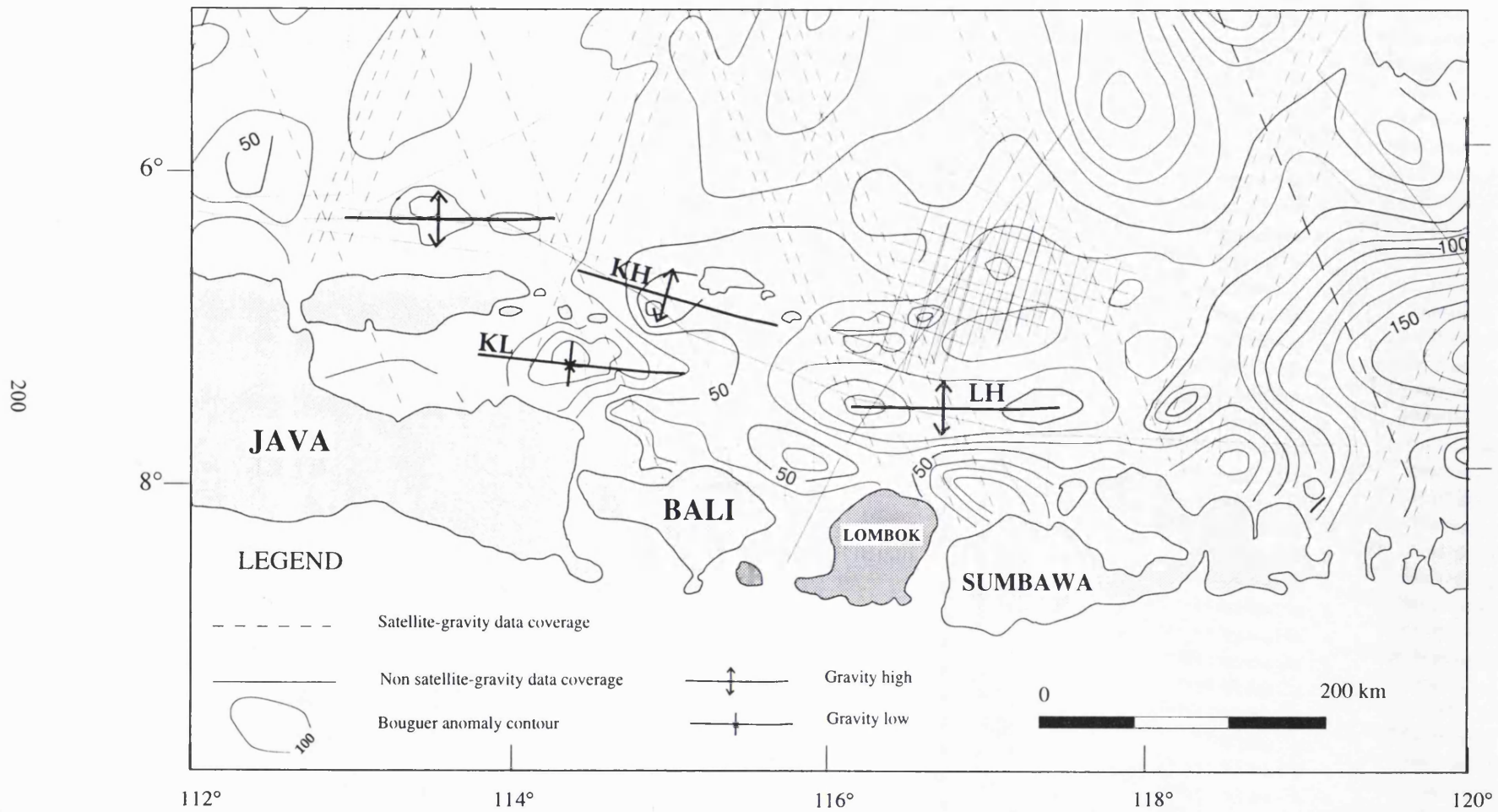


Figure 8.9: Bouguer anomaly map in the East Java Sea (Modified from Edcon 1991)

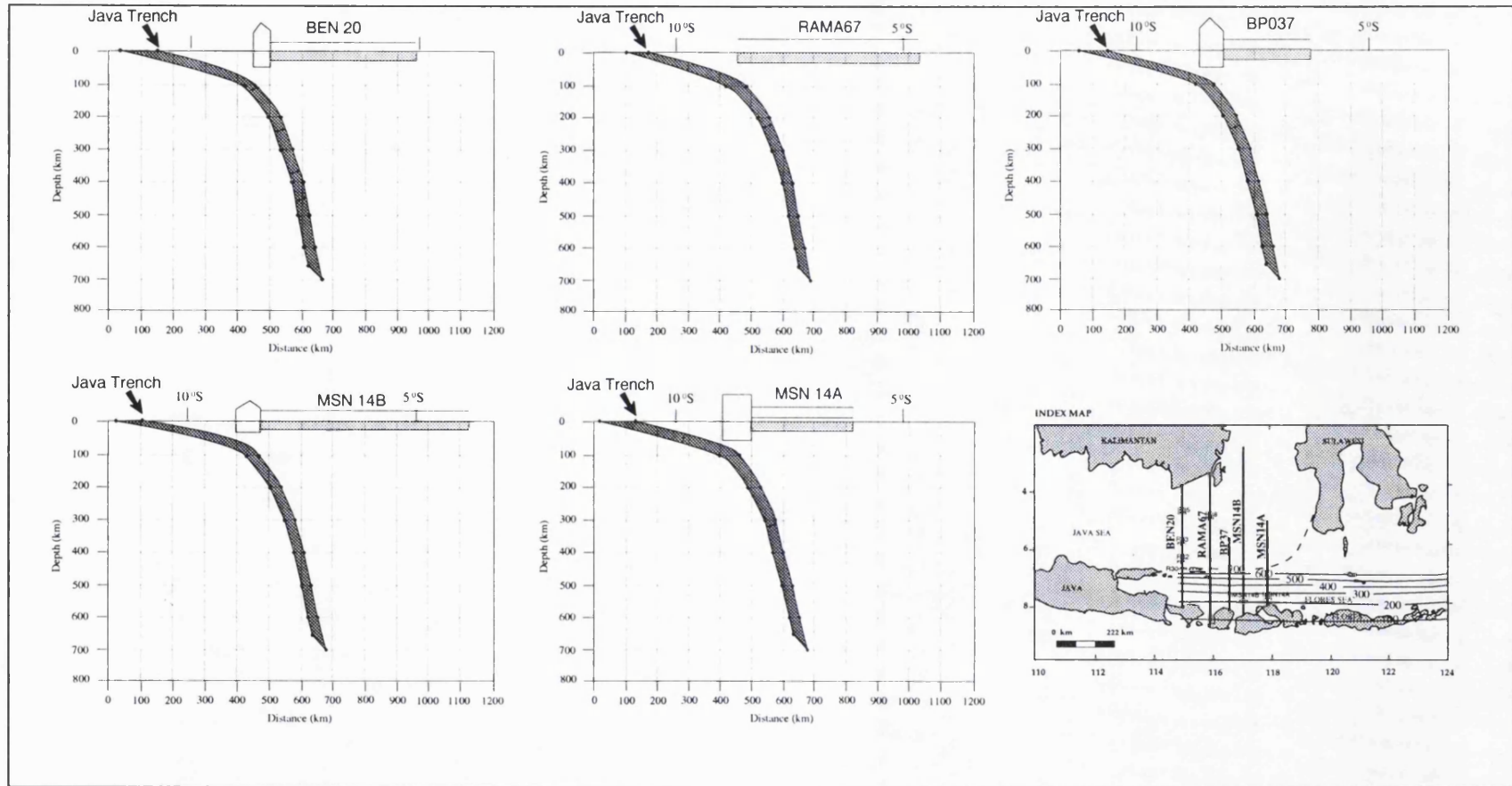


Figure 8.10: The geometry of the slab subduction of the Indo-Australian plate beneath the Sunda-Banda arcs to the effect of the gravity models in the East Java Sea

velocities obtained from radiosonobuoy data (Ben-Avraham and Emery 1973) and refraction stations (Curry *et al.* 1977); velocities were converted into densities using the velocity-density relations of Nafe and Drake (1963). The models were simplified by assigning only one or two densities to the sedimentary layer except in model BP 037, which was constrained by seismic reflection. The average seismic velocity in sediments, using data from stations R30, R32, R33, R35 and R38 was 2.435 km/s, equivalent to a density of about 2.1 Mg/m³. The crust was assigned a density of 2.67 Mg/m³, and the mantle was assigned a density of 3.3 Mg/m³. The reference crustal density used was 2.67 Mg/m³ and the thickness of standard crust was taken as 30 km.

8.7.3.2 The effect of subducted lithosphere on the gravity models

The most prominent earthquakes in the Indonesian region occur along a line from south of Sumatra through Java to the Banda Sea and define a zone that dips northward from the Java Trench to a depth of 700 km beneath Java and the Banda Sea (Cardwell and Isacks 1978). This zone of earthquakes is associated with the subducted Indian-Australian plate. The effect of this subducted material must be considered in constructing gravity models.

The effect of a subducted lithospheric slab on the gravity field has been discussed by many authors (e.g. Grow and Bowin 1974; Watts and Talwani 1974; McCaffrey and Nabelek 1984). All believed that a strong positive anomaly should be expected on the down dip side of the subducted plate, although Talwani and Watts (1974) pointed out that computation of the gravity is complicated by lack of knowledge of the density distribution and configuration of the slab. In this thesis the slab configuration has been constrained by the location of the inclined seismic zone in the Java-Banda seas proposed by Cardwell and Isacks (1978). The thickness of the subducted slab was estimated from the inclined seismic zone in the Banda Arc as 30 km and the density contrast as 0.04 Mg/m³. The geometry of the slab for each of the gravity models is shown in Fig. 8.10.

8.7.3.3 Gravity model BEN 20

This model relates to a N-S line across the Lombok Sea north of Lombok Island, i.e. a line perpendicular to structure and gravity anomalies. It was named after geophysical profile line 20 (Ben-Avraham and Emery 1973), which has been used to constrain the

model along with four sets of radiosonobuoy data (R30, R32, R33 and R35 which gave information on the thicknesses and velocities of the sediments. The final model (Fig. 8.11) produces a good match between observed and calculated gravity anomalies, and is consistent with the known geology.

There are five major Bouguer anomaly features, these being, from south to north, the Bali High, the Bali Low, the Kangean High, the Kangean Low and the Meratus High. The Bali High, with a maximum Bouguer anomaly of +60 mGal, corresponds to the uplifted basement seen on Line 20. The Kangean High (with a maximum Bouguer anomaly +62 mGal) is situated west of Kangean Island and close to refraction stations R30 and R32. The source of this high was modelled as an igneous intrusion, as seen on Line 20. Between these two highs is the Bali Low, reaching down to +38 mGal, which corresponds to a structural low infilled by sediments approximately 3 km thick.

Further north, over the Kangean Low, Bouguer anomaly values decrease gradually to +35 mGal in the axial depression, and then slightly increase to +40 mGal at the location of R35 on the Meratus High before again decreasing towards SE Kalimantan. The source of the Meratus High was modelled as an ophiolitic body as the high is situated very close to Laut Island.

The depth to the mantle is about 26.5 km in the south, near the island arc, and nearly 30 km in north, near SE Kalimantan. Beneath the Bali Low the depth to the mantle decreases slightly to 24.5 km. Crustal thicknesses along this profile are typical of stretched continental crust.

8.7.3.4 Gravity model RAMA 67

This profile runs parallel to BEN 20 and about 40 km farther east. The model is named after seismic line RAMA 67 (Silver *et al.* 1983), which was used to constrain the model in the south. The model shown in Fig. 8.12 produces a good match between observed and calculated gravity anomalies and is compatible with the known geology.

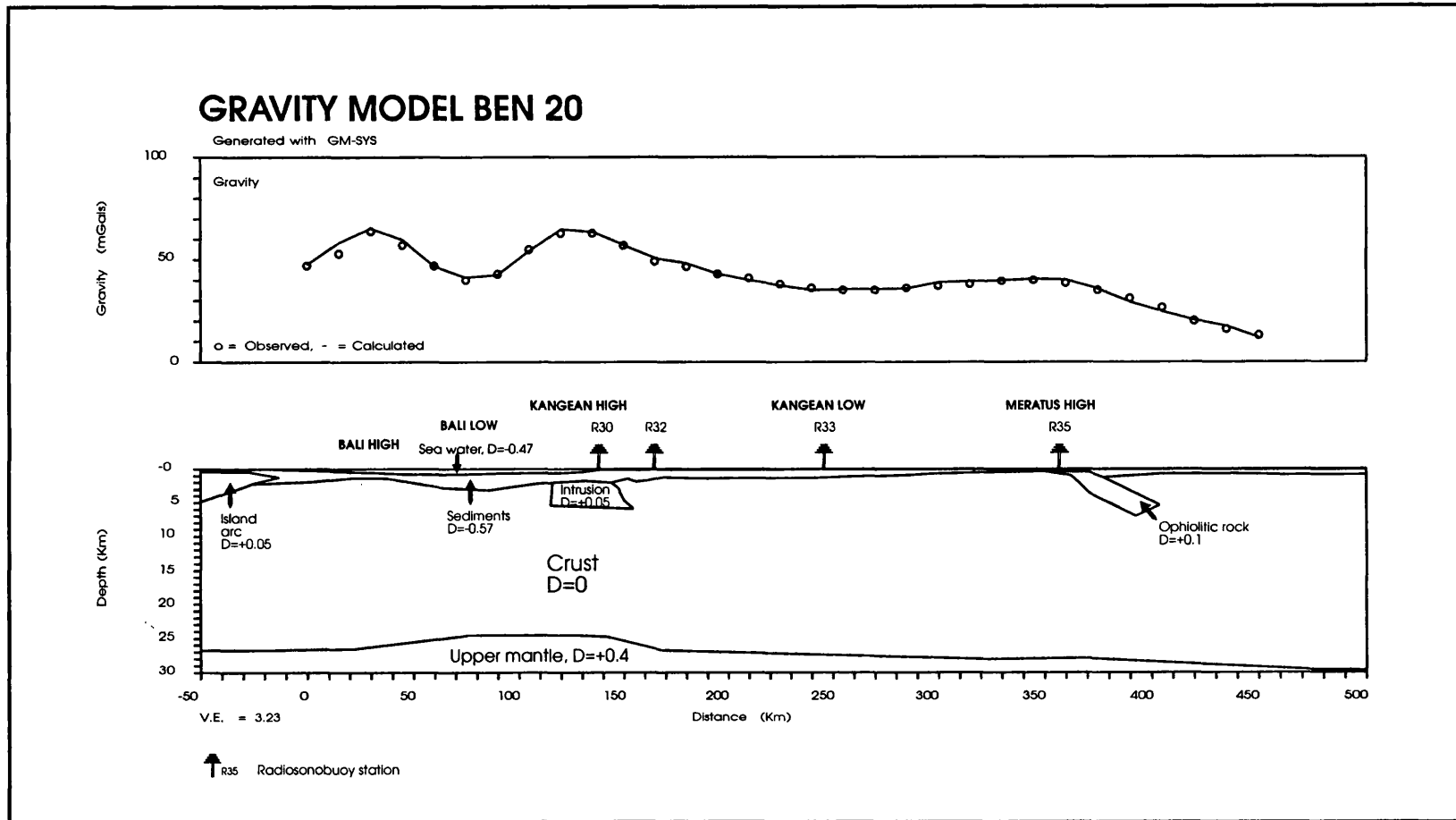


Figure 8.11: Gravity model BEN 20

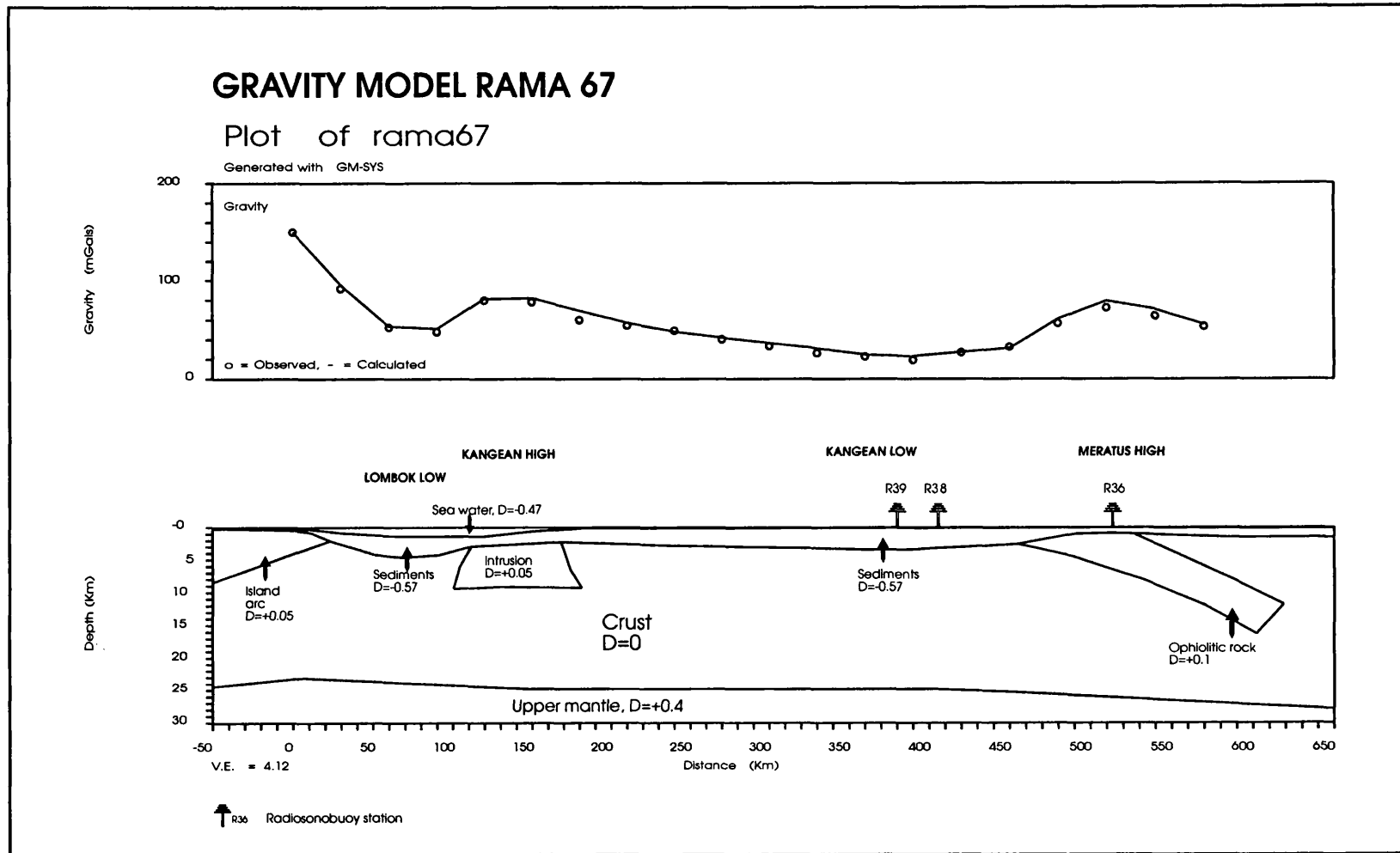


Figure 8.12: Gravity model RAMA 67

There are four major gravity features, these being, from south to north, the Lombok Low, the Kangean High, the Kangean Low and the Laut High. Towards the island arc the Bouguer anomalies increase to +150 mGal. They decrease sharply to +50 mGal over the Lombok Low, where the water depth is approximately 1500 m. In the model the Lombok Low is filled by sediments with a thickness of more than 4.5 km. On the Kangean High, the Bouguer anomaly increases again to +80 mGal. The source of this high was modelled as an igneous intrusion, as is seen on seismic profile RAMA 67. Further to the north, over the Kangean Low, the Bouguer anomaly drops up to +21.5 mGal in a region where basement is covered by 3 km sediments. On the Laut High, the Bouguer anomaly increases again to +72.5 mGal. In the model, the ophiolitic source body dips to the north. If this is correct, the ophiolites may be slices of oceanic crust emplaced when collision occurred at the eastern margin of Sundaland.

The depth to the mantle is roughly constant at about 24 km - 25 km. The Moho is shallowest beneath the Lombok Low (about 23 km) and deepens towards the island arc and SE Kalimantan.

8.7.3.5 Gravity model BP 037

This model was prepared for a line which runs parallel to profile RAMA 67 and approximately 60 km to the east. The model was named after seismic line BP 037 which was used to constrain it. The result is shown in Fig.8.13. There is a good match between observed and calculated gravity anomalies and consistency with the known geology.

There is a Bouguer anomaly high, the Lombok High, north of Lombok reaching +82 mGal. The source of this was modelled as an igneous intrusion, as supported by the interpretation of seismic line BP 037. The Bouguer high over this intrusion does not correlate with any magnetic feature and the intrusion was therefore considered to be granitic and was assigned a density contrast of 0.05 Mg/m^3 . Another Bouguer anomaly high, the Kangean High, corresponds to a basement uplift as interpreted on the seismic profile and does coincide with a high magnetic anomaly.

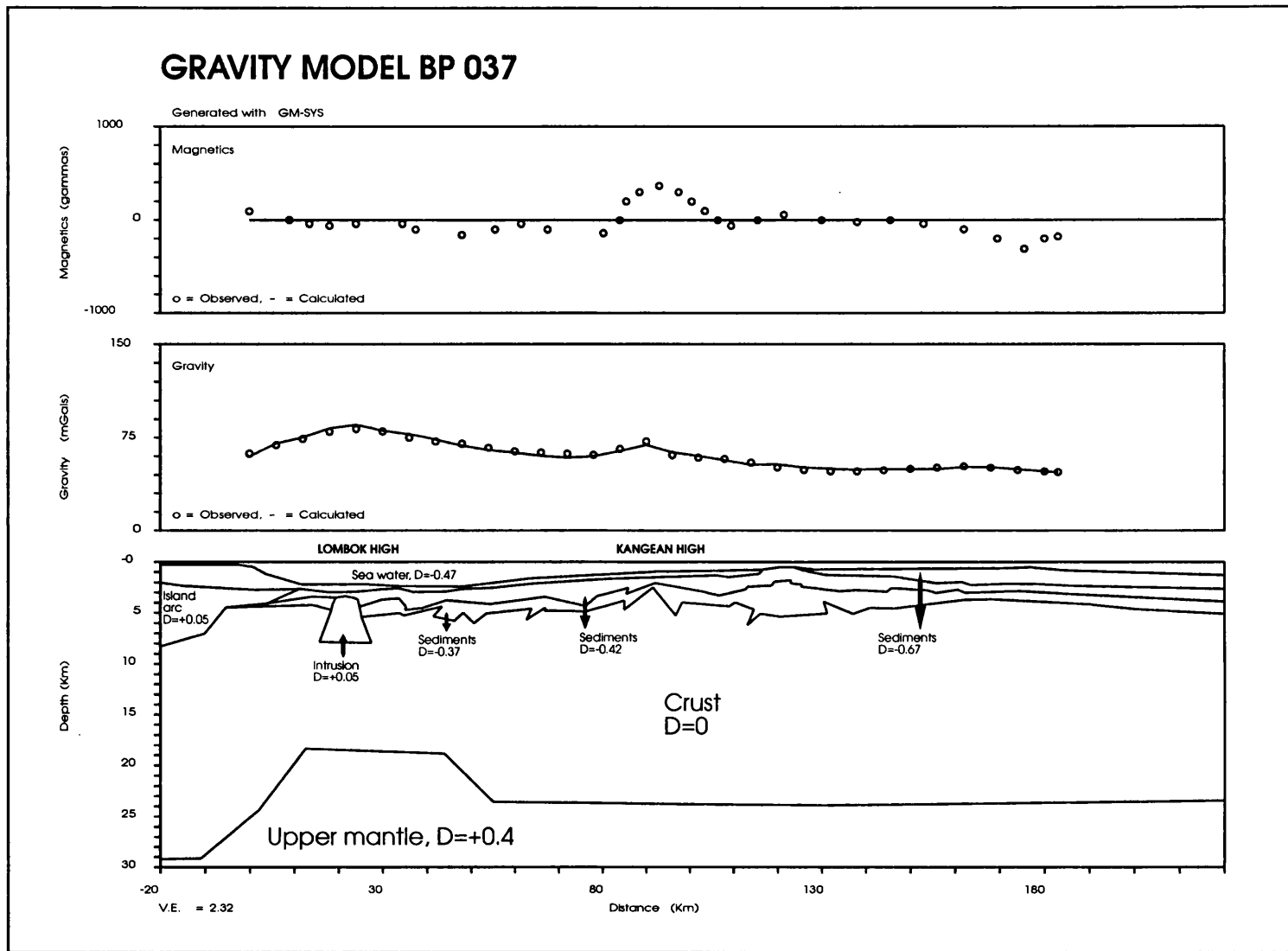


Figure 8.13: Gravity model BP 037

The depth of the Moho near Lombok is nearly 30 km. Beneath the Lombok trough the depth of the mantle decreases sharply to approximately 18 km and increases again to the north, to about 24 km. These thicknesses suggest stretched continental crust.

8.7.3.6 Gravity model MSN 14B

This model relates to a N-S line across the Lombok Sea, parallel to profile BP91-037 and approximately 50 km to the east. The model was named after seismic refraction station MSN 14B (Curry *et al.* 1977) which was used to it. The result of modelling is shown in Fig. 8.14. There is a good match between observed and calculated gravity anomalies and consistency with what is known of the geology.

The Lombok Low, with a minimum Bouguer anomaly of +15 mGal, occurs approximately 30 km north of the Lombok trough, in a region where basement is covered by 5 km sediments. Farther to the north, on the Lombok High, the values increase sharply to +90 mGal. The source of the high was modelled as a basement uplift of about 2.5 km, compared to a depth of 5 km to the south. Towards the Makassar Strait, Bouguer anomaly values slightly decrease from +90 mGal to +30 mGal in a distance of about 300 km. This decreasing Bouguer anomaly value is interpreted as due to the effect of increasing crustal thickness. On the Paternoster High the Bouguer anomaly increases again to +60 mGal, which is interpreted as due to uplifted basement.

The most interesting feature of this profile is that the maximum Bouguer anomaly does not occur over the Lombok Trough, which indicates that the crust does not thin beneath the trough, and that the trough is not locally compensated. The maximum is shifted approximately 30 km to the north of the centre of the Lombok Trough, and is approximately coincident with the Lombok Thrust zone.

8.7.3.7 Gravity model MSN 14A

This model relates to a N-S line across the Sumbawa Sea, i.e. perpendicular to the regional structure and Bouguer anomaly contours. It was named after seismic refraction station MSN 14a (Curry *et al.* 1977) which was used to constrain the model. There is a

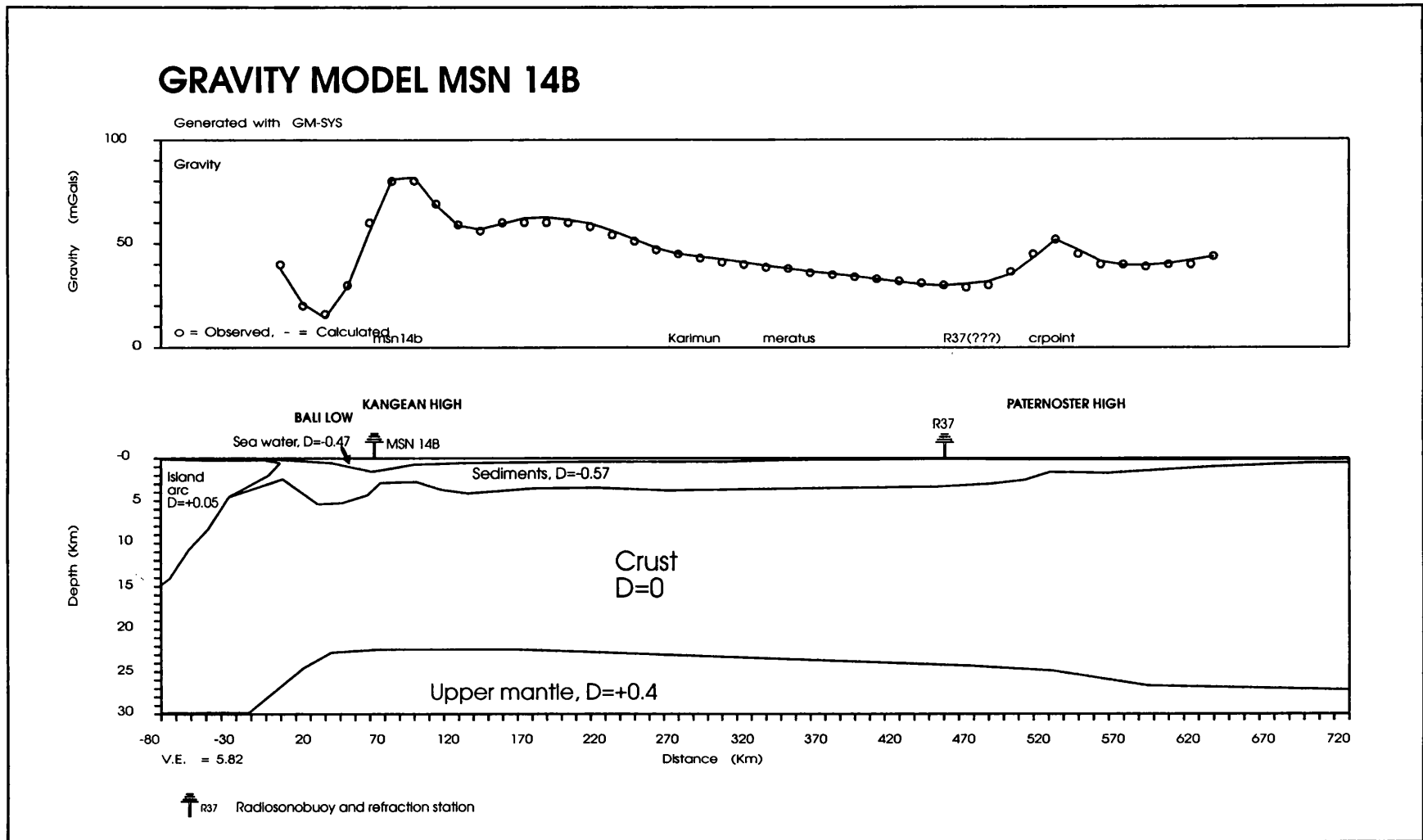


Figure 8.14: Gravity model MSN 14B

good match between observed and calculated gravity anomalies and consistency with the known geological constraints. The model is shown in Fig. 8.15

Bouguer anomaly values increase from +40 mGal north of Lombok to +70 mGal and then decrease to +10 mGal. The Bouguer anomaly high (the Sumbawa High) is situated approximately 30 km north of the point of minimum water depth, indicating that the bathymetry is only partially compensated. From Km 180 to Km 255, Bouguer anomaly values decrease gradually from +40 mGal to +10 mGal, and this is interpreted as the effect of the Moho deepening northwards. The depth to the Moho near the island arc is nearly 30 km, and towards the Makassar Strait it is about 27 km. In the centre of the profile the Moho is uplifted to about 21 km, suggesting crustal thinning.

8.8 CRUSTAL STRUCTURE

Comparison between the Bouguer and free-air anomalies and bathymetric profiles (Fig 8.16) shows that, in general, the minimum free-air anomalies do not correspond to the bathymetric minima but are shifted approximately 15-30 km to the south. The westernmost profile (Ben 20) is an exception, with the minimum free-air anomaly shifted 45 km to the north. This suggests that the area is not locally compensated, the lack of equilibrium being due to the northward subduction of Indian-Australian lithosphere beneath the Sunda and Banda arcs. This conclusion is also supported by the relatively high free-air and Bouguer anomalies which could be the effect of this subducted lithosphere.

Bouguer and free-air anomaly values decrease from east to west (From the Bali-Lombok Sea towards the Central Java Sea), showing that the crust thickens to the west.

The five gravity models described above show the mantle rising to the east to about 21 km. The highest Moho level occurs beneath BP 037 and is about 18 km. This suggests that the centre of the rifted basin is situated around this line, where the interpreted depth to basement reaches 6 km. In summary, the formation of the rift structures in the East Java Sea is interpreted as a result of attenuation of continental crust.

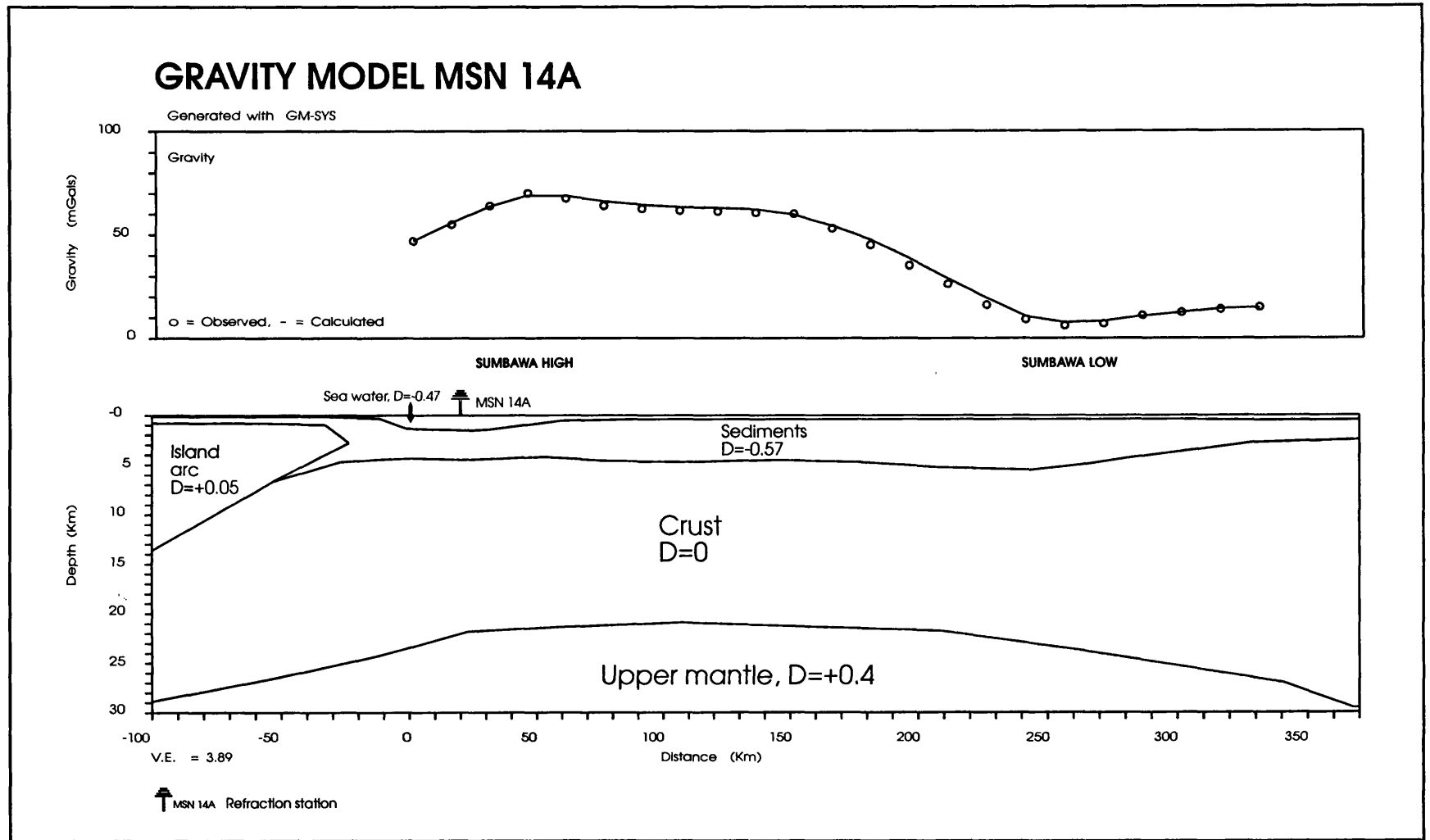


Figure 8.15: Gravity model MSN 14A

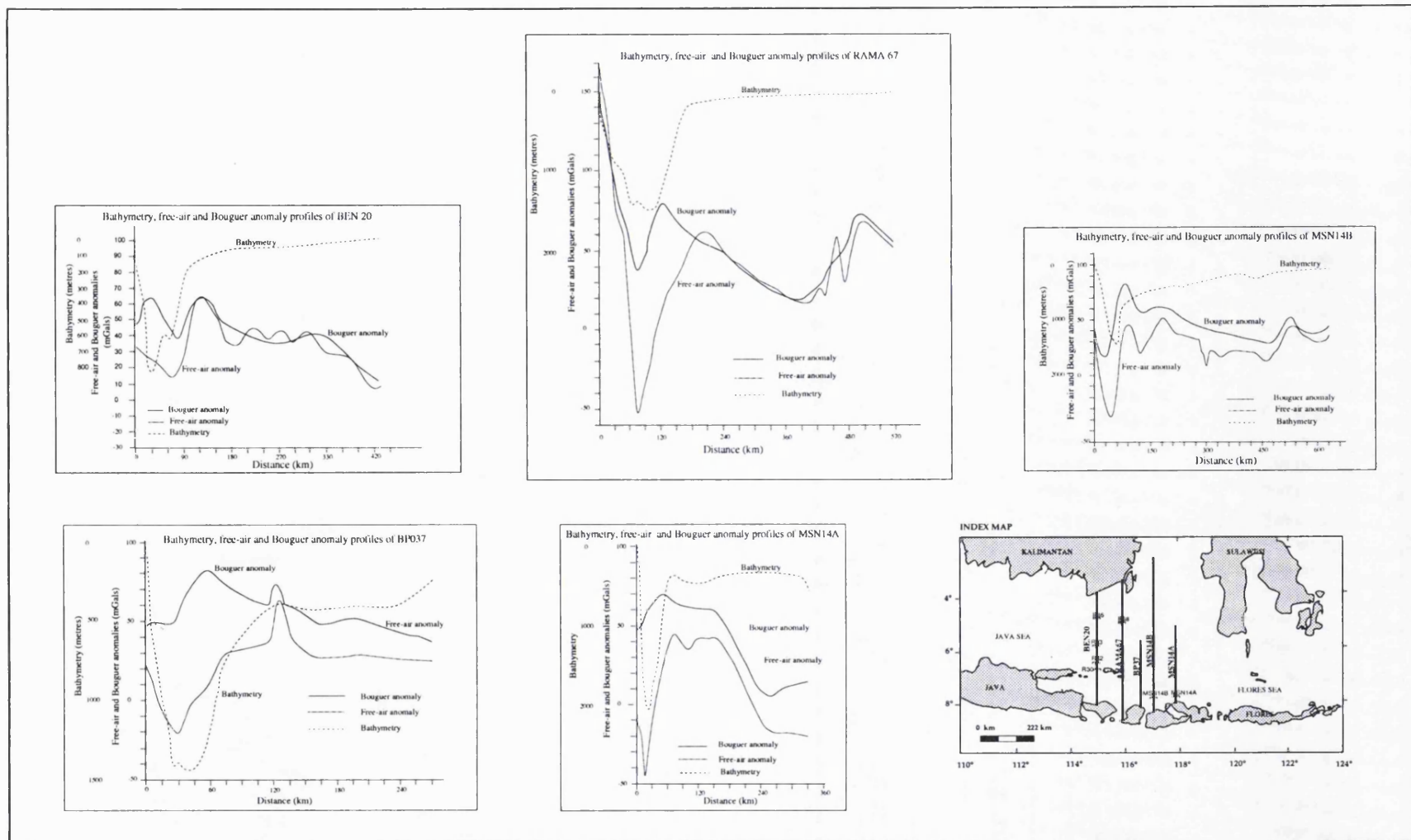


Figure 8.16: Comparison of bathymetry, free-air and Bouguer anomaly profiles of BEN 20, RAMA 67, BP 037, MSN 14A and MSN 14B in the East Java Sea

8.9 TECTONIC IMPLICATIONS AND STRUCTURAL INTERPRETATION

The geological history of the East Java Sea province can be summarised on the basis of seismic stratigraphy analyses, gravity data, geological information and published seismic interpretations.

The East Java Sea has experienced three major tectonic events, these being Cretaceous crustal compression, Palaeogene crustal extension and Neogene inversion. The changes between these structural regimes, indicated by distinct basin geometries, styles of faulting and structural deformation since the Cretaceous, imply changes in the intraplate stresses or plate boundaries and movements which can be linked to the evolution of subduction and collision around the SE Sunda Shelf. From the information of Well JS 25-1, basement complexes are present in the Central Lombok Block. These are suggested to be part of the Late Cretaceous accretionary complexes formed at the southeastern margin of the Sundaland.

From the seismic stratigraphic analyses outlined above, the basin of the East Java Sea is believed to have existed since the Cretaceous. The basin might have extended in a NE-SW direction as far as SE Kalimantan; basement complexes which might correlate with those in SE Kalimantan and SW Sulawesi trend in NE-SW directions. The succession of the Cretaceous folded and thrust sediments can be correlated with the Paniungan Formation in the SE Kalimantan and also with the folded and thrust-faulted sediments in west Sulawesi seen on Line IND 116 (see Fig.10.3 in Chapter 6).

Extension took place in the Paleocene-Eocene, with some of the normal faults reactivating former E-W thrust faults. The period was characterised by the formation of horsts and grabens. The cause of this rifting is still poorly understood. Gravity modelling (see section VIII.7.3.2) suggests that the thickness of the crust, including sediments, in the East Java Sea ranges from 18-30 km, which is characteristic of attenuated continental crust. There is no indication of the presence of oceanic crust. The tectonic style in the west is dominated by folding, with thrusting becoming weaker. This would seem to rule out the possibility of arc reversal in this region as suggested by Silver *et al.* (1983) and Prasetyo (1992). Rifting in the East Java Sea may have been caused by the separation

between SE Kalimantan and SW Sulawesi in the Early Palaeogene. Matthews (1990) suggested that the East Java Sea basin had undergone a bulk clockwise rotation of approximately 20-30 degrees since the cessation of rifting, and therefore the current margin of the system (West Sulawesi, and the main rift axis in the Makassar Strait) would have been orientated approximately NNW-SSE during extension. Rotation was followed by subsidence and deposition of post-rift sediments which are nearly undisturbed. The latest compression took place between the Middle Miocene and the Pleistocene, with reactivation of older normal faults as thrust faults.

Regional studies have shown the presence of a continuous zone of Neogene back-arc thrusting from Flores to the Bali Sea (McCaffrey and Nabelek 1984;1987 and Prasetyo 1992). However, the seismic reflection observations outlined above, and also published seismic profiles, indicate that the structural framework of the Bali and Lombok seas changes gradually from east to west with deformation becoming weaker westwards. On the westernmost profile of Rama 67 (McCaffrey and Nabelek 1987), the Flores thrust zone loses its surface expression north of Bali. However, broad folding continues and involves the entire sedimentary section.

Matthews (1990) proposed three possible controls on Neogene fault reversal and resultant uplift, these being; compression from the NW Borneo collision (Late Early Miocene), Sulawesi collisions (Middle Miocene and younger) and the Australian collision (Early Miocene and younger). He argued that of these three crustal-scale mechanisms, the only one likely to have resulted in Neogene strike-slip in the East Java Sea would have been the Sulawesi collisions, and if this were the uplift mechanism, then the East Java Sea uplifts would be explained as transpressional bend folds within a subvertical crustal-scale shear zone. Nonetheless, the Neogene thrust faults on the seismic profiles (Line BP91-037, Line BP91-010 and Line BP91-110) show either positive flower structures as defined by Harding (1990), or pop-up structures as defined by McClay and Buchanan (1992). These two types of structure have different mechanisms. Flower structures occur in strike-slip fault regimes whilst pop-up structures are inversion structures involving reactivation of extensional listric faults. The presence of high angle thrusts, footwall shortcut and harpoon structures on the seismic profiles is typical of inversion along the

bounding faults of crustal collapse grabens in listric fault systems as suggested by McClay and Buchanan 1992. These characteristics are seen in the seismic profiles in the East Java Sea (see Fig. 8.6 and 8.7). Considering these data, it is unlikely to relate the inversion of Neogene thrust faults in the East Java Sea to the Sulawesi collision having tranpressional regime, but it is more likely to relate the inversion to the collision the Indo-Australian continent to the Sunda-Banda arcs.

CHAPTER NINE

GEOLOGICAL AND GRAVITY OBSERVATIONS ON THE FLORES SEA ISLANDS

9.1 THE FLORES SEA ISLANDS SURVEY

9.1.1 Introduction

Several groups of small islands in the Flores Sea between Sulawesi and Flores, referred to as the Flores Sea Islands, were visited by a joint University of London and Geological Research and Development Centre (GRDC), Bandung team in May 14 - 1 June 1993.

The survey was carried out for the purpose of collecting geological and gravity data, since there were no onshore geology and gravity data from the Flores Sea Islands. The geological and gravity data obtained from the islands are needed to constrain geophysical modelling and to better understand about geological evolution of the Flores Sea Islands and the vicinity.

9.1.2 Survey area

The survey area comprises several groups of islands which are situated in the Flores Sea between Sulawesi and Flores (Fig. 9.1). The area is bounded by 120°E 15' to 122°E longitude and 6°30' to 7°30' S latitude, and is located within Selayar District, Pasimasunggu Sub-district. This area is referred to in this report as the Flores Sea islands of which there are several groups of islands, all lying on separate plateaus rising from great depths. Kepulauan Macan reef complexes are the largest group situated to the southeast of Selayar, and surrounding this complex in an elliptical form from northwest to southeast are: Selayar group (Selayar, Pasi, Bahuluang, Tambolongan and Pulasi islands); Bonerate group (Kajuadi, Tanahjampea, Tanahmalala, Kalao and Bonerate islands); Kalaotoa group (Kalaotoa, Madu, Karompa Cadi and Karompo Lompo islands). Topographic maps of the areas can be obtained from the Direktorat Geologi Bandung (scale 1:250,000, Sheets SB 51-9 and SB 51-13). Aerial photographs of Tanahjampea, Kalao and Kalaotoa islands were obtained from BAKOSURTANAL, Jakarta but for security reasons have been examined only in Indonesia.

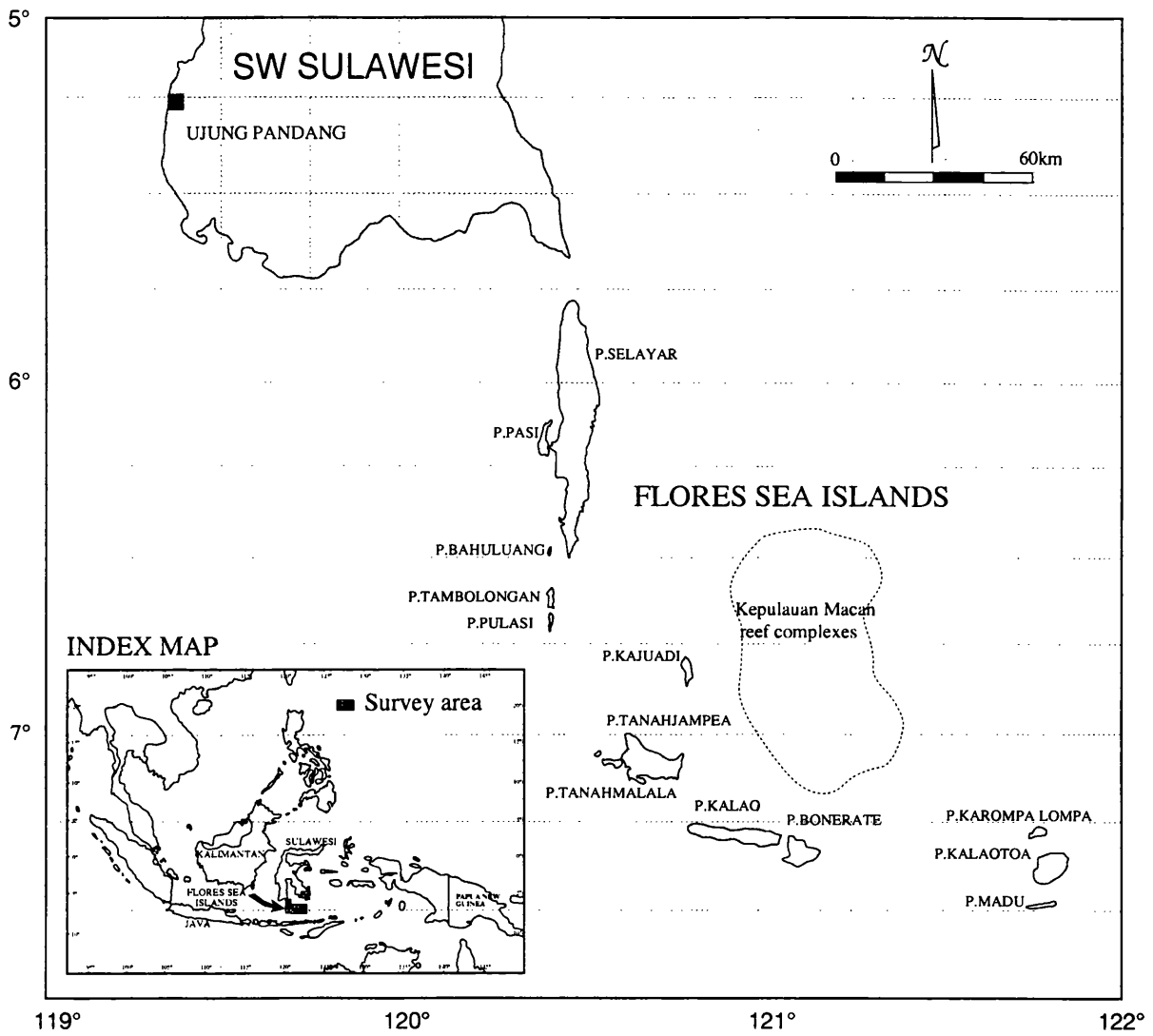


Figure 9.1: Geological and gravity survey area in the Flores Sea Islands

9.1.3 Type and period of survey

9.1.3.1 Gravity survey

The aim of this survey is to obtain gravity data of the islands by using gravimeter (La Coste and Romberg). In the survey area, the nearest base station is situated at Hasannudin Airport (Ujung Pandang), of which the absolute gravity value is 978119.9800 mGal. Speed boats or larger trading vessels were used to go around the islands, and motor bikes or "Mikrolet" buses to make traverses along roads.

Location: Selayar, Kajuadi, Tanahmalala, Tanahjampea, Kalao, Bonerate, Kalaotoa

Duration of work: May 14 to May 23, 1993.

9.1.3.2 Reconnaissance geological mapping

The aims of this survey are: to map geology of Tanahjampea and Tanahmalala and to study the lateral as well as vertical distribution of the rocks in order to gather information regarding the structure and stratigraphy of the Flores Sea Islands.

Field observations were carried out using compass clinometer, aerial photographs (scale 1:50,000) and 1:250,000 topographic maps

This survey was carried out on foot but a speed boat was used for transport between the surveyed areas and base camp.

Location: Tanahjampea and Tanahmalala. In addition, limited geological observations were made in conjunction with the gravity survey described above.

Duration of work: May 14 to June 6, 1993

9.1.4 Communication and access

Geographically, Selayar Island is situated in the south of Southwest Sulawesi. It is a big island (about 80 km long and 12 km wide) easily accessible from the mainland of South Sulawesi. The survey area can be reached from a small port called Lapee in Bulu Kumba, three hours journey by car, south of Ujung Pandang. From there the journey to Selayar can be made either by a ferry which runs three times a week or by a daily trading vessel. The journey takes approximately seven hours. Tanahjampea, Kalao,

Bonerate and Kalaotoa can be reached from Selayar by trading vessels and the journeys take nine, six, two and seven hours consecutively to the capitals of each island. For the gravity survey, a boat of 30 tonnes was hired from Selayar for ten days. The boat was suitable as a base and for transportation between islands, but could not be used to conduct actual survey work as it could not approach the shore, except in a few places such as the ports on some of the islands. On Selayar the gravity survey was conducted by hired car and a small boat was hired to cross to Pasi and Bahuluang islands. On Bonerate, motor cycles were used to cross the island, and on Tanahjampea, Kalao and Kalaotoa local boats with capacities of about 3 tonnes were hired. Transportation for moving from one village to others when geological mapping in Tanahjampea and Tanahmalala was conducted using a 3 tonnes boat of equipped with 25 HP engine and sometimes using public-sea transportation.

Food and fuel can be obtained in Benteng, the capital city of Selayar. In Bonerate, food is very difficult to obtain. A limited amount of fuel can be obtained at Benteng, Tanahjampea. In this survey food was brought from Ujung Pandang and the fuel was bought on Selayar. Documentation for the fieldwork was arranged through GRDC in Bandung and further arrangements are needed in Ujung Pandang, Benteng Selayar and Benteng Tanahjampea.

Porters can normally be hired on a daily basis through the head of villages on each islands. Nearly all islands are inhabited, especially along their coasts, where people live mainly by fishing, coconut cultivation, boat building and farming. The religion of the area is dominantly Islam. The people have their own languages but communication can be conducted through Bahasa Indonesia.

9.1.5 Currents, Climate and Weather

In the Flores Sea the west-going current runs from June to October and the east-going currents from December to May. Both the west-going and east-going currents are, on average, a little stronger than those of the Java Sea and the east-going current is somewhat stronger than the west-going one, the average rate during December to May being approximately 30 km per day.

The climate of the area is hot and humid, with temperatures between 26⁰C and 35⁰C. The wet season is from November or December to March, and the dry season is at its height from July to September. In May-September, the winds are usually very strong. Fieldwork during the wet season is not advisable due to the common flooding of rivers and rough seas.

9.2 GEOLOGICAL SURVEY

9.2.1 Introduction

9.2.1.1 Type of geological information

Geological information on the islands in this report are considered in three parts: (1) islands which were not visited during this fieldwork where geological information has been obtained from literature studies (Pulasi and Tambolongan islands and Macan islands) (2) islands where geological information has been obtained along the coast in conjunction with gravity and minor geological observations conducted inland (Selayar, Kajuadi, Kalao, Bonerate and Kalaotoa islands); (3) islands where reconnaissance geological mapping was done in a systematic fashion (Tanahmalala and Tanahjampea).

As ground geological survey inland was limited by poor outcrops, dense forest and ruggedness of terrain, geological boundaries have, in many cases, been interpreted from air photographs.

9.2.1.2 Vegetation and outcrop condition

The Flores Sea Islands are situated in the wet tropics and they are in most cases covered by very thick forest which extends up to the ridges of the mountains. Exceptions are Bonerate, which is relatively densely populated and largely given over to agriculture, and Tanahmalala, which is covered by coarse grass. Along the coasts, there are extensive areas of thick mangrove forest and swamp.

In general, good outcrops in the surveyed areas are present only along the coasts. Rivers are rare and the occasional creeks run only in the wet season.

9.2.1.3 Previous surveys

The earliest geological report on the islands in the Flores Sea was provided by Hetzel (1930). This report was written in Dutch but the main results have been summarised by van Bemmelen (1949). Since then, no geological ground surveys were conducted until 1991, when a team from the Geological Research and Development Centre (Bandung) carried out geological mapping of the islands. Preliminary copies of their geological maps have been made available (Koswara *et al.* 1991;1993). Information on the topography, sea currents and climate is contained in Eastern Archipelago Pilot, Vol II (Royal Navy, 1961).

9.2.2 Topography of the Flores Sea Islands

9.2.2.1 Tanahjampea

Tanahjampea, the largest of the islands in the western part of the area, is high, thickly wooded and deeply indented on its western side, off which lie many smaller islands. The numerous summits are approximately of the same elevation and are difficult to identify from the coast. On the topographic map the highest peak recorded is 521 m.

9.2.2.2 Kajuadi

Kajuadi lies at the northern end of the bank extending north from Tanahjampea, and in some places rise steeply from the sea. The island is dominated by three hills. Dato Besar is the highest hill at the northernmost, with an elevation of 287m, and it is fringed by steep reefs. The top of which is 0.5 - 2m below the surface.

9.2.2.3 Kalao and Bonerate

Kalao lies about 15 km south-southeastward of Tanahjampea. The island is higher at the eastern and western parts than in the middle. The western peak, named Baringke (270 m), and the eastern peak, named Popoking (335 m), are both good landmarks.

Bonerate is separated from the eastern end of Kalao by a small channel about two km wide. It is much lower than Kalao, with three flat hills, the highest of which is Bingkung at the northern extremity of the island, which has an elevation of 150 m.

9.2.2.4 Madu and Kalaotoa

Madu, the more southerly of these hilly islands, lies about 60 km east-southeastward of Bonerate and has a 120 m high plateau in its middle.

Kalaotoa, separated from Madu by a deep passage about five km wide, is the principal and the most populated island on this group. Cornelia peak, on the south-eastern side, is a steep 342 m high hill. The south-western peak of the island, 330 m high, appears as the highest summit when seen from the west and is somewhat conical in shape.

9.2.2.5 Taka Lambaena and Karompa

Taka Lambaena is an extensive and steep sided coral atoll lying northwest of the Kalaotoa Island. Karompa Lompo, the largest and the only permanently inhabited island in this group, is 82 m high and lies 4 km north of Kalaotoa. Karompa Cadi, 60 m high, with Anak Karompa islet to the south of it, occupies the northeastern extremity of the reef, 2.5 km further north.

9.2.2.6 Kepulauan Macan

Kepulauan Macan or Taka Bonerate is a group of small coral islands forming an extensive reef complex which occupies a large area between Taka Lambaena and southeast Selayar. These islands are visited regularly by local trading vessels, which call at Rajuni Kecil for copra.

The central part of the group consists of numerous uplifted reefs. The large reefs are nearly always marked by discoloured water when submerged. The difference in appearance of the area at high water, when nearly all the reefs are covered, and at low water, when all the large reefs are dry, is very pronounced.

9.2.3 Regional Geological study of South Sulawesi

9.2.3.1 Introduction

Sulawesi is divided into two main tectonic units; the eastern and western arcs or provinces (van Leeuwen 1981). The eastern arc or province is characterised by thrust tectonics associated with the emplacement of an ophiolite-metamorphic suite. The western arc or province consists of folded metamorphic, sedimentary and volcanic

sequences of Mesozoic to Tertiary which are intruded by acid and intermediate plutonic rocks (van Leeuwen 1981). Southwest Sulawesi is located at the southern end of the western province and is dominated by three major structural units; the Western Divide Mountains, Bone Mountains and Walanae Depression (Fig.9.2).

Since the Flores Sea Islands are nearest to the South Sulawesi, it is useful to compare the results of the geological observations in these islands with those from the South Sulawesi where the geological conditions are better understood.

9.2.3.2 Stratigraphy

The stratigraphy of South Sulawesi, with reference to the Biru area (see Fig.9.2 for location), 70 km east of Ujung Pandang, has been summarised by van Leeuwen (1981). A simplified stratigraphy of the region is shown in Fig.9.3. The rock units present are predominantly of Cainozoic age, with minor outcrops of pre-Tertiary sedimentary and metamorphic rocks of the Bantimala Tectonic Complex (see Chapter 3.1.2.4). The Tertiary rock units consist largely of thick volcanic and volcanoclastic sequences. The description of the formation is based on van Leeuwen (1981) from the oldest to youngest as follows;

Marada Sandstone Formation

This Upper Cretaceous formation crops out in the eastern part of the Biru area, and it is the oldest formation exposed in Southwest Sulawesi. It consists predominantly of an arenaceous succession of alternating impure sandstone, siltstone and shale characterised by monotonous lithology. The thickness is difficult to estimate because the formation is poorly exposed and strongly faulted, but is estimated at more than 750 m.

The base and top of this formation are not exposed. The formation is overlain with angular unconformity by rocks belonging to the Pamesurang and Walanae Formations.

Langi Volcanic Formation

This formation consists of lavas and pyroclastics of andesitic to trachy-andesitic composition with rare intercalations of limestone and shale. The thickness is difficult to

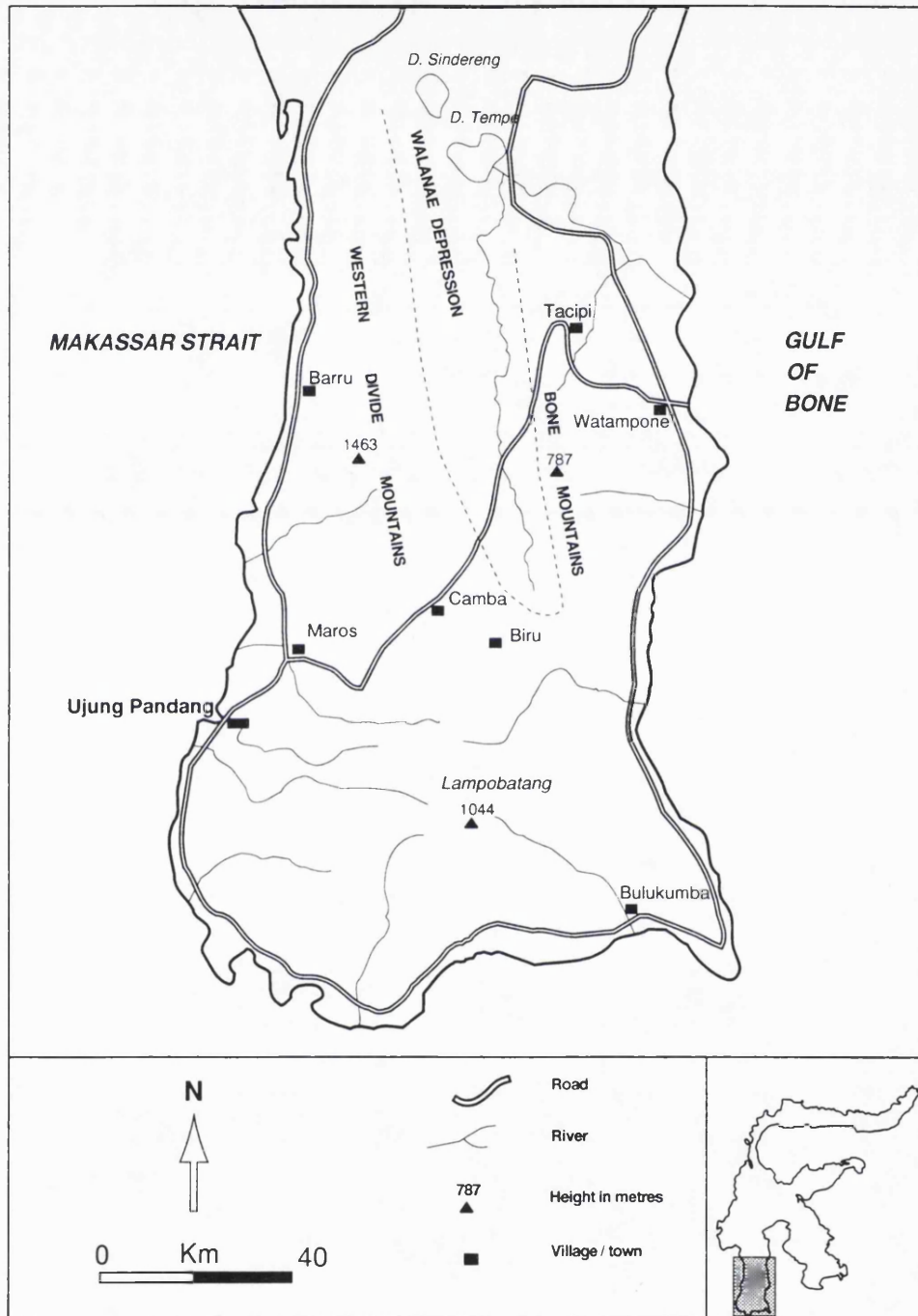


Figure 9.2: Three major morphological units in SW Sulawesi; the Western Divide Mountains, the Bone Mountains and the Walanae Depression (Leeuwen 1981)

AGE	FORMATION	MEMBER	THICKNESS (M)	LITHOLOGY	ENVIRONMENT	REMARKS	
PLIOCENE (?) ↑ U. MIOCENE 6.2 my	LEMO VOLCANICS		350 +	V V V V V V V V △ △ △ △ △ △ △ △ V V V V V V V V △ △ △ △ △ △ △ △ V V V V V V V V	Lavas and breccias predominantly of andesitic composition; alkaline basaltic rocks in basal part.	Sub-aerial (?)	Alkaline and Calc-alkaline vlc
U. MIOCENE	WALANAE VOLCANICS		100	V V V V V V V V △ △ △ △ △ △ △ △ V V V V V V V V △ △ △ △ △ △ △ △ V V V V V V V V	Tuffs, tuffaceous sandstones, breccias, and lavas, predominantly andesitic, lesser trachyte, minor shale and limestone.	Shallow marine	Alkaline and Calc-alkaline vlc DYKES (11my)
U. MIOCENE (?) ↑ M. MIOCENE 13 my	PAMMESURANG VOLCANICS	G	0 - 80	V V V V V V V V △ △ △ △ △ △ △ △	Leucite tephrite	Sub-aerial (?)	Alkaline volcanism
		F	0 - 110	V V V V V V V V △ △ △ △ △ △ △ △	Litic tuffs and tuff breccias, minor marl and tuffaceous sandstone	Shallow marine	Alkaline volcanism
		E	0 - 40	V V V V V V V V △ △ △ △ △ △ △ △	Trachyte ignimbrite	Sub-aerial	Alkaline volcanism
M. MIOCENE	SOFO VOLCANICS		0 - 250	V V V V V V V V △ △ △ △ △ △ △ △ V V V V V V V V △ △ △ △ △ △ △ △ V V V V V V V V	Andesitic and basaltic lavas and breccias; minor tuff.	Sub-marine (?)	Alkaline vlc
M. MIOCENE	TONASA LIMESTONE	D	65	V V V V V V V V △ △ △ △ △ △ △ △ V V V V V V V V △ △ △ △ △ △ △ △ V V V V V V V V	Tuffaceous marls, limestones, tuff and lavas, exotic limestone blocks	Deep neritic with influx of shallow marine and volcanic material, erosion of submarine fault scarps	Calc-alkaline vlc FOLDING
M. MIOCENE ↑ L. MIOCENE		C	150	V V V V V V V V △ △ △ △ △ △ △ △ V V V V V V V V △ △ △ △ △ △ △ △ V V V V V V V V	Thin bedded to massive limestone with abundant coral/algal debris	Shallow to mid-neritic	FAULTING BIRU GRD (19 my) & DYKES
U. OLIGOCENE (?)							
NON - DEPOSITION (?)							
L. OLIGOCENE	TONASA LIMESTONE	B	60	V V V V V V V V △ △ △ △ △ △ △ △ V V V V V V V V △ △ △ △ △ △ △ △ V V V V V V V V	Massive limestone	Lagoonal	UPLIFT
U. EOCENE		A	205	V V V V V V V V △ △ △ △ △ △ △ △ V V V V V V V V △ △ △ △ △ △ △ △ V V V V V V V V	Thick bedded limestone, abundant chert	Lagoonal to mid-neritic	
U. EOCENE ↑ PALEOCENE (?) 63 my	LANGI VOLCANICS		400 +	V V V V V V V V △ △ △ △ △ △ △ △ V V V V V V V V △ △ △ △ △ △ △ △ V V V V V V V V	Lavas, breccias and tuffs of andesitic and trachy/andesitic composition. Near top intercalations of limestone and shale.	Sub-marine Sub-aerial (?)	Calc-alkaline volcanism
NOT EXPOSED IN MAPPED AREA							
U. CRETACEOUS	MARADA SANDSTONE		1000 +	V V V V V V V V △ △ △ △ △ △ △ △ V V V V V V V V △ △ △ △ △ △ △ △ V V V V V V V V	Monotonous sequence of alternating graywackes, argillites, siltstones and shale, rare sills or flows of trachy-andesite.	Deep neritic to ? bathyal	FOLDING

Figure 9.3: Simplified stratigraphy of Southwest Sulawesi with the special reference to the Biru Area (Leeuwen 1981)

estimate because the volcanic rocks are for the most part unbedded. Probably it exceeds 400 m.

The base of the Langi Volcanics is not exposed. The formation is conformably overlain by the Tonasa Limestone Formation.

Tonasa Limestone Formation

This thick sequence of Eocene to Middle Miocene limestone is widely distributed throughout the western part of Southwest Sulawesi. It is developed into four members A, B, C and D from bottom to top. The 'A' member consists of well bedded calcarenites composed of broken or disintegrated fragments of algae, bryozoa and hydrozoa mixed in various proportions with complete shells of benthonic foraminifera. The 'B' Member is composed of a thickly-bedded to massive limestone crowded with foraminifera. The 'C' Member consists of a thick sequence of detrital limestones. It carries numerous foraminifera together with small gastropods, brachiopods and ostracods in a fine calcarenite matrix. The upper part of 'C' Member contains alternating thinly-bedded limestone, largely made up of plankton, and lenses and massive beds of calcarenites and calcirudites, composed of a mixture of benthic foraminifera, abundant coral-algae debris, limestone clasts and plankton. The 'D' Member is characterised by the abundant presence of volcanic materials of andesitic composition. The total thickness of the formation is about 400 m. The Tonasa Limestone Formation rests conformably on the Langi volcanics and has an angular unconformable contact with the overlying Sopo and Walanae Volcanics.

Sopo Volcanic Formation

This formation rests unconformably above the Tonasa Limestone. It consists of andesitic and basaltic lava flows and breccias with minor tuff intercalations. In the basal part these formation contains abundant limestone fragments. The thickness of the Sopo Volcanics is about 250 m. This formation is equivalent to the Lower Camba Formation from Sukamto (1975) and Sukamto and Supriatna (1982).

Pamesurang Volcanic Formation

This formation rests with pronounced angular unconformity above the Marada Sandstone and Langi Volcanics. It is assumed to be younger than the Sopo Volcanics on the basis of regional considerations. It is exposed only in the southeastern part of the Biru area, and is divided into three members (E,F and G from bottom to top). The 'E' Member is an ignimbrite consisting of welded and non-welded ashflow tuffs, with rare, thin intercalations of tuff breccia. The 'F' Member is a poorly stratified sequence of unsorted calcareous lithic-tuffs and tuff breccias with minor tuffaceous marl and tuffaceous sandstone. The 'G' Member is composed of several massive flows of blocky microporphyritic leucite tephrite which is locally highly vesicular. Members 'E' and 'F' locally contain fragments of the Biru Granodiorite and Tonasa Limestone. This formation is equivalent to the Upper Camba Formation from Sukamto (1975) and Sukamto and Supriatna (1982).

Walanae Volcanic Formation

The Upper Miocene Walanae Volcanics unconformably overlie the Pamesurang Volcanics. It is exposed in the Walanae Valley and in the southern part of the Biru area, and consists of alternating tuff, conglomerates and volcanic breccias with intercalations of sediments and lava flows. The thickness of the Walanae Volcanic Formation is estimated to be 100 m.

Lemo Volcanic Formation

This formation is widely distributed in the southeastern part of the Biru area and consists largely of volcanic breccias. A dating of basalt at the base of the formation yielded Lower Miocene age. The upper part of the formation may have been deposited in Pliocene times.

Biru Granodiorite

In the eastern part of Biru area, the Biru Granodiorite is exposed. It varies in composition from granite to diorite with biotite granodiorite as the dominant rock type. The Biru Granodiorite intrudes into the Marada Sandstone and Langi Volcanics which are either silicified and pyritised or metamorphosed into hornfels near the contact with the intrusion.

The granodiorite does not intrude the Pamesurang, Walanae and Lemo Volcanics.

Fission track dating of this granodiorite gave an age of 19 ± 3.4 Ma.

9.2.4 Review geology on the Flores Sea Islands

9.2.4.1 Selayar

Verbeek (1908, in Hamilton 1979) described Selayar as consisting of volcanic and Neogene sedimentary rocks. Hamilton (1979) interpreted a seismic reflection profile showing thick strata east of Selayar, dipping west toward a deep and narrow trough at the base of the long and straight island, and suggested that this trough was a young inactive trench. He also proposed that the volcanic rocks of Selayar, the ridge to the southeast of it and the large inactive volcano in the southwest corner of the South Arm of Sulawesi belonged to this inactive subduction system.

A more recent geological map of Selayar Island published by Sukanto and Supriatna (1982) shows the oldest sedimentary rocks as belonging to the Upper Miocene Volcanic Camba Formation, which consists of breccia, lava, conglomerate and tuff. This formation interfingers with the Camba Formation which consists of marine sedimentary rocks interbedded with volcanic rocks.

Unconformably overlying these two formations are the Pliocene Walanae Formation and the Selayar Member of Walanae Formation. The Walanae Formation consists of sandstones, conglomerate, tuff, siltstone, limestone and marl. The Selayar Member consists of limestone.

9.2.4.2 Kajuadi

Hetzel (1930) described Kajuadi as consisting of undated andesite and basalt and highly alkaline volcanic and intrusive rocks, overlaid by raised reef limestone. However, according to Koswara *et al.* (1991), the island is mainly covered by tuffaceous sandstone interbedded with volcanic rocks.

9.2.4.3 Tanahjampea and Tanahmalala

The geology of Tanahjampea and Tanahmalala was reported by Hetzel (1930) and van Bemmelen (1949). The islands consist largely of igneous rocks. They described that

along the east and northwest coast there are some elevated coral reefs whereas on the south coast there are thick limestones with large *Lepidocyclina* foraminifera. Tanahmalala, the largest of the small islands along the west coast, consists totally of eruptive products and similar rocks form most of Tanahjampea. The calc-alkaline rocks (aplite, syenite porphyry, synoaplite and andesite) were found predominantly in the eastern part of the Tanahmalala and along its southwest coast. The rest of the island appears generally to be formed by alkalic rocks (quartz monzonite, nepheline monzonite and aplite nepheline monzonite).

The age of the eruptive rocks cannot be determined with certainty but the age of syenitic intrusions may be compared with the granodioritic intrusions of Flores, which are probably Miocene (Bemmelen 1949). Ehrat (in Hetzel 1930) recognised, with some reservation, a post-Miocene age; Kemmerling (in Hetzel 1930) simply described the rocks as Neogene; Musper (in Hetzel 1930), in contrast, noted that a Neogene age has not been proved and that the rocks could be pre-Neogene.

Koswara *et al.* (1991) map nearly all Tanahjampea and Tanahmalala as covered by granitic rocks, and suggested an Early-Middle Miocene age, based on correlation with the granitic rocks of South Sulawesi.

9.2.4.4 Kalao

Hetzel (1930) and van Bemmelen (1949) described the geology of Kalao, and this section is based on their work.

The island consists primarily of uplifted coral reefs, and the basement consists partly of andesite and possibly basaltic rocks. In the west, andesite was overlain by reef limestone, and on the east side it is overlain by Tertiary massive tuffs and tuffaceous sandstones alternating with Globigerina limestone. It is considered to be of post-Lepidocyclina age (young Neogene). The Tertiary sediments dip about 40° to the southwest.

Koswara *et al.* (1991) described the presence of ophiolite on the north coast in fault contact with the Walanai Formation, which consists of conglomerate, sandstone, tuff, calcareous tuff, clay and marl. On the west coast there is an intrusion of granite.

9.2.4.5 Kepulauan Macan (Tiger Islands)

These islands were not visited. They consist of a group of about twenty small islands built from coral debris on a large complex reef. The reef occupies a roughly elliptical area about 75 km long and 40 km wide.

Geological information on these islands has been provided by Hetzel (1930). Mollengraff (in Hetzel 1930) suggested that this largest reef complex in the Indonesian archipelago was formed by sea level changes during the Pleistocene. In contrast, Rutten (in Hetzel 1930) suggested that subsidence has been of tectonic origin. Keunen (in Hetzel 1930) combined both views by proposing that Kepulauan Macan (and P. Tukang Besi) were already in existence as reefs before the Pleistocene, when former land area subsided, and that during the sea level fall in the Pleistocene the edges were abraded and any lagoons were completely filled. The reef owes its present form to later sea level rise. However, Hetzel (1930) disagreed with these three views, arguing that seen from the west and the south, the islands show signs of young uplift and that one would expect tectonic control to be important in the forming the reefs.

9.2.5 Geological observation on the Flores Sea Islands

9.2.5.1 Selayar

Geological observations made at this island, along gravity stations GS 003 to GS 014 (Fig.9.4) were predominantly of coarse volcanogenic sandstone. However, locally reef carbonates were present. The island is mountainous with ridges which are assumed to be formed by a series of west dipping normal faults.

9.2.5.2 Kajuadi

The island was visited during the gravity survey. There are four gravity stations (Fig.9.5), three along the west coast from north to south, GS 072, GS 074, GS 073 and one (GS 075) in the centre of the island. Of the four stations, geological exposure was present only at GS 075, consisting of reef carbonate.

9.2.5.3 Tanahjampea and Tanahmalala

Mapping carried out following the gravity survey showed that the rocks exposed are mainly granite, granodiorite, diorite, andesite, basalt and rhyolite. In some areas igneous

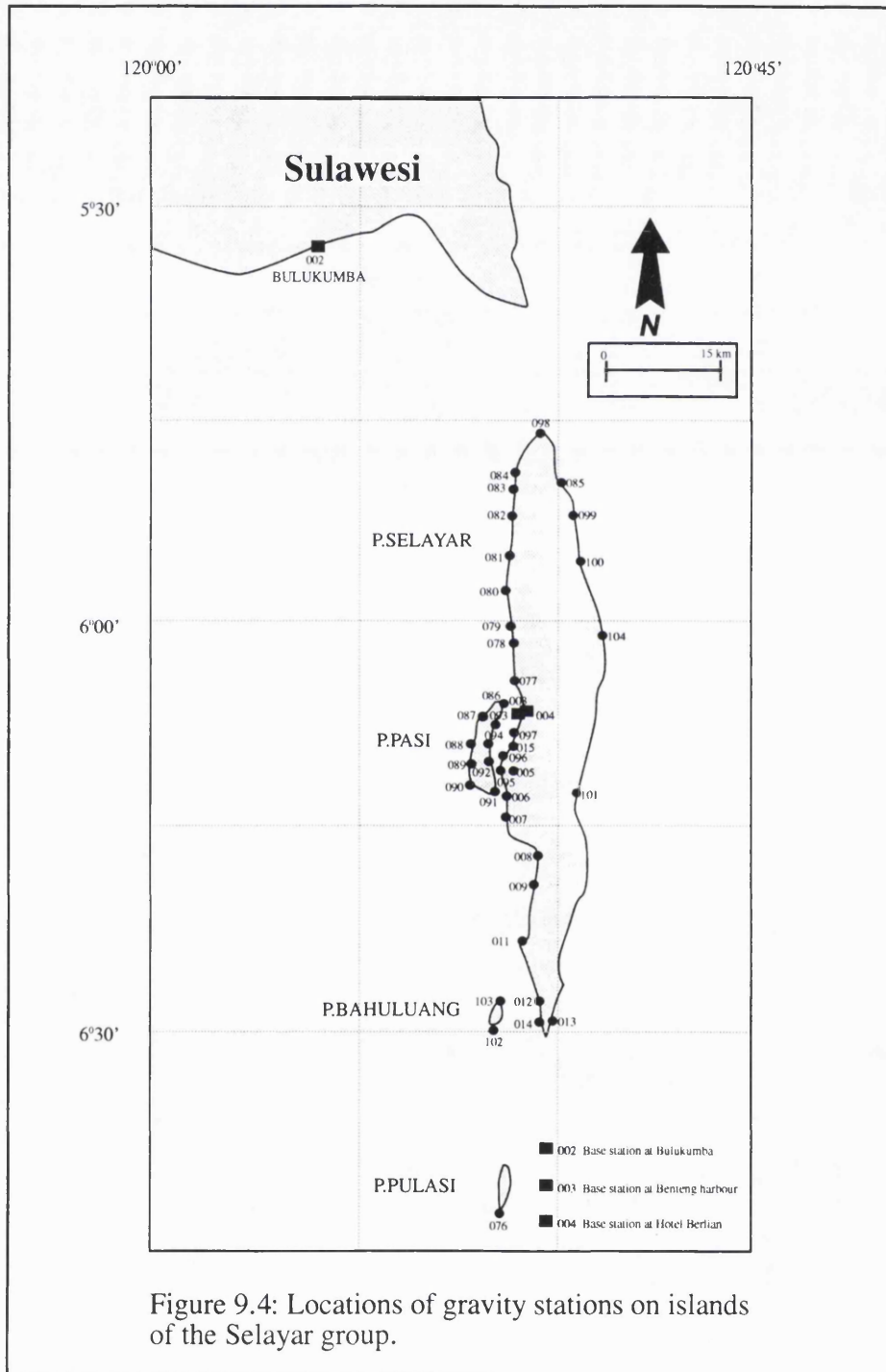


Figure 9.4: Locations of gravity stations on islands of the Selayar group.

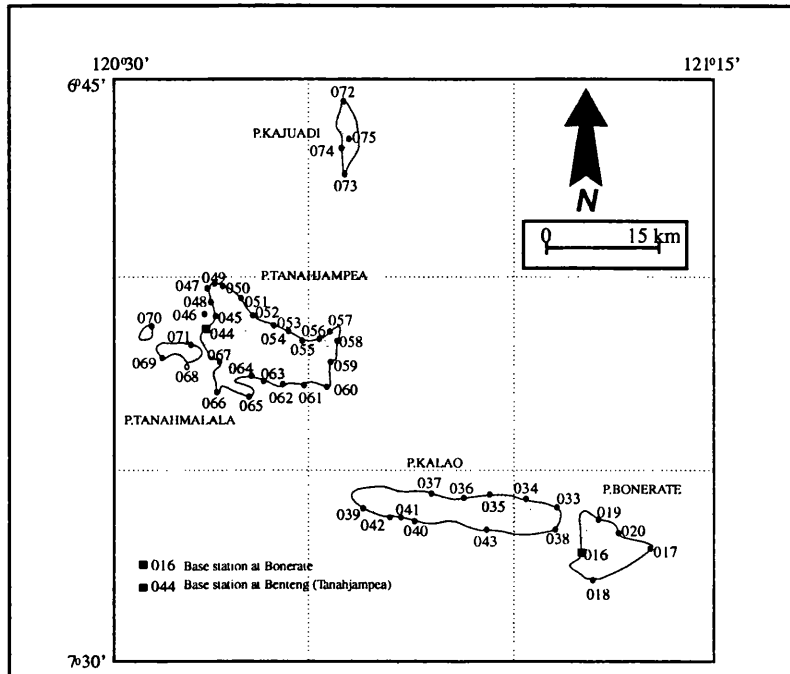


Figure 9.5a: Locations of gravity stations on islands of the Bonerate group

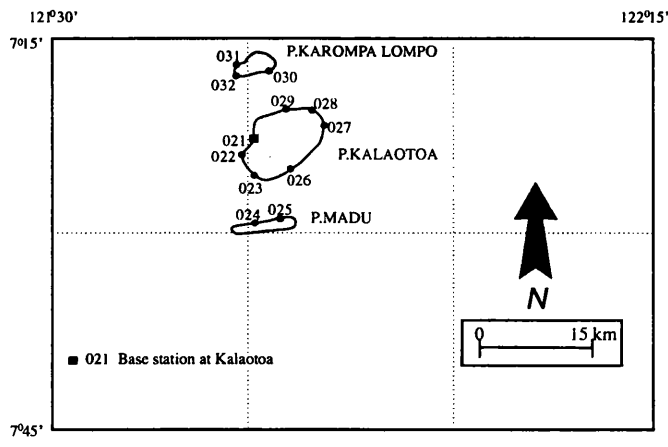


Figure 9.5b: Locations of gravity stations on islands of the Kalaotoa group

rocks are covered by volcanic breccia and carbonate rocks. The geological map of Tanahjampea and Tanahmalala is shown in Fig. 9.6 and the reconnaissance geological mapping are described below.

9.2.5.3.1 Old volcanic breccia

Observed in Kampung Tengah at gravity station GS 065 where it is unconformably overlaid by bioclastic limestone (Photo. 9.1). The base of the formation was not found and contact with granitic rocks was not seen.

Description - This unit consists of dark-brownish, grain-supported volcanic breccia, with poorly sorted, angular to subangular, coarse sand-pebble size clasts of basalt and andesite in a calcareous and tuffaceous sandstone matrix.

Interpretation - This unit is interpreted to be deposited in the shallow marine environment and marks the activity of volcanism.

Correlation and age - This unit was not mapped and described in the preliminary geological map of Koswara *et al.* 1991. The age of this unit is not known.

9.2.5.3.2 Bioclastic limestone

The rock was observed at Tanjung Kanpe, Kampung Tengah and Pulau Janggut. It is well bedded and jointed extensively. Joints are infilled with calcite and sulphide (Photo.9.2). The bedding attitude is N132E/57.

Description - This bioclastic limestone is partly altered to crystalline limestone. It is yellow-brownish, massive and hard, and contains medium to very coarse grained, poorly sorted, angular fragments of coral and fossils, and calcite veins.

Microscopic analysis of the lower part of the formation (close to contact with old volcanic breccia at GS 065) reveals an interstitial calcisiltite matrix and skeletal fragments, approximately 30% of which consist of larger foraminifera, smaller benthic and planktic foraminifera, red algae, echinoderms and fragments of andesitic rock. Stylolite structures were present, indicating compaction to various burial depth (Flugel

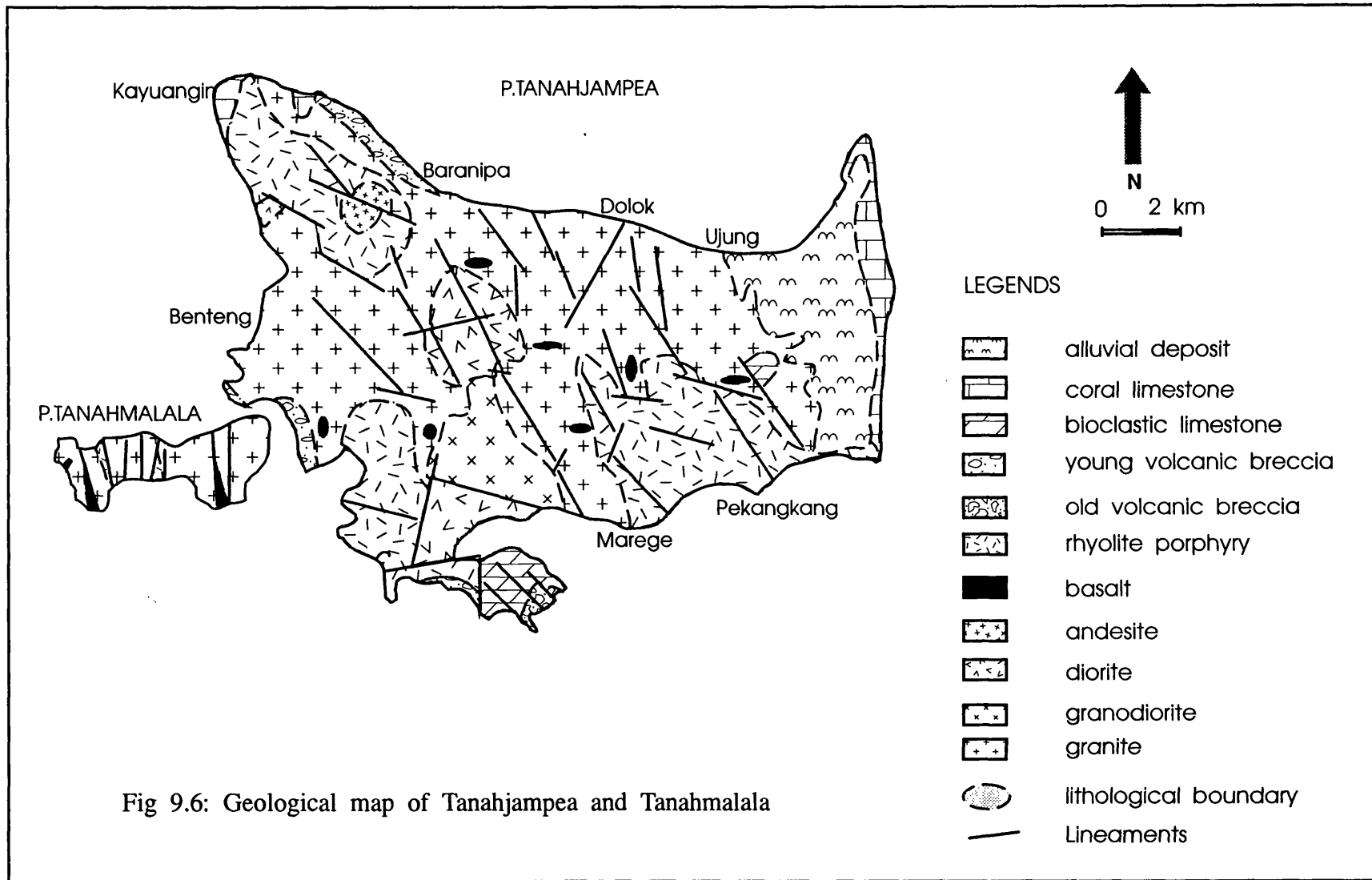


Fig 9.6: Geological map of Tanahjampea and Tanahmalala

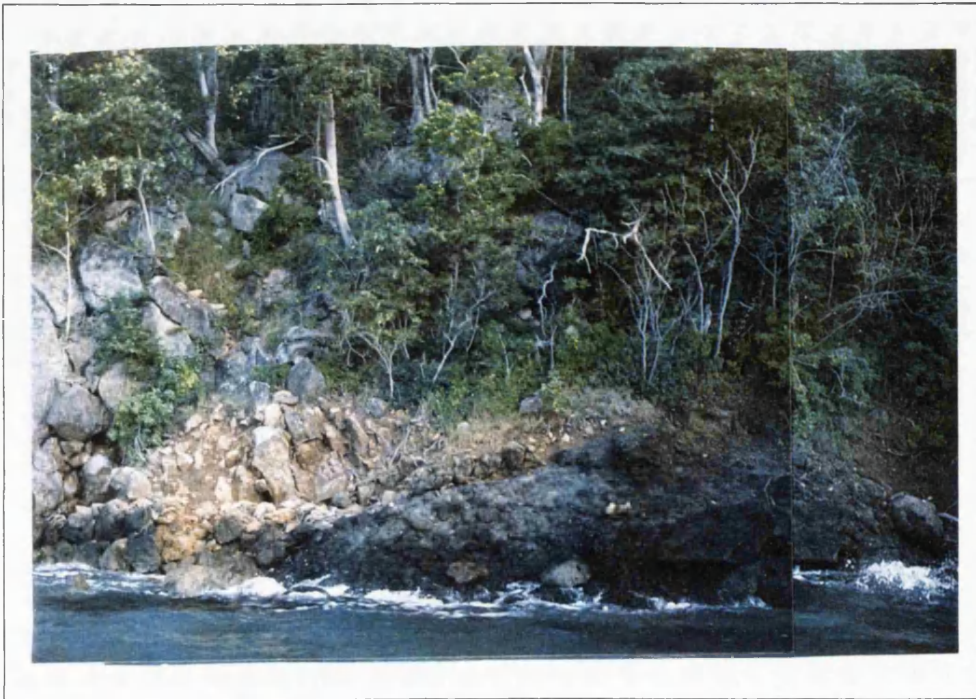


Photo 9.1: Outcrop showing unconformable contact between old volcanic breccia and bioclastic limestone

Location: GS 065

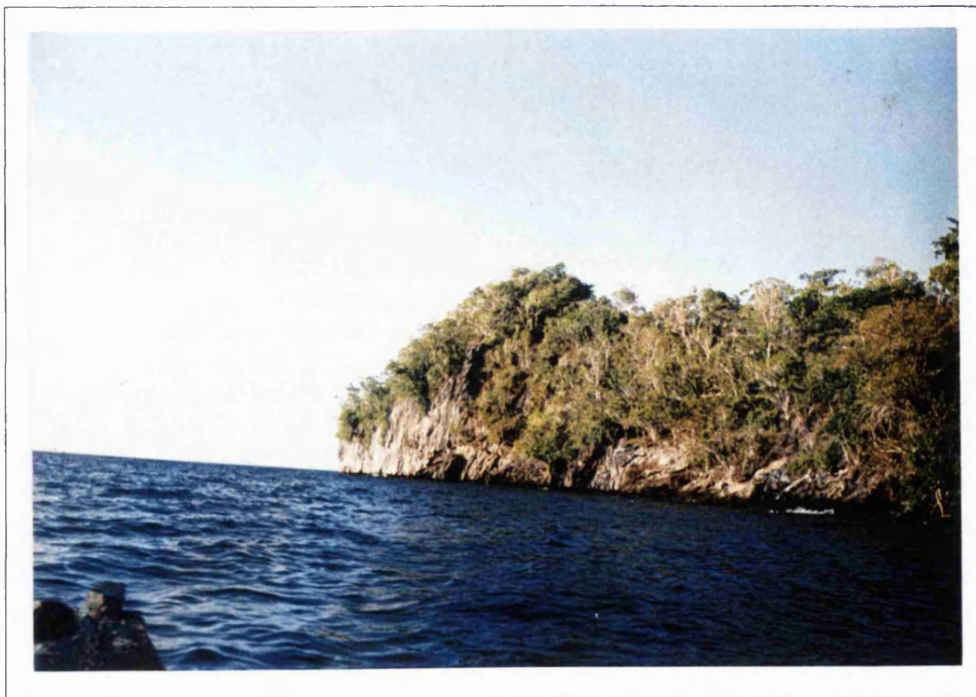


Photo 9.2: Outcrop of bioclastic limestone with extensive vertical joints

Location: GS 065

1982). This type of rock can be classified as a wackestone-packstone (Dunham 1960). In the upper part of the formation, the coral has recrystallised to pseudospar. This type of rock can be classified as coral boundstone (Dunham 1962).

Interpretation - In the lower part of this limestone, the diversity of biota and the presence of large numbers of planktic and benthic foraminifera indicate deposition in a shallow open marine environment near the fore-slope (Ascaria, pers. comm., 1994). The presence of large foraminifera (*Lepidocyclina*) indicates a fore-reef position (Spencer, pers. comm., 1994).

The wackestone texture and the occurrence of whole bioclasts with minimal abrasion suggests deposition in a generally low energy environment. Moderate to fair sorting suggest fluctuating energy levels, but a predominantly low energy environment. The high percentage of micrite indicates current reworking in low energy conditions, where wave/current activity was weak enough to allow the accumulation of fine grained muds.

In the upper part, the occurrence of subangular fragments of corals suggests proximity to a reefal complex and high energy conditions resulting in mechanical destruction of the reef by waves and tides. The facies difference between the lower and upper parts of the formation indicate the progradation of the slope seawards.

In thin section, post sedimentation tectonic activity was recorded by fractures filled with calcite and the offset of some large foraminifera, and the presence of stylolite structure.

Correlation and age - This limestone can be correlated with the Batu Formation of Koswara *et al.* (1993), the type locality of which is on Batu Island, a small island 15 km north of Ujung Village. Micropaleontological analysis indicates Oligocene to Late Miocene age (Koswara *et al.* 1993).

9.2.5.3.3 Igneous rocks

1. Granite

Granitic and associated rhyolitic rocks cover nearly 70% of the Tanahjampea and Tanahmalala. The rocks commonly show very extensive fracturing or jointing in NE-

SW and NW-SE directions (Photo.9.3). Basalt and andesite commonly fill fractures as dykes, ranging from a few centimetres to two metres in thickness.

The granitic rocks can be largely divided into three types: biotite granite, hornblende granite and microgranite.

- Biotite Granite

This is mainly exposed in the northern part of Tanahjampea, and good outcrops were seen at Dolok, Bonalambere and Ujung.

Description - Light grey, porphyritic, holocrystalline, medium-coarse to very coarse and massive. Contains biotite (both as phenocryst and matrix), feldspar and quartz.

- Hornblende Granite Porphyry

This rock is dominant on Tanahmalala and around, Benteng and Mangati. Feldspar phenocrysts up to 1 cm long show strong orientation. On Tanahmalala, there are xenoliths of diorite in the granite at some locations e.g. at GS 069 (Photo.9.4).

Description - Grey-pinkish, porphyritic, medium to very coarse grained and massive. Contains feldspar and hornblende (as phenocrysts and matrix), biotite and quartz.

- Microgranite

This rock is predominant in the south of Tanahjampea. Good exposures were seen at Marege, Binanga Baka and Aerompa.

Description - Light grey, holocrystalline, medium grained size, compact. Contains biotite, plagioclase, feldspar, quartz and minor pyrite.

2. Granodiorite

This rock is exposed at Kampung Tengah and Binangabaka and is considered to be the more basic equivalent of the granite.

Description - Dark grey, holocrystalline, fine to medium grained and massive. Contains hornblende, biotite, feldspar and rare quartz.

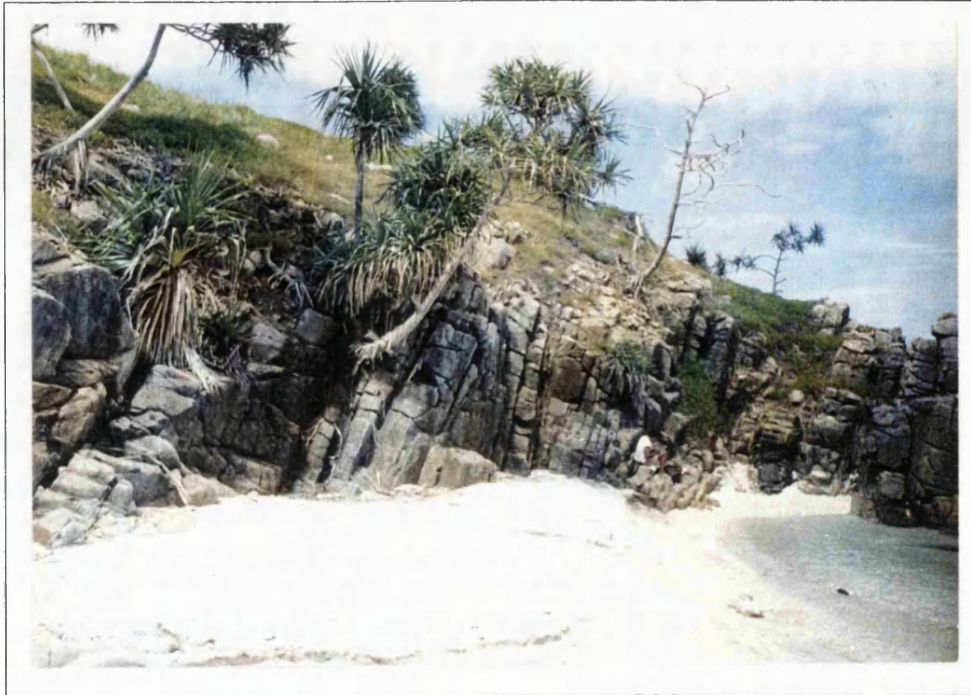


Photo 9.3: Outcrop of granite showing very extensive vertical joints, which was intruded by andesite as dykes
Location: GS 068

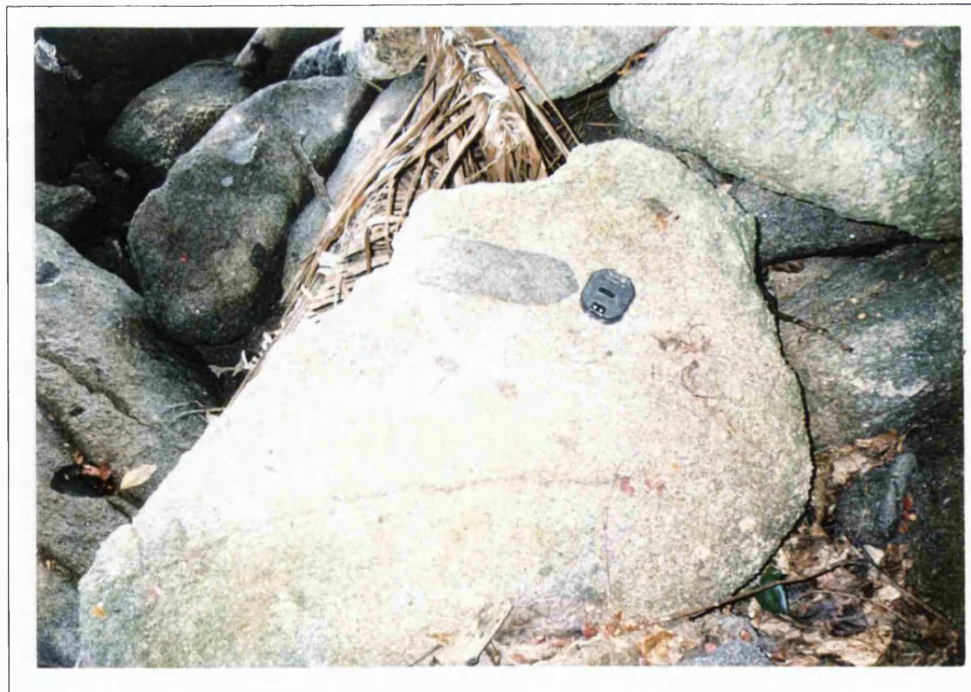


Photo 9.4: Diorite xenoliths within the granite
Location: GS 069

3. Diorite

These rocks were found at Bonelambere, Doda and Kampung Tengah. No contact with granite has been observed in the field, but its distribution suggests that the diorite intrudes the granite.

Description - Grey, holocrystalline, medium to coarse grained, porphyritic texture and massive. Contains pyroxene, biotite, alkali feldspar, plagioclase and quartz.

4. Basalt - Andesite

These rocks occur as dykes and sills in the granitic and rhyolitic rocks, filling fractures ranging from a few centimetres to a few metres in width. Good outcrops are seen at GS 069 and GS 050. At GS 069, five sheets of basaltic dykes occur within a distance of about 50 m with attitudes from N325°E/85° to N350°E/80°.

Description - Basalt: dark green to blackish (dark brown on weathered surface), aphyric.

Andesite: grey-black, feldspar-phyric, medium-coarse grain, massive. Contains pyroxene, feldspar, ore minerals (in some places) and biotite.

5. Porphyritic Rhyolite

This rock was seen at Aerompa, Binangabaka, Pekangkang, Kampung Tengah, Doda and Tanahmalala, apparently occurring as lava flows or dykes. It is usually associated with tuff. In Batusobo, on the south coast, at GS 066 the rocks are layered, with layering directions of N80°E/53° and N100°E/65°. Locally the sequence is folded with attitudes of the flanks of N310°E/35° and N105°E/49° (Photo. 9.5). Folding is tectonic, characterised by fracturing or jointing. In some parts, porphyritic rhyolite is intruded by basalt.

Description - Porphyritic rhyolite: Light grey, fine to coarse phenocrysts. Contains plagioclase and biotite (as phenocrysts and matrix), quartz and glass.

Welded Tuff: yellowish-pink, fine to medium grained and massive.

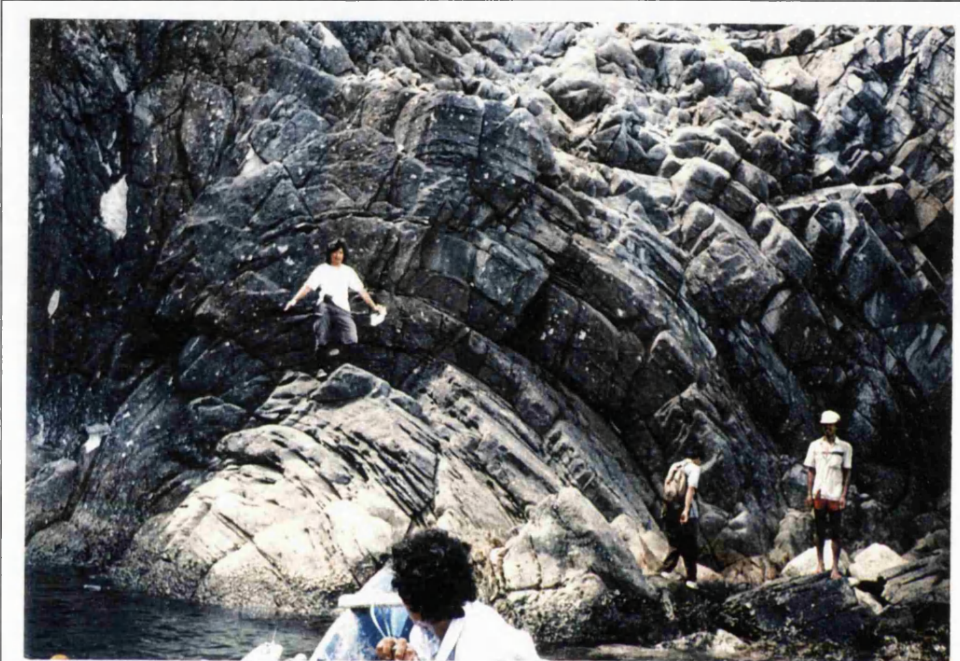


Photo 9.5: Outcrop of rhyolite showing layerings, jointings and foldings
Location: GS 066 (Tanahjampea Island)

Interpretation of igneous rocks on Tanahjampea

The granitic rocks of Tanahjampea and Tanahmalala consist of calc-alkaline and alkaline assemblage (Hetzl 1930). Commonly, calc-alkaline rocks are associated with subduction-derived magma and alkaline rocks with extensional processes. This leads to the conclusion that the island is part of a magmatic arc related to an active subduction zone represented by granitic and associated rhyolitic rocks. The alkaline rocks resulting from extensional process are interpreted to be younger than the granitic volcanism, and are represented by andesitic and basaltic rocks as dykes and sills.

Stratigraphy, age and correlation

Contacts between the granitic and other rocks have not been seen in the field. However, the presence of xenoliths of dioritic rocks, which probably belong to old volcanic breccia in the granitic rocks, as found in some parts in Tanahmalala and Tanahjampea, suggests that the granitic rocks intruded the old volcanic breccia.

In a granitic batholith, it is usual to find finer grained phases along the contact with host rocks as the molten magma has cooled more rapidly by contact with the surrounding wall. Since the granitic rocks of Tanahjampea and Tanahmalala can be divided into biotite granite (exposed in the north of the islands), hornblende granite (exposed in the west of the islands) and micro granite (exposed in the south of the islands), it is likely that boundaries of the intrusion is in the south, where the old volcanic breccia and bioclastic limestone are exposed.

The associated mineralogies of granite and monzonite in Tanahjampea and Tanahmalala are similar to those of South Sulawesi (Koswara, pers. comm., 1993). It is, therefore, suggested that Tanahjampea and Tanahmalala are part of the western arc of Sulawesi or Western Sulawesi Plutono Volcanic Belt (see Chapter 5, section 5.3). The intrusive could have the same age as similar rocks elsewhere in the belt, i.e. Early - Middle Miocene.

Basalt and andesite intrude through all the above units. The age of this volcanism is thought to be Plio - Pleistocene, which was the time of the last tectonic event in the Southwest Sulawesi (van Leeuwen, 1981) and the time of major tectonic activity on the

Walanae Fault. This dating is supported by similar orientations of the Walanae Fault and intrusions of basalt and andesite.

9.2.5.3.4 Young volcanic breccia

This rock is distributed in western and northern Tanahjampea (Mangati, Kampung Tengah and Kayu Angin). In general, this unit forms rugged mountains and steep cliffs with good exposures. At GS 050 and GS 067, it consists of intercalations of volcanic breccia and vitric tuff (Photo. 9.6). Calcite and silica veins are common in the outcrops.

Description - The volcanic breccia is dark-brownish, grain-supported breccia with poorly sorted, angular to sub angular, coarse sand to pebble size clasts of basalt and andesite in a tuffaceous and calcareous sandstone matrix.

Interpretation - The presence of calcareous matrix and extensive calcite veins in the rocks is interpreted to be deposited in marine environment. The intercalation of volcanic breccia and vitric tuff may be as a result of sediment gravity flows.

Correlation and age - In the area where this rock is exposed it was mapped as Middle Miocene Kajuadi Formation (Koswara *et al.* 1991). However, field observation (see Photo 9.6) is more likely to interpret this rock as young volcanics of probably Pliocene age where it marked the last volcanic event in South Sulawesi (van Leeuwen 1981).

9.2.5.3.5 Coral limestone

Exposed along the east coast of Tanahjampea as terraces. Well lithified and locally crystalline. The thickness is about 7m. The base of this unit was not seen in the field.

Description - White-cream, compact and massive, It consisting of corals, shells and fossil fragments.

Interpretation - This coral is interpreted as uplifted coral limestone of Quaternary age.



Photo 9.6: Outcrops showing intercalation between volcanic breccia and tuff with extensive calcite veins
Location: GS 067 (Tanahjampea Island)

Correlation and age - On the basis of its stratigraphical position, this coral is the youngest formation on the islands. This coral can be correlated to the other coral reef in the Flores Sea Islands, and the age of this rock is thought to be Quaternary.

9.2.5.4 Kalao

The gravity survey on Kalao consisted of four stations on the south coast, four stations on the north coast and a single station at Lambego village on the east coast. The latter station was occupied at night and no geological observations could be made. On the north coast the geological party remained close to the site of the first gravity station, in an area mapped as underlain by ophiolite, whilst gravity readings were taken further along the coast. A stream section running inland for a distance of 2 km was logged and coastal exposures were examined. On the south coast the rocks in the vicinity of the three gravity stations near to the western end of the island were briefly examined; the fourth station, in the central part of the south coast, was established on the fringing reef, which dries at low tide. The region of acid igneous rocks in the extreme western part of the island was not visited. A modified geological map of Kalao can be seen in Fig. 9.7.

The rocks seen in this observation belong to two groups;

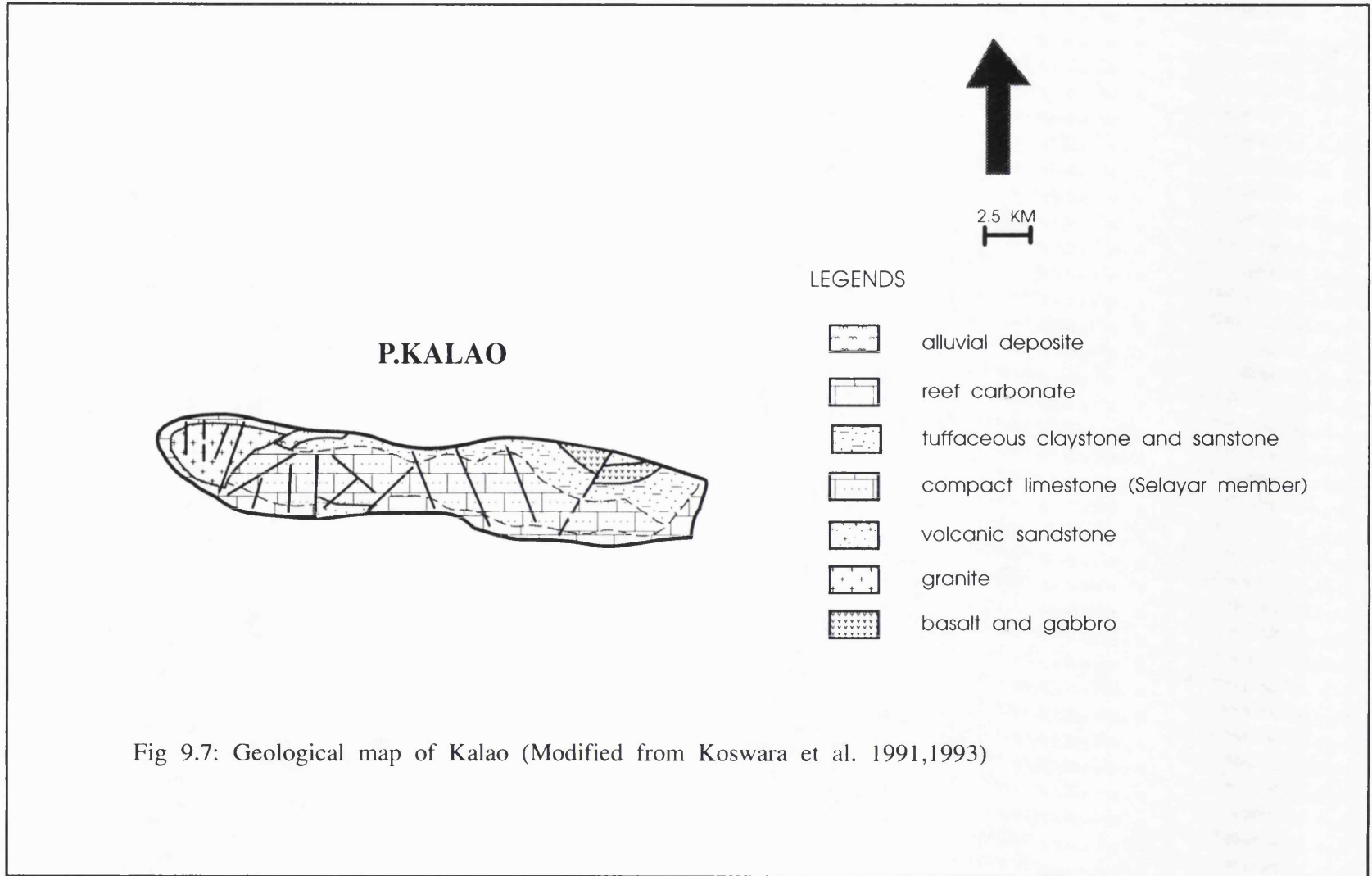
1. Ophiolitic rocks
2. Sedimentary rocks

9.2.5.4.1 Ophiolitic rocks

This group was observed inland over a distance of about 2 km southeast from gravity station GS 034 on the north coast. The stream section is seen in Fig. 9.8, through extensively weathered gabbro and basalt, although locally there are fresh surfaces. The basalt is stratigraphically above the gabbro and some fresh outcrops show very extensive deformation, brecciation (fault-gouge) and jointing. Bearings measured on brecciation in the basalt are trending in WNW.

Description - Gabbro: dark green to black, holocrystalline, medium-coarse grained. Composed primarily of pyroxene and plagioclase.

Basalt: dark brown-black, aphyric, fine grained.



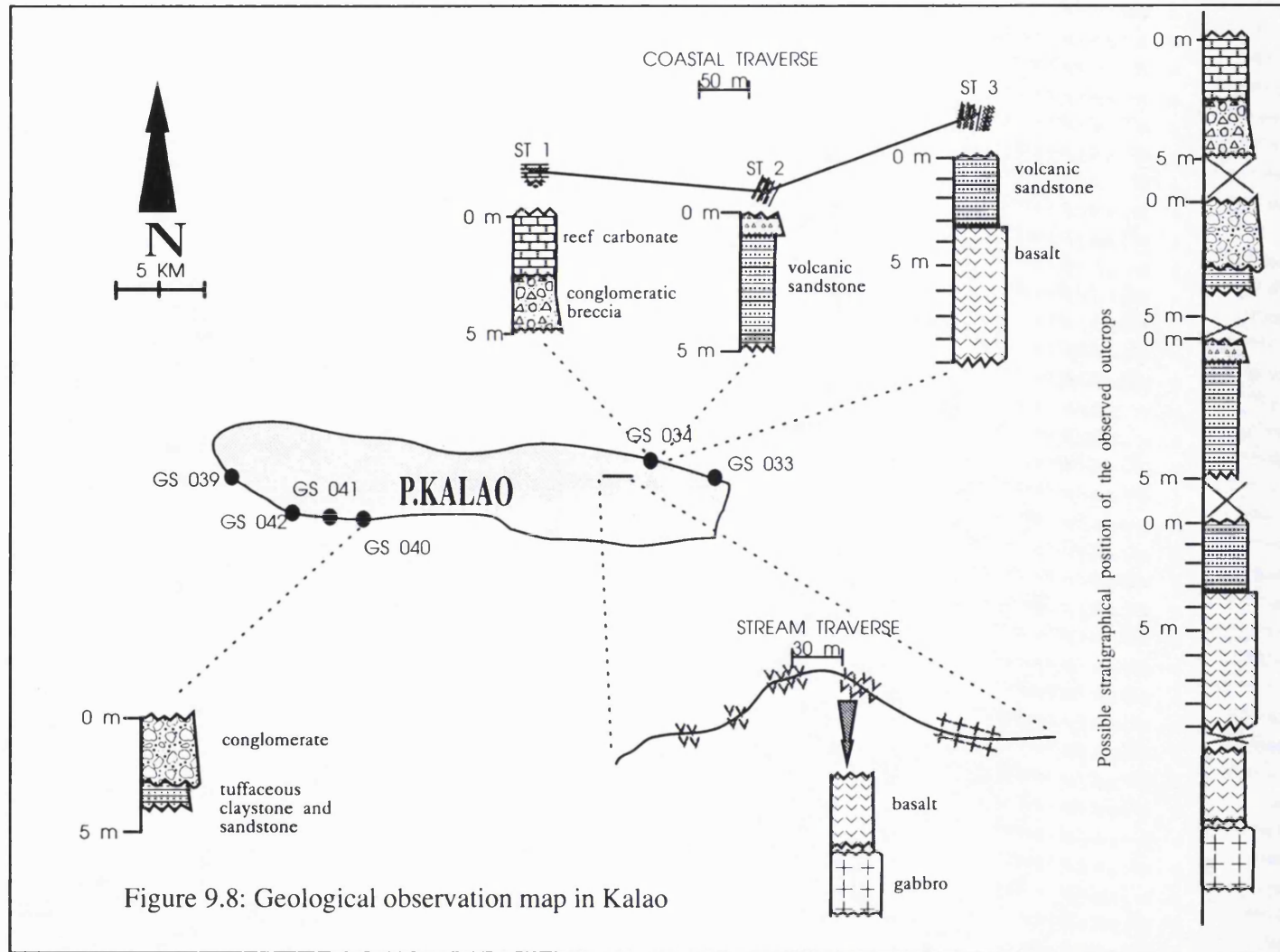


Figure 9.8: Geological observation map in Kalao

Interpretation - In the field, rocks of this unit are extensively weathered and jointing. Brecciation was also found in nearly all fresh outcrops of basalt. These observations may indicate that the emplacement of this unit was associated with intensive fault activity.

Stratigraphy and age - The base and top of this unit were not seen, but this rock unit is considered as the oldest exposed not only on Kalao but also in the Flores Sea Islands. The age is not known.

9.2.5.4.2 Sedimentary rocks

These rocks consist of volcanoclastic sandstone, tuffaceous sandstone, conglomerate, conglomeratic breccia and coral limestone.

Volcanoclastic sandstone

This was observed as coastal exposures on the south coast at GS 040 and on the north coast about 200 m to the east of GS 034 at observation point St 2 and St 3 (see Fig. 9.7). At St. 2 the outcrop was affected by minor normal faults, with displacement about 10 cm. The directions of fault planes are N164°E/76° & N145°E/25° (Photo.9.7), with conjugate shear and extension joint. The attitudes of the shear joint are in NE-SW and NW-SE. The directions of extension joints are in E-W to NW-SE. The bedding attitudes of the outcrop are N90°E/64° and N100°E/64°, and the thickness is about 6m. At St. 3 there is a fault contact (attitude of N90°E/65°). The rock consists of volcanoclastic sandstone and volcanic breccia. The base and top of the formation were not seen in the field. At St 3, the rocks are in fault contact with basalt.

Description - It is grey-brownish, friable, fine-very coarse grained. Grains are angular-subangular with poor-moderate sorting and comprise volcanic lithic fragments, mafic minerals of pyroxene and amphibole, plagioclase and iron ore. The beds are parallel laminated on a cm scale. Microscopic analysis reveals the presence of alteration minerals (pumpellyite and zeolite) replacing the matrix and filling veins.

Stratigraphically above the volcanoclastic sandstone is a grain-supported volcanic breccia which is lithologically similar to the sandstone, with coarse sand to pebble-size clasts in a sandy matrix. A 0.3 m bed of volcanic breccia has graded bedding structure.



Photo 9.7: Outcrop of volcanic sandstone showing minor faults and joints
Location: Gravity Station 034 (St. 02, Kalao Island)



Photo 9.8: Outcrop of conglomerate clast and intercalation between tuffaceous sandstone and claystone showing irregular contact
Location: Gravity station 040 (Kalao Island)

Interpretation - The immature texture of this sequence indicates short transportation and possibly rapid deposition under unstable conditions. The composition suggests that it was derived from volcanic rocks. It is difficult to interpret the depositional setting of these rocks, due to the limited exposure but it might represent a deep marine environment where turbidite with Ta and Tb interval deposited). The presence of secondary minerals (pumpellyite and zeolite) indicates that these rocks have been affected by low-temperature, low-pressure metamorphism, possibly due to burial (Malaihollo, pers. comm., 1994).

The bedding directions, faults and joints suggest the compression in N-S direction, and this is in contrast to the major stress in SW Sulawesi, Selayar and Tanahjampea which is in E-W direction.

Correlation and age - This rock was not described and mapped by Koswara *et al.* (1991) in their preliminary geological map, and the age is not known. The rocks have steeper dips, with more extensive deformation than any other sedimentary rocks in the region and may therefore be older than any of the other sedimentary rocks exposed on the island.

Tuffaceous sandstone

At GS 040, there is an irregular contact between polymict conglomerate and a sequence of alternating tuffaceous claystones and sandstones (5 - 15 cm) (Photo.9.8). The rocks are rather friable, so therefore very difficult to sample. The bedding direction is N138E/17 and N134E/15. The base and top of this unit are not seen.

Description - Tuffaceous claystone; white-cream and contains abundant foraminifera. Tuffaceous sandstone: grey-white, medium grained, moderately sorted, angular grains of tuff, mafic minerals, feldspar and quartz. Contains cm-scale parallel lamination. Conglomerate: grey-dark, matrix supported, very poorly sorted, subrounded-subangular, coarse sand to pebble size clasts (1 cm - 35 cm in diameter) of coral limestone, basalt, gabbro, claystone and sandstone. Matrix is fine to coarse grained sandstone.

Interpretation - The presence of facies A1.1 (disorganized gravel) and C2.3 (thin bedded sand-mud couplet) of Pickering *et al.* (1989) in the sedimentary structures is interpreted as a turbidity current deposit. According to Pickering *et al.* (1989), facies A1.1 demonstrates transport by high concentration turbidity currents or debris flows, followed by 'freezing' on decreasing bottom slopes due to intergranular friction and cohesion. Facies C2.3 indicates deposition from relatively dilute currents. The facies analyses indicate deposition by intermediate turbidity currents which dissipated their energy as they traveled down slope.

Correlation and age - Based on the similarities in lithological characteristics, this rock unit can be correlated with the Middle Miocene Kalao Formation described by Koswara *et al.* (1991). However, in the location where this rock exposed it was not mapped as Kalao Formation, it was mapped as coral limestone unit. Tuffaceous claystone at ST 40 has been described by GRDC (Table 9.1) as containing *Globorotalia merotumida*, *Globigerinoides canimarensi*, *Globorotalia plesiotumida*, *Hastigerina aequilaterallis* and *Sphaeridinella subdehiscens*. These fossils indicate that the age is N17-N18 (Miocene-Pliocene).

Conglomeratic breccia

This rock is exposed at low tide near St.3 over an area about 8m long and 5m wide. It is unconformably overlain by coral limestone.

Description - Grey-dark in colour, very poorly sorted and displaying a chaotic fabric, clast-supported, grain size very coarse sand to pebble (1 - 15 cm), subangular and subrounded. Fragments of basalt and basaltic scoria occur in tuffaceous and calcareous sandstone matrixes.

Interpretation - This rock is interpreted to be deposited in a shallow marine environment.

Correlation and age - On the basis of lithology, this rock is similar to the young volcanic breccia on Tanahjampea. The age is not known.

Coral limestone

Coral limestone was mainly observed along southeast and south coast of Kalao. According to Hetzel (1930) on the south coast of Kalao it consists of 11 terraces.

Description - White-yellowish, massive and hard coral reefs.

Interpretation - This unit is interpreted as carbonate reef deposited in a shallow water environment.

Correlation and age - This coral can be correlated with all the coral limestones in the Flores Sea Islands and probably up to the SW Sulawesi. The age is probably of Quaternary.

9.2.5.5 Bonerate

There are five gravity stations on this island (Fig. 9.9a); one on the west coast (GS 016), one on the east coast (GS 017), one on the south coast (GS 018) and two on the north coast (GS 019 and GS 020). Geological observations were made at every gravity station and also on the traverses from GS 016 (the local base) to the other gravity stations. All the rocks seen were coral limestone. At GS 20 the upper part of the limestone shows horizontal laminations. The thickness of this unit is about 7m at the gravity stations. A modified geological map of Bonerate is shown as Fig. 9.9b.

Description - Coral limestone; white-yellowish, massive and hard coral limestone containing coral and other fossil fragments and calcite

Interpretation - These coral limestone are probably recently elevated reefs.

Correlation and age - This coral can be correlated to the all coral limestones in the Flores Sea Islands and probably to SW Sulawesi. The age is probably of Quaternary.

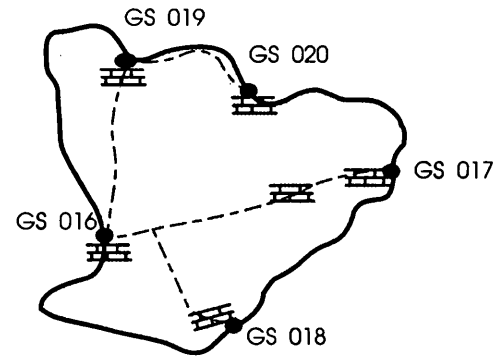
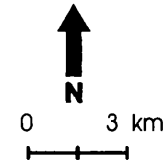


Figure 9.9a : Traverse map in Bonerate



LEGENDS

-  coral limestone
-  bioclastic limestone
-  coral limestone
-  GS 016 gravity station
-  traverse

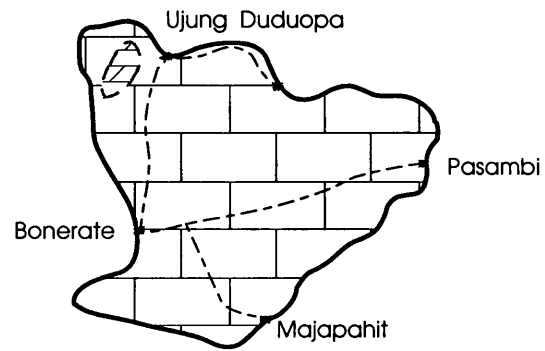


Figure 9.9b: Geological map of Bonerate (Modified from Koswara et al. 1991;1993)

9.2.5.6 Kalaotoa

In Kalaotoa there are six gravity stations around the island (Fig. 9.10a). Geological observation was carried out on a one-day geological traverse from Buranga to Latodo, Goraupa and back to Buranga.

Outcrops of coral limestone and sandy limestone were seen in some locations, however the quality was poor because of extensive weathering. Koswara *et al.* (1991;1993) reported that ophiolitic rocks are exposed on the beach in the Latodo area on the east coast, and these are shown on the preliminary geological map as occurring widely throughout southern Kalaotoa. However, observations made in the course of the current survey indicate that ophiolitic rocks do not extend far inland. A modified geological map of Kalaotoa can be seen in Fig. 9.10b.

Description - Coral limestone: white-yellowish, massive and hard, containing coral and other fossil fragments and calcite.

Interpretation - They are interpreted as uplifted coral limestone of Quaternary age. Van Bemmelen (1949) noted that on Kalaotoa elevated coral reefs are found at heights of up to 518 m.

Correlation and age - These limestones are similar to coral limestone as seen on other islands on the Flores Sea Islands, and is interpreted as Quaternary age.

Description - Sandy limestone; white-yellowish, massive and compact containing poorly sorted, subangular, medium-coarse grains of fossil fragments, calcite and quartz.

Interpretation - The texture of the rocks is immature, suggesting that the deposition was not far from the source in a shallow marine environment.

Correlation and age - In the locations where these rocks exposed, Koswara *et al.* (1993) mapped them as Selayar Limestone, a member of Walanae Formation. They suggested the age of this member is Middle-Upper Miocene.

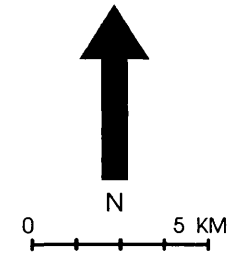
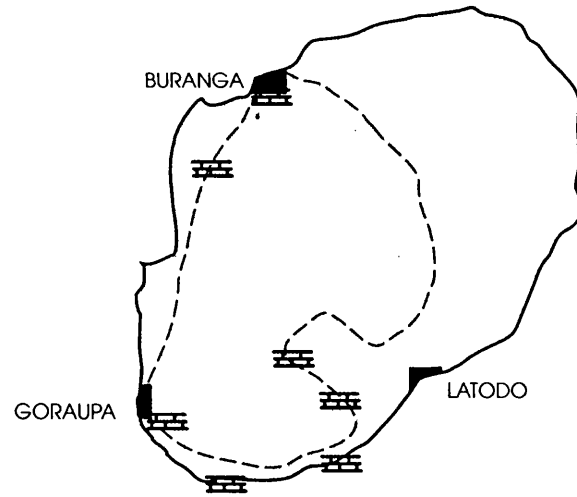
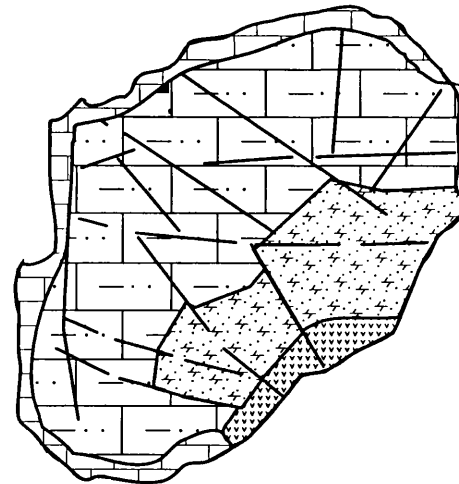


Figure 9.10a :Traverse map in Kalaotoa



LEGENDS

-  corral limestone
-  sandy limestone and marl
-  tuffaceous sandstone and marl
-  basalt

Figure 9.10b: Geological map of Kalaotoa (Modified from Koswara et al. 1991;1993)

9.2.5.7 Summary of stratigraphy of the Flores Sea islands

In this section, the stratigraphy and tectonic aspects of the Flores Sea Islands are summarised. There is, however, a considerable lack of detailed information in published literature. The summary of the stratigraphy of the Flores Sea Islands (Fig.9.11) is correlated to the stratigraphy in SW Sulawesi. To some extent, there are similarities in the stratigraphical sequences between the Flores Sea Islands and SW Sulawesi as summarised by van Bemmelen (1949) and van Leeuwen (1981, see Fig. 9.3). All rocks exposed provide evidence for extensive volcanic and tectonic activity since the Eocene, making plausible a tectonic link between SW Sulawesi and the Flores Sea Islands.

The oldest rocks present are thought to be ophiolites consisting of gabbro and basalt. These are known from Tambolongan, Pulasi, Madu, Kalao and Kalaotoa islands (Koswara *et al.* 1991;1993). The ophiolite is extensively brecciated and jointed, and the age is not known. The simplest explanation is that they may be related to the Cretaceous ophiolitic rocks in SW Sulawesi where the emplacement is very complicated and poorly understood. Parkinson (1991) suggested the emplacement took place in the Oligocene when East Sulawesi collided with West Sulawesi, whereas Silver *et al.* (1981) suggested the emplacement took place in the Middle Miocene when Banggai Sula Microcontinent collided with East Sulawesi. Another alternative is that the ophiolite may be associated with thrust fault activities during the Neogene due to the collision of the northern margin of the Australian continent and the Banda Arc.

The old volcanic breccias probably correspond to the Eocene Langi Volcanic of SW Sulawesi. Their presence indicates that there may have been a west-dipping subduction zone to the east of this region. Therefore it is sensible to link SW Sulawesi and Selayar and Tanahjampea in the same Early Tertiary magmatic belt.

Unconformably above the old volcanic breccia is the bioclastic limestone. This relationship is also supported by the presence of andesitic fragment in the bioclastic limestone, indicating erosion of old volcanic breccia. It shows some similarities to the 'C' and 'D' members of Tonasa Limestone in SW Sulawesi, e.g. in the presence of andesitic fragments in the 'D' Member and the abundance planktic and benthic foraminifera and

AGE		LITHOLOGICAL UNITS	STRATIGRAPHICAL UNITS	IGNEOUS ROCKS	DESCRIPTION	
QUATERNARY	HOLOCENE	Alluvium		OPHIOLITE GRANITIC ROCKS DIORITE BASALT-ANDESITE	Granule, sand, silt, clay and mud	
		Coral Limestone			Coral limestone, massive and hard	
TERTIARY	PLEISTOCENE	Young volcanic breccia			intercalations of volcanic breccia and vitric tuff, calcite and silica veins are common	
		PLIOCENE	Tuffaceous sandstone and claystone			Volcanic sandstone, with lithic fragment grained
MIOCENE	LATE		Volcanic sandstone			Conglomerate and alternating tuffaceous claystone and sandstone
		MIDDLE	Sandy limestone			sandy limestone with coral fragments
			EARLY		Bioclastic limestone	
OLIGOCENE	?				HIATUS	
	EOCENE	Old volcanic breccia				volcanic breccia, poorly sorted, clasts of basalt and andesite in tuffaceous sandstone matrix
		PALEOCENE				
MESOZOIC	CRETACEOUS					

Figure 9.11: Summary of stratigraphy of the Flores Sea islands

large foraminifera (*Lepidocyclina* and *Cycloclypeous*) in the 'C' Member. The bottom of the bioclastic limestone was not seen.

In SW Sulawesi, the relationship between the Langi Volcanics and Tonasa Limestone is conformable (van Leeuwen 1981), but on Tanahjampea the contact between the old volcanic breccia (which corresponds to the Langi Volcanics) and the bioclastic limestone (corresponding to the 'C' and 'D' members of Tonasa Formation) is unconformable. This can be explained by noting that equivalents of the 'A' and 'B' members, which lie in the lower part of Tonasa Limestone, are not deposited on Tanahjampea. The occurrence of this bioclastic limestone can be correlated to a period of regional tectonism without igneous activity. This regional tectonism was recorded in this period in nearly all areas of the East Java Sea, causing widespread uplift and marine regression. The resulting structural high was covered by carbonate buildups in many part of the East Java Sea (Tyrrel *et al.* 1986). The highs later became source regions for carbonate deposition in the surrounding areas. In SW Sulawesi the correlated carbonate rock is known as the Tonasa Limestone Formation. The periods of uplift and formation of carbonate buildups in SW Sulawesi and Tanahjampea may coincide with the cessation of west-dipping subduction as there are no concurrent volcanic products.

An assemblage of plutonic and volcanic rocks ranging from granitic to rhyolitic was intruded as batholiths. No contact between these rocks and other rocks was seen in the field but the presence of dioritic xenoliths in granitic rocks in many parts in Tanahjampea and Tanahmalala indicate that the granitic rocks were intruded after the formation of the xenoliths, which are interpreted as belonging to the old volcanic breccia. Therefore the granitic rocks are Eocene or younger. The relationship with the bioclastic limestone is not known. The granitic rocks may be correlated to Lower-Middle Miocene granites in SW Sulawesi (Koswara, pers. comm., 1993) and/or to the granodioritic rocks of the Flores (van Bemmelen 1949). The presence of significant quantities of calc-alkaline and alkaline rocks as reported by Hetzel (1930) and associated granitoid plutons and volcanics in Tanahjampea and Tanahmalala suggest a subduction origin. Such rocks have also been found in SW Sulawesi (van Leeuwen 1981), pointing to a more or less continuous history of subduction along the east of SW Sulawesi and Tanahjampea and probably further southwards to the present Sumba

Fracture (south of Flores). The alkaline rocks have been interpreted as having formed later, during extension.

The culmination of volcanic activity in the Middle Miocene in SW Sulawesi is inferred by the Walanae depression separating the Western Divide Mountains and the Bone Mountain (van Bemmelen 1949). Van Bemmelen (1949) argued that the culmination of magmatic activity caused the collapse in the middle of the volcanic centres. On the physiographic map it appears that the Walanae Depression propagated southward flanked by two structural highs. The first extends from the Western Divide Mountain to Selayar and Tanahjampea, the second extends from the Bone Mountains to the Tiger islands and Kalaotoa. This tectonic process is suggested to control the lateral and vertical variation of facies in the proto Flores Sea Islands basin, in particular in the area between Tanahjampea and Kalaotoa where younger rocks are exposed.

The volcanoclastic sandstone with basaltic-andesitic fragments indicating derivation from volcanic sources and showing immature texture is interpreted to be deposited in the unstable conditions resulting from sediment gravity flows. Considering from the presence of Ta and Tb intervals of Bouma (1962), it was interpreted to be deposited in the upper slope. This unit can be correlated with the Walanae Formation in SW Sulawesi, which was deposited after the formation of the Walanae Depression. The next sediments to be deposited were tuffaceous sandstones and claystone consisting of resedimented conglomerates intercalated with sandstones and siltstones. These are also thought to represent turbidity current deposits in a deep marine basin.

The relationship with the older unit (volcanic sandstone) reveals a progradation of a turbidity sequence from upper fan to middle fan, perhaps as block-faulting became more intense.

The young volcanic breccia consists of volcanic tuff, breccia volcanic and conglomerate of andesitic and basaltic composition and might indicate volcanic activity in the Pleistocene. Van Bemmelen (1949) noted two major periods of uplift associated with volcanic activity in the South Arm of Sulawesi. The first took place in the Middle

Miocene, and was marked by granitic intrusions. The second took place in the Plio-Pleistocene, when the young volcanic breccia is thought to have been deposited.

Raised coral reefs found throughout the entire Flores Sea Islands region are considered the youngest rock unit, and are thought to mark global Quaternary tectonic uplift in Eastern Indonesia as a result of continuing collision between the Australian continental margin and the Banda Arc.

Hamilton (1979) suggested that the elevated young coral reefs on the islands of the Banda outer-arc ridge as evidence of rapid uplift resulting from the buoyancy effects of the light subducted sediments. Price and Audley-Charles (1987) proposed that rupture of the subducted Australian Plate in the Late Pliocene resulted in isostatic uplift (unflexing). On the Flores Sea islands, raised coral reefs form a number of terraces. Hetzel (1930) noted there are 11 terraces in Kalao. On Bonerate, it is estimated that coral reefs have been raised by up to 100 m. These data support the conclusion that at least since the Pleistocene the Flores Sea and its adjacent area have been subject to compression as a result of collision between northern margin Australian platform and Banda Arc. The continuous compressional stress of this collision caused periodic uplift, forming reef carbonate terraces in Eastern Indonesian region. Audley-Charles (1986) suggested uplift rates of 3 mm yr^{-1} for the Pliocene and 1.5 mm yr^{-1} for the Quaternary in Central Timor. Vita-Finzi and Syarif (1991), on the basis of paleontological analyses, proposed that during the Holocene the uplift rate on Timor decayed to a negligible level, and suggested that the 6 km of relief on Timor was attained largely by uplift during the early stages of collision.

9.3 GRAVITY SURVEY ON THE FLORES SEA ISLANDS

9.3.1 Introduction

9.3.1.1 Purpose of study

The purpose of the gravity survey was to provide data to constrain models of the crustal structure of the Flores Sea Islands and the more general Flores Sea area. Interpretation is itself constrained by geological observations made on the islands and by seismic data.

9.3.1.2 Location of gravity stations

The islands on which the gravity survey was conducted were, from north to southwest; the Selayar group (Selayar, Pasi, Bahuluang and Pulasi islands, Fig. 9.4); the Bonerate group (Kajuadi, Tanahjampea, Tanahmalala, Kalao and Bonerate islands, Fig. 9.5a); and the Kalaotoa group (Kalaotoa, Madu and Karampo Lompo islands; Fig. 9.5b). 104 coastal gravity stations were established, composed of 41 gravity stations on islands of the Selayar group, 47 stations on islands of the Bonerate group and 12 stations on islands of the Kalaotoa group.

9.3.1.3 Instrumentation

The instrument used to conduct this survey was a La Coste & Romberg type, model "G" geodetic gravimeter, serial number 286. Three 12 volt batteries were used in alternation providing power to maintain the instrument at constant temperature. A generator on the boat was used to recharge the batteries every day. On Selayar the batteries were charged at the Hotel Berlian and on Tanahjampea there was also a town electricity supply so it was possible to charge batteries there.

Readings were tied to the Indonesian national base station at Hasanudin Airport, Ujung Pandang. The gravimeter has a reading precision of 0.01 mGal and should drift less than 1 mGal/month. However, in this survey when the survey loop was closed at Hasanuddin airport base station after 19 days, the drift was 10.2 milligal.

9.3.1.4 Method of investigation

The stations were located using topographic maps at a scale of 1:250,000 and aerial photographs at a scale of 1:50,000. The coastal topographic maps did not describe the

present day coast lines very well and the aerial photographs were, therefore, very useful in determining the station locations.

Gravity measurements were taken along the coasts close to mean sea level. Free-air and Bouguer corrections were therefore minimal at most stations and Bouguer and free-air anomaly values are similar. The distance between gravity stations was planned to be about 5 km but in places where there was no access by land and no place suitable for landing from a boat; the distance could be as much as 10 km. On the east coast of Selayar, where there is no vehicle access to the beach from the main road, station separations are up to 30 km. Additional gravity stations were established in some places where the gravity values increased sharply from a previous station.

9.3.1.5 Observed Gravity

The observed gravity is the value of gravity obtained from the measurement in the field using gravimeter. There are some procedures to be applied to a gravity reading in order to derive an observed gravity value as follows (Dobrin 1988);

1 Calibration

A reading of a gravimeter is recorded in scale divisions and it is necessary to convert this to milligal. This was done using the conversion table specific to the G-286 gravimeter.

2 Earth tide correction

This correction is applied to allow for the effects of the periodic variations in the gravitational effects of the Sun and Moon associated with their orbital motions. These cause absolute gravity at fixed locations to vary with time. They have a maximum amplitude of some 0.3 mGal and a minimum period of about 12 hours. The tidal effects are predictable and published every year in the geophysical press. In this survey, however, tide corrections were calculated using the approach of Honkasalo (1964) which was available as a computer program.

3 Gravity base station

A gravimeter measures only the gravity differences between stations so that in order to obtain an absolute gravity value there must be at least one base station near or in the survey area at which the absolute gravity value is already known. Measurements can then be referred to this base station to obtain observed gravity values. Absolute gravity values are obtained by reference to the International Gravity Standardization Network 1971 (IGSN 71), a network of stations at which the absolute values of gravity have been determined by reference to sites of absolute gravity measurements.

In the survey area the nearest IGSN 71 gravity base station to which the gravity readings could be referenced was station No. 7693.1063 at Hasanuddin Airport, Ujung Pandang (Adkins *et al.* 1978). A description of this base station is given in Appendix 9.1

Generally, if the location of the nearest IGSN or base station is inconvenient, a gravimeter can be used to establish a local base by measuring the gravity difference between the base station and the local base. This procedure was used in this survey because the base station at Hasanuddin Airport (Ujung Pandang) is a long way from the surveyed area. Moreover, the area was very large, and it was necessary to establish secondary base stations at the Hotel Ramayana (Ujung Pandang), Lapee Port (Bulu Kumba), Benteng (Selayar), Bonerate, Kalaotoa and Benteng (Tanahjampea). The calculation of gravity values for these subsidiary base station is shown in Table 9.2, and descriptions gravity stations are shown in Appendix 9.2-8.

4 Drift correction

This correction compensates for the gradual change in reading due to the imperfect elasticity of the meter springs which undergo inelastic creep with time. Also, the elastic properties vary with temperature. To estimate this correction, repeated readings are taken at a base station at recorded times during the survey. The meter reading is plotted against time and the drift is assumed to be linear between consecutive base readings. The drift correction for each reading is then given by the formula:

$$D(n)=(R2 - R1)*(Tn - T1)/(T2 - T1)$$

BONERATE GRAVITY SURVEY MAY14 - JUNE1, 1993

CALCULATION OF Gobserved ON THE SUBSIDIARY BASE STATIONS WITH THE REFERENCE TO THE HASANNUDIN AIRPORT

BASE STATION OF HASANNUDIN AIRPORT

First reading										Last reading
Date: May 14										Date: June 1
Time: 12:38 PM	758	minutes								Time: 10:17 AM
Ref. Reading	1763.6637	mGals								Tide corrected=1773.8433
										The length of overall survey
Gabsolute	978119.94	mGals								25779
Drift corr	10.1796	mGals								minutes

Date	Subsidiary base stations	Time	Time in minute	Reading (mGals)	Tide correction (mGals)	Tide corrected (mGals)	Drift correction (mGals)	Drift corrected (mGals)	Gobserved (mGals)
May14	H.Ramayana	01:13:00 PM	793	1759.1021		1759.1021	0.0138	1759.0883	978115.3646
		02:28:00 PM	868	1759.0918		1759.0918	0.0434	1759.0484	978115.3247
May15	H.Ramayana Bulukumba Benteng H.Berlian	06:35:00 AM	395	1758.9786		1758.9786	0.4253	1758.5533	978114.8296
		09:53:00 AM	593	1802.3472		1802.3472	0.5035	1801.8437	978158.1200
		10:06:00 PM	1326	1880.8620	0.0390	1880.9000	0.7929	1880.1071	978236.3834
		10:39:00 PM	1359	1876.1908	0.0230	1876.2138	0.8059	1875.4079	978231.6842
May16	H.Berlian Benteng	06:36:00 AM	393	1876.1805	0.0400	1876.2205	0.9931	1875.2274	978231.5037
		08:46:00 AM	526	1876.1703	0.0800	1876.2503	1.0456	1875.2047	978231.4810
		02:38:00 PM	878	1876.3143	-0.0650	1876.2493	1.1846	1875.0647	978231.3410
		03:35:00 PM	935	1880.9958	-0.0630	1880.9328	1.2071	1879.7257	978236.0020
May17	Bonerate	10:26:00 AM	626	1930.9900	0.1660	1931.1560	1.6538	1929.5022	978285.7785
		11:41:00 AM	701	1931.1444	0.1230	1931.2674	1.6834	1929.5840	978285.8603
		12:58:00 PM	778	1931.2267	0.0660	1931.2927	1.7138	1929.5789	978285.8552
		05:07:00 PM	1027	1931.3913	0.0230	1931.4143	1.8121	1929.6022	978285.8785
May18	Kalaotoa	08:28:00 AM	508	1927.2037	0.1710	1927.3747	2.1758	1925.1989	978281.4752
		04:49:00 PM	1009	1928.7985	-0.0070	1928.7915	2.3736	1926.4179	978282.6942
May19	Bonerate	06:46:00 AM	406	1933.8195	0.0530	1933.8725	2.7041	1931.1684	978287.4447
		06:56:00 AM	416	1933.8092	0.0630	1933.8725	2.7081	1931.1644	978287.4407
		07:09:00 AM	429	1933.7661	0.0750	1933.8431	2.7132	1931.1299	978287.4062
		07:15:00 AM	435	1933.7784	0.0810	1933.8594	2.7156	1931.1438	978287.4201
		07:22:00 AM	444	1933.7887	0.0880	1933.8767	2.7191	1931.1576	978287.4339
		07:51:00 AM	471	1933.7681	0.1660	1933.9341	2.7298	1931.2043	978287.4806
		07:55:00 AM	475	1933.7681	0.1190	1933.8871	2.7314	1931.1557	978287.4320
		10:57:00 PM	1377	1934.8073	0.1670	1934.9743	3.0876	1931.8867	978288.1630
May20	Bonerate	07:12:00 AM	432	1934.9822	0.0450	1935.0272	3.2830	1931.7442	978288.0205
		08:06:00 PM	1206	1935.5275	0.0540	1935.5815	3.5887	1931.9928	978288.2691
May21	T.Jampea	08:29:00 AM	509	1939.8180	0.0550	1939.8720	3.8821	1935.9899	978292.2662
May22	T.Jampea	03:54:00 PM	954	1939.6842	0.0210	1939.7052	4.6264	1935.0788	978291.3551
May23	P.Kajuadi T.Jampea	10:50:00 AM	650	1969.8837	0.0950	1869.9787	5.0750	1864.9037	978221.1800
		06:20:00 PM	1100	1940.7955	-0.0580	1940.7375	5.2527	1935.4848	978291.7611
May24	P.Pulasi Benteng H.Berlian	10:00:00 AM	600	1896.9335	-0.0020	1896.9315	5.6239	1891.3076	978247.5839
		04:24:00 PM	984	1886.8399	0.0230	1886.8629	5.7755	1881.0874	978237.3637
		07:46:00 PM	1186	1882.2408	-0.1110	1882.1766	5.8553	1876.3213	978232.5976
May25	H.Berlian	08:39:00 AM	519	1882.2716	-0.0950	1882.1766	6.1605	1876.0161	978232.2924
		01:36:00 PM	816	1882.1173	0.1070	1882.2243	6.2778	1875.9465	978232.2228
May26	H.Berlian	08:22:00 AM	502	1882.2408	-0.0810	1882.1598	6.7224	1875.4374	978231.7137
		12:44:00 PM	764	1885.5744	0.0390	1885.6134	6.8259	1878.7875	978235.0638
May27	Hotel Berlian	09:22:00 AM	562	1885.7082	-0.0640	1885.6442	7.3147	1878.3295	978234.6058
		01:23:00 PM	803	1886.0374	0.0220	1886.0594	7.4099	1878.6495	978234.9258
May28	H.Berlian	07:12:00 AM	432	1885.9551	0.0380	1885.9931	7.8320	1878.1611	978234.4374
		04:44:00 PM	1004	1885.9242	0.0830	1886.0072	8.0579	1877.9493	978234.2256
May29	H.Berlian	06:44:00 AM	404	1885.9139	0.0790	1885.9929	8.3896	1877.6033	978233.8796
		04:20:00 PM	980	1886.3461	0.0360	1886.3461	8.6171	1877.7290	978234.0053
May30	H.Berlian Benteng	06:41:00 AM	401	1886.2843	0.0870	1886.3713	8.9571	1877.4142	978233.6905
		03:42:00 PM	942	1886.3769	-0.0410	1886.3359	9.1707	1877.1652	978233.4415
		07:54:00 PM	1194	1886.2329	0.0960	1886.3289	9.2702	1877.0587	978233.3350
		08:05:00 PM	1205	1890.9453	0.0960	1890.9453	9.2745	1881.6708	978237.9471
May31	BuluKumba H.Ramayana	05:21:00 AM	321	1812.5745	0.0530	1812.6275	9.4941	1803.1334	978159.4097
		01:28:00 PM	808	1769.2677		1769.2677	9.6864	1759.5813	978115.8576
June1	H.Ramayana Bandara UP	09:15:00 AM	555	1769.1031		1769.1031	10.1551	1758.9480	978115.2243
		10:17:00 AM	617	1773.6303	0.2130	1773.84	10.1796	1763.6637	978119.9400

THE AVERAGE OF Gobserved at EVERY SUBSIDIARY BASE STATION

Hotel Ramayana(001)	978115.3201	mGals
Bulu Kumba(002)	978158.7649	mGals
Benteng(003)	978236.9240	mGals
Hotel Berlian(004)	978233.1359	mGals
Bonerate(016)	978287.1345	mGals
Kalaotoa(021)	978282.0847	mGals
Tanahjampea(044)	978291.7941	mGals
P.Pulasi(076)	978247.6239	mGals

Table 9.2: Calculation of Gobserved on the subsidiary base stations with reference to the Hasannudin Airport

where: $D(n)$ = Drift correction at station 'n'
 R_1 = First reading at the base station
 R_2 = Last reading at the base station
 T_n = Time recorded when reading is conducted at station 'n'
 T_1 = Time recorded when the first reading is conducted
 T_2 = Time recorded when the last reading is conducted

In the Flores Sea gravity survey the drift was very large and clearly non-linear. The treatment of this drift is discussed below.

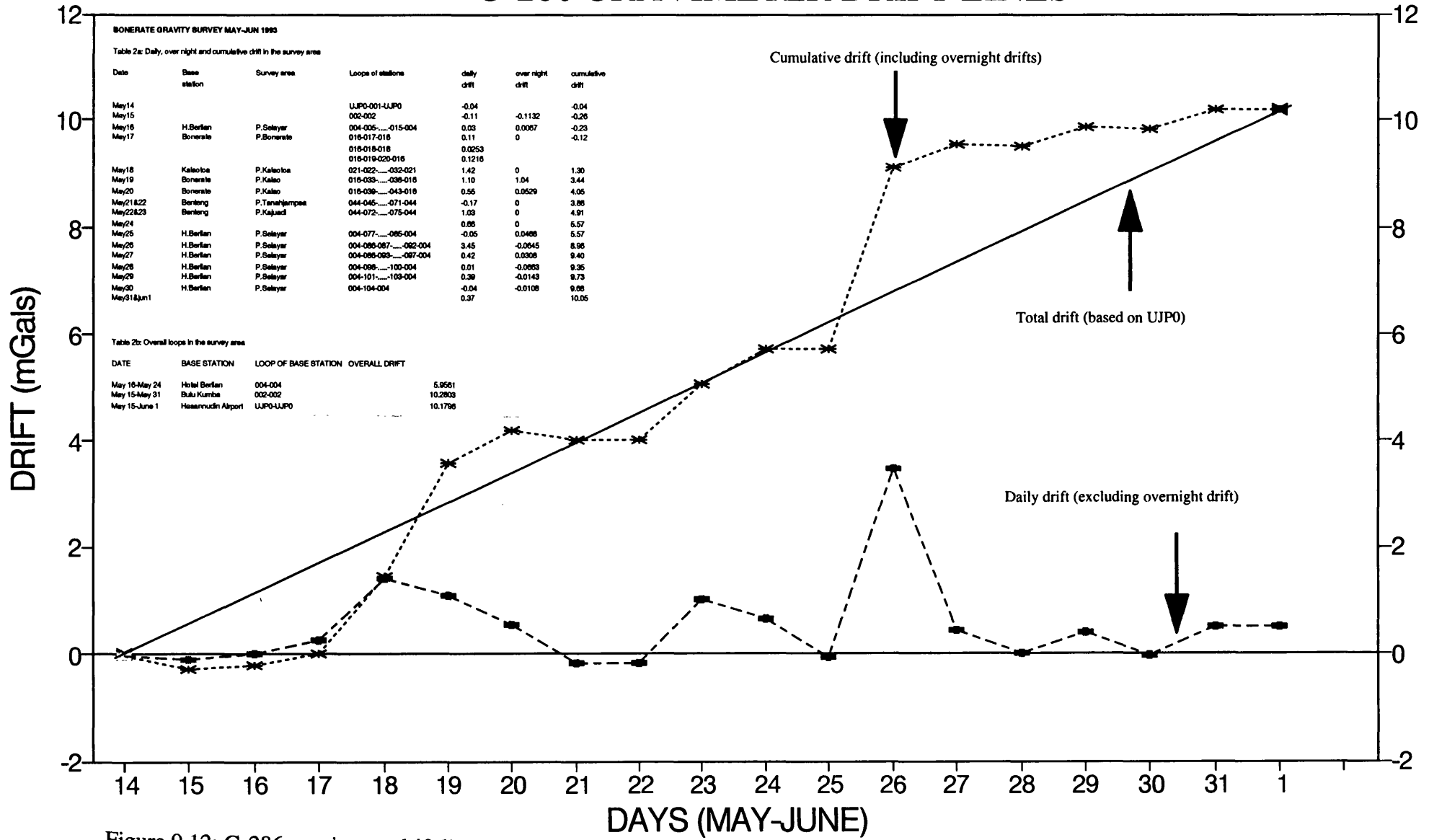
9.3.1.6 Survey loops

Survey loops used to control the gravimeter drift involve reading a gravimeter at a base station at the beginning and at the end of observation. In the Flores Sea, the survey pattern consisted of long and rather complicated loops. There was one main base station, at Hasanuddin Airport, and seven subsidiary base stations which were established in the survey area. The gravity values of the subsidiary bases were tied directly to the main base station at Hasanuddin Airport and all other gravity stations were tied to the nearest subsidiary base station.

Drift corrections for subsidiary base stations were performed as follows. The overall survey loop was closed at the end of the survey at the base station at Hasanuddin Airport after 19 days, during which time the drift was 10.196 mGal. Although generally drift is assumed to be linear, in this survey, daily observation showed that the drift fluctuated irregularly and when the cumulative drifts were plotted from the beginning up to the end of the survey, the curve was not linear (Fig.9.12). The maximum discrepancy between the assumed linear drift curve and the cumulative drift curve, which is real and non-linear, was about 2 mGal. In order to obtain maximum accuracy in gravity values at subsidiary base stations, the drift corrections for these stations used the cumulative drift curve.

Drift during subsidiary loops were assumed to be linear; such loops were normally completed in a day, except on Tanahjampea where the loop took two days. On Bonerate three small loops were obtained in one day. On May 24 a loop which began at Base

BONERATE GRAVITY SURVEY, MAY-JUNE 1993 G-286 GRAVIMETER DRIFT LINES



BONERATE GRAVITY SURVEY MAY-JUN 1993

Table 2a: Daily, over night and cumulative drift in the survey area

Date	Base station	Survey area	Loops of stations	daily drift	over night drift	cumulative drift
May 14			UJPO-001-UJPO	-0.04		-0.04
May 15			002-002	-0.11	-0.1132	-0.26
May 16	H.Berlan	P.Soleyar	004-005.....015-004	0.03	0.0067	-0.23
May 17	Bonerate	P.Bonerate	018-017-018	0.11	0	-0.12
			018-018-018	0.0253		
			018-019-020-018	0.1216		
May 18	Kalaloa	P.Kalaloa	021-022.....032-021	1.42	0	1.30
May 19	Bonerate	P.Kalao	018-033.....038-018	1.10	1.04	3.44
May 20	Bonerate	P.Kalao	018-039.....043-018	0.56	0.0529	4.06
May 21 & 22	Berlong	P.Tanahjampai	044-045.....071-044	-0.17	0	3.88
May 22 & 23	Berlong	P.Kajauad	044-072.....075-044	1.03	0	4.91
May 24				0.86	0	5.57
May 25	H.Berlan	P.Soleyar	004-077.....085-004	-0.05	0.0488	5.57
May 26	H.Berlan	P.Soleyar	004-086-087.....092-004	3.45	-0.0645	8.96
May 27	H.Berlan	P.Soleyar	004-089-089.....097-004	0.42	0.0308	9.40
May 28	H.Berlan	P.Soleyar	004-089.....100-004	0.01	-0.0553	9.35
May 29	H.Berlan	P.Soleyar	004-101.....103-004	0.39	-0.0143	9.73
May 30	H.Berlan	P.Soleyar	004-104-004	-0.04	-0.0108	9.68
May 31 & Jun 1				0.37		10.05

Table 2b: Overall loops in the survey area

DATE	BASE STATION	LOOP OF BASE STATION	OVERALL DRIFT
May 16-May 24	Hotel Berlan	004-004	5.9561
May 15-May 31	Buku Kuriba	002-002	10.2803
May 15-June 1	Hasanudin Airport	UJPO-UJPO	10.1798

Figure 9.12: G-286 gravimeter drift lines

Station 044 (Tanahjampea) was not closed at that base but at Base Station 004 (Hotel Berlian, Selayar). The overall drift was obtained by the loop based on the Hotel Berlian which lasted from May 16 - May 24. The drift on May 24 was then assumed to be equal to the overall drift from May 16 - May 24 (5.95 mGal) at Base Station 004, Hotel Berlian minus the total cumulative drift from May 16 - May 23 (4.94 mGal), giving a drift on May 24 of 0.656 mGal. The same method was used to obtain drifts on May 31 and June 1 because these loops were also closed at different base stations. Fig. 9.12 shows the daily, cumulative and overall drift curves; the table included in the figure shows the way in which the values were obtained. Overnight drifts were obtained by measuring the gravity difference between the last reading on one day and the first reading on the next. The maximum overnight drift of 1.04 mGal occurred on May 19 at Bonerate base station (GS 016). Drift on legs connecting islands could not be measured directly as in these cases. There was no loop, but the values themselves have been integrated into the overall drift curve. Fig. 9.12 also shows small and rather linear drifts in the period of May 14 to May 17 and May 27 to June 1, the range being from about -0.04 mGal to +0.26 mGal, and that in contrast in the period May 18 to May 26, drift fluctuated irregularly. The highest drift recorded in one day (3.46 mGal) was on May 26 at the Hotel Berlian base station (004).

It is difficult to explain these high drifts. On the first occasion it was thought to be due to inadequate charging of the batteries causing unstable temperature of the gravimeter, which would cause significant errors in the gravity readings. This possibility was considered because the generator used to charge the battery in the boat did not work properly. However, the problem still occurred even the batteries had enough charge, as even when the survey was based at the Hotel Berlian (Selayar) and the batteries were charged using main electricity. The highest drift was encountered in this place on May 26.

9.3.2 Gravity data processing

9.3.2.1 Gravity data reduction

Gravity data obtained in the field are the result of the superposition of many effects, many of which are not geological, and the data must be corrected by a process known as gravity reduction. Generally this is a reduction to the geoid, as sea level is usually the

most convenient datum level. The types of corrections are as follow (Telford *et al.* 1976):

- Latitude correction
- Free-air correction
- Bouguer correction
- Terrain correction

The sequence of gravity data reduction in the Flores Sea survey can be seen in Appendix 9.9.

9.3.2.1.1 Latitude correction

Because of the Earth's rotation, the Earth is not actually spherical and the gravitational acceleration has a maximum value at the poles and a minimum at the equator. The difference in gravity value between poles (latitude=90⁰) and equator (latitude=0⁰) is about 5300 mGal.

The latitude correction is usually made by subtracting the 'normal' gravity calculated from the 1967 International Gravity Formula from the absolute 'observed' gravity as follow:

$$g_l = 978031.8 (1 + 0.0053024 \sin^2 \phi - 0.0000059 \sin^2 2\phi)$$

where g_l = the 'normal' gravity (in mGal)

ϕ = latitude

The accuracy of this correction depends on the accuracy in determining the location of gravity station. As already noted, the positions of the stations were determined using topographic maps at a scale of 1:250,000, aerial photographs at a scale of 1:50,000 and by identifying coastal and topographic features. The accuracy of the location using this method is estimated to be about ± 100 m. The difference produced by a change of 100 m in a north-south direction in the theoretical gravity is 0.02 mGal.

9.3.2.1.2 Free- air correction

Because there is a variation in distance between the gravity station and the datum level (sea level), the gravity values have to be corrected to sea level. This correction can be

obtained by applying Newton's Law, according to which the gravity value at the surface of the Earth is given by the following formula (Dobrin 1988):

$$g = Gm/r^2$$

where g = theoretical value of gravity with g in milligals

m = mass of the earth

r = radius of the earth (6.37×10^5 km)

This formula defines the changes of gravity values in response to changes in ' r ' and show that ' g ' will increase when ' r ' decreases and vice versa. From this formula the free-air correction can be calculated to be +0.3086 mGal for every meter above sea level. This correction does not deal with the effect of rock material between the sea-level datum and the station.

9.3.2.1.3 Bouguer Correction

This correction is applied to compensate for the effect of the rock between the observation point and the datum, because this mass will increase the gravity field at a point above it. The amount of attraction caused by this material is estimated using the equation (Dobrin 1988):

$$\begin{aligned} BC &= 2 \pi \rho G h \\ &= 0.04191 \rho h \text{ mGal} \end{aligned}$$

Where BC = Bouguer correction

π and G = have their usual values

ρ = density

h = elevation

It is assumed that the rocks form an infinite horizontal slab of uniform density with a bottom surface at sea level and a top surface at the elevation of the station. If the

material in this slab has a standard density of 2.67 Mg/m^3 , the attraction will be 0.1112 mGal/m . If the observation point is situated above sea level the correction is negative.

The free-air and Bouguer corrections are often combined and referred to as the elevation correction. Using a standard density of 2.67 Mg/m^3 , the elevation correction becomes 0.1968 mGal/m . In the Flores Sea, the density of 2.2 Mg/m^3 was used, as it was the value used by Edcon (1991) to make Bouguer corrections in the off-shore area of the East Java Sea. The accuracy of the combined corrections depends on the accuracy in determining the elevations of the stations. Elevations of stations were estimated by reference to mean sea level, the accuracy was estimated to be about $\pm 0.5 \text{ m}$ and this is equal to 0.1 mGal for the combined free-air and Bouguer corrections.

9.3.2.1.4 Terrain correction

This correction is applied to the gravity value because of the topographic relief in the vicinity of the gravity station. If there are considerable differences in elevation, especially close to the station, these local irregularities of topography will have effects on the gravity attraction which must be taken into account in reducing the gravity values (Nettleton 1940). The excess masses of hills above a gravity station give an upward component of gravitational attraction, which counteracts a part of the downward pull exerted by the rest of the Earth, while valleys below a gravity station produced a smaller downward pull at the station than was assumed present in making the simple Bouguer correction. Therefore hills and valleys in the surrounding survey area will both reduce the gravity value and the correction is always positive.

Terrain corrections can be estimated manually using a circular graticule divided by radial and concentric lines into a large number of compartments. This is known as a Hammer chart. Alternatively, the topography can be digitised and the correction can be calculated by computer.

In this report terrain corrections were not applied due to the unavailability of small scale topographic maps. However, the correction is considered to be very small due to the smooth topography in the surveyed area. A "worst case" estimate of the terrain correction was calculated using GMSYS Gravity Modelling at Gravity Station 034 on

Kalao since this is located close to steep hills. The correction in this case was about 0.60 mGal. The most extreme terrain correction was at Gravity Station 104 on Selayar, located near very steep slopes. Using GMSYS Gravity modelling, with density 2.2 Mg/m³, the terrain correction was estimated 5.96 mGal. However this value is regarded as an exception and is not representative of the terrain correction at other gravity stations. In this single case, a terrain correction was applied.

9.3.2.2 Error Estimation in reduction of the gravity data

The errors in the calculations of Bouguer anomaly values are due to errors in determining the positions and elevations of the stations and also those due to the terrain effect, for which no correction was applied. As seen, errors in determining position and elevation were low (0.118 mGal) compared to the size of the gravity correction. However errors due to lack of terrain correction were much higher, the maximum likely terrain correction being about 0.60 mGal. Therefore the maximum errors in the calculation of Bouguer anomalies are thought to be about 0.72 mGal. The effect of such errors on gravity maps contoured at 10 mGal intervals is insignificant.

9.3.2.3 Bouguer anomaly and contouring

The Bouguer gravity anomaly for every station was obtained by applying the following formula:

$$BA = G_o - G_n + FAC - BC + TC$$

where BA = Bouguer anomaly

G_o = observed gravity value

G_n = theoretical value of gravity on a certain latitude

FAC = Free-air correction

BC = Bouguer correction

TC = Topographic correction

A Bouguer anomaly contour map was constructed on a scale of 1:375000. Bouguer anomaly contours in the surrounding sea areas were constrained by the Bouguer

anomaly map prepared by Edcon for BP Exploration (1991) using data from marine cruises.

9.3.2.4 Description of Bouguer anomaly maps

Fig. 9.13a,b and c shows the Bouguer anomaly maps of the Flores Sea Islands contoured at 10 mGal interval. The station distributions are also shown. There is a gradual change of contour orientation from roughly north-south on Selayar to northwest-southeast on Tanahjampea and finally to east-west on Kalao and Bonerate. On and to the south of Kalaotoa the contours may be defining a closed Bouguer anomaly high and to the east, towards to the Banda Sea, contour lines resume a north-south alignment.

On Selayar, Bouguer anomaly values increase from east to west, from +60 mGal to +200 mGal. The gravity gradients also become steeper from east to west, from 3-4 mGal/km to 8-10 mGal/km. The highest value (+205 mGal) is on Pasi Island and this is thought to associate with basement uplift and intrusion of mantle material into the upper crust.

On Tanahjampea, Bouguer anomaly values increase from NE to SW, from +145 mGal to +195 mGal. The gravity gradients are also steeper from NE to SW. The highest Bouguer anomaly, of about +195 mGal, occurs at the village of Mangati in the southern part of Tanahjampea (GS 064).

On Kalao, Bouguer anomaly values increase from south to north and also from west to east, from +150 mGal to +170 mGal. On the adjacent island of Bonerate, 5 km east of Kalao, the contour values increase from north to south (+160 mGal to +175 mGal). This suggests that Kalao and Bonerate have different geological structure and are probably separated by a major fault. On Kalao the highest value measured (at GS 034 on the north coast) coincides with the area where ophiolite was mapped whilst the lowest value measured (at GS 039 on the southeast coast) coincides with the area where granite was mapped by Koswara *et al.* (1991). The distribution of ophiolite and granite on the geological map (which is largely based on aerial photograph interpretation) seems in agreement with the Bouguer anomaly contours.

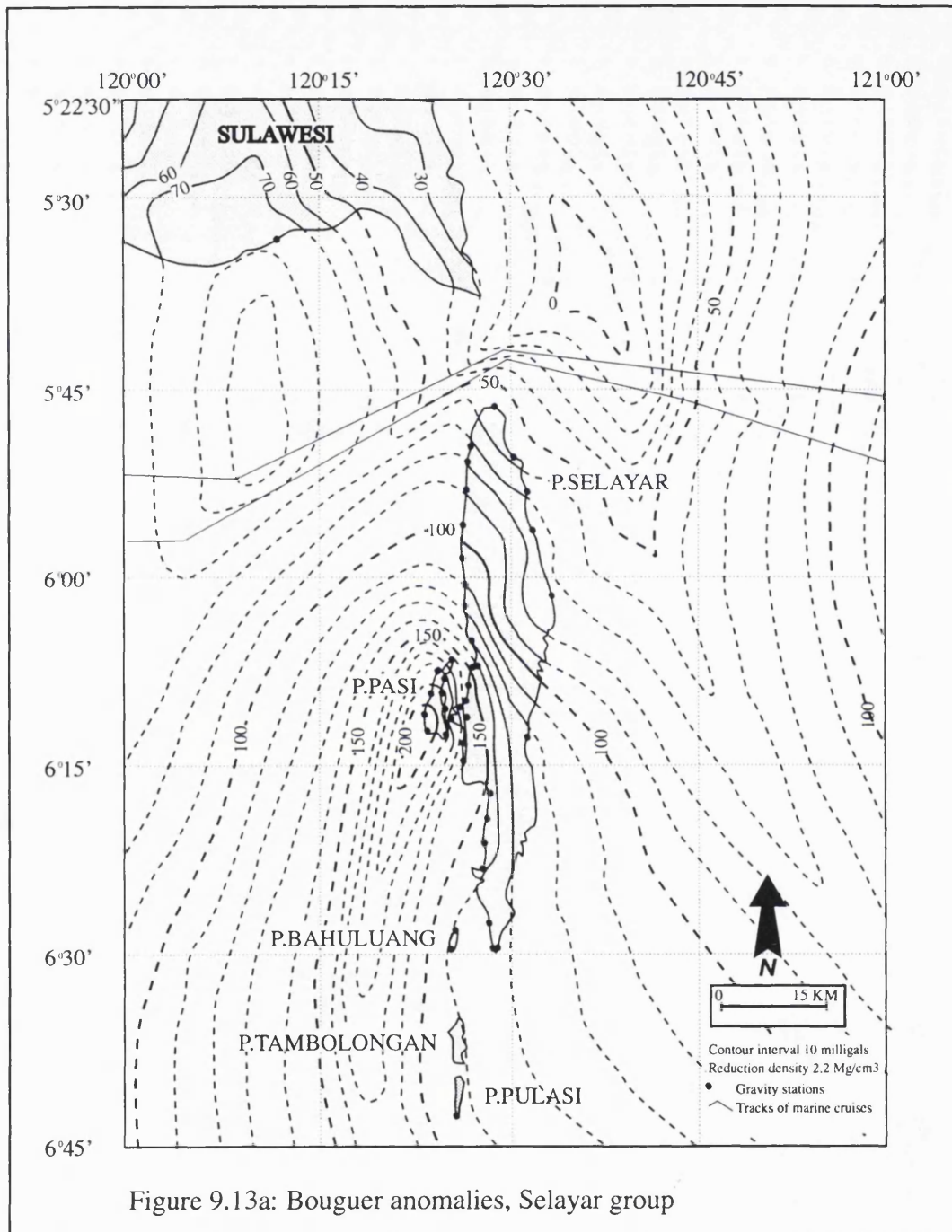


Figure 9.13a: Bouguer anomalies, Selayar group

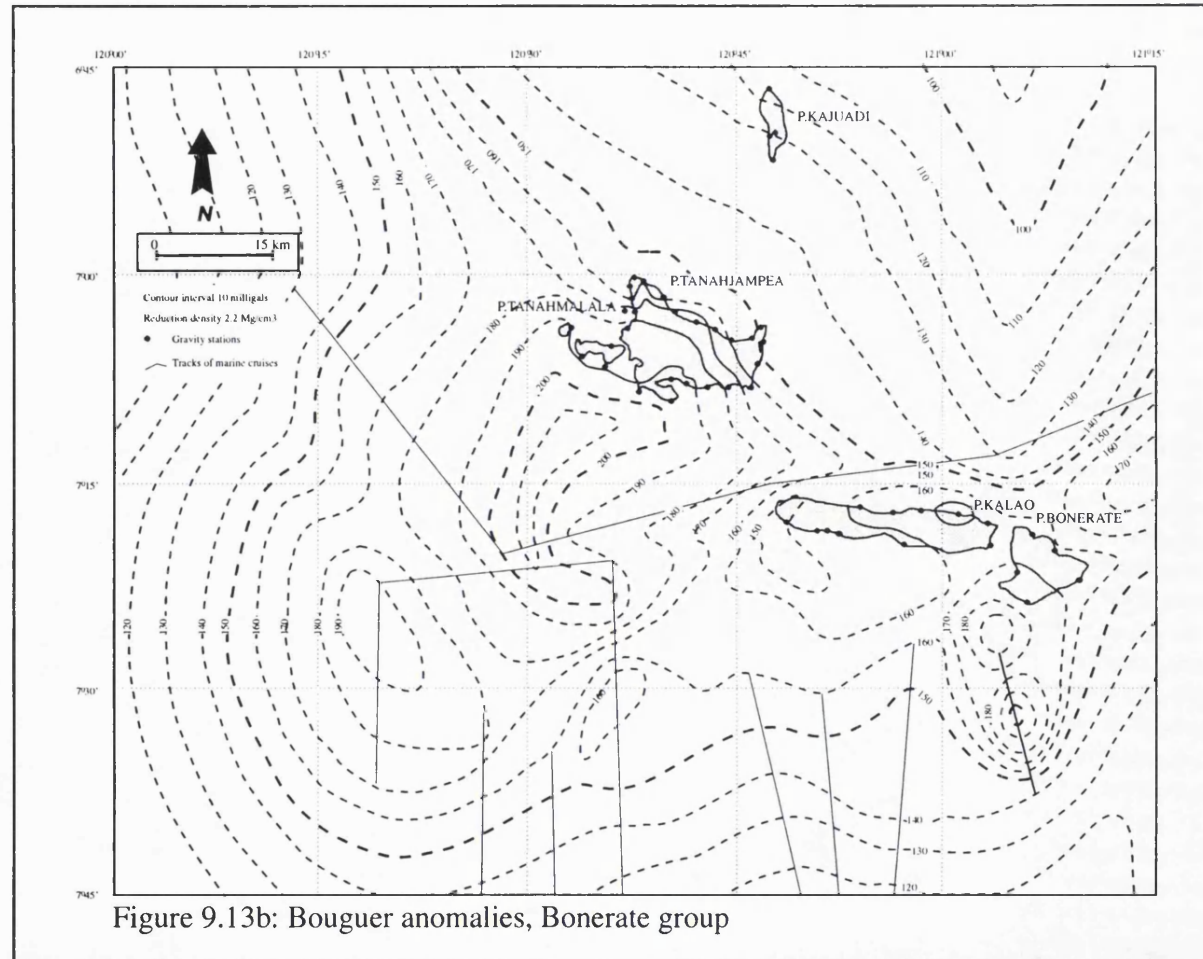
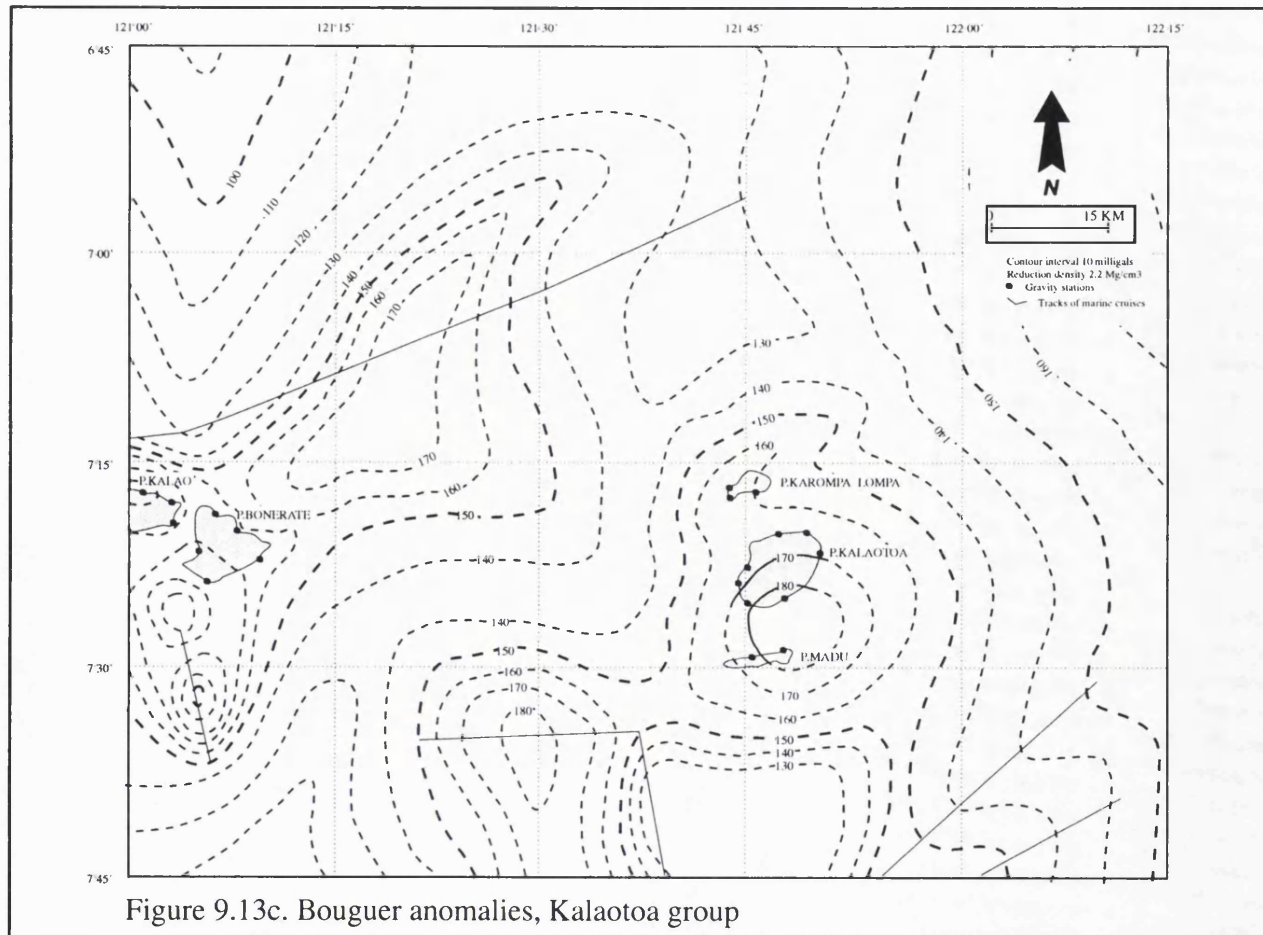


Figure 9.13b: Bouguer anomalies, Bonerate group



On Kalaotoa, Bouguer anomaly values increase from north to south, from +165 mGal to +180 mGal. On Madu, Bouguer anomaly values increase from west to east, from +177 mGal to 182 mGal. The highest value is recorded in the locality where ophiolite was mapped by Koswara *et al.* (1991;1993). On Karompa Lompa, the values range from 160 mGal to 165 mGal from east to west.

9.3.2.5 Summary

The Bouguer anomaly map of the Flores Sea is characterised by a broad positive anomaly and an extremely large range of gravity values (0 mGal to +200 mGal). The trends of gravity anomalies are mainly parallel to the main geological structures. Different gravity values may indicate different crustal thicknesses, which may reflect different tectonic settings. Local gravity anomalies can in some cases be correlated with surface geological formations; the outcrops of basaltic rocks on Kalao, Kalaotoa and Madu islands are associated with high Bouguer anomalies whereas outcrops of granitic rocks in western Kalao are associated with low Bouguer anomalies. However, in other cases, the gravity anomalies are not correlated exposed geology; on Pasi Island, which is covered mainly by Pliocene and Quaternary carbonate rocks, Bouguer anomalies in places exceed +210 mGal, indicating concealed subsurface structures and perhaps mantle uplift.

CHAPTER TEN

GEOPHYSICAL STUDY OF THE FLORES SEA ISLANDS AND VICINITY

10.1 INTRODUCTION

The geology and gravity fields of the Flores Sea Islands, defined as the small islands between South Sulawesi and Flores, have been described in Chapter 9. This chapter will examine the marine geology of the surrounding area using geophysical data available in the region, which will be integrated with the geological and gravity data obtained in the course of the Flores Sea Islands Survey.

10.2 FLORES BASIN

The Flores Basin is a Tertiary sedimentary basin about 135 km E-W by 35 km N-S which is bounded to the northeast by the Bonerate Ridge, which separates it from the Banda Sea to the east, and to the west by the NE trending slope of the southeastern flank of the Sunda Shelf (Fig.10.1). The basin reaches oceanic depths of more than 5000 m. The floor is composed of Neogene volcanic and sedimentary rocks which dip to the west and southwest (Silver *et al.* 1986). The Flores Basin has a relatively dense coverage of single channel reflection seismic lines as well as Sea MARC II side-scan mosaics. Results obtained from a seismic refraction station MSN 13 north of Flores (see Fig.10.1 for location) have been interpreted by Curray *et al.* (1977) as showing that the oceanic layer was not detected. The Moho lies at only 14.3 km, which is slightly greater than oceanic average but significantly less than its depth under continental areas. It has been concluded that the crust of the Flores Basin was originally oceanic and may resemble the crust in the enclosed Sulu and Sulawesi basins (Hamilton 1979).

At refraction stations MSN 14A and 14B, north of Sumbawa at the eastern end of the Flores Sea, a thick oceanic crustal layer was detected and the mantle was interpreted as lying at more than 22 Km (Curray *et al.* 1977). This crustal thickness is very similar to that in the arc-trench gap south of Java and Bali.

10.2.1 Tectonic setting of the Flores Basin

In Eastern Indonesia, the phenomena of back arc thrusting has attracted considerable attention and various hypotheses have been proposed to explain its initiation and driving

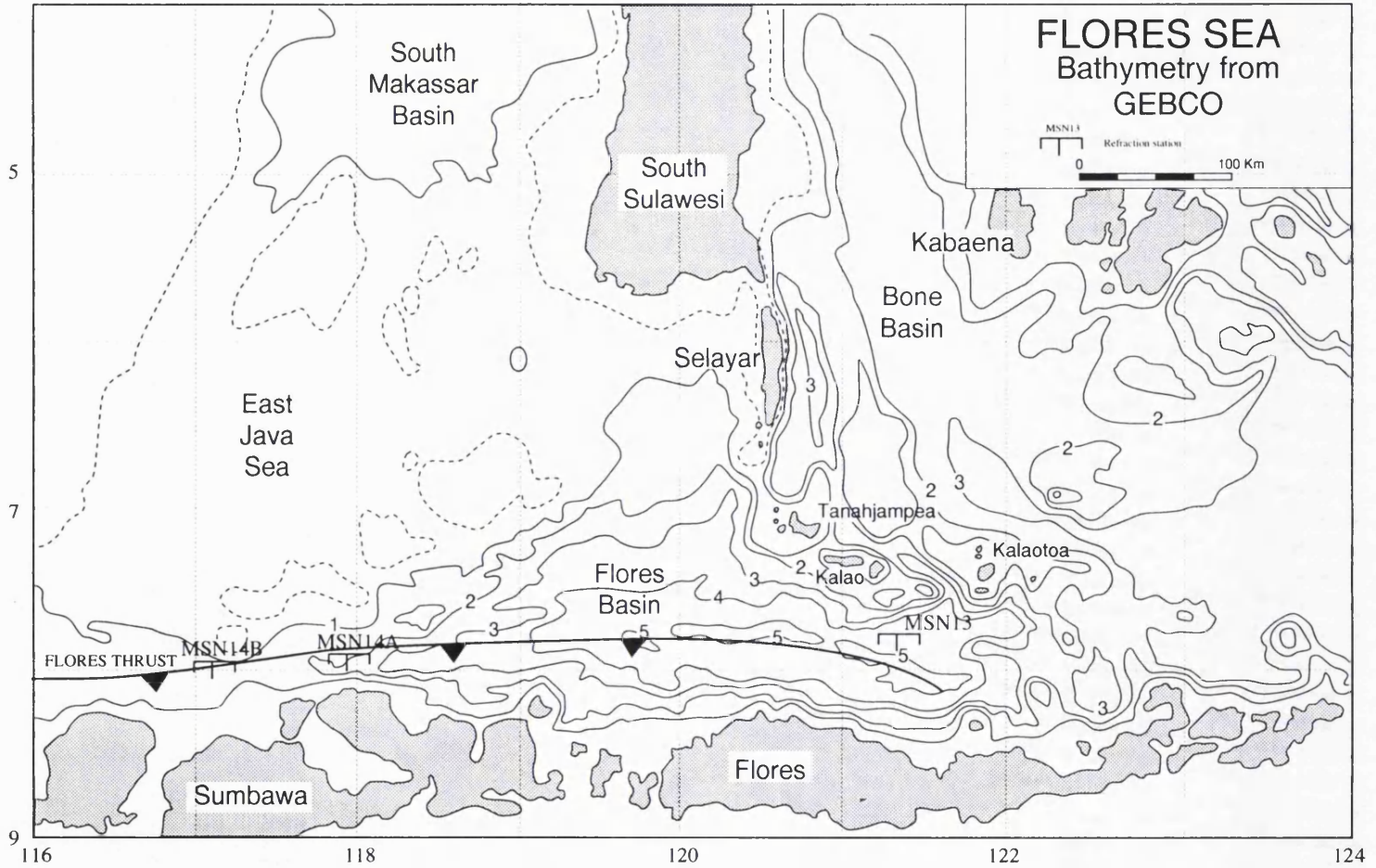


Figure 10.1: Bathymetric map of the Flores Sea

mechanism. Silver *et al.* (1983) listed some of these hypotheses, including gravitational body forces as the sole mechanism, gravity spreading as a result of existing relief or injection of magma in the volcanic arc, low angle subduction resulting in back arc thrusting and collisional stress. Silver *et al.* (1983, 1986) considered back-arc thrusting to be a precursor of arc polarity reversal.

In Eastern Indonesia there are two major zones where back arc thrusting occurs (Silver *et al.* 1986; Prasetyo and Dwiyanto 1986); one is to the north of Wetar and Alor (Wetar Thrust), the other is to the north of Flores and Sumbawa islands (Flores Thrust). Hamilton (1979) proposed that these back arc thrusts indicated subduction polarity reversal due to the difficulty of subducting the buoyant continental margin of Australia, whereas Silver *et al.* (1983) related the distribution of back arc thrusts to the thickness of the forearc crust. Thick forearc crust, represented by Sumba Island and Timor Island, respectively is correlated with the formation of the Flores and Wetar thrusts.

Silver *et al.* (1986) interpreted seismic reflection profiles from immediately north of Flores as showing thrusting at the base of the slope of the volcanic pile, with the oceanic crust of the Flores Basin being overridden by the volcanic islands. The amount of convergence between the Flores Basin and the island arc is about 30 - 60 km, judging from the volume of material accreted to the toe of the volcanic arc (Silver *et al.* 1983). The crust of the Flores Basin was suggested by McCaffrey and Nabelek (1984) to dip beneath the small back-arc accretionary prism at an angle of about 6° or to thicken considerably under the southern Flores Basin. This dip angle is similar to that of many subducting plates at trenches in the western Pacific (Watts and Talwani 1974).

Large negative free-air anomalies (reaching -110 mGal over the accreted wedge 30 km south of the deepest part of the Flores Basin) have been interpreted as indicating that the crust is out of isostatic equilibrium and suggest that the underthrusting plate is pulled down as in more developed subduction zones (McCaffrey and Nabalek 1984). The load represented by crustal material between Flores Island and the Flores Thrust cannot completely explain the deflection of the Flores Basin lithosphere if this is being bent as an elastic plate and McCaffrey and Nabalek (1984) proposed that either the underthrusting plate extends as far south as Flores Island (which is characterised by

negative free-air gravity anomalies) and/or that its gravitational instability is pulling it down into the asthenosphere.

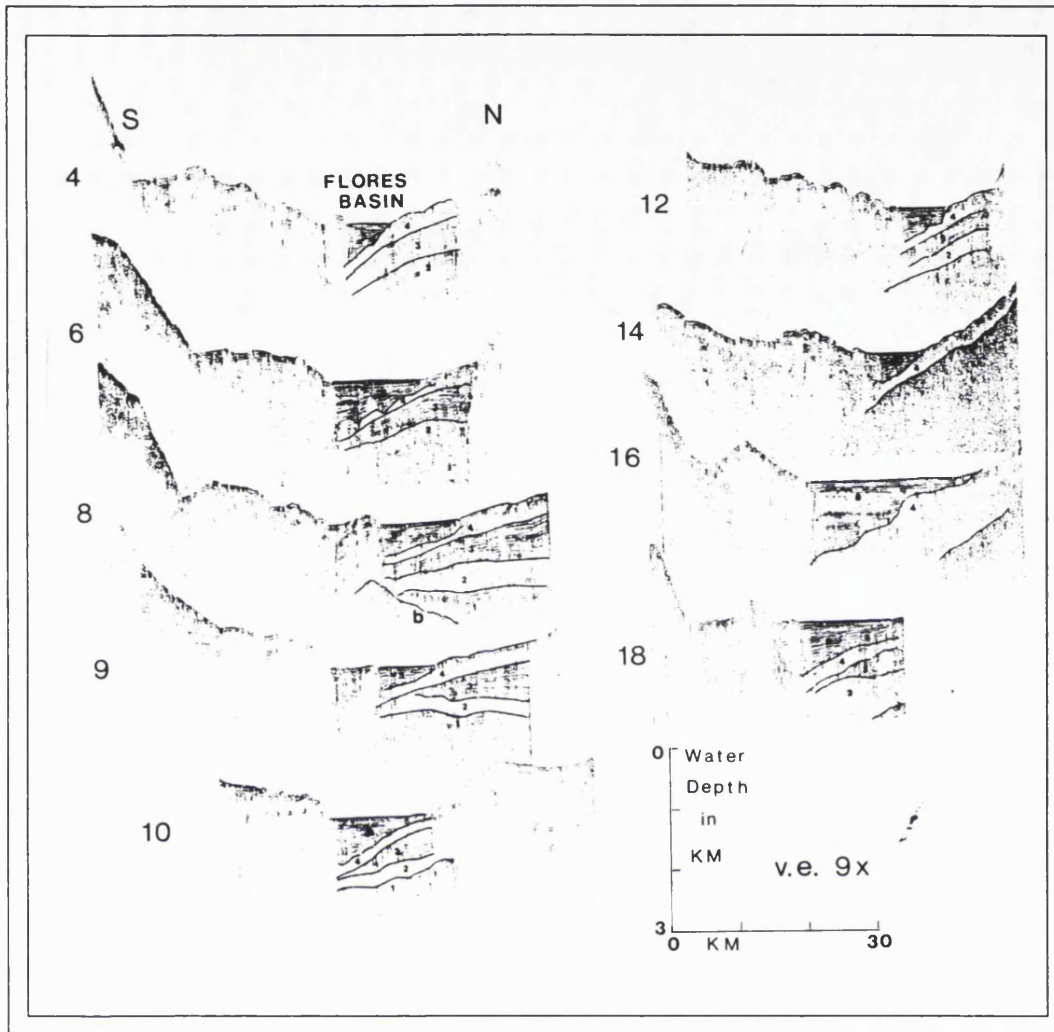
10.2.2 Stratigraphy of the Flores Basin

Silver *et al.* (1986) divided the outer slope and trench sediments in the Flores Basin into five recognizable seismic stratigraphic units (Fig. 10.2), but not all units appear on all sections. The following divisions are based on their description. The lowest reflector (B) is irregular, hummocky, and considered to be acoustic basement. It was suggested that on Line 14, at least, this basement may consist of young (Pliocene ?) lava flows, consistent with the occurrence of volcanic products on the islands of the Bonerate Group to the north. Unit 1, which immediately overlies basement, is highly reflective and very variable in thickness. On Lines 8-12 this unit can be seen clearly and may thicken westward.

Above Unit 1 is a poorly reflective Unit 2 which is inferred to have been deposited under pelagic or hemipelagic conditions. Unit 3 is well layered with variable thickness and is interpreted as a turbidite deposit. Above Unit 3 is another poorly bedded hemipelagic layer which generally forms the top of the slope sequence. This unit appears on all sections and is very thick in some places, although the average thickness is nearly constant at a few hundred metres. Unit 5 consists of trench turbidites. These are present on all profiles but vary greatly in thickness and lateral extent.

On Line 14 (Fig.10.2), the major change in slope stratigraphy occurs just south of the westernmost end of the Selayar - Bonerate ridge, which is consistent with the expectation that the basement and sediment source rocks to the east and west of this point are very different.

A number of mud diapirs are present in the southern part of the Flores Basin, indicating abnormally high fluid pressures. They occur in all parts of the wedge and may be associated with lateral propagation of the thrust zone. The presence of circular mud volcanoes in the inner part of the wedge indicates that they have formed in their present setting, rather than at the toe of the wedge. The distribution of mud volcanoes is interpreted as indicating that they form continually within and in front of the accretionary



INDEX MAP

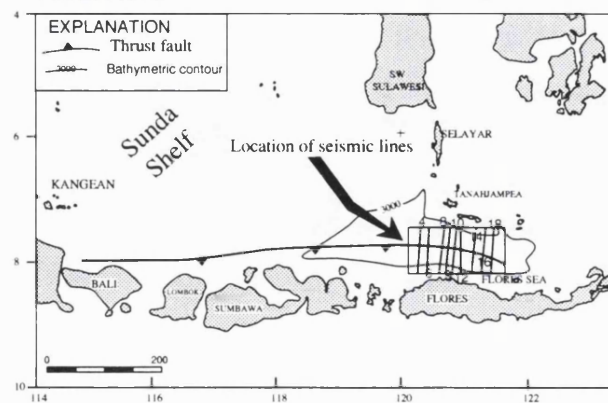


Figure 10.2: Seismic stratigraphy of the Flores Basin from single channel seismic reflection (Silver et al. 1986)

wedge, although there is a tendency for them to form more toward the toe than towards the rear of the wedge.

The most interesting result from the Silver *et al.* (1986) seismic interpretation is the presence of faults cutting the lower plate sediments. They suggested that the faults may represent reactivations of older basement faults because they are parallel to buried basement faults mapped in the Java Sea where the collision possibly reactivated faults north of the Flores Thrust zone. They also suggested an alternative cause might be strike-slip faulting related to the collision.

10.3 SEISMIC INTERPRETATION

Some additional multi channel seismic reflection profiles have been interpreted in the region as part of this study to determine structural characteristics. In general, the area is dominantly formed by normal faults, block faulting the basement and by volcanic activity. Figure 10.3 shows an interpretation of line IND 116, west of Selayar. The major angular unconformity is interpreted to be Middle Miocene age, the time of major orogenesis in South Sulawesi. Intrusion-like structures are also observed in the middle and east of the profile and are seen as continuations of the volcanism of South Sulawesi. The basin configuration indicates extension with sediment thickness reaching 3 sec TWT. Figure 10.4 is a seismic interpretation of Line PAC 203, situated 30 km south of line IND 116. There is a major unconformity on this line which correlates with that on line IND 116. The section also shows basement uplift and extensive block faulting.

Figure 10.5 shows single channel seismic reflection, bathymetric and gravity data obtained along the line Mariana 09 which crossed the Flores Sea from south to near Kabaena Island in the northeast, a total distance of about 400 km. The seismic profile shows that the region is dominated by series of down thrown basement blocks and magmatic activity. The Flores Ridge, the Flores Thrust, the Flores Basin, Selayar Ridge, Selayar Basin, Bone Ridge, Kabaena Basin and Kabaena Ridge can all be identified. The sediments accumulated in several sub basins separated by oceanic topographic highs. There are two principal types of reflectors. The first is characterised by rounded, conelike structures, irregular surfaces and high morphology, which can be seen in the Selayar Ridge, Bone Ridge and Kabaena Ridge. The second reflector type is sub-parallel to horizontal. In the Kabaena and Selayar basins

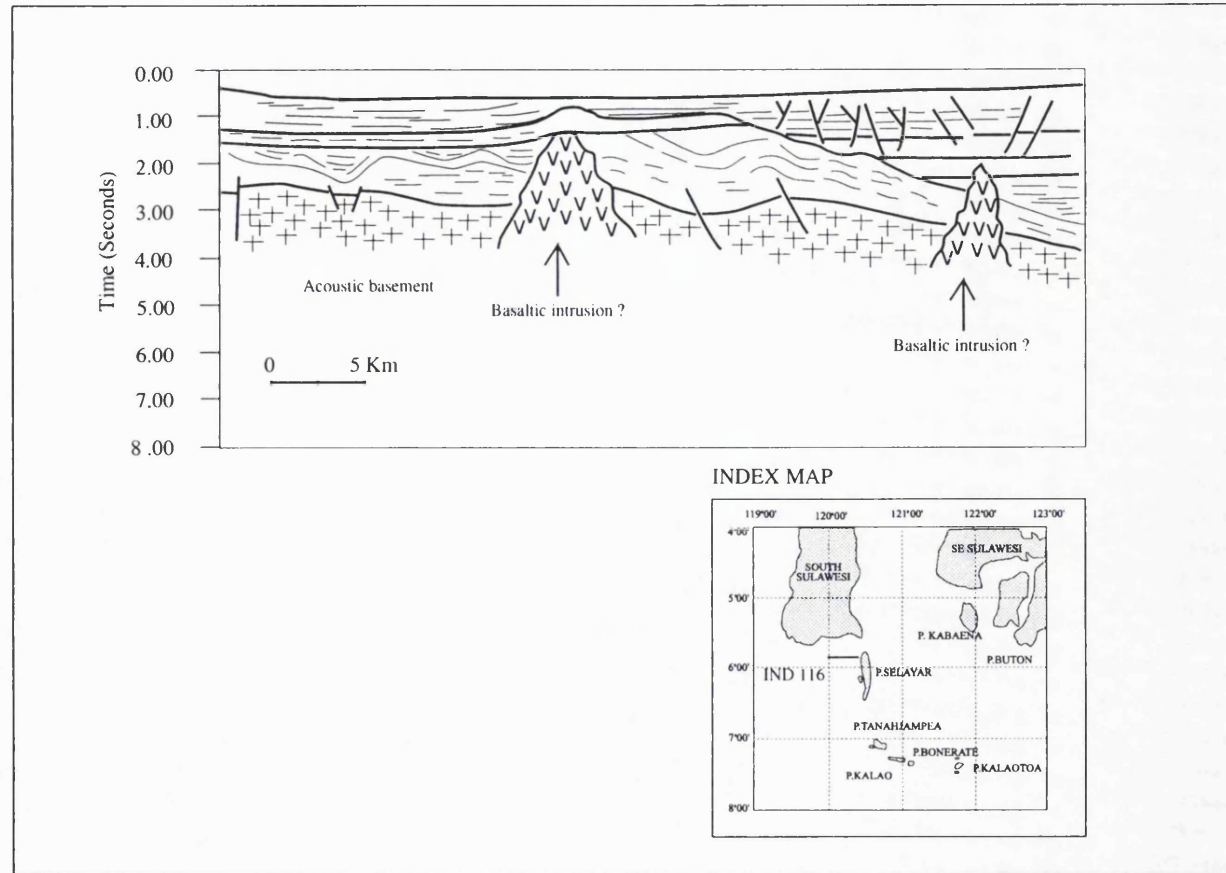


Figure 10.3: Seismic interpretation of line IND 116 showing basement faults, angular unconformity and intrusion of more basaltic rocks.

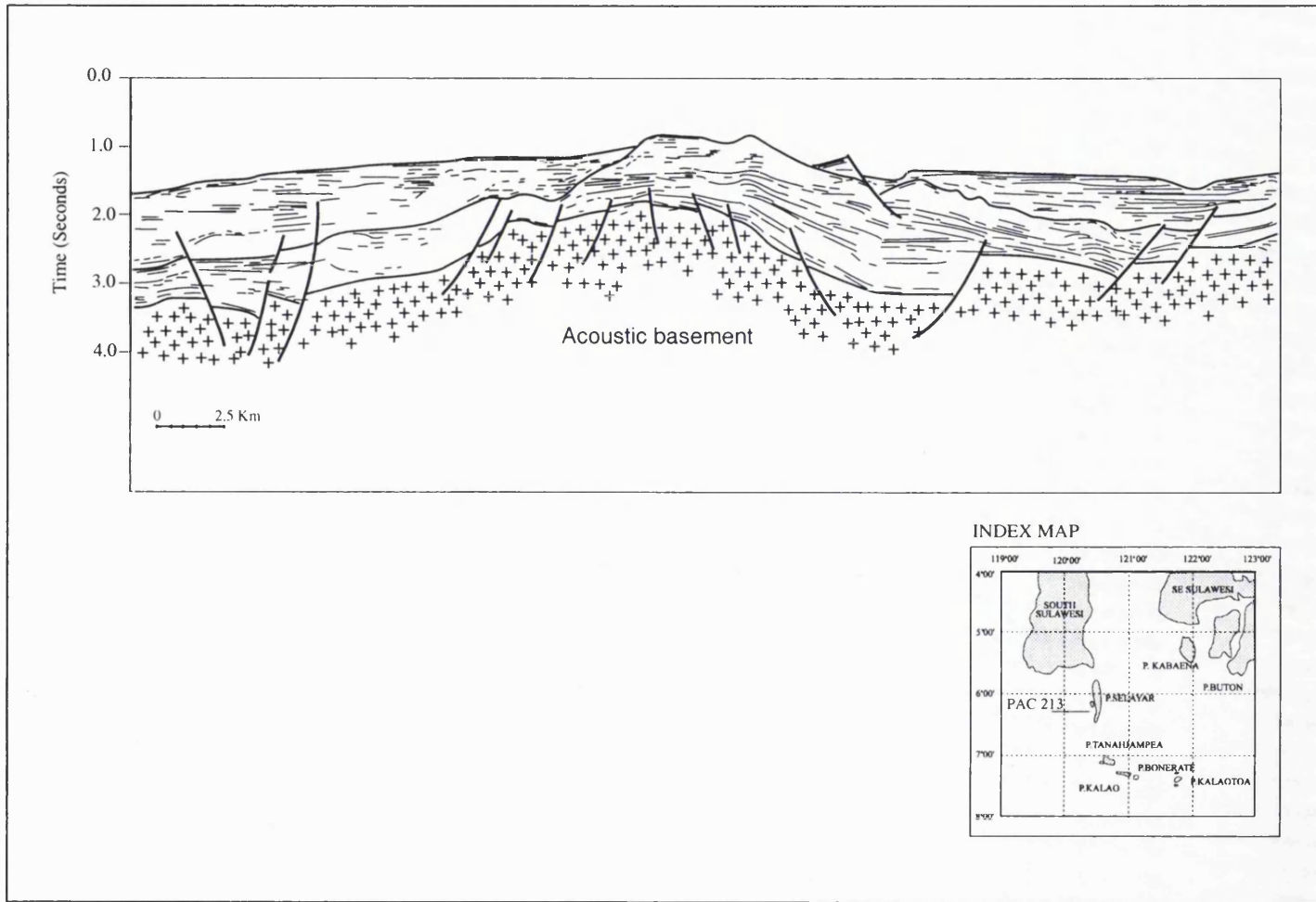


Figure 10.4: Seismic interpretation of line PAC213 showing basement uplift

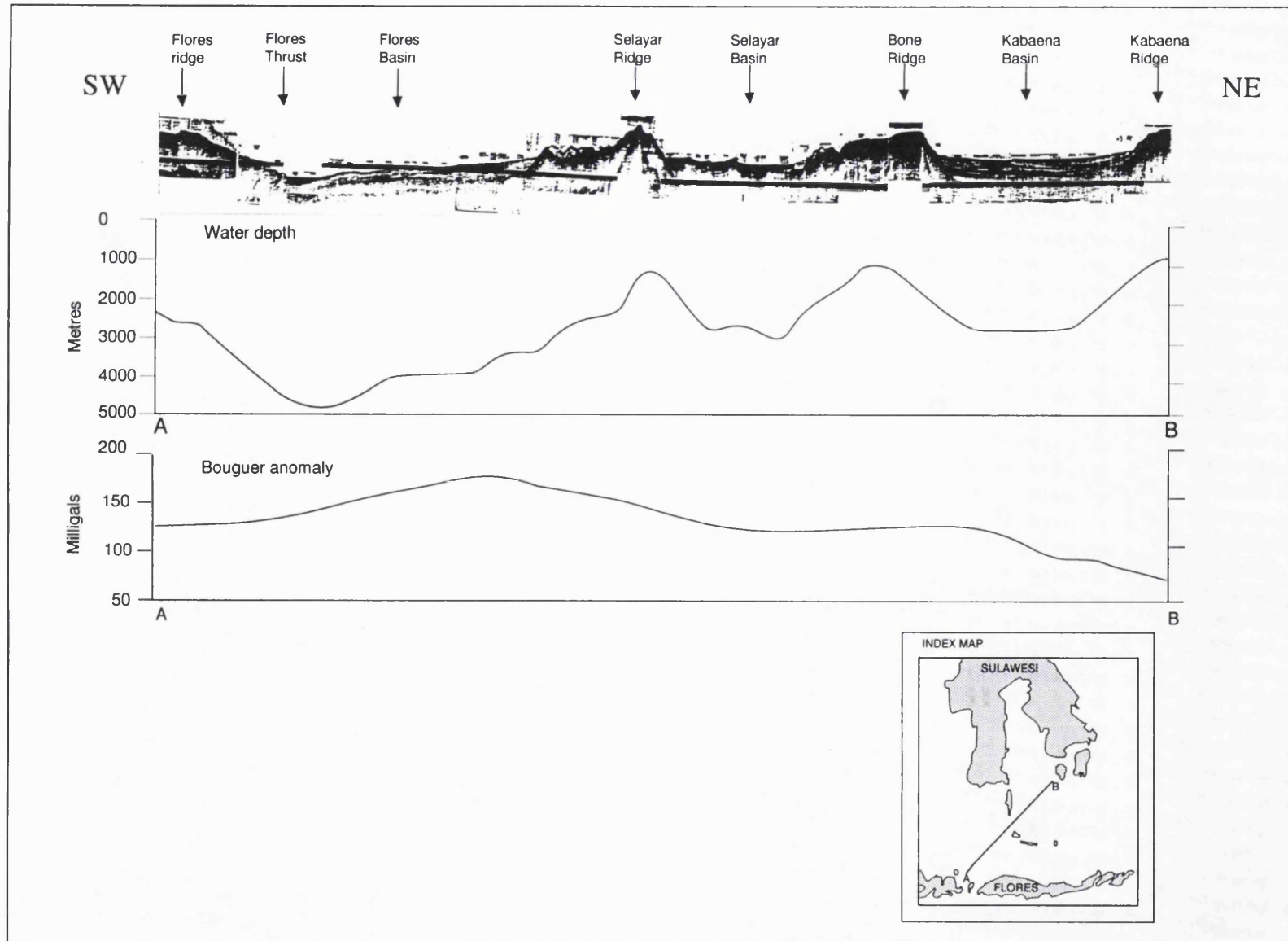


Figure 10.5: Correlation between single channel seismic reflection, bathymetry and gravity profiles of Mariana 09

this reflector is interpreted as indicating flat-lying sediments but in the Flores Basin, where reflectors are smoother than in the Kabaena and Selayar basins, they probably mark basaltic lava flows with thin sedimentary cover.

10.4 GRAVITY DATA

10.4.1 Introduction

The free-air anomaly map of the Flores Sea Islands and vicinity (Fig.10.6) has been prepared by integrating the gravity data from the 1993 Flores Sea Islands gravity survey (Chapter IX.3) with the free-air anomaly map of Bowin *et al.* (1980) and free-air anomaly map of Edcon (1991).

10.4.2 Qualitative gravity interpretation

The free-air anomaly map in the Flores Sea Islands and vicinity is characterised by two distinctive trends of anomaly contours. The first occurs around the Selayar-Tanahjampea region and is oriented N-S to NNW-SSE. The gravity anomaly values range from -100 mGal to +250 mGal. This trend parallels the orientation of Bone Bay (see Chapter 5). The second trend occurs to the south of the first, in the area of Kalao, Kalaotoa and Flores islands. The orientation is E-W and the gravity values range from -125 mGal to +175 mGal.

On the basis of contour patterns and gravity values, the Flores Sea Islands and vicinity can be divided into several structural domains (see Fig. 10.6), these being the Selayar-Tanahjampea High, Selayar Low, Bone High and Bone Low with a N-S to NNW-SSE trend and the Kalao-Kalaotoa High and Flores Low in the E-W trend.

The Selayar-Tanahjampea High extends from Selayar to Tanahjampea. To the north, the high may continue onto South Sulawesi but to the south it terminates abruptly at the E-W trending Kalao-Kalaotoa High. The highest gravity values are +210 mGal on Pasi Island (west of Selayar) and +210 mGal on southwestern Tanahjampea. Pasi Island is covered by Pliocene and Quaternary carbonate rocks while exposures on Tanahjampea are dominantly of granitic rocks. Pulasi and Tambolongan, situated in the region of lower gravity between Selayar and Tanahjampea are reportedly ophiolitic (Koswara *et al.* 1993).

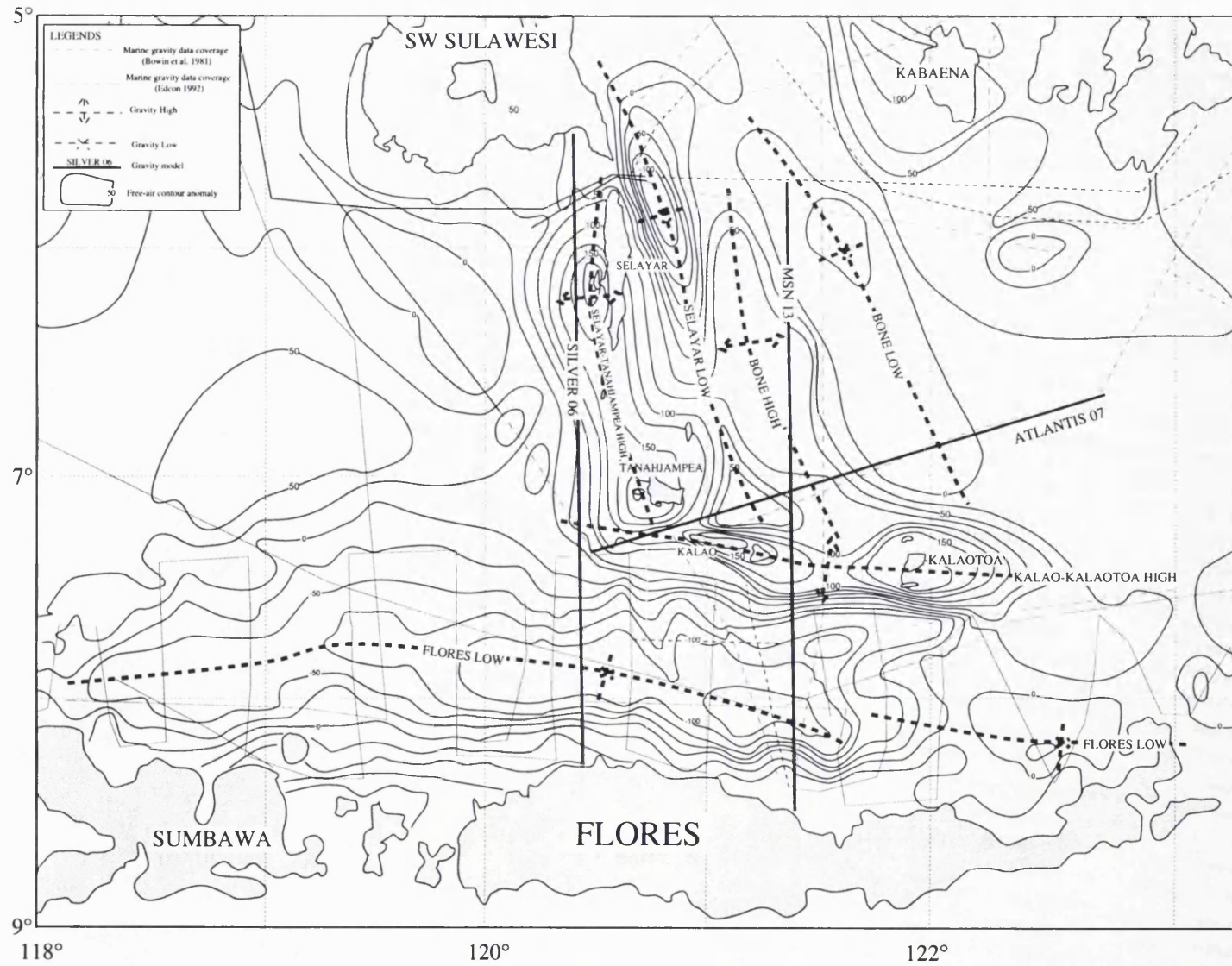


Figure 10.6: Free-air anomaly map of the Flores Sea islands and vicinity (compiled from 1993 Flores Sea Islands gravity survey; free-air anomaly map of Bowin (1980); free-air anomaly map of Edcon (1991))

Parallel and to the east of the Selayar-Tanahjampea High is the Selayar Low where the free-air gravity values range from -100 mGal to +50 mGal. The northern part of this low has been discussed in the part of Chapter 5 which deals with the southernmost part of Bone Bay; it continues into South Sulawesi as the Walanae Low in the Walanae Depression. The southern part of this low terminates to the north of Kalao where it is cut by the E-W trending Kalao-Kalaotoa High. In total, this low extends over more than 600 km.

Parallel and to the east of the Selayar Low is the Bone Low, separated from it by the narrow zone of the Bone High. Free-air gravity values in the Bone Low range from -25 mGal to 0 mGal. The low continues into Bone Bay where it corresponds to a rifted basin filled with thick sediments (see Chapter 5, Section 5.5).

The Kalao-Kalaotoa High which terminates the four gravity domains described above is characterised by an E-W trending free-air anomaly contour closure and by gravity values in the range from +100 mGal to +184 mGal. The highest values (+174 mGal in Kalao and +185 mGal in Kalaotoa) were measured where ophiolite has been mapped on this high, and is therefore considered to mark the presence of ophiolite.

To the south of the Kalao-Kalaotoa High is the Flores Low, situated in the centre of Flores Sea and characterised by E-W trending free-air anomaly contours, extending from 115°E (north of Bali) to 125°E (north of Sumba). The free-air anomaly values range from -125 mGal to 0 mGal, with the lowest values in areas where the water is at least 5 km deep. The contour trends are parallel to the main young structures in Java and the lesser Sunda islands. This structural trend is probably related to the collision of the Australian continent with the Sunda-Banda arcs in the Pliocene. In contrast, the N-S to NNW-SSE trending structures are believed to be associated with the plate boundary at the eastern margin of Sundaland, associated with Cretaceous subduction which later migrated eastwards. It is clear that the N-S to NNW-SSE gravity trends are older than the E-W trends because the former are cut by the latter.

10.4.3 Gravity models

10.4.3.1 Introduction

Three gravity models have been constructed using the two dimensional GM-SYS gravity modelling program, these being the Atlantis 07, MSN 13 and Silver 06 models.

10.4.3.2 Gravity model Atlantis 07

This model relates to an ENE-WSW line between Tanahjampea and Kalao which is approximately 255 km long. The line is named after the single channel seismic reflection line Atlantis 07 (Bowin *et al.* 1980), which also constrains the model. The final model (Fig.10.7) produces a good match between observed and calculated gravity anomalies and is consistent with the known geology.

Free-air anomaly levels decrease gradually eastward. The free-air highs and lows are, from west to east, the Selayar-Tanahjampea High, Selayar Low, Bone High and Bone Low. The Selayar-Tanahjampea High, reaching +125 mGal, and Bone High, reaching +100 mGal, correspond to basement uplifts covered by thin (less than 0.5 km) sediments. The depths to the Moho are about 17 km beneath the Selayar-Tanahjampea and Bone highs.

The Selayar Low, reaching 0 mGal, corresponds to a deep basin flanked by basement uplifts and filled with thick (more than 1 km) sediments. This basin may have been originally formed by rifting. The depth to the Moho is about 25 km.

The Bone Low, reaching -50 mGal, corresponds to a basin filled with more than 1.5 km sediments. The depth to the Moho is about 17 km.

10.4.3.3 Gravity model MSN 13

This model relates to a line across the Flores Sea in a N-S direction, perpendicular to structure and gravity anomalies. The model is named after seismic refraction station MSN 13, which constrains the model. The effect of subducted lithosphere of the Indo-Australian Plate beneath the Sunda-Banda arcs is also included in the model, using the same parameters as in Chapter 8, section 8.7.3.2. The model, shown in Fig.10.8, produces a good match between observed and calculated gravity anomalies. There are

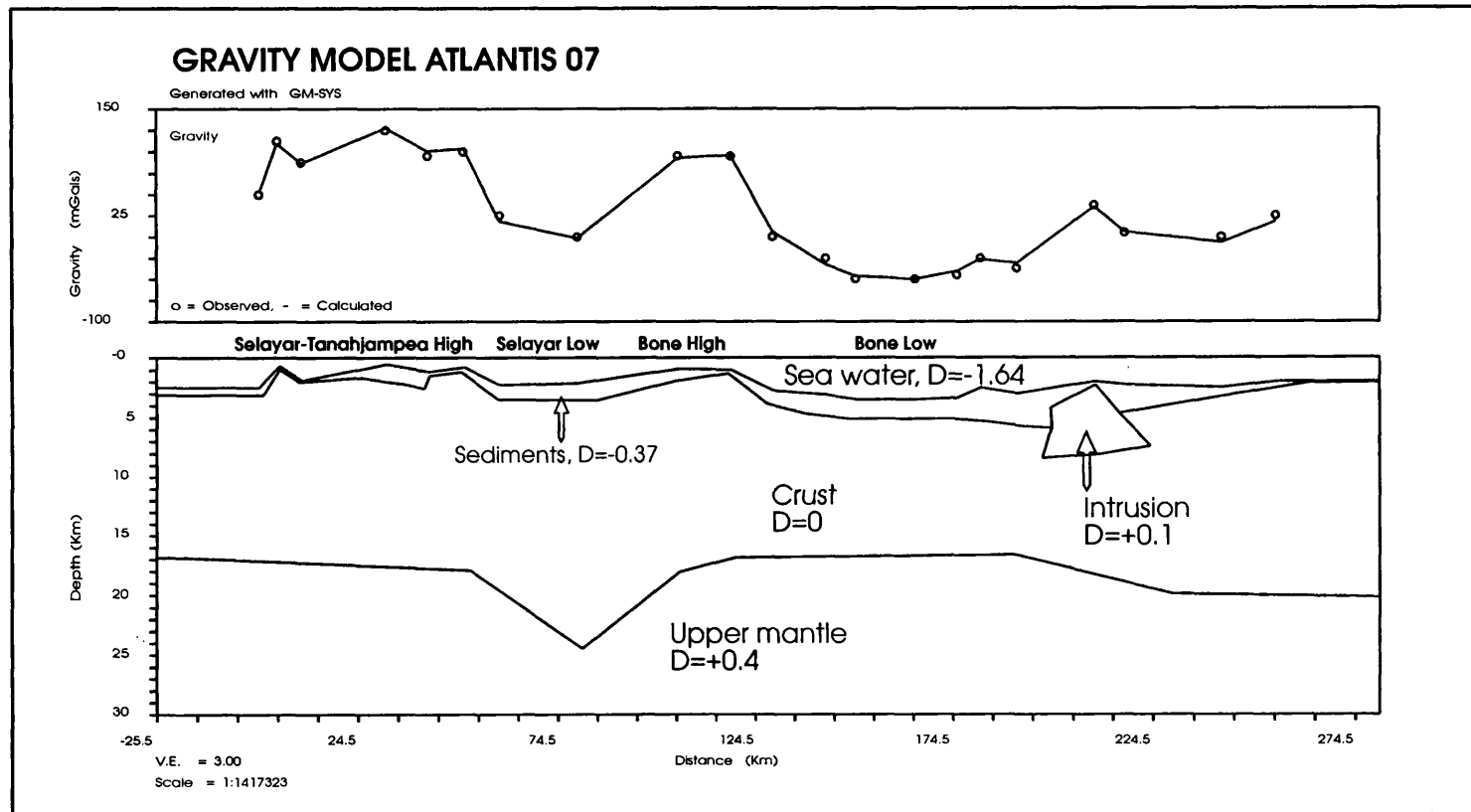


Figure 10.7: Gravity model Atlantis 07 showing the crustal thickening beneath the Selayar Low and crustal thinning beneath the Bone Low

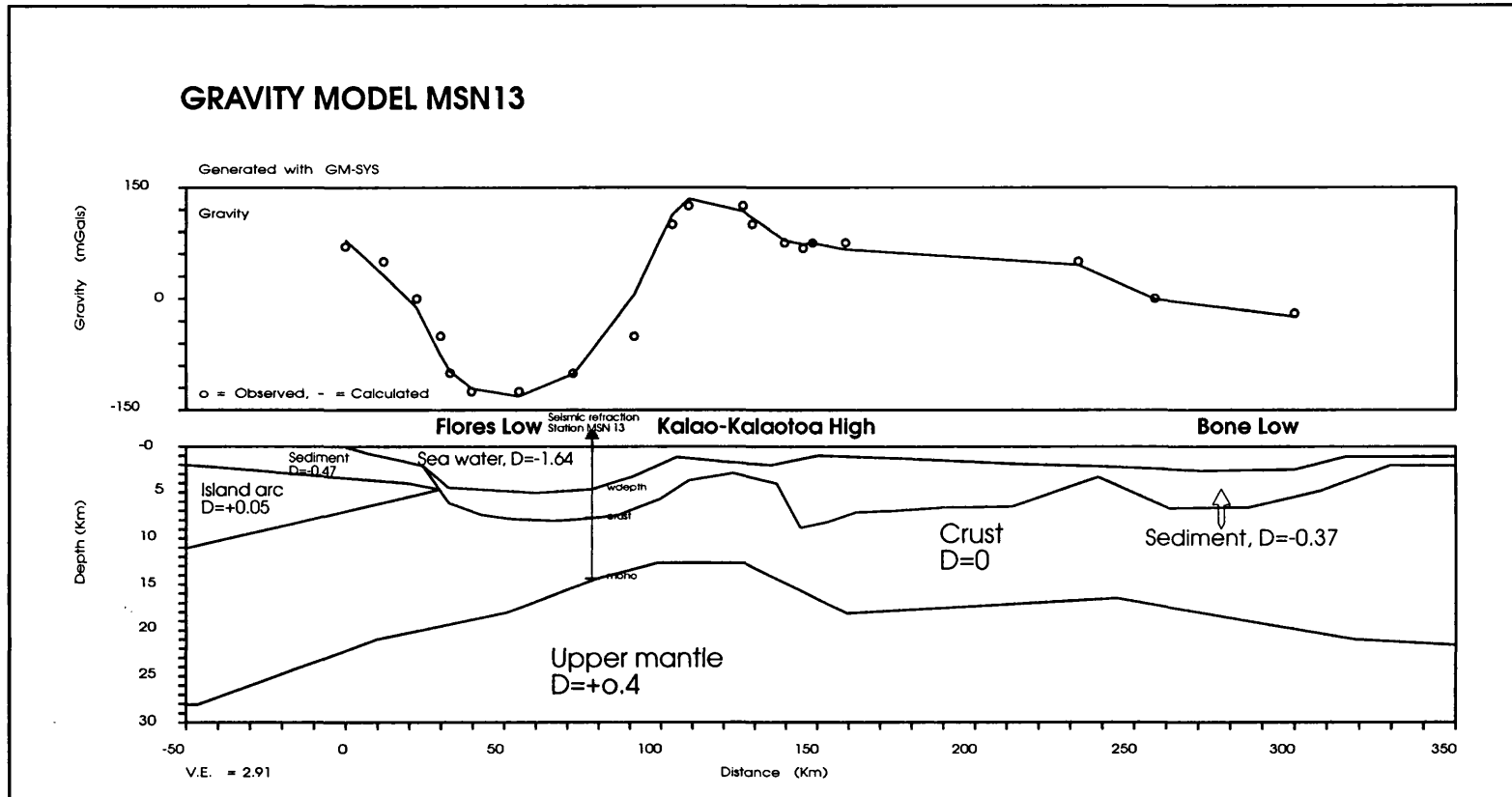


Figure 10.8: Gravity model MSN 13 showing crustal thinning beneath Flores Low in the Flores Sea, suggesting the presence of oceanic crust

three major structural domains, these being the Flores Low, Kalao-Kalaotoa High and Bone Low.

The Flores Low corresponds to the deepest part of the Flores Sea, and has minimum free-air anomaly of -125 mGal. The maximum sediment thickness is about 3 km. The depth to Moho is 14 km and increases sharply to the south to more than 23 km towards the island arc.

To the north of the Flores Low is the Kalao-Kalaotoa High, where the free-air anomaly reaches +125 mGal. This high corresponds to a basement uplift which is probably associated with the ophiolitic emplacement. The sediment is thin over this high (less than 0.5 km). The depth to the Moho is 12 km and increases sharply to the north, to about 17 km toward Bone Bay.

The Bone Low reaches a minimum free-air anomaly of -20 mGal. This low corresponds to a basin containing more than 1.5 km sediments. The depth to the Moho is about 21 km.

10.4.3.4 Gravity model Silver 06

The model is named after seismic line 06 (Silver *et al.* 1986), which is used to constrain the model. This line runs parallel to the profile MSN 13 and about 90 km farther west. The effect of subducted lithosphere of the Indo-Australian Plate beneath the Sunda-Banda arcs is considered using the same parameters as in Chapter 8, section 8.7.3.2. The model is shown in Fig.10.9. There is a good match between observed and calculated gravity anomalies and with the known geology.

Towards the island arc the free-air anomaly increases to +50 mGal, and the depth to the Moho reaches nearly 30 km. To the north the value decreases sharply to - 100 mGal over the centre of the Flores Sea where the water depth is approximately 5 km. The thickness of sediments beneath this low is about 2.5 - 3 km, and the depth to the Moho is 15 km.

To the north of the Flores Low is the Selayar-Tanahjampea High where the maximum free-air anomaly reaches +150 mGal. The high corresponds to a basement uplift which

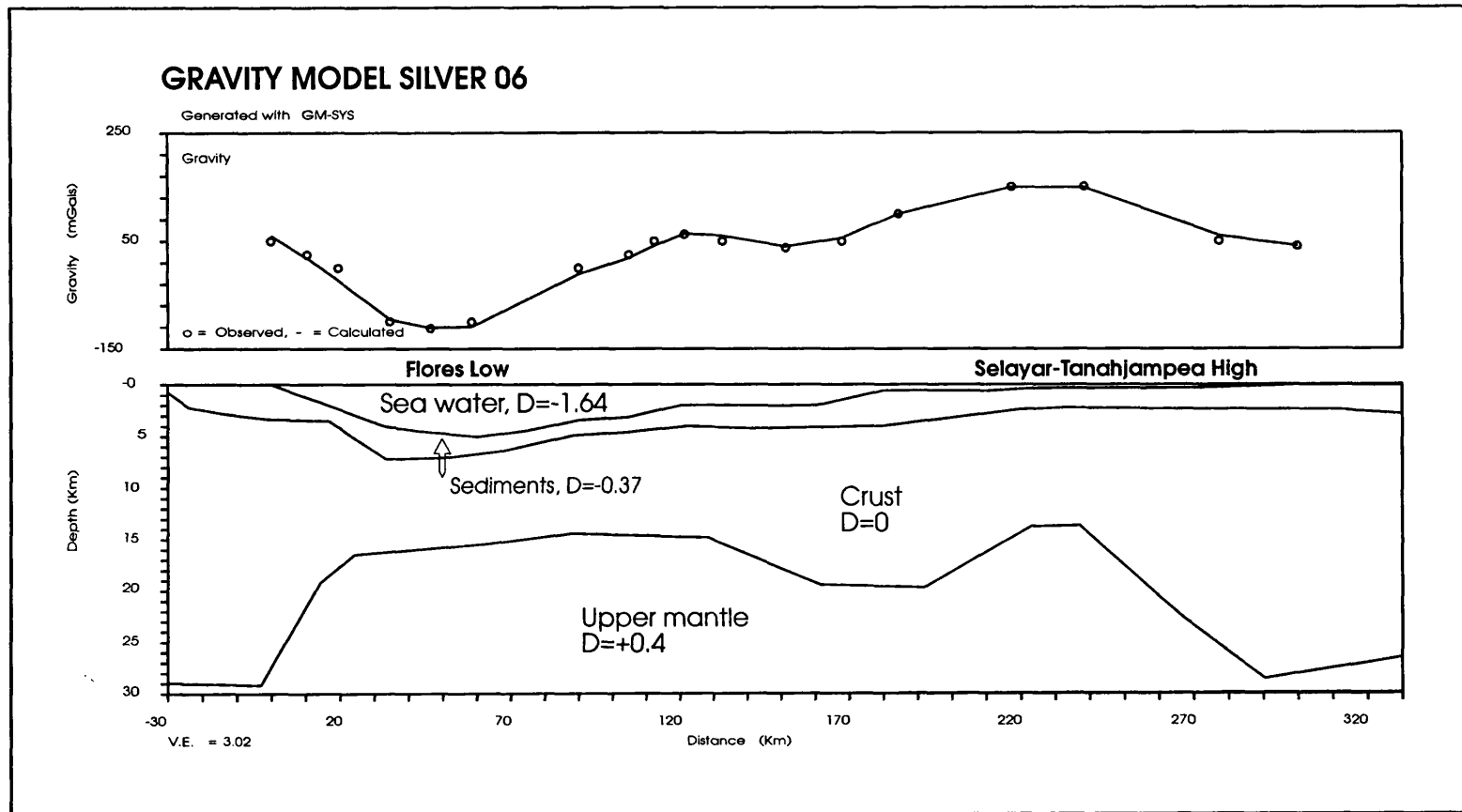


Figure 10.9: Gravity model Silver 06 showing cruatal thinning beneath Flores Low, suggesting the presence of oceanic crust

may be due to a basic igneous intrusion (Fig.10.3). The depth to Moho is about 14 km. Towards the margin of South Sulawesi the free-air anomaly decreases to +20 mGal and the depth to Moho increases to 29 km.

10.5 CRUSTAL STRUCTURE

Profiles Silver 06 and MSN 13 show that the minimum free-air anomaly does not correspond to the deepest water but is shifted approximately 15 km to the south. This is interpreted as due either to the northward subduction of Indo-Australian lithosphere beneath the Sunda-Banda arcs or to arc polarity reversal in the Flores Sea in which oceanic crust has been subducted southwards by about 30 km (Silver *et al.* 1983). The two models show that the Moho beneath the Flores Sea lies at about 14 km - 15 km in a maximum water depth of 5 km and with a maximum sediment thickness of 3.5 km. Therefore the minimum thickness of the crust, excluding the sediments, is about 6 km. Such thickness is typical of oceanic crust.

In the gravity model Atlantis 07, the Selayar Low, which continues onto south Sulawesi as the Walanae Low, is underlain by Moho at a depth of about 25 km and the basin is defined by block faulting flanked by uplifted topography. In the gravity model IND 116 (Chapter 5, Section 5.6.3.2.2) the low was interpreted as indicating former subduction; the low on gravity model Atlantis 07 is therefore also interpreted in this way.

In general, the Flores Sea and vicinity are characterised by crustal thinning, and the gravity highs on Tanahjampea and in the Bone Basin are thought to be due to not only igneous intrusion but also to significant uplift of mantle material.

10.6 TECTONIC IMPLICATION

The Selayar Low, extending from South Sulawesi (Walanae Low) in the north almost to Kalao in the south, a distance of about 600 km, is interpreted as a regional structure. Further gravity models (IND 116 in Chapter 5 and Atlantis 07) suggest that this low is associated with a basement fault and with Moho depths of 30 km and 25 km respectively. This is interpreted as a site of former subduction associated with the migration of subduction at the eastern margin Sundaland since the Cretaceous. The presence of ophiolitic rocks in the Latimojong Mountains (South Sulawesi) can be

correlated with the presence of ophiolite on Kalao and Kalaotoa, based on the continuation of the gravity trend between these ophiolites. The emplacement of these ophiolites at their present sites is interpreted as associated with the collision between East and West Sulawesi in the Oligocene, a period marked by the absence of volcanism in South Sulawesi.

In Chapter IX.2, the similarity between granitic rocks in South Sulawesi and Tanahjampea was noted. From gravity contours, these two areas are also linked continuously by a gravity trend without significant disturbance. This strongly indicates that South Sulawesi and Selayar-Tanahjampea form a magmatic arc related to subduction to the east since the Eocene.

Between and on Sulawesi and Tanahjampea, the gravity contours show N-S to NNW-SSE trends, parallel to the main structures in Sulawesi and roughly to the geometry of subduction in the Late Cretaceous. In contrast, on Kalao-Kalaotoa and between there and Flores the gravity contours show strongly E-W directions. These trends are parallel to the main structures in Java and the lesser Sunda islands, and to the present-day subduction to the south. It is, therefore, likely that the opening of the young Flores Basin is associated with the change of structural patterns discussed above. It is interpreted that the opening was caused by the rupture of Cretaceous-Early Tertiary subduction, which was probably related to the movement of one of the splays of the Sorong Fault Zone. Old basement faults have been mapped by Silver *et al.* (1986) to the north of Flores thrust (see Section IX.2.3). The rupture caused the clockwise rotation of Java and the lesser Sunda Islands. Later on, the impact of the Australian continent on the Sunda-Banda arcs was accommodated by reactivation of strike-slip faults, forming the present Flores Thrust Zone.

CHAPTER ELEVEN

SUMMARY AND TECTONIC EVOLUTION

11.1 SUMMARY OF GEOLOGICAL PROVINCES

The following is a summary of the conclusions which can be drawn from this study regarding the geology and crustal structure of each province in the Central Indonesian region and vicinity.

11.1.1 BONE BAY PROVINCE

There is relatively little geological and geophysical information to be obtained from previous published studies in this province. This area can, therefore, be regarded as frontier area. Daly *et al.* (1991) suggested that the opening of Bone Bay was caused by the collision of northern margin of the Australian continent with the Sunda-Banda arcs in the Pliocene.

The present study has provided some additional information about its evolution using techniques of gravity and seismic interpretation. Some of the major conclusions which can be drawn are as follows;

1. Bone Bay is an extensional basin which is marked by syn-rift and post-rift sediments. However, the area at the head of the bay is marked by compression. The pattern of compression in the northern part and extension in the southern part is interpreted to be due to the collision of the Banggai-Sula microcontinent with East Sulawesi in the Middle Miocene. The collision was with a left lateral component to this collision allowed compression in the north and extension in the south.

2. The Selayar Trough is linked in the north to the Walanae Depression of SW Sulawesi and in the south extends to the region north of Kalao. These areas are marked by continuity of low free-air anomaly. Gravity models suggested that this gravity low marks the trace of Early Tertiary subduction. This subduction ceased in the Oligocene when East Sulawesi collided with West Sulawesi, an event

marked by the emplacement of the Latimojong basement complex in SW Sulawesi.

3. Gravity models suggest the thickness of the crust in the middle of Bone Bay may be as little as 5 km. This such a thickness may suggest that Bone Bay is underlain by oceanic crust.

11.1.2 MAKASSAR STRAIT PROVINCE

There have been several previous studies of the Makassar Strait but the evolution and crustal structure are still controversial. Ideas of the crustal structure beneath the strait can be grouped into two; the first of these is that oceanic spreading has taken place and the strait is underlain by oceanic crust (Katili 1978; Hamilton 1979), the second that only continental rifting has occurred and that the strait is underlain by attenuated continental crust (Burrolet and Salle 1981, Situmorang 1982). The time of opening of the Makassar Strait is also still uncertain; Katili (1978) suggested that opening took place in the Quaternary, whilst Daly *et al.* (1991) suggested that a deep basin had formed in the Makassar Strait by Miocene times. Situmorang (1982) proposed that the rifting in the Makassar Strait started in Lower-Middle Eocene and continued until the Lower Miocene. The Makassar Strait has recently been interpreted as a foreland basin bounded on both sides by converging Neogene thrust belts (Bergman *et al.* 1994).

Conclusions from the present study for the Makassar Strait Province are as follows:

1. Seismic interpretation indicates that the Makassar basin is a rifted basin marked by the deposition of syn-rift and post-rift sediments. An Eocene opening of the Makassar Strait is inferred from the deposition of syn-rift sedimentary rocks.
2. The separation between the North Makassar Basin and South Makassar Basin occurred after Middle Miocene, when thrust faults displaced Horizon H5 in the seismic profile PAC 201. These complex thrust faults are confined to the region between two major right lateral strike-slip faults (the Paternoster and Sangkulirang faults) and local compression in this region produced characteristics of a foreland basin here.

3. Gravity models suggest that the thickness of crust in the centre of the Makassar Strait may in places be as little as 6 km. This thickness suggests that parts of the strait are underlain by oceanic crust.

11.1.3 CENTRAL JAVA SEA PROVINCE

In this thesis the term of Central Java Sea is used to defined an area which has NE-SW structural trends and is bounded to the west and east, respectively by the West Java Sea, which has N-S structural trends, and East Java Sea which has E-W structural trends.

This region is part of what is known as the East Java Sea in the literature.

From the present study, some conclusions pertinent to the evolution of the Central Java Sea Province can be drawn as follows:

1. Seismic interpretation suggests that the Tertiary basin was formed by block faulting. It is interpreted as a rifted basin which developed in the Eocene.
2. Four major Bouguer anomaly highs can be correlated with the main pre-Tertiary structural trends of SE Kalimantan, and thus support the existence of a tectonic link between the Java Sea and SE Kalimantan in the Cretaceous.
3. Gravity models suggest that the crustal thickness in Central Java Sea reaches nearly 30 km, consistent with continental crust underlying this province.
4. The crust is thickest in the eastern part of the province, suggesting crustal thickening due to compression. The limit of the thickened crust provide a constraint on the geometry of the plate boundary in the Early Cretaceous.

11.1.4 EAST JAVA SEA PROVINCE

The term East Java Sea in this thesis is used to defined an area rather different from that in the literature. In this thesis the East Java Sea is defined as the area where gravity, bathymetry and structural trends are in E-W directions, and is separated from the Central Java Sea to the west, which is characterised by NE-SW trends. The crustal structure in the region is still controversial. Hamilton (1979) suggested that the crust in the Bali Basin is transitional in thickness character, and the East Java Sea is underlain by a

basement of composition and origin quite different from that of the Sunda Shield to the northwest. Ben-Avraham and Emery (1973) inferred that oceanic crust is present beneath the Bali and Madura basins.

The conclusions from the present study for the East Java Sea Province are as follows:

1. Seismic interpretation suggests that the basin in the East Java Sea experienced three major tectonic events, these being; Cretaceous compression, Eocene crustal extension and Neogene inversion.
2. In the Cretaceous, the East Java Sea is believed to have been part of the East Java Microplate, which originally had structural orientations in NE-SW directions. Folded and thrustured Cretaceous sediments in the East Java Sea appear similar to those observed on seismic section west of Selayar (Flores Sea Province). The trends of magnetic contours also have these orientations.
3. Extension in the Eocene may be related to subduction roll-back east of west Sulawesi.
4. The Neogene inversion structures were produced by the collision between the northern margin of the Australian continent and the Sunda-Banda arcs.
5. The high Bouguer anomaly in the East Java Sea is interpreted as partly due to the northward subduction of Indo-Australian lithosphere beneath the Sunda-Banda arcs.
6. Crustal thickness deduced from gravity models varies from 18 to 24 km, suggesting the region is underlain by stretched continental crust.

11.1.5 FLORES SEA PROVINCE

The Flores Sea Islands are situated between SW Sulawesi and Flores. Geological and geophysical data for this region were previously very limited but geological and gravity surveys carried out on the islands as part of this study provide new constraints on and

insights into the evolution of the region. Some data and conclusions for the Flores Sea Province can be drawn from this thesis as follows:

1. The Flores Sea Islands can be grouped into two major geological provinces on the basis of structural trends; the Selayar-Tanahjampea and Kalao-Kalaotoa islands. The implication of this division is that these two provinces have different origins. The Selayar-Tanahjampea structural trends are thought to have derived from Early Tertiary subduction stress, whilst the Kalao-Kalaotoa islands, where structural trends are parallel to the young trends of Java and the Sunda arcs are interpreted as a result of the collision of the northern margin of Australian continent with the Sunda-Banda arcs.

2. Geological mapping on the Flores Sea Islands has confirmed that Tanahjampea is mainly composed of granitic rocks, and that these can be correlated with granitic rocks on SW Sulawesi and probably with granodioritic rocks on Flores which are of Middle Miocene age. This interpretation suggests the presence and continuity of a subduction zone to the east of these regions.

3. Although Tanahjampea and the Kalao-Kalaotoa islands are divided into different geological provinces, Bouguer anomaly values are not very different; on Tanahjampea the values range from +145 mGal to +195 mGal, whereas on Kalao the range is from +150 mGal to +170 mGal and on Kalaotoa the range is from +165 mGal to +180 mGal. The implication of this is that Tanahjampea and Kalao-Kalaotoa islands are likely to be underlain by similar basement rocks. These magmatic rocks were probably a result of previous subduction.

4. The E-W strike directions of the Kalao-Kalaotoa islands are interpreted as having developed when the subduction zone was ruptured followed by the opening of the Flores Sea in the Late Miocene. The opening process transported some of the magmatic rocks to their present position.

5. Gravity modelling suggests the crustal thickness in the central Flores Sea is only 6 km. This is taken to indicate that the Flores Sea is underlain by oceanic crust.

11.2 EVOLUTION OF THE CENTRAL INDONESIAN REGION

The present configuration of the Indonesian archipelago is considered to be a result of the interaction of the Eurasian, Indo-Australian and Pacific plates since at least the Cretaceous. The tectonic evolution of the CIR which lies at the triple junction of plate interaction began in the Early Cretaceous and was influenced later by collision with some microcontinents derived from the northern margin of the Australian continent. In Chapter 3.1.1 the Central Indonesian Region (CIR) has been defined as consisting of the Makassar Strait, Central Java Sea and East Java Sea provinces. The Bone Bay and Flores Sea provinces are not included in the CIR, but their position at its eastern margin is considered crucial in explaining the evolution of CIR as a whole, and they have therefore also been studied in detail in this thesis.

Taken together, geological and geophysical studies suggest that the Central Indonesian Region and vicinity are characterised by faulting, rifting, compressional deformation, magmatic events producing both plutonic and volcanic rocks, basement complexes, ophiolites and metamorphism. The complex geological phenomena are interpreted as involving many geological processes such as deformation of an previously tectonically fragmented terrane, juxtaposition of sweeping of fragments against unrelated terranes, thrusting of oceanic and mantle material over island-arcs of different ages, closing of deep sea basins behind arcs, trapping of old oceanic crust, formation of marginal basins by the spreading of the sea floor behind the arc and development of small subduction zones with reverse polarities, etc. The region represents a continental margin which has been repeatedly deformed at a subduction boundary. All these phenomena have occurred in the CIR and understanding of these processes is vital in any synthesis of the tectonic evolution of the Central Indonesian Region.

Figures 11.1-6 show possible models of plate kinematic reconstruction from Late Cretaceous to Late Miocene. These reconstructions summarise the geological and

geophysical data from the CIR and also integrate previous models from Hamilton (1979), Daly *et al.* (1991) and Parkinson (1991).

The Cretaceous basement complexes in Java, the Java Sea, SE Kalimantan and SW Sulawesi are believed to constrain the geometry of subduction between the East Java Sea microplate and the Indo-Australian Plate (Fig. 11.1). The trends on magnetic and gravity maps (see Fig. 3.10 and 3.16) are also continuous from Java to SE Kalimantan through the Java Sea, and palaeomagnetic results also indicate that SW Sulawesi lay close to its present position relative to East Kalimantan during the Mesozoic (Haile 1978; 1981). There is strong evidence from the distribution of sediments for the presence of west-dipping subduction at the eastern margin of the East Java Sea microplate and the close juxtaposition of SW Sulawesi and SE Kalimantan in the Late Cretaceous. The presence of the Alino Formation, the Paniungan beds, the Manunggul Formation and the plutonic and volcanic rocks in the Meratus Mountains are considered to support the presence a Cretaceous subduction zone in the eastern margin of the East Java Sea microplate (Katili 1978; Sikumbang 1990). There are also similarities between the Upper Cretaceous Manunggul Formation (SE Kalimantan) and the Upper Cretaceous Balangbaru Formation (SW Sulawesi), suggesting that these two areas once lay close together (Hasan 1990).

In the Late Cretaceous, the Pacific Plate pushed Western Sulawesi against SE Kalimantan causing the closure of the intervening oceanic basin, which finally led to collision (Sikumbang 1986). This event resulted in the uplift of the Meratus Mountains and the emplacement of basement complexes in the Meratus range and SW Sulawesi (Fig. 11.2).

Shortly following this collision, the passive margin east of Western Sulawesi changed to an active margin to accommodate the compression from the continuing movement of the Pacific Plate. West-dipping subduction was active again, forming the Pompangeo Schist Complex in the present Central Sulawesi and is thought to have been responsible for the volcanic activity in SE Kalimantan. Some authors (Barber 1981, Sikumbang 1986 and Parkinson 1991) considered that the Bantimala Complex (SW Sulawesi) and Pompangeo Schist Complex have the same Late Cretaceous age and interpreted them as

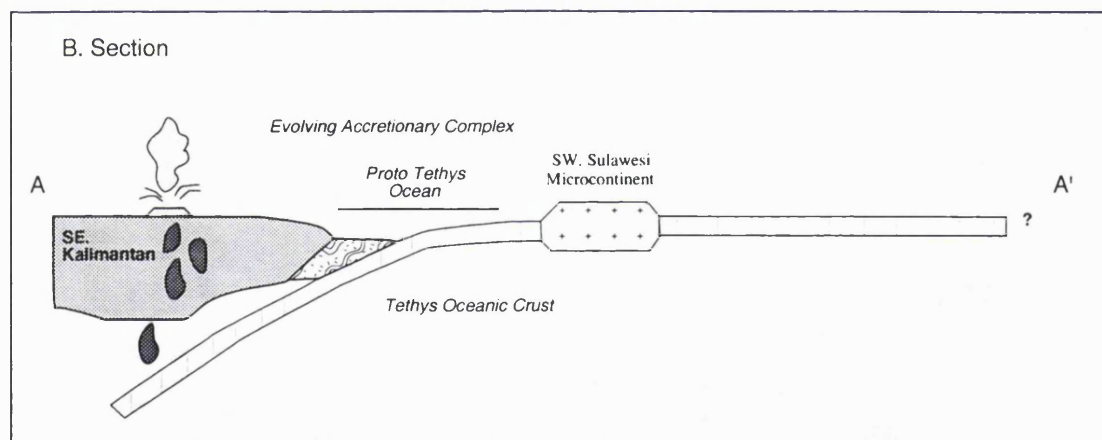
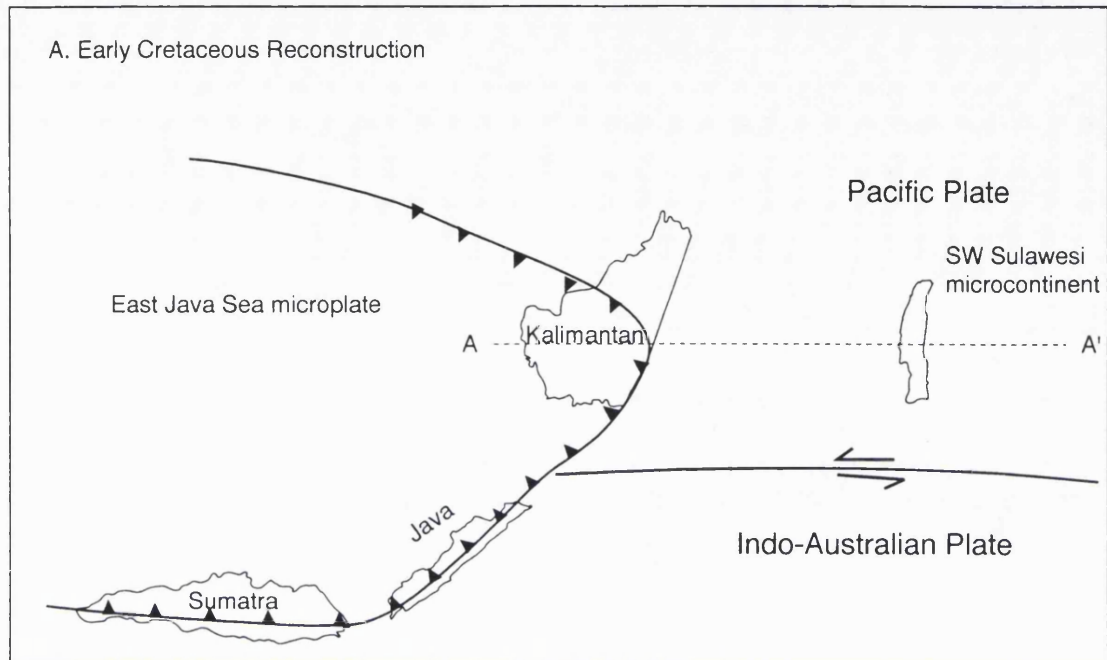


Figure 11.1: Early Cretaceous reconstruction (a) and section (b) showing the configuration of the junction between the East Java Sea microplate, the Pacific Plate and the Indo-Australian Plate. Subduction extends from Sumatra through Java, the proto Java Sea and SE Kalimantan, generating an accretionary complex. The boundary between the Indo-Australian and Pacific Plates is probably a transform fault. In the east, the SW Sulawesi microcontinent was conveyed along this transform.

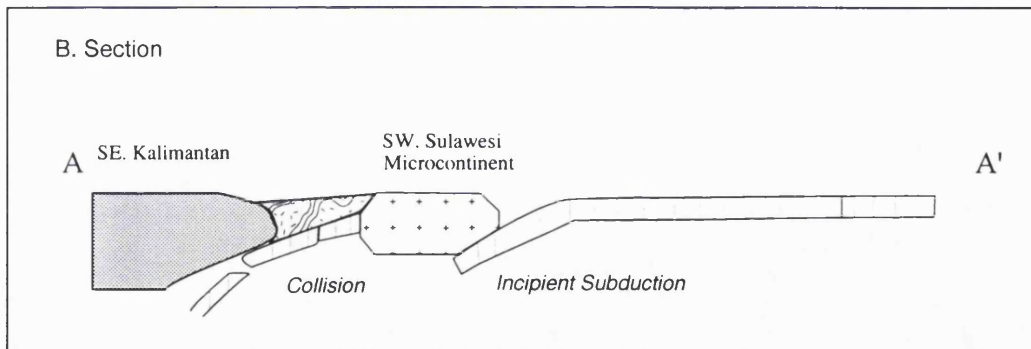
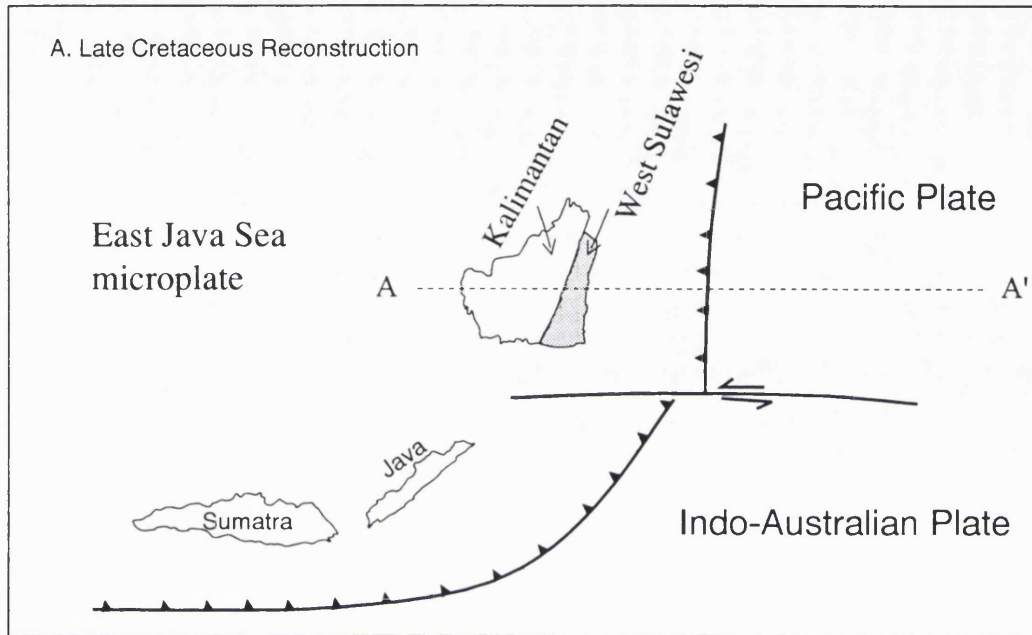


Figure 11.2: Late Cretaceous reconstruction (a) and section (b) showing how, after collision of the SW Sulawesi microcontinent with SE Kalimantan and emplacement of basement complexes, the passive margin east of SW Sulawesi changed to an active margin to accommodate continuing movement of the Pacific Plate.

part of the same accretionary terrane. However, the Bouguer and free-air anomaly contours associated with the two complexes have different trends, suggesting different basement configurations. The Bantimala Complex is dominated by NNE-SSW trends, linking it to Java, the Java Sea and SE Kalimantan, whereas orientations in the Pompangeo Schist Complex are N-S to NNE-SSW and continue southwards towards Flores. Therefore these two complexes are regarded here as separate accretionary terranes.

In the Paleocene, the whole area of the Meratus mountains was uplifted and associated with block faulting (Fig. 11.3).

In the Eocene, an increase in plate convergence is thought to have caused vertical sinking of the subducting plate east of Western Sulawesi and to have led to trench-rollback (Fig. 11.4). This vertical sinking was accommodated by extension and rifting of the crust located in the previous site of collision behind the subduction zone, and interpreted to cause the opening of the Makassar Strait, Central Java Sea and East Java Sea.

In the Lower Oligocene, collision and obduction of the Eastern Sulawesi ophiolite against SW Sulawesi, as suggested by Parkinson (1991), may have terminated the rifting of the CIR (Fig. 11.5) where this period is marked by the deposition of post-rift sedimentary rocks. Thrust faults which interspersed slivers of oceanic crust with the Peluru Melange Complex were a result of this collision. Later this thrust complex was covered by sedimentary rocks. This model provides an explanation for the westward thickening of the ophiolite, the emplacement of the Peluru Melange Complex beneath the ophiolite, the presence of undeformed sedimentary rocks over the basement complex, and also relates the opening of the basins in the CIR to the trench-rollback. Additional evidence for this subduction and collision is provided by the presence of the Latimojong Basement Complex in SW Sulawesi and ophiolite on Kalao (see Chapter 9). Gravity data (Chapter 5 and 10) show a continuous free-air anomaly low extending from Latimojong through Selayar to the region north of Kalao where it is cut by the Kalao-Kalaotoa structural high. This low is interpreted as marking the site of subduction which in the Oligocene stretched from Central Sulawesi to the region north of Kalao and

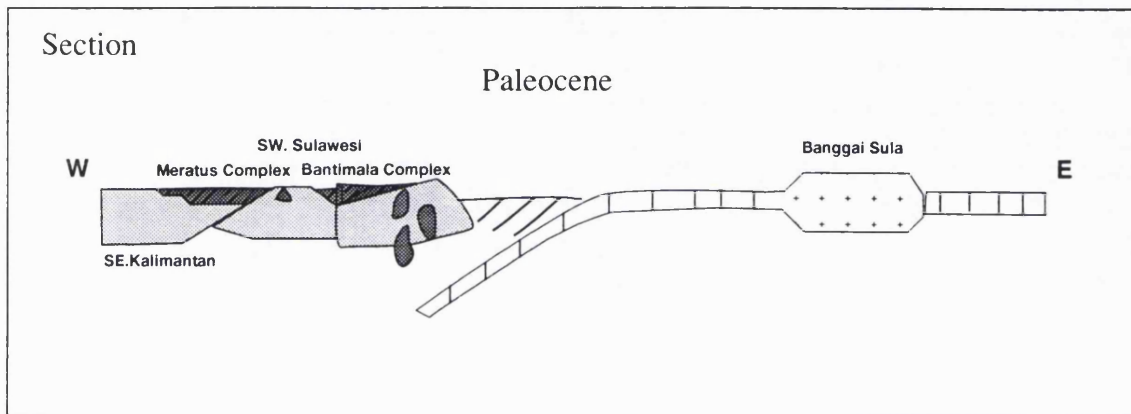


Figure 11.3: Paleocene section showing the uplift and block faulting of the collision region between SE Kalimantan and SW Sulawesi. The continuous magmatic activity in SE Kalimantan is interpreted to result from this subduction

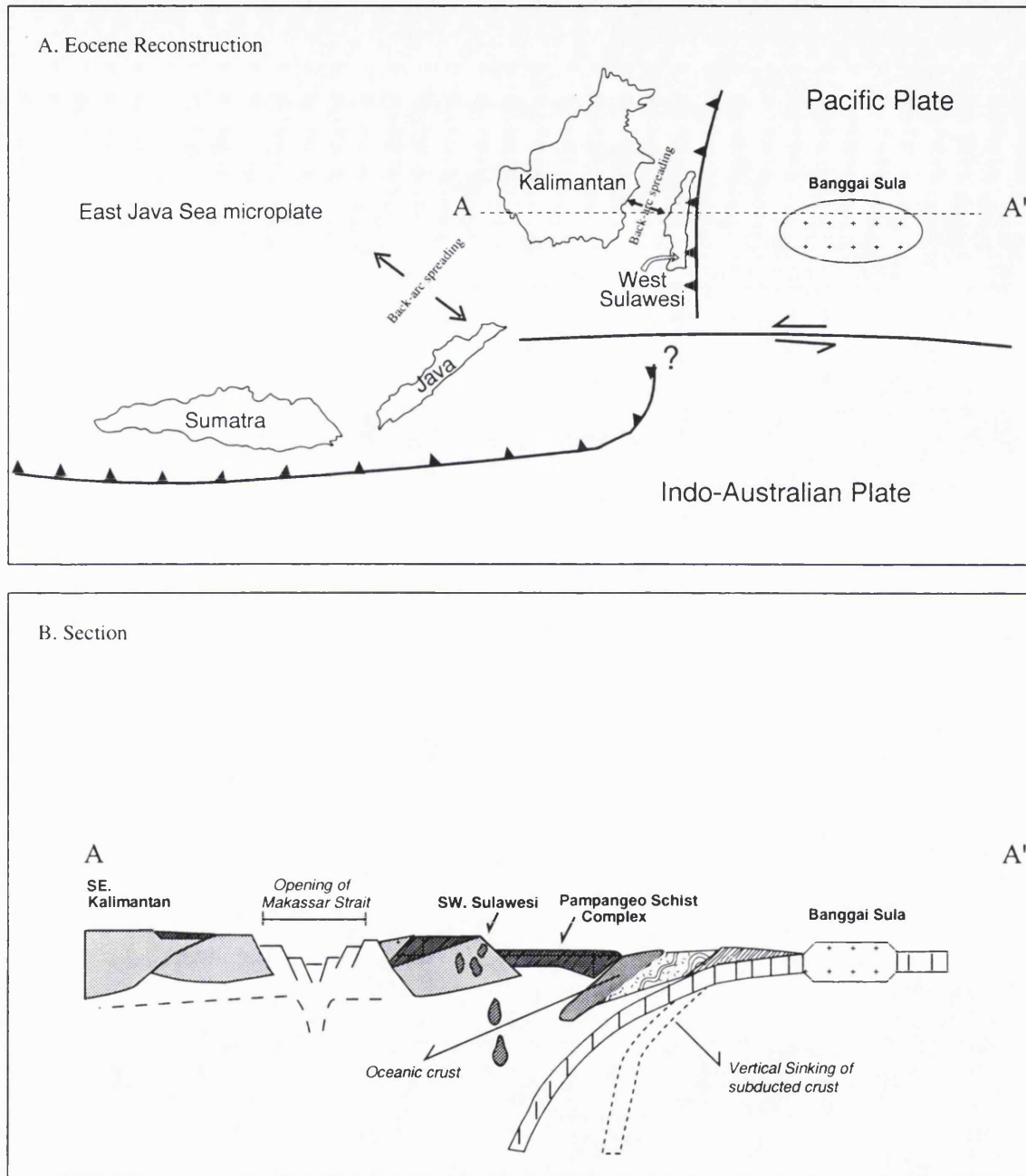


Figure 11.4: Eocene reconstruction map (a) and section (b) showing increasing plate convergence due to vertical sinking of the subducting plate causing back-arc spreading in the Makassar Strait and Java Sea, generating horst and graben structures accompanied by the deposition of rift sediments

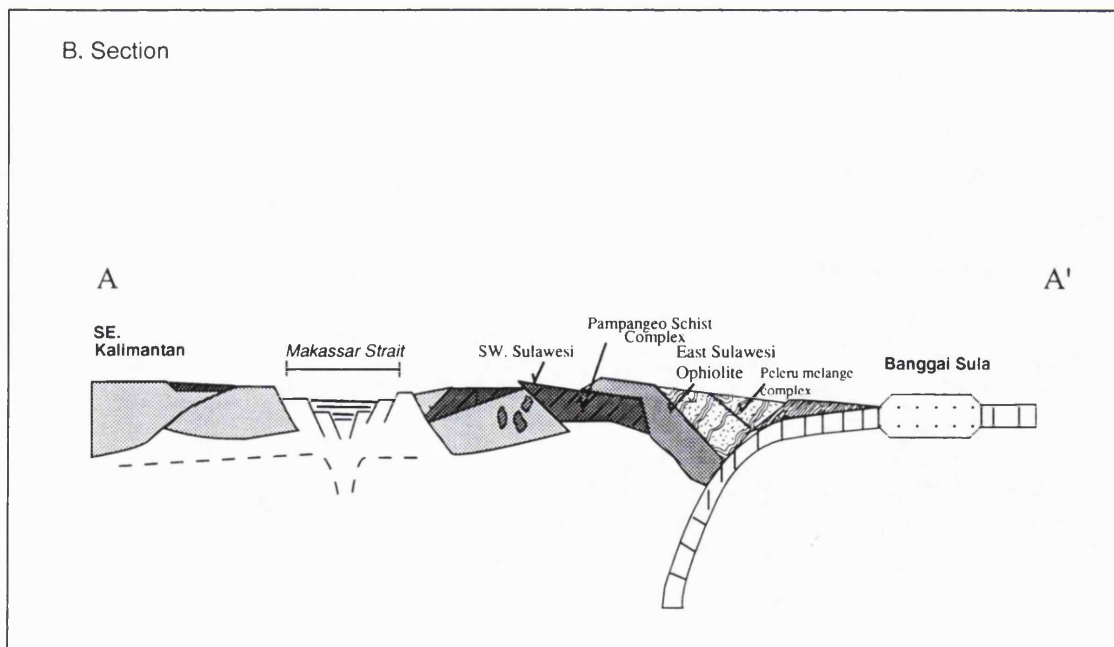
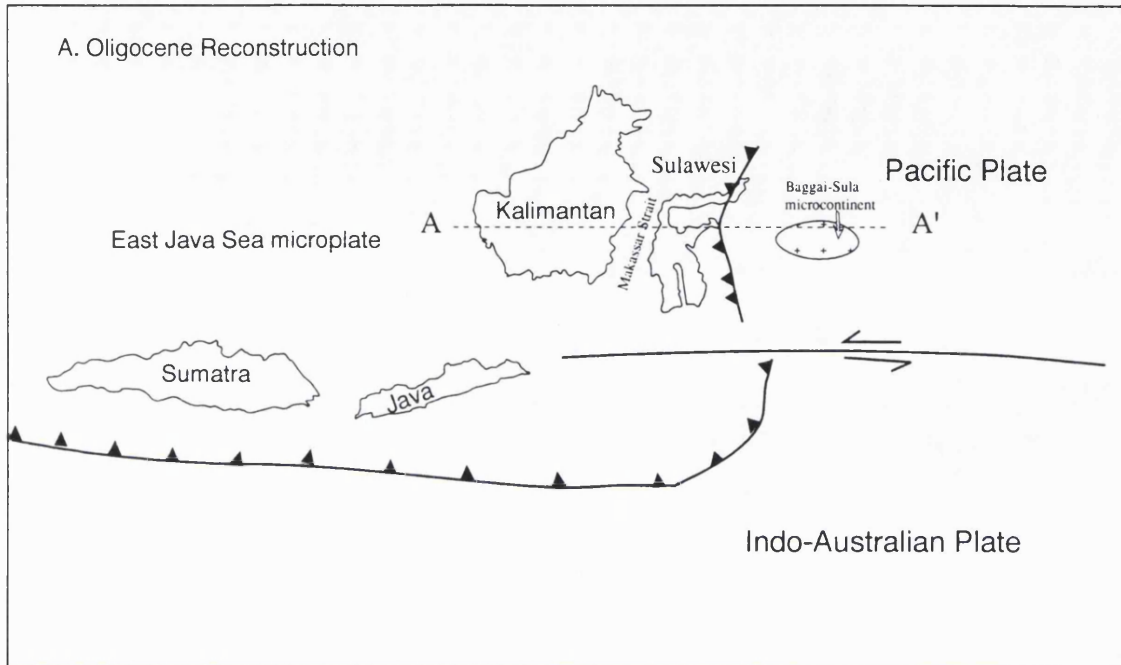


Figure 11.5: Oligocene reconstruction (a) and section (b) showing the collision of the East Sulawesi ophiolite with SW Sulawesi, causing the formation of the Peluru melange complex and the emplacement of the Latimojong ophiolite in SW Sulawesi.

probably from there southward to the Sumba Fracture, south of Flores. This Sumba Fracture was suggested by Audley-Charles (1975) as a major discontinuity between Western and Eastern Indonesia.

The continuing volcanic activity in SW Sulawesi during the Neogene is interpreted as due to active subduction east of Sulawesi which conveyed the Banggai-Sula microcontinent westwards along the Sorong Fault after detachment from New Guinea (Fig.11.6) (Hamilton 1979). The microcontinent probably collided with East Sulawesi in the Middle Miocene (Hamilton 1979; Silver *et al.* 1981, Simandjuntak 1990, and Parkinson 1991). This collision is marked by the formation of the Kolokolo Melange which contains fragments detached from both the ophiolite suite and the continental margin sequence (Simandjuntak 1990). The boundary between these two terranes is placed at the Batui-Balantak Fault (Simandjuntak 1990, Silver *et al.* 1981). The collision is inferred to have reactivated the Median Line as a thrust fault and emplaced the Pompangeo Schist Complex structurally on top of lithologies of the Western Sulawesi Plutono-Volcanic Belt. Deformation following the collision of Banggai-Sula microcontinent is thought to have caused the opening of Bone Bay along the Median Line by reactivation of the left-lateral faults (see Chapter 5, Section 5.11).

The Banggai-Sula collision is also thought to have ruptured the subduction zone, which ceased to exist in the north but persisted further south where it is now marked by oceanic depths along the line of the Tolo Thrust. The rupture also permitted the rotation of eastern Sumbawa and western Flores by some 45° CW relative to Sulawesi and the continental shelf of the Java Sea, opening up the Flores Sea in the Late Miocene (Hamilton 1979). Hamilton (1979) also suggested the islands of the presently active inner magmatic arc extending from Java expose rocks as old as Middle Miocene only as far east as central Flores, beyond which the volcanic ridge is narrower and the oldest rocks seen are Late Miocene or Pliocene. Before the rupture of the subduction zone this magmatic arc continued to the broad Neogene magmatic terrain of the South Arm of Sulawesi via northern Kalao, where granites have been reported.

In the Pliocene the tectonic development of the CIR was influenced by the collision of the Indo-Australian plate with the Banda-Sunda arc system. This caused inversion in the marginal basins and the development of back thrusts along the south margin of the CIR,

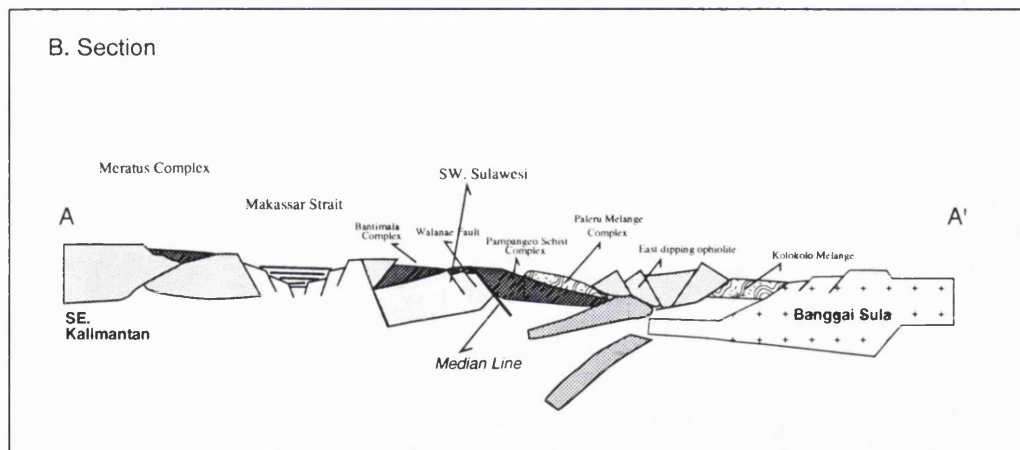
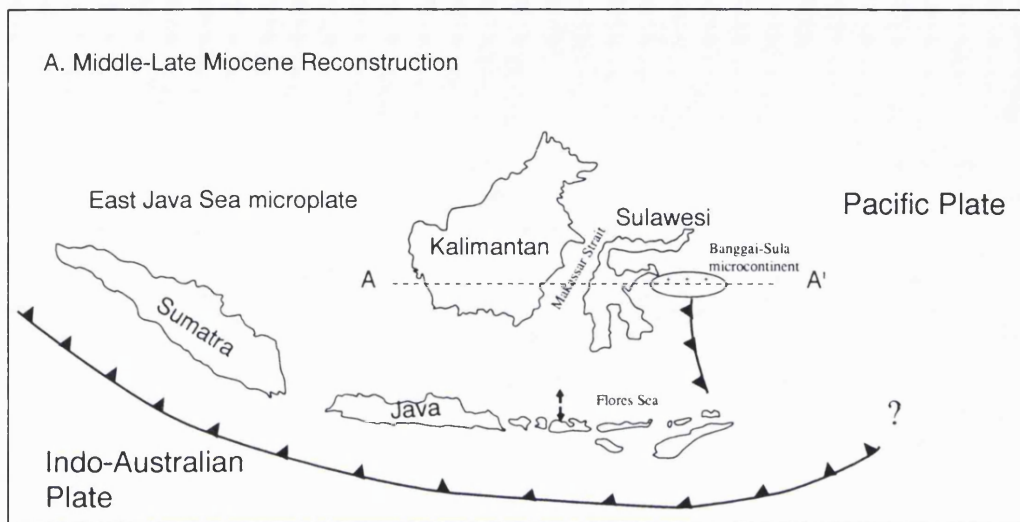


Figure 11.6: Middle-Late Miocene reconstruction (a) and section (b) showing collision between the Banggai-Sula microcontinent and East Sulawesi followed by the opening of Bone Bay. Clockwise rotation of Java, Sumbawa and West Flores was followed by the opening of the Flores Sea.

especially where blocks of thickened crust were being incorporated into the forearc further south.

11.3 RECOMMENDATIONS FOR FUTURE WORK

One of the main difficulties in explaining the tectonic evolution in the Indonesian region during the Cretaceous to Early Tertiary is that the past plate boundaries are still poorly constrained. A major conclusion of the present study is that there was a plate boundary stretching from Central Sulawesi and passing east of Selayar to the Sumba Fracture. This hypothesis needs testing; a more detailed understanding of the Flores Sea Islands is vital as they are the key to this framework since they are situated on this proposed boundary. Detailed geological mapping and palaeomagnetic study of the igneous rocks of the islands are recommended to obtain some more data to test the hypothesis. Gravity data should also be collected from the Tiger islands (Kepulauan Macan) and Kabaene Island, which both lie very close to the Flores Sea Islands. This information, which would supplement the data presented here from the Flores sea Islands, is vital to an understanding of the tectonic evolution of the Indonesian region as a whole since the Flores Sea was situated at the eastern margin of the major accretionary complex development in the Cretaceous.

REFERENCES

- ADKINS, J. S., SUKARDI, S., SAID, H., and UNTUNG, M. 1978. A Regional Gravity Base Station Network for Indonesia. *Publikasi Teknik-Seri Geofisika, No.6, Geological Survey of Indonesia*.
- ASIKIN, S. 1974. Evolusi geologi Jawa Tengah dan sekitarnya, ditinjau dari segi tektonik-dunia yang baru. *Unpublished PhD thesis, Institute Teknologi Bandung, Indonesia*.
- AUDLEY-CHARLES, M. G. 1975. The Sumba fracture: A major discontinuity between Eastern and Western Indonesia. *Tectonophysics, 26, 213-228*.
- AUDLEY-CHARLES, M. G. 1986. Rates of Neogene and Quaternary tectonic movements in the southern Banda Arc based on micropaleontology. *J. Geol. Soc. Lond. 143, 161-175*.
- AUDLEY-CHARLES, M. G. 1976. Mesozoic evolution of the margin in the Tethys in Indonesia and the Philippines. *IPA, Proceedings 5th, Annual Convention, Jakarta*.
- BARBER, A. J. 1981. Structural interpretations of the island of Timor, Eastern Indonesia. The Geology and Tectonics of Eastern Indonesia, *Geological Research and Development Centre, Bandung, Special Publication, No. 2, 183-197*.
- BEN-AVRAHAM, Z. 1978. The evolution of marginal basins and adjacent shelves. East and Southeast Asia. *Tectonophysics, 45, 269-288*.
- BEN-AVRAHAM, Z., and K. O. EMERY. 1973. Structural framework of Sunda Shelf. *American Association of Petroleum Geologist Bulletin, Vol. 57, 2323-2366*.
- BERGMAN, S. C., LOFFIELD, D. Q., TALBOT, J. P., and GARRAD, R. A. 1994. Late Tertiary tectonic and magmatic evolution of SW Sulawesi and the Makassar Strait: Evidence for a Miocene continental collision (Abstract). *Tectonic Evolution of SE Asia, The geological Society London, Burlington House, Dec. 7-8*.
- BIANTORO, E., MURITNO, B. P., and MAMUAYA, J. M. B. 1992. Inversion faults as the major structural control in the northern part of the Kutai Basin, East Kalimantan. *Indonesian Petroleum Association, Proceedings 21st Annual Convention, Jakarta, 45-68*.
- BISHOP, W. F. 1980. Structure, stratigraphy and hydrocarbons offshore southern Kalimantan, Indonesia. *American Association of Petroleum Geologist Bulletin, Vol. 4, 37-58*.

- BOWIN, C. O., PURDY, G. M., JOHNSTON, C., SHOR, G., LAWVER, L., HARTONO, H. M. S. and JEZEK, P. 1980. Arc-continent collision in the Banda Sea region. *American Association of Petroleum Geologist Bulletin*, Vol. 64, 868-915.
- BOUMA, A. H., 1962. Sedimentology of some flysch deposits. *Elsevier, Amsterdam*, 168 pp.
- BRANSDEN, P. J. E., and MATTHEWS, S. J. 1992. Structural and stratigraphic evolution of the East Java Sea, Indonesia. *Indonesian Petroleum Association, Proceedings 21th, Annual Convention, Jakarta*, 417-453.
- BUROLLET, P. F., and SALLE, C. 1981. Seismic reflection profiles in Makassar Strait. The Geology and Tectonics of Eastern Indonesia, Geological Research and Development Centre, Bandung, *Special Publication, No. 2*, 273-276.
- CARDWELL, R. K., and ISACKS, B. L. 1978. Geometry of subducted lithosphere beneath the Banda Sea in Eastern Indonesia from seismicity and fault plane solution. *J. Geophys. Res.*, 83, 2825-2838, 1978.
- CHAMALAUN, F. H., LOCKWOOD, K., and WHITE, A. 1976. The Bouguer gravity field and crustal structure of eastern Timor. *Tectonophysics*, 30, 241-259.
- CHASE, C. G. 1978. Plate kinematics: the Americas, East Africa and the rest of the world. *Earth Planet, Sci., Lett.*, 37, 355-368.
- COX, A., and HART, R. B. 1986. Plate Tectonics: How it works. *Blackwell Scientific Publication, Inc. Boston, Oxford*.
- CURRAY, J. R., G. G. SHOR, RAITT, R. W, and HENRY, M 1977. Seismic refraction and reflection studies of crustal structure of the eastern Sunda and western Banda arcs. *J. Geophys. Res.*, 82, 2479-2497.
- DALY, M. C., HOOPER, B. D. G., and SMITH, D. G. 1987. Tertiary plate tectonics and basin evolution in Indonesia. *Indonesian Petroleum Association, Proceedings 16th, Annual Convention, Jakarta*, 399-428.
- DALY, M. C., COOPER, M. A., WILSON, I., SMITH, D. G., and HOOPER, B. D. G. 1991. Cenozoic plate tectonics and basin evolution in Indonesia. *Marine and Petroleum Geology*, 8, No.1, 2-21.
- DEWEY, J. F. 1980. Episodicity, sequence and style at convergent plate boundaries. *Spec. Pap. Geol. Assoc., Can.*, 20, 553-574.
- DOBRIN, M. B. 1988. Introduction to Geophysical Prospecting. *New York. Mc.Graw Hill*.

DUNHAM, R. J. 1962. Classification of carbonate rocks according to depositional texture. *Ham W.E (ed.), Classification of Carbonate rocks. Mem. American Association of Petroleum Geologist, 1, 108-121.*

EDCON, Inc. 1991. Merge of public domain and proprietary gravity, magnetic and bathymetry data. *Edcon, Inc.*

FLUGEL, E. 1982. Microfacies Analysis of Limestones. *Springer-Verlag, Berlin, 633pp.*

GROW, J. A., and BOWIN, C. O. 1975. Evidence for high-density crust and mantle beneath the Chile Trench due to the descending lithosphere. *J. Geophys. Res., Vol. 80, 1449-1458.*

HAILE, N. S., McELHINNY, M. W., and McDOUGALL, I. 1977. Paleomagnetic data and radiometric ages from the Cretaceous of West Kalimantan (Borneo) and their significance in interpreting regional structure. *Jour. Geol. Soc. Lond., 133 (2), 133-145.*

HAILE, N. S. 1978. Reconnaissance palaeomagnetic results from Sulawesi, Indonesia, and their bearing palaeogeographic reconstructions. *Tectonophysics, 46, 77-85.*

HAILE, N. S. 1981. Palaeomagnetic evidence and the geotectonic history and palaeogeography of Eastern Indonesia. *The Geology and Tectonics of Eastern Indonesia, Geological Research and Development Center, Bandung, Special Publication, No. 2, 81-87.*

HAMILTON, W. 1979. Tectonics of the Indonesian Region. *US Geol. Surv. Prof. paper 12078.*

HARDING, T. P. 1990. Identification of wrench faults using subsurface structural data: criteria and pitfalls. *American Association of Petroleum Geologist Bulletin, 74, 1590-1609.*

HARJONO, H., and PRASETYO, H. 1993. Catatan gempa bumi Flores; Flores'92. *Sinyal, No. 01, Tahun XVI, 30-37.*

HARTONO, M. H. S, and TJOKROSAPOETRO, S. 1984. Preliminary account and reconstruction of Indonesia terranes. *Indonesian Petroleum Association, Proceedings 13th, Annual Convention, Jakarta, 185-226.*

HASAN, K. 1987. Preliminary report on the Upper Cretaceous flysch in the Balangbaru region, SW Sulawesi, Indonesia. *Univ. of London, Report No. 62 (Internal Report, Unpublished).*

HASAN, K. 1990. The Upper Cretaceous flysch succession of the Balangbaru Formation, Southwest Sulawesi, Indonesia. *Unpublished PhD thesis, RHBNC, University of London.*

- HATHERTHON, T and DICKINSON, W. R. 1969. The relationship between andesitic volcanism and seismicity in Indonesia, the Lesser Antilles, and other island arcs. *J. Geophys. Res.*, Vol. 74, 5301-5310.
- HELMERS, H., MAASKANT, P., and HARTEL, T. H. D. 1989. Garnet peridotite and associated high grade rocks from Sulawesi, Indonesia. *Third International Eclogite Conference (Okrusch, M., Ed.) Lithos 25 (1/3), 171-188.*
- HETZEL, W. H. 1930. Over de geologic der Eilanden in de Flores-Zee, Overgenomen De Mijningenieur, 53-56.
- HONKASALO, T. 1964. On the tidal gravity correction. *Bulletin., Geof. Teor., ed., appl. VI, 21, 34-36.*
- HOWELL, D. G., and JONES, D. L. 1983. The principles of terrane analysis and some key definitions. (*Unpublish*)
- HSU, K. J. 1968. Principles of melanges and their bearing on the franciscan-Knoxville paradox. *Geol. Soc. Am. Bull.*, v. 79, 1063-1074.
- HUTCHISON, C. R. 1981. Review of Indonesian volcanic arc. *Geology and tectonics of Eastern Indonesia, Geological Research and Development Centre, Bandung, Special Publication, No. 2, 65-80.*
- JARRAD, R. D. 1986. Cause of compression and extension behind trenches. *Tectonophysics, 132, 89-102.*
- JOHNSTON, C. R. 1981. A review of Timor tectonics, with implications for the development of the Banda Arc. *The Geology and Tectonics of Eastern Indonesia, Geological Research and Development Centre, Bandung, Special Publication, No. 2, 199-216.*
- KARIG, D. E. 1971. Origin and development of marginal basins in the Western Pacific. *J. Geophys., Res.*, 76, 2542-2561.
- KARIG, D. E and SHARMAN. G. F. 1975. Subduction and accretion in trenches. *Geol. Soc. Am. Bull.*, Vol. 86, 377-389.
- KATILI, J. A. 1971. A review of the geotectonic theories and tectonic maps of Indonesia. *Earth Sciences Review 7, 143, 146.*
- KATILI, J. A. 1973. Geochronology of west Indonesia and its implication on plate tectonics. *Tectonophysics*, v.26, 165-188.
- KATILI, J. A. 1978. Past and present geotectonic position of Sulawesi, Indonesia. *Tectonophysics, 45 (1978), 289-322.*

- KATILI, J. A. 1981. Geology of Southeast Asia with particular reference the South China Sea. *Energy*, 6 (11), 1077-1091.
- KATILI, J. A. 1991. Tectonic evolution of Eastern Indonesia and its bearing on the occurrence of hydrocarbons. *Marine and Petroleum Geology*, 8, No.1, 70-83.
- KERTAPATI, E. K., SOEHAIMI, A., and DJUHANDA. 1992. Peta Seismotektonik Indonesia (Seismotectonic Map of Indonesia). *Pusat Penelitian dan Pengembangan Geologi (PPPG), Bandung, Indonesia*.
- KETNERS, K. B., KASTOWO, MODJO, SUBROTO, NAESER, C. W., OBRADOVICH, J. D., ROBINSON, KEITH, SUPTANDAR, TATAN and WIKARNO. 1976. Pre-Eocene rocks of Java, Indonesia. *U.S. Geol. Survey Jour. Res.*, v.4, 605-614.
- KOESOEMADINATA, R. P, and PULUNGGONO, A. 1971. Offshore Tertiary sedimentary basins in Indonesia (*Abstract*). *The twelfth Pacific Science Congress. Canberra, Australia, Aug. 26*.
- KOESOEMADINATA, R. P., and PULUNGGONO, A. 1975. Geology of the Southern Sunda Shelf in reference to the tectonic framework of Tertiary sedimentary basins of Western Indonesia. *Geologi Indonesia, J.2, No. 2*
- KOHAR, A. 1985. Seismic expression of Late Eocene Carbonate build up features in the JS 25 and P.Sepajang trend, Kangean Block. *Indonesian Petroleum Association, Proceeding 14th, Annual Convention, Jakarta, 437-452*.
- KOSWARA, A., PANGGABEAN, H., and BAHARUDDIN. 1991. Preliminary geological map of Bonerate islands (*unpublished*).
- KOSWARA, A., PANGGABEAN, H., and BAHARUDDIN. 1993. Geological map of Bonerate islands (*unpublished*).
- MATTHEWS, S. J. 1990. Cenozoic structural evolution of Western Indonesia with specific reference to the development and deformation of Palaeogene basins around the Sunda Shield margin. (*Unpublished BP Report*).
- MATTHEWS, S. J., and BRANSDEN, P. J. E. 1993. Late Cretaceous and Cenozoic tectonostratigraphic development of the East Java Sea Basin, Indonesia. (*Unpublished BP Report*).
- McCAFFREY, R., MOLNAR, P., ROEKER, S., and JOYODIWIRYO, Y. 1985. Microearthquake seismicity and fault plane solutions related to arc-continent collision in the eastern Sunda Arc, Indonesia. *J. Geophys. Res.*, 90 (B6), 4511-4528.
- McCAFFREY, R. 1988. Active tectonics of the eastern Sunda and Banda arcs. *J. Geophys. Res.*, 93, 15163-15182.

- McCAFFREY, R., and NABELEK, J. 1984. The geometry of back-arc thrusting along the Sunda Arc, Indonesia: Constraints from earthquake and gravity data. *J. Geophys. Res.*, Vol. 89, No. B7, 6171-6179, 1984.
- McCAFFREY, R., and NABELEK, J. 1987. Earthquake, gravity and the origin of the Bali Basin: An example of a nascent continental fold and thrust belt. *J. Geophys. Res.*, Vol. 92, No. 1B, 441-460.
- McCLAY, K. R., and BUCHANAN, P. G. 1992. Thrust faults in inverted extensional basin. *Thrust Tectonics*, Ed. K.R McClay, Chapman and Hall.
- McKENZIE, D. P. 1978. Some remarks on the development of sedimentary basins. *Earth Planet, Sci. Lett.*, 40, 25-32.
- MOLNAR, P., and ATWATER, T. 1978. Interarc spreading and cordilleran tectonics as alternates related to the age of subducted oceanic lithosphere. *Earth and Planetary Science Letters*, 41, 330-340.
- NAFE, J. E., and DRAKE, C. L. 1963. Physical properties of marine sediments. *M.N. Hill (ed.), The Sea, Interscience Pub., New York*, 3, 784-815.
- NAYOAN, G. A. S. 1975. Contribution to the knowledge of the offshore extension of the Tertiary-Pre-Tertiary of S. Kalimantan, Indonesia (Abstract). *The Conference on the Geology of Kalimantan, Jakarta*.
- NETTLETON, L. L. 1940. Geophysical Prospecting for Oil. *McGraw-Hill Book Company, Inc. New York and London*.
- NISHIMURA, S., OTOFUJI, Y., IKEDA, T., ABE, E., YOKOYAMA, T., KOBAYASHI, Y., HADIWISASTRA, S., SOPAHELWAKAN, and HEHUWAT, F. 1981. Physical geology of the Sumba, Sumbawa and Flores islands. *The Geology and Tectonics of Eastern Indonesia, Geological Research and Development Centre, Bandung, Special Publication, No.2, 105-114*.
- PARK, R. G. 1988. Geological Structures And Moving Plates. *Blackie & Son, Glasgow*, 337pp.
- PARKER, E. S., and GEALEY, W. K. 1983. Plate tectonic evolution of the Western Pacific-Indian Ocean region. *Energy*, Vol. 10, No. 374, 249-261.
- PARKINSON, C. D. 1991. The Petrography Structure and Geologic History of the Metamorphic Rocks of Central Sulawesi. (*Unpublished PhD thesis, University of London*).
- PARKINSON, C. D. 1994. The tectonic evolution of Sulawesi (Abstract). *Tectonic Evolution of SE Asia, The Geological Society London, Burlington House, Dec. 7-8*.

- PICKERING, K. T., HISCOTT, R. N., and HEIN, F.J. 1989. Deep-marine environments: clastic sedimentation and tectonics. *Unwin Hyman, London, 416pp.*
- PRASETYO, H. 1992. The Bali-Flores Basin: Geological transition from extensional to subsequent compressional deformation. *Indonesian Petroleum Association, Proceedings 21th Annual Convention, Jakarta, 455-478.*
- PRASETYO, H. and DWIYANTO, B. 1986. Single channel seismic reflection study of the Eastern Sunda Back-arc basin, North Central Flores, Indonesia. *Bulletin of the Marine Geological Institute of Indonesia, 2, 1, 3-11.*
- PRICE, N. J., and AUDLEY-CHARLES, M. G. 1983. Plate rupture by hydraulic fracture resulting in overthrusting. *Nature, 396-121.*
- P.T. TRIAS JAYAGUNA. 1989. Palaeogene hydrocarbon potential study of Java and adjacent offshore (*Pertamina Report, Unpublished*)
- ROSE, R., and HARTONO, P. 1978. Geological evolution of the Tertiary Kutei - Melawi Basin, Kalimantan, Indonesia. *Indonesian Petroleum Association, Proceeding 7th Annual Convention, Jakarta, 225-252.*
- ROYAL NAVY. 1961. *Eastern Archipelago Pilot, vol.II.*
- SASAJIMA, S., NISHIMURA, S., OTOFUJU, Y., HIROOKA, K., LEEUWEN, T. H., and HEHUWAT, F. 1981. Paleomagnetic studies combined with fission-track dating on the western arc of Sulawesi, East Indonesia. *The Geology and Tectonics of Eastern Indonesia, Geological Research and Development Centre, Bandung, Special Publication, No. 2, 305-311.*
- SCOTT, J., and ATKINS, D. 1991. The Cretaceous to Eocene age rocks of Southwest Sulawesi: Implication for palaeogeographic developments of the East Java Sea area. (*Unpublished BP Report*)
- SIKUMBANG, N. 1986. Geology and tectonics of Pre-Tertiary rocks in the Meratus Mountains, Southeast Kalimantan, Indonesia. *Unpublished PhD thesis, University of London, 400pp.*
- SIKUMBANG, N. 1990. The geology and tectonics of the Meratus mountains, South Kalimantan, Indonesia. *Geologi Indononesia, V 13, No. 2, 1-31.*
- SILITONGA, F., and HAKIM, S. 1990. Seismic investigation on the southern part of the Karimunjawa Arc. *Himpunan Ahli Geofisika Indonesia, Proceedings 15th, Yogyakarta, 348-358.*
- SILVER, E. A., McCaffrey, R., and JOYODIWIRYO, Y. 1981. Gravity result and emplacement geometry of the Sulawesi ultramafic belt, Indonesia. *The Geology and*

Tectonics of Eastern Indonesia, Geological Research and Development Centre, Bandung, Special Publication, No. 2, 343-347.

SILVER, E. A., REED, D. and McCAFFREY, R. 1983. Back-arc thrusting in the Eastern Sunda arc, Indonesia: A consequence of arc-continent collision. *J. Geophys. Res.*, Vol. 88, No. B9, 7429-7448.

SILVER, E. A., BREEN, N. A. and PRASETYO, H. 1986. Multibeam study of the Flores back-arc thrust belt Indonesia. *J. Geophys. Res.*, Vol. 91, No. B3, 3489-3500.

SIMAMORA, H., and MARZUKI, S. 1990. Bouguer anomaly map of the Ujung Pandang and Sinjai Quadrangles, Sulawesi. *Geological Research and Development Centre, Bandung.*

SIMANDJUNTAK, T. O. 1986. Sedimentology and tectonics of the collisions complex in the east arm of Sulawesi, Indonesia. *Unpublished PhD thesis, RHBNC, University of London.*

SIMANDJUNTAK, T. O. 1990. Sedimentology and tectonics of the collision complex in the east arm of Sulawesi, Indonesia. *Bulletin of Geology Indonesia*, Vol. 13, n. 1, 1-35.

SITUMORANG, B. 1982. The formation and evolution of the Makassar Basin, Indonesia. *Unpublished PhD thesis, University of London, 313 pp.*

SUKAMTO, R. 1975. Geologic map of Indonesia sheet VII Ujung Pandang, scale 1:1,000,000. *Geological Survey Indonesia.*

SUKAMTO, R and SUPRIATNA, S. 1982. Peta geologi lembar Ujung Pandang, Benteng dan Sinjai (Geologic map of the Ujungpandang, Benteng and Sinjai quadrangles, Sulawesi). *P3G, Bandung, Indonesia*

SUKAMTO, R., and SIMANJUNTAK, T. O. 1983. Tectonic relationship between geologic province of Western Sulawesi, Eastern Sulawesi and Banggai-Sula in the light of sedimentological aspects. *Bulletin Geological Research and Development Centre*, 7, 1-12.

SUTISNA, K., SAMODRA, H., AND KOSWARA, A. 1986. Peta geology lembar Kangean dan Sapudi, Jawa Timur (Geologic map of Kangean and Sapudi quadrangles, East Java). *P3G, Bandung, Indonesia.*

TELFORD, W. M., GELDART, L. P., AND SHERIFF, R. E., and KEYS, D. A. 1976. *Applied Geophysics. Cambridge University Press.*

TAPPONNIER, P., PELTZER, G., LE DAIN, Y. Y., ARMIJO, R. and COBBING, P. 1982. Propagating extrusion tectonics in Asia: new insights from simple experiments with plasticine. *Geology* 10, 611-616.

- THAYIB, E. S., SAID, E. L., SISWOYO, SUMARSO, P. 1977. The status of the melange complex in Ciletuh area, south-west Java. *Indonesian Petroleum Association, Proceedings 6th, Annual Convention, Jakarta, 241-253.*
- TYRREL, W. W., DAVIS, R. G., and DOWELL, H. G. 1986. Miocene carbonate shelf margin, Bali-Flores Sea, Indonesia. *Indonesian Petroleum Association, Proceedings 15th, Annual Convention, Jakarta, 123-140.*
- UYEDA, S., and KANAMORI, H. 1979. Back-arc opening and the mode of subduction. *J. Geophys., Res.*, 84, 1049-1061.
- VAIL, P. R., MITCHUM, R. M and THOMPSON, S. 1977. Seismic stratigraphy and global changes of sea-level, part 4: global cycles of relative changes of sea level. *Mem. American Association of Petroleum Geologist*, v.26.
- VAN BEMMELEN, R. W. 1949 (2nd edition 1970). The Geology of Indonesia. (3 Vols). Vol. 1a: General Geology of Indonesia and Adjacent Archipelagos. Vol. 1b: Portfolio (maps, charts, indexes and references). Vol. 2: Economic Geology. Government Printing Office, Nijhoff, The Hague (2nd edition, 1970), 732pp.
- VAN LEEUWEN, M. Th. 1981. The Geology of Southwest Sulawesi with special reference to the Biru area. *The Geology and Tectonics of Eastern Indonesia, Geological Research and Development Centre, Special Publication, No. 2, 277-304.*
- VITA-FINZI, C., and SYARIF, H. 1991. Holocene uplift in West Timor. *Journal of Southeast Asian Earth Sciences*, Vol. 6, No. 3/4, 387-393.
- WATTS, A. B., and TALWANI, M. 1974. Gravity anomalies seaward of deep-sea trenches and their tectonic implications. *Geophys. J.R. Astron. Soc.*, 36, 57-90, 1974.

APPENDIX 9.1

DESCRIPTION OF GRAVITY BASE STATION AT HASANUDDIN AIRPORT UJUNG PANDANG

COUNTRY INDONESIA	NEAREST CITY UJUNG PANDANG	GRAVITY STATION DESCRIPTION				
STATE/PROVINCE SULAWESI		STATION NAME HASANUDDIN AIRPORT #1				
LATITUDE 5°4.05'S	LONGITUDE 119°12.0'W	ELEVATION 32.0 m	U.S.G. STATION NO. 7693.0163	GRAVITY VALUE (g)		
POSITION CONTROL DESCRIPTION Airport Location						
ELEVATION CONTROL DESCRIPTION Airport Elevation						
DESCRIPTION		DESCRIBED BY John S. ADKINS		DATE 10/76		
<p>Station is located outside against the concrete wall pillar, one metre to the right of the glass doors of the Departure Lounge.</p>						
DIAGRAM		DIAGRAM BY John S. ADKINS		DATE 10/76		
STATION ALIAS						
DATE	OBSERVED BY	INSTRUMENT	STATION OF REFERENCE	REFERENCE VALUE	Δg	REMARKS
University of New England, Australia.					JSA.78	

Appendix 4.1: Description of gravity base station at Hasanuddin Airport, Ujung Pandang (Adkins et al. 1978)

APPENDIX 9.2 - 9.8

DESCRIPTION OF SUBSIDIARY GRAVITY BASE STATIONS ON THE FLORES SEA ISLANDS

COUNTRY INDONESIA		NEAREST TOWN UJUNG PANDANG	GRAVITY STATION DESCRIPTION	
STATE PROVINCE COUNTY	SOUTH SULAWESI	STATION NAME	HOTEL RAMAYANA	STATION No. 9381.9001
LATITUDE		LONGITUDE		ELEVATION
POSITION CONTROL				GRAVITY VALUE 978115.4347 mGals
ELEVATION CONTROL				BOUGUER ANOMALY
DESCRIPTION				
<p>The station is situated at the left corner in front of travel agent office "MUTIARA NUSANTARA" which opens out on to the fare court of the Hotel Ramayana. The site suffers from minor vibration effects due to traffic in the nearby main road.</p>				
DESCRIBED BY GUNTORO,A.				DATE MAY 14, 1993
DIAGRAM				
<i>GENERAL</i>		<i>DETAIL</i>		
<p>The general diagram shows the layout of Hotel Ramayana. A large rectangle represents the hotel building. Inside, there is a 'TRAVEL AGENT MUTIARA NUSANTARA' office. A 'Main entrance to the Hotel' is shown. Below the office is a 'PARKING AREA IN THE HOTEL'. The building is bounded by a 'WALL'. Two 'GATE' points are marked. Below the hotel is 'Jl. Bawakaraeng'. A 'Gravity base station 001' is indicated by a circle with a crosshair at the left corner of the travel agent office.</p>		<p>The detail diagram shows a close-up of the station location. It features a 'WALL' and a 'Door'. The 'Gravity base station 001' is located at the corner where the wall meets the ground. A vertical dimension of '1 m' is shown from the station to the door. A horizontal dimension of '0.5 m' is shown from the station to the wall. An 'Overhang' is also indicated.</p>		
DIAGRAM BY JOHN MILSOM				DATE OCT 25, 1993
STATION HISTORY				
<p>The station was established as subsidiary base station in the cause of the 1993 Flores Sea islands gravity survey It is tied to the Hasannudin Airport base station by a well controlled A-B-A-B-A tie On 14-5-93 and reoccupied 31-5-93.</p>				
SOURCE ORGANISATION Geological Sciences, University College London & Geological Research and Development Centre, Bandung				

COUNTRY INDONESIA		NEAREST TOWN BULU KUMBA	GRAVITY STATION DESCRIPTION	
STATE PROVINCE COUNTY	SOUTH SULAWESI	STATION NAME BULU KUMBA		STATION No. 9381.9002
LATITUDE 5.5567°		LONGITUDE 120.2023°	ELEVATION 1.5 m	
POSITION CONTROL TOPOGRAPHIC MAP			GRAVITY VALUE 978159.0003 mGals	
ELEVATION CONTROL REFERENCE TO SEA LEVEL			BOUGUER ANOMALY 79.11 mGals	
DESCRIPTION				
The station was positioned on the parking area of Lapee Port (Bulu Kumba), near at the left corner to the way to the pier on a concrete platform				
DESCRIBED BY GUNTORO.A.				DATE May 15, 1993
DIAGRAM				
<i>GENERAL</i>		<i>DETAIL</i>		
<i>LAPEE PORT, BULU KUMBA</i>				
DIAGRAM BY GUNTORO.A.				DATE OCT 25, 1993
STATION HISTORY				
This subsidiary base station was established at the point of departure for the 1993 Flores Sea islands survey and was tied to the Hasanuddin Airport base station via station 9381.9002 at the Hotel Ramayana in Ujung Pandang.				
SOURCE ORGANISATION Geological Sciences, University College London & Geological Research and Development Centre, Bandung				

COUNTRY INDONESIA		NEAREST TOWN BENTENG SELAYAR	GRAVITY STATION DESCRIPTION	
STATE PROVINCE COUNTY	SOUTH SULAWESI	STATION NAME HOTEL BERLIAN		STATION No. 9831.9004
LATITUDE 6.1133°		LONGITUDE 120.4667°		ELEVATION
POSITION CONTROL TOPOGRAPHIC MAP			GRAVITY VALUE 978232.8914 mGals	
ELEVATION CONTROL REFERENCE TO SEA LEVEL			BOUGUER ANOMALY 142.54 mGals	
DESCRIPTION				
The station is situated at the left corner of the entrance to the HOTEL BERLIAN on the concrete floors.				
DESCRIBED BY GUNTORO.A.			DATE May 15, 1993	
DIAGRAM				
<i>GENERAL</i>		<i>DETAIL</i>		
DIAGRAM BY SARJONO			DATE OCT 26, 1993	
STATION HISTORY				
The station was established for use as a regional base for the 1993 Flores Sea islands survey. It was tied directly to the National Base at Hasanuddin Airport via stations in Ujung Pandang, Bulu Kumba and Benteng Selayar.				
SOURCE ORGANISATION Geological Sciences, University College London & Geological Research and Development Centre, Bandung				

COUNTRY		INDONESIA		NEAREST TOWN		BONERATE		GRAVITY STATION DESCRIPTION	
STATE PROVINCE COUNTY		SOUTH SULAWESI		STATION NAME		BONERATE		STATION No. 9381.9016	
LATITUDE		7.34°		LONGITUDE		121.0833°		ELEVATION 0.60 m	
POSITION CONTROL						Topographic map and aerial photograph		GRAVITY VALUE 978287.5632 mGals	
ELEVATION CONTROL						Reference to sea level		BOUGUER ANOMALY 171.62 mGals	
DESCRIPTION									
<p>This station is situated in front of the first house of principal road from the beach to Bonerate village. The reading was taken on the ground to the right of the steps.</p>									
DESCRIBED BY GUNTORO.A.						DATE May 17, 1993			
DIAGRAM									
<i>GENERAL</i>					<i>DETAIL</i>				
DIAGRAM BY JOHN MILSOM						DATE OCT 25, 1993			
STATION HISTORY									
<p>The station was established for use as a regional base for the 1993 Flores Sea islands survey. It is tied to the National Base at Hasanuddin Airport via stations No. 9831.0001-9831.002- 9831.003 and 9831.004.</p>									
SOURCE ORGANISATION Geological Sciences, University College London & Geological Research and Development Centre, Bandung									

COUNTRY INDONESIA		NEAREST TOWN BONERATE	GRAVITY STATION DESCRIPTION	
STATE PROVINCE COUNTY	SOUTH SULAWESI	STATION NAME	KALAOTOA	STATION No. 9381.9021
LATITUDE 7.3783°		LONGITUDE 121.7533°		ELEVATION 1 m
POSITION CONTROL Topographic map and aerial photograph			GRAVITY VALUE 978283.7710 mGals	
ELEVATION CONTROL Reference to sea level			BOUGUER ANOMALY 167.04 mGals	
DESCRIPTION				
The station was positioned on the ground at the right corner of the first house from the beach in Buranga village.				
DESCRIBED BY GUNTORO.A.				DATE May 18, 1993
DIAGRAM				
<i>GENERAL</i>		<i>DETAIL</i>		
<p>Base Station 021</p> <p>Coast line</p> <p>approximately 10 m from the high tide</p> <p>IBRAHIM'S HOUSE</p> <p>BURANGA VILLAGE</p>		<p>IBRAHIM'S HOUSE</p> <p>Base Station 021</p>		
DIAGRAM BY GUNTORO, A.				DATE OCT 25, 1993
STATION HISTORY				
The station was established for use as a regional base for the 1993 Flores Sea islands survey. It is tied to the National Base at Hasanuddin Airport via stations No. 9381.0001-9381.002- 9381.003- 9831.004 and 9381.0016				
SOURCE ORGANISATION Geological Sciences, University College London & Geological Research and Development Centre, Bandung				

COUNTRY INDONESIA		NEAREST TOWN BENTENG TANAHJAMPEA		GRAVITY STATION DESCRIPTION	
STATE PROVINCE COUNTY SOUTH SULAWESI		STATION NAME TANAHJAMPEA			STATION No. 9381.9044
LATITUDE 7.0633°		LONGITUDE 120.6138°		ELEVATION 0.60 m	
POSITION CONTROL Topographic map and aerial photograph				GRAVITY VALUE 978292.1564 mGals	
ELEVATION CONTROL Reference to sea level				BOUGUER ANOMALY 182.42 mGals	
DESCRIPTION					
The station is situated at the "welcome" gate on the principal road from the beach to the village.					
DESCRIBED BY GUNTORO,A.				DATE MAY 21, 1993	
DIAGRAM					
<i>GENERAL</i>			<i>DETAIL</i>		
DIAGRAM BY GUNTORO,A.				DATE OCT 25, 1993	
STATION HISTORY					
The station was established for use as a regional base for the 1993 Flores Sea islands survey It is tied to the National Base at Hasanuddin Airport via station No. 9381.9001-9381.9002-9381.9003-9381.9004-9381.9016					
SOURCE ORGANISATION Geological Sciences, University College London & Geological Research and Development Centre, Bandung					

APPENDIX 9.9

**GRAVITY DATA REDUCTION
ON
THE FLORES SEA ISLANDS**

BONERATE GRAVITY SURVEYS MAY-JUNE 1993, SOUTH SULAWESI

GRAVITY DATA PROCESSING IN THE FLORES SEA ISLANDS

GRAVITY BASE STATION IN UJUNG PANDANG IS 978119.94 mGAL

GRAVITY FORMULA (1967) $G_n = 978031.8 (1 + 0.0053024 \sin^2 A - 0.000059 \sin^2 2A)$

Date	Area	Time	St. Number	Latitude	Longitude	Elevation	Gravity Reading	Equivalent (mGal)	Tide correction (mGal)	Drift correction (mGal)	Tide corrected (mGal)	Drift & tide corrected (mGal)	Gobserve (mGal)	Gnormal (mGal)	FAC (mGal)	BC (mGal)	BA (mGal)
May14	Bandung	05:21	DG0				157365	1620.1314			1620.1314	1620.1314					
	Bandera U.P	12:38	UJPO	5.0675	119.5500	32	171310	1763.6087	0.055	0.0000	1763.6637	1763.6637	978119.9400	978072.0834	9.8752	2.9505	54.78
	H.Ramayana U.P	13:13	001				170872	1759.1021		-0.0367	1759.1021	1759.1388	978115.4151			0.0000	
		13:50	UJPO	5.0675	119.5500	32	171308	1763.5881		-0.0756	1763.5881	1763.6637	978119.9400	978072.0834	9.8752	2.9505	54.78
	H.Ramayana U.P	14:28	001				170871	1759.0918			1759.0918	1759.0918	978115.3601			0.0000	
May15	H.Ramayana U.P	06:35	001				170860	1758.9786		0.0000	1758.9786	1758.9786	978115.4347			0.0000	
	BuluKumba	09:53	002	5.5567	120.2023	1.50	175075	1802.3472		0.0000	1802.3472	1802.3472	978159.0003	978080.2108	0.4629	0.1383	79.11
	BuluKumba	14:39	002	5.5567	120.2023	1.50	175084	1802.4398	-0.004	0.0886	1802.4358	1802.3472	978159.0003	978080.2108	0.4629	0.1383	79.11
	Benteng(Selayar)	22:06	003	6.1150	120.4600	2.80	182706	1880.8620	0.038	0.0000	1880.9000	1880.9000	978237.6195	978090.3885	0.8641	0.2582	147.84
	H.Berlian(selayar)	22:39	004	6.1133	120.4667		182252	1876.1908	0.023	0.0000	1876.2138	1876.2138	978232.8914	978090.3561	0.0000	0.0000	142.54
May16	H.Berlian(selayar)	06:36	004	6.1133	120.4667		182251	1876.1805	0.04	0.0000	1876.2205	1876.2205	978232.8914	978090.3561	0.0000	0.0000	142.54
	H.Berlian(selayar)	08:46	004	6.1133	120.4667		182250	1876.1703	0.08	0.0078	1876.2503	1876.2425	978232.9134	978090.3561	0.0000	0.0000	142.56
		09:29	005	6.1850	120.4500	1.50	183785	1891.9639	0.073	0.0103	1892.0369	1892.0265	978248.6974	978091.7323	0.4629	0.1383	157.29
		09:50	006	6.2350	120.4467	0.50	184338	1897.6537	0.067	0.0116	1897.7207	1897.7091	978254.3800	978092.7013	0.1543	0.0461	161.79
		10:11	007	6.2433	120.4433	0.50	184092	1895.1226	0.059	0.0128	1895.1816	1895.1688	978251.8396	978092.8630	0.1543	0.0461	159.08
		10:45	008	6.2867	120.4783	0.50	183231	1886.2638	0.043	0.0149	1886.3068	1886.2919	978242.9628	978093.7114	0.1543	0.0461	149.36
		11:10	009	6.3183	120.4750	0.50	183207	1886.0168	0.029	0.0163	1886.0458	1886.0295	978242.7003	978094.3328	0.1543	0.0461	148.48
		11:33	010	6.3517	120.4683	0.50	182860	1882.4465	0.016	0.0177	1882.4448	1882.4448	978239.1157	978094.9930	0.1543	0.0461	144.23
		11:50	011	6.3867	120.4667	0.60	182589	1879.6582	0.006	0.0187	1879.6642	1879.6455	978236.3163	978095.6884	0.1852	0.0553	140.78
		12:23	012	6.4583	120.4733	0.50	182096	1874.5857	-0.012	0.0207	1874.5737	1874.5530	978231.2239	978097.1228	0.1543	0.0461	134.21
		12:42	013	6.4933	120.4833	0.50	181943	1873.0115	-0.022	0.0218	1872.9895	1872.9677	978229.6386	978097.8297	0.1543	0.0461	131.92
		12:58	014	6.4933	120.4767	0.50	181980	1873.3922	-0.05	0.0228	1873.3422	1873.3194	978229.9903	978097.8297	0.1543	0.0461	132.27
		14:23	015	6.1633	120.4483	0.60	183793	1892.0462	-0.065	0.0279	1891.9812	1891.9533	978248.6242	978091.3141	0.1852	0.0553	157.44
	H.Berlian(selayar)	14:38	004	6.1133	120.4667		182264	1876.3143	0.065	0.0288	1876.2493	1876.2205	978232.8914	978090.3561	0.0000	0.0000	142.54
	Benteng(Selayar)	15:35	003	6.1150	120.4600	2.80	182719	1880.9958	-0.063	0.0000	1880.9328	1880.9328	978237.6195	978090.3885	0.8641	0.2582	147.84
May17	P.BONERATE	10:26	016	7.3400	121.0833	0.60	187578	1930.9900	0.166	0.0000	1931.1560	1931.1560	978287.5632	978116.0717	0.1852	0.0553	171.62
		11:02	017	7.3683	121.1550	0.75	187176	1926.8539	0.151	0.0232	1927.0049	1926.9617	978283.3888	978116.7192	0.2315	0.0692	166.83
	P.BONERATE	11:41	016	7.3400	121.0833	0.60	187593	1931.1444	0.123	0.1113	1931.2674	1931.1560	978287.5632	978116.0717	0.1852	0.0553	171.62
		12:03	018	7.3917	121.0933	0.60	188013	1935.4658	0.112	0.0625	1935.5778	1935.5153	978291.9224	978117.2564	0.1852	0.0553	174.80
	P.BONERATE	12:58	016	7.3400	121.0833	0.60	187601	1931.2267	0.066	0.1366	1931.2927	1931.1560	978287.5632	978116.0717	0.1852	0.0553	171.62
		13:57	019	7.3167	121.1017	0.50	186739	1922.3576	0.026	0.1359	1922.3836	1922.2477	978278.6548	978115.5404	0.1543	0.0461	163.22
		15:17	020	7.3350	121.1250	0.50	186575	1920.6702	0	0.1874	1920.6702	1920.4828	978276.8899	978115.9576	0.1543	0.0461	161.04
	P.BONERATE	17:07	016	7.3400	121.0833	0.60	187617	1931.3913	0.023	0.2583	1931.4143	1931.1560	978287.5632	978116.0717	0.1852	0.0553	171.62
May18	P.KALAO TOA	08:28	021	7.3783	121.7533	1.00	187210	1927.2037	0.171	0.0000	1927.3747	1927.3747	978283.7710	978116.9486	0.3086	0.0922	167.04
		09:31	022	7.3983	121.7433	0.70	187315	1928.2840	0.196	0.1782	1928.4800	1928.3019	978284.6982	978117.4082	0.2160	0.0645	167.44
		09:55	023	7.4217	121.7533	0.40	188555	1941.0424	0.2	0.2460	1941.2424	1940.9964	978297.3927	978117.9476	0.1234	0.0369	179.53
		10:38	024	7.4867	121.7567	1.30	188673	1942.2565	0.198	0.3676	1942.4545	1942.0869	978298.4832	978119.4545	0.4012	0.1199	179.31
		11:07	025	7.4817	121.7950	1.90	188997	1945.5901	0.185	0.4496	1945.7751	1945.3255	978301.7218	978119.3381	0.5863	0.1752	182.79
		11:52	026	7.4167	121.7967	1.00	189109	1946.7425	0.151	0.5789	1946.8935	1946.3166	978302.7129	978117.8322	0.3086	0.0922	185.10
		12:53	027	7.3633	121.8383	0.50	187531	1930.5065	0.096	0.7494	1930.6025	1929.8531	978286.2494	978116.8046	0.1543	0.0461	169.75
		13:22	028	7.3350	121.8217	0.70	187193	1927.0288	0.068	0.8314	1927.0968	1926.2654	978282.6617	978115.9576	0.2160	0.0645	166.86
		13:56	029	7.3400	121.7900	1.50	187083	1925.8970	0.041	0.9276	1925.9380	1925.0104	978281.4067	978116.0717	0.4629	0.1383	165.66
		14:37	030	7.2883	121.7633	1.80	186574	1920.6599	0.008	1.0435	1920.6679	1919.6244	978276.0207	978114.8951	0.5555	0.1660	161.52
		15:13	031	7.2833	121.7333	0.60	187118	1926.2571	-0.01	1.1453	1926.2471	1925.1018	978281.4981	978114.7818	0.1852	0.0553	166.85
		15:32	032	7.2967	121.7317	0.55	186958	1924.6109	-0.015	1.1990	1924.5969	1923.3968	978279.7931	978115.0857	0.1697	0.0507	164.83
	P.KALAO TOA	16:49	021	7.3783	121.7533	1.00	187365	1928.7965	-0.007	1.4188	1928.7915	1927.3747	978283.7710	978116.9486	0.3086	0.0922	167.04

May19	P.BONERATE	06:46	016	7.3400	121.0833	0.60	187853	1933.8195	0.053	0.0000	1933.8725	1933.8725	978287.5632	978116.0717	0.1852	0.0553	171.62		
	P.BONERATE	06:56	016	7.3400	121.0833	0.60	187852	1933.8092	0.063	-0.0128	1933.8722	1933.8850	978287.5757	978116.0717	0.1852	0.0553	171.63		
	P.BONERATE	07:09	016	7.3400	121.0833	0.60	187848	1933.7681	0.075	-0.0294	1933.8431	1933.8725	978287.5632	978116.0717	0.1852	0.0553	171.62		
	P.BONERATE	07:15	016	7.3400	121.0833	0.60	187849	1933.7784	0.081	-0.0132	1933.8594	1933.8725	978287.5632	978116.0717	0.1852	0.0553	171.62		
	P.BONERATE	07:22	016	7.3400	121.0833	0.60	187850	1933.7887	0.088	0.0000	1933.8767	1933.8767	978287.5632	978116.0717	0.1852	0.0553	171.62		
	P.BONERATE	07:51	016	7.3400	121.0833	0.60	187848	1933.7681	0.166	0.0340	1933.9341	1933.9000	978287.5866	978116.0717	0.1852	0.0553	171.64		
	P.BONERATE	07:55	016	7.3400	121.0833	0.60	187848	1933.7681	0.119	0.0387	1933.8871	1933.8483	978287.5349	978116.0717	0.1852	0.0553	171.59		
			10:09	033	7.3000	121.0500	0.50	187385	1929.0043	0.199	0.1960	1929.2033	1929.0072	978282.6938	978115.1607	0.1543	0.0461	167.64	
			10:55	034	7.2850	121.0167	0.30	187999	1935.3217	0.197	0.2500	1935.5187	1935.2687	978288.9552	978114.8203	0.0926	0.0277	174.20	
			11:53	035	7.2833	120.9700	0.50	187467	1929.8480	0.172	0.3181	1930.0200	1929.7018	978283.3884	978114.7818	0.1543	0.0461	168.71	
			12:54	036	7.2850	120.9350	0.75	187498	1930.1669	0.124	0.3897	1930.2909	1929.9012	978283.5877	978114.8203	0.2315	0.0692	168.93	
	8		14:01	037	7.2767	120.8963	1.00	186800	1922.9852	0.059	0.4684	1923.0442	1922.5758	978276.2624	978114.6323	0.3086	0.0922	161.85	
			21:32	038	7.3233	121.0517	0.50	187280	1927.9239	0.146	0.9978	1928.0699	1927.0721	978280.7586	978115.6908	0.1543	0.0461	165.18	
		P.BONERATE	22:57	016	7.3400	121.0833	0.60	187949	1934.8073	0.167	1.0976	1934.9743	1933.8767	978287.5632	978116.0717	0.1852	0.0553	171.62	
	May20	P.BONERATE	07:12	016	7.3400	121.0833	0.60	187966	1934.9822	0.045	0.0000	1935.0272	1935.0272	978287.5632	978116.0717	0.1852	0.0553	171.62	
			12:06	039	7.2933	120.8117	0.30	185734	1912.0171	0.191	0.2106	1912.2081	1911.9976	978264.5336	978115.0086	0.0926	0.0277	149.59	
			14:16	040	7.3083	120.8717	0.75	186565	1920.5673	0.077	0.3037	1920.6443	1920.3406	978272.8767	978115.3493	0.2315	0.0692	157.69	
		14:52	041	7.3017	120.8583	0.75	186199	1916.8015	0.04	0.3294	1916.8415	1916.5121	978269.0481	978115.1993	0.2315	0.0692	154.01		
		15:17	042	7.2850	120.8467	0.50	185927	1914.0029	0.015	0.3473	1914.0179	1913.6706	978266.2066	978114.8203	0.1543	0.0461	151.49		
		17:30	043	7.3200	120.9483	-0.50	186768	1922.6560	-0.04	0.4426	1922.6160	1922.1734	978274.7094	978115.6156	-0.1543	-0.0461	158.99		
P.BONERATE		20:06	016	7.3400	121.0833	0.60	188019	1935.5275	0.054	0.5543	1935.5815	1935.0272	978287.5632	978116.0717	0.1852	0.0553	171.62		
May21	P.T.JAMPEA	08:29	044	7.0633	120.6183	0.60	188436	1939.8180	0.055	0.0000	1939.8730	1939.8730	978292.1564	978109.8695	0.1852	0.0553	182.42		
		09:24	045	7.0417	120.6267	0.50	187734	1932.5951	0.111	-0.0049	1932.7061	1932.7110	978284.9944	978109.3952	0.1543	0.0461	175.71		
		10:00	046	7.0417	120.6133	0.60	187805	1933.3256	0.143	-0.0081	1933.4686	1933.4767	978285.7601	978109.3952	0.1852	0.0553	176.49		
		10:27	047	7.0100	120.6183	0.80	185863	1913.3444	0.159	-0.0105	1913.5034	1913.5139	978265.7973	978108.7016	0.2469	0.0738	157.27		
		10:38	048	7.0233	120.6200	0.40	186126	1916.0504	0.167	-0.0115	1916.2174	1916.2289	978268.5123	978108.9922	0.1234	0.0369	159.61		
		10:56	049	7.0033	120.6250	1.50	185584	1910.4738	0.173	-0.0131	1910.6468	1910.6599	978262.9433	978108.5554	0.4629	0.1383	154.71		
		11:18	050	7.0050	120.6350	0.70	186110	1915.8858	0.179	-0.0150	1916.0648	1916.0798	978268.3632	978108.5925	0.2160	0.0645	159.92		
		11:41	051	7.0250	120.6633	0.40	185965	1914.3939	0.183	-0.0171	1914.5769	1914.5940	978266.8774	978109.0294	0.1234	0.0369	157.93		
		12:03	052	7.0283	120.6750	0.30	187466	1929.8377	0.181	-0.0191	1930.0187	1930.0377	978282.3211	978109.1016	0.0926	0.0277	173.28		
		12:26	053	7.0533	120.7017	0.50	187477	1929.9509	0.176	-0.0211	1930.1269	1930.1480	978282.4314	978109.6497	0.1543	0.0461	172.89		
		12:52	054	7.0650	120.7450	1.40	186934	1924.3639	0.163	-0.0234	1924.5269	1924.5503	978276.8337	978109.9069	0.4320	0.1291	167.23		
		13:25	055	7.0783	120.7483	1.10	186220	1917.0176	0.14	0.0000	1917.1576	1917.1576	978269.4410	978110.1997	0.3395	0.1014	159.48		
		13:59	056	7.0750	120.7683	0.40	185625	1910.8956	0.107	-0.0350	1911.0026	1911.0376	978263.3210	978110.1270	0.1234	0.0369	153.28		
		14:35	057	7.0617	120.7800	0.30	185091	1905.4013	0.068	-0.0720	1905.4693	1905.5413	978257.8247	978109.8343	0.0926	0.0277	148.06		
		15:12	055	7.0783	120.7483	1.10	186220	1917.0176	0.03	-0.1100	1917.0476	1917.1576	978269.4410	978110.1997	0.3395	0.1014	159.48		
		23:59																	
	May22		07:11	055	7.0783	120.7483	1.10	186228	1917.0999	-0.048	-0.1212	1917.0519	1917.1731	978269.4565	978110.1997	0.3395	0.1014	159.49	
		08:10	058	7.0767	120.7933	0.50	184626	1900.6169	0.001	-0.1264	1900.6179	1900.7444	978253.0278	978110.1645	0.1543	0.0461	142.97		
		08:44	059	7.1033	120.7767	0.50	185589	1910.5252	0.039	-0.1295	1910.5642	1910.6937	978262.9771	978110.7517	0.1543	0.0461	152.33		
		09:19	060	7.1333	120.7683	0.50	186596	1920.8862	0.08	-0.1326	1920.9662	1921.0988	978273.3822	978111.4165	0.1543	0.0461	162.07		
		09:47	061	7.1300	120.7400	0.70	187803	1933.3051	0.109	-0.1351	1933.4141	1933.5491	978285.8325	978111.3432	0.2160	0.0645	174.64		
		10:14	062	7.1300	120.7117	1.20	188865	1944.2320	0.136	-0.1375	1944.3680	1944.5055	978296.7889	978111.3432	0.3703	0.1106	185.71		
		10:44	063	7.1250	120.6867	0.50	189516	1950.9301	0.16	-0.1402	1951.0901	1951.2303	978303.5137	978111.2323	0.1543	0.0461	192.39		
		11:08	064	7.1217	120.6683	0.50	189820	1954.0580	0.176	-0.1423	1954.2340	1954.3763	978306.6597	978111.1591	0.1543	0.0461	195.61		
		11:37	065	7.1483	120.6683	0.60	189539	1951.1668	0.192	-0.1449	1951.3588	1951.5036	978303.7870	978111.7499	0.1852	0.0553	192.17		
		12:12	066	7.1333	120.6333	1.50	189443	1950.1790	0.196	-0.1480	1950.3750	1950.5230	978302.8064	978111.4165	0.4629	0.1383	191.71		
		13:02	067	7.1017	120.6333	1.00	188825	1943.8204	0.181	-0.1524	1944.0014	1944.1539	978296.4373	978110.7163	0.3086	0.0922	185.94		
		13:40	068	7.1050	120.5867	0.80	189226	1947.9463	0.159	-0.1558	1948.1053	1948.2611	978300.5445	978110.7893	0.2469	0.0738	189.93		
		14:05	069	7.0917	120.5600	1.20	188903	1944.6230	0.137	-0.1581	1944.7600	1944.9180	978297.2014	978110.4953	0.3703	0.1106	186.97		
		14:43	070	7.0600	120.5483	0.80	189112	1946.7734	0.097	-0.1614	1946.8704	1947.0318	978299.3152	978109.7969	0.2469	0.0738	189.69		
		15:21	071	7.0800	120.5983	0.70	188406	1939.5093	0.058	-0.1648	1939.5673	1939.7322	978292.0155	978110.2372	0.2160	0.0645	181.93		
P.T.JAMPEA		15:54	044	7.0633	120.6183	0.60	188423	1939.6842	0.021	-0.1678	1939.7052	1939.8730	978292.1564	978109.8695	0.1852	0.0553	182.42		

May23	P.KAJUADI	10:50	072	6.7817	120.7900	1.00	181639	1869.8837	0.095	0.7392	1869.9787	1869.2395	978221.5229	978103.7973	0.3086	0.0922	117.94		
		12:15	073	6.8667	120.7933	1.50	183327	1887.2515	0.157	0.7945	1887.4085	1886.6140	978238.8974	978105.6046	0.4629	0.1383	133.62		
		12:49	074	6.8317	120.7833	0.60	183154	1885.4715	0.159	0.8167	1885.6305	1884.8139	978237.0972	978104.8577	0.1852	0.0553	132.37		
		13:16	075	6.8250	120.7967	5.00	182815	1881.9835	0.156	0.8342	1882.1395	1881.3053	978233.5887	978104.7152	1.5430	0.4610	129.96		
		18:20	044	7.0633	120.6183	0.60	188531	1940.7955	-0.058	1.0322	1940.7375	1939.7052	978291.9886	978109.8695	0.1852	0.0553	182.25		
May24	P.PULASI	10:00	076	6.7080	120.6750	0.50	184268	1896.9335	-0.002	0.0000	1896.9315	1896.9315	978248.2978	978102.2480	0.1543	0.0461	146.16		
		16:24	003	6.1150	120.4600	2.80	183287	1886.8399	0.023	0.0000	1886.8629	1886.8629	978237.6195	978090.3885	0.8641	0.2582	147.84		
		19:46	004	6.1133	120.4667		182840	1882.2408	-0.111	0.0000	1882.1298	1882.1298	978232.8914	978090.3561	0.0000	0.0000	142.54		
May25	H.Berlian(Selayar)	08:39	004	6.1133	120.4667		182843	1882.2716	-0.095	0.0000	1882.1766	1882.1766	978232.8914	978090.3561	0.0000	0.0000	142.54		
		09:01	077	6.0795	120.4545	0.50	181779	1871.3241	-0.086	0.0035	1871.2381	1871.2346	978221.9494	978089.7128	0.1543	0.0461	132.34		
		09:23	078	6.0352	120.4455	0.75	180395	1857.0842	-0.073	0.0071	1857.0112	1857.0041	978207.7189	978088.8750	0.2318	0.0692	119.01		
		09:41	079	6.0092	120.4500	0.50	179613	1849.0391	-0.061	0.0100	1848.9781	1848.9682	978199.6829	978088.3861	0.1543	0.0461	111.41		
		09:59	080	5.9727	120.4477	0.50	178961	1842.3306	-0.046	0.0128	1842.2846	1842.2718	978192.9866	978087.7033	0.1543	0.0461	105.39		
		10:17	081	5.9297	120.4133	0.50	178044	1832.8955	-0.029	0.0157	1832.8665	1832.8508	978183.5656	978086.9041	0.1543	0.0461	96.77		
		10:31	082	5.8830	120.4523	0.50	177148	1823.6765	-0.014	0.0180	1823.6625	1823.6445	978174.3593	978086.0426	0.1543	0.0461	88.42		
		10:43	083	5.8387	120.4545	0.75	176055	1812.4305	-0.001	0.0199	1812.4295	1812.4096	978163.1244	978085.2316	0.2315	0.0692	78.06		
		10:58	084	5.8182	120.4567	0.50	175360	1805.2796	0.014	0.0223	1805.2936	1805.2713	978155.9860	978084.8584	0.1543	0.0461	71.24		
		11:27	085	5.8375	120.5113	0.75	174076	1792.0684	0.038	0.0270	1792.1064	1792.0794	978142.7942	978085.2097	0.2315	0.0692	57.75		
		13:36	004	6.1133	120.4667		182828	1882.1173	0.107	0.0477	1882.2243	1882.1766	978232.8914	978090.3561	0.0000	0.0000	142.54		
		May26	H.Berlian(Selayar)	08:22	004	6.1133	120.4667		182840	1882.2408	-0.081	0.0000	1882.1598	1882.1598	978232.8914	978090.3561	0.0000	0.0000	142.54
				08:53	086	6.1092	120.4307	0.30	184965	1904.1049	-0.083	0.4086	1904.0219	1903.6132	978254.3449	978090.2779	0.0926	0.0277	164.13
				09:17	087	6.1227	120.4092	0.30	186909	1924.1067	-0.082	0.7250	1924.0247	1923.2997	978274.0313	978090.5356	0.0926	0.0277	183.56
09:39	088			6.1500	120.4023	0.30	188227	1937.6676	-0.078	1.0150	1937.5896	1936.5746	978287.3062	978091.0585	0.0926	0.0277	196.31		
10:06	089			6.1795	120.3920	0.50	189197	1947.6479	-0.069	1.3709	1947.5789	1946.2080	978296.9397	978091.6262	0.1543	0.0461	205.42		
10:36	090			6.2057	120.3988	0.50	189253	1948.2241	-0.055	1.7664	1948.1691	1946.4028	978297.1344	978092.1326	0.1543	0.0461	205.11		
11:00	091			6.2067	120.4205	0.50	187780	1933.0684	-0.04	2.0827	1933.0284	1930.9457	978281.6773	978092.1519	0.1543	0.0461	189.63		
11:34	092			6.1750	120.4182	0.50	187595	1931.1650	-0.016	2.5309	1931.1490	1928.6180	978279.3497	978091.5394	0.1543	0.0461	187.92		
12:44	004			6.1133	120.4667		183164	1885.5744	0.039	3.4536	1885.6134	1882.1598	978232.8914	978090.3561	0.0000	0.0000	142.54		
May27	H.Berlian(Selayar)			09:22	004	6.1133	120.4667		183177	1885.7082	-0.064	0.0000	1885.6442	1885.6442	978232.8914	978090.3561	0.0000	0.0000	142.54
		09:58	086	6.1092	120.4307	0.30	185314	1907.6957	-0.067	0.0620	1907.6287	1907.5667	978254.8140	978090.2779	0.0926	0.0277	164.60		
		10:56	093	6.1318	120.4193	0.50	187223	1927.3374	-0.059	0.1620	1927.2784	1927.1165	978274.3637	978090.7097	0.1543	0.0461	183.76		
		11:15	094	6.1523	120.4137	0.50	187867	1933.9636	-0.053	0.1947	1933.9106	1933.7159	978280.9631	978091.1027	0.1543	0.0461	189.97		
		11:37	092	6.1750	120.4182	0.50	187663	1931.8646	-0.044	0.2326	1931.8206	1931.5880	978278.8352	978091.5394	0.1543	0.0461	187.40		
		11:51	095	6.1817	120.4262	0.30	186630	1921.2361	-0.037	0.2567	1921.1991	1920.9423	978268.1896	978091.6686	0.0926	0.0277	176.59		
		12:14	096	6.1682	120.4398	0.60	185929	1914.0235	-0.024	0.2964	1913.9995	1913.7031	978260.9504	978091.4084	0.1852	0.0553	169.67		
		12:43	097	6.1408	120.4488	-0.50	184902	1903.4567	-0.005	0.3463	1903.4517	1903.1054	978250.3526	978090.8820	-0.1543	-0.0461	159.36		
		13:23	004	6.1133	120.4667		183209	1886.0374	0.022	0.4152	1886.0594	1885.6442	978232.8914	978090.3561	0.0000	0.0000	142.54		
		May28	H.Berlian(Selayar)	07:12	004	6.1133	120.4667		183201	1885.9551	0.038	0.0000	1885.9931	1885.9931	978232.8914	978090.3561	0.0000	0.0000	142.54
09:14	084			5.8182	120.4567	0.50	175728	1809.0660	-0.004	0.0030	1809.0620	1809.0590	978155.9573	978084.8584	0.1543	0.0461	71.21		
09:54	098			5.7705	120.4887	0.30	174002	1791.3070	-0.017	0.0040	1791.2900	1791.2860	978138.1843	978083.9949	0.0926	0.0277	54.25		
11:48	099			5.8842	120.5307	0.75	175588	1807.6255	-0.042	0.0068	1807.5835	1807.5767	978154.4750	978086.0647	0.2315	0.0692	68.57		
14:18	100			5.9317	120.5342	0.50	176334	1815.3012	0.018	0.0105	1815.3192	1815.3086	978162.2069	978086.9411	0.1543	0.0461	75.37		
16:44	004			6.1133	120.4667		183198	1885.9242	0.083	0.0141	1886.0072	1885.9931	978232.8914	978090.3561	0.0000	0.0000	142.54		

May29	H.Berlian(Selayar)	06:44	004	6.1133	120.4667		183197	1885.9139	0.079	0.0000	1885.9929	1885.9929	978232.8914	978090.3561	0.0000	0.0000	142.54
		09:05	101	6.2125	120.5250	1.50	181844	1871.9929	0.026	0.0953	1872.0189	1871.9237	978218.8221	978092.2643	0.4629	0.1383	126.88
		12:13	014	6.4933	120.4767	0.50	182932	1883.1873	-0.055	0.2223	1883.1323	1882.9101	978229.8085	978097.8297	0.1543	0.0461	132.09
		13:01	102	6.4932	120.4227	0.00	183668	1890.7601	-0.056	0.2547	1890.7041	1890.4494	978237.3478	978097.8277	0.0000	0.0000	139.52
		13:28	103	6.4705	120.4273	0.50	183631	1890.3794	-0.053	0.2729	1890.3264	1890.0534	978236.9519	978097.3688	0.1543	0.0461	139.69
	H.Berlian(Selayar)	16:20	004	6.1133	120.4667		183239	1886.3461	0.036	0.3891	1886.3821	1885.9929	978232.8914	978090.3561	0.0000	0.0000	142.54
May30	H.Berlian(Selayar)	06:41	004	6.1133	120.4667		183233	1886.2843	0.087	0.0000	1886.3713	1886.3713	978232.8914	978090.3561	0.0000	0.0000	142.54
		12:12	104	6.1025	120.5637	2.00	175915	1810.9900	-0.04	-0.0217	1810.9500	1810.9717	978157.4917	978090.1502	0.6172	0.1844	67.77
	H.Berlian(Selayar)	15:42	004	6.1133	120.4667		183242	1886.3769	-0.041	-0.0354	1886.3359	1886.3713	978232.8914	978090.3561	0.0000	0.0000	142.54
	H.Berlian(Selayar)	19:54	004	6.1133	120.4667		183228	1886.2329	0.096	-0.0424	1886.3289	1886.3713	978232.8914	978090.3561	0.0000	0.0000	142.54
	Banteng(Selayar)	20:05	003	6.1150	120.4600	2.80	183686	1890.9453	0.096		1891.0413	1891.0413	978236.9240	978090.3885	0.8641	0.2582	147.14
May31	BuluKumba	05:21	002	5.5567	120.2023	1.50	176069	1812.5745	0.053	0.0000	1812.6275	1812.6275	978159.0003	978080.2108	0.4629	0.1383	79.11
		H.Ramayana U.P	13:28	001				171860	1769.2677		0.0000	1769.2677	1769.2677	978115.4347	978031.8000	0.0000	0.0000
Jun1	H.Ramayana U.P	09:15	001				171844	1769.1031		0.0000	1769.1031	1769.1031	978115.4347	978031.8000	0.0000	0.0000	
		Bandara U.P	10:17	UJPO	5.0675	119.5500	32.00	172284	1773.6303	0.213	10.0216	1773.8433	1763.8217	978119.9400	978072.0834	9.8752	2.9505